

Dr. Cooke  
Best Wishes  
Charlie

LATE QUATERNARY GEOLOGICAL HISTORY

OF MAKKOVIK BAY, LABRADOR

by

Charles Q. Barrie

Submitted in partial fulfillment of the

requirements for the degree of

Master of Science

at

Dalhousie University

Halifax, Nova Scotia

May, 1980

Examiners:

---

---

---

---

---

TABLE OF CONTENTS

	<u>Page</u>
TABLE OF CONTENTS	i
LIST OF FIGURES	v
LIST OF PLATES	x
LIST OF TABLES	xii
ABSTRACT	xiii
ACKNOWLEDGEMENT	xvi
Chapter I	INTRODUCTION
	1.1 Scientific Objectives 1
	1.2 Practical Applications 5
	1.3 Approach 6
Chapter II	GEOLOGY OF MAKKOVIK AREA
	2.1 Bedrock Geology 8
	2.2 Surficial Land Geology 11
	2.3. Coastal Geomorphology 18
Chapter III	PHYSICAL OCEANOGRAPHY
	3.1 Previous Work 24
	3.2 Bathymetry 25
	3.3 Physical Oceanographic Measurements 27
	3.4 Suspended Sediments 29
	3.5 Sediment Traps 32
	3.6 Discussion 36

Chapter IV	ACOUSTIC STRATIGRAPHY	
4.1	Physical Guidelines for High Resolution Acoustic Stratigraphy	48
	Equipment	49
	Propagation of Sound	49
	Acoustic Reflection	50
	Horizontal Resolution and Side Effects	51
	Vertical Resolution	53
	Sub-bottom Composition	55
4.2	Acoustic Stratigraphy of Makkovik Bay	56
	Evidence of Lithological Stratum	56
	Descriptive Techniques	57
	Description of Basinal Acoustic Stratigraphy	62
	Specific Interpretational Problems	83
4.3	Interbasin Correlation of Acoustic Stratigraphy	85
	Upper Basin-Fill Unit	85
	Conformable Cover Unit	89
	Lower Basin-Fill Unit	91
	Erosional Unconformities	92
4.4	Surficial Distribution of Acoustic Units	93
4.5	Depositional Interpretation	93
	Upper Basin-Fill Environment	93
	Conformable Cover Environment	96
	Lower Basin-Fill Environment	97
4.6	Model of Acoustic Stratigraphy	98
Chapter V	LABORATORY TECHNIQUES	101
Chapter VI	SURFICIAL SEDIMENT DISTRIBUTION	
6.1	Purpose	105

	6.2 Short Core Sediment Types	105
	6.3 Detailed Grain Size Distribution	109
	6.4 Discussion	115
	6.5 Clay Intertidal Platforms	119
	6.6 Interpretation of Grain Size Trends	121
Chapter VII	PISTON CORE FACIES DESCRIPTIONS	
	7.1 Introduction	126
	7.2 Facies Description	126
	7.3 Facies Distribution	140
Chapter VIII	PISTON CORE CORRELATION AND FACIES INTERPRETATION	
	8.1 Introduction	143
	8.2 Piston Core-Acoustic Correlation Techniques	143
	8.3 Piston Core 78-020-003	144
	8.4 Piston Core 78-020-004	144
	8.5 Lithologic Correlation	146
	8.6 Chronologic Correlation	150
	8.7 Stratigraphic Correlation	153
	8.8 Facies Interpretation	156
Chapter IX	CLAY MINERALOGY	
	9.1 Introduction	160
	9.2 Distribution of Clay and Clay-Size Mineralogy	160
	9.3 General Interpretations	175
	9.4 Discussion: General Aspects of Clay Mineral Segregation	181
	9.5 Hypothesis for Deposition of Clay Minerals	184
Chapter X	FORAMINIFERA	
	10.1 Introduction	190
	10.2 Surficial Distribution	190

	10.3 Discussion of Surficial Distribution	194
	10.4 Distribution Within Piston Cores	196
	10.5 Discussion of Ecology of Benthonic Foraminifera	202
	10.6 Interpretation	207
Chapter XI	FACIES MODEL OF POSTGLACIAL DEPOSITION	
	11.1 Factors Controlling Deposition	212
	11.2 Facies Model of Deposition	216
	11.3 Stratigraphic Facies Model of Deposition	223
	11.4 Application to Recent Concepts of Postglacial Development	225
Chapter XII	CONCLUSIONS AND SUGGESTIONS FOR FURTHER RESEARCH	
	12.1 Oceanography	231
	12.2 Stratigraphy	231
	12.3 Model of Postglacial Development	232
	12.4 Suggestions for Further Research	234
	REFERENCES	237
Appendix 1	RS-5 PLOTS	247
Appendix 2	SEDIMENT TRAP DATA	254
Appendix 3	PISTON CORE LABELLING	256
Appendix 4	SEDIMENT STATISTICS	259
Appendix 5	CLAY AND CLAY-SIZE MINERALOGY	264

LIST OF FIGURES

		<u>Page</u>
FIGURE 1.1	Location Map of Makkovik Bay	2
FIGURE 1.2	Bathymetry of Makkovik Bay	4
FIGURE 2.1	Geological Map of the Makkovik Bay Area	9
FIGURE 2.2	Classification of Contemporary Shoreline Energy Levels	20
FIGURE 3.1	Track Chart, Makkovik Bay	in pocket
FIGURE 3.2(a)	Downbay Water Temperature Profile	28
FIGURE 3.2(b)	Downbay Water Salinity Profile	30
FIGURE 3.2(c)	Downbay Water Density Profile	31
FIGURE 3.3	Downbay Profile of Suspended Sediments	33
FIGURE 3.4	Sketch of Sediment Trap Operation	35
FIGURE 3.5	Downbay Profile of Sediment Accumulation by Sediment Trap	37
FIGURE 3.6	Hypothetical Explanation for the Distribution of Near Bottom, Suspended Sediments	42
FIGURE 3.7	Water Depth for Threshold of Sediment Motion	43
FIGURE 4.1	Relative Effects of Sea Floor on Recorder Trace	52
FIGURE 4.2	Profile Showing Stratal Reflection Superimposed by Side Effects	54
FIGURE 4.3	Smoothed Track Chart and 13 Representative Basins	58

FIGURE 4.4	Illustration of Three Morphologic Types of Acoustic Strata	61
FIGURE 4.5	Interbasin Correlation Chart	86
FIGURE 4.6	Isopach Map of the Upper Basin-Fill Unit	88
FIGURE 4.7	Isopach Map of the Conformable Cover Unit Plus the Lower Basin-Fill Unit	90
FIGURE 4.8	Surficial Distribution of the Acoustic Stratigraphic Units	94
FIGURE 4.9	Model of Postglacial Development: Acoustic Stratigraphy	99
FIGURE 5.1	Representative X-Ray Diffractograms	103
FIGURE 6.1	Surficial Distribution of Sediment Types	107
FIGURE 6.2	Ternary Plot of Grain Size Distributions From All Surficial Sedimentary Units	110
FIGURE 6.3	Plots of Percent Sand vs Depth	111
FIGURE 6.4	Six Detailed Grain Size Frequency Histograms Taken Along Tom's Cove Profile	114
FIGURE 6.5	Plot of the Silt-Clay Ratio vs Depth for the Outer Bay Samples	116
FIGURE 6.6	Cross-sectional Profile of a Clay Intertidal Platform	120
FIGURE 6.7	Schematic Description of the Mode of Deposition along the Tom's Cove Profile	122
FIGURE 6.8	Superposition of the Tom's Cove Profile Grain Size Distributions on the 3.5 kHz Seismic Profile, 1230-1242/22	125
FIGURE 7.1	Piston Core 78-020-003	128
FIGURE 7.2	Piston Core 78-020-004	129
FIGURE 7.3	Sketch of X-Radiograph of Facies A, Core 78-020-003	131

FIGURE 7.4	Modal Analysis of Facies A	132
FIGURE 7.5	Sketch of X-Radiograph of Wispy Silt Laminae of Facies B	134
FIGURE 7.6	Modal Analysis of Facies B	135
FIGURE 7.7	Representative Grain-Size Analysis of Facies C	137
FIGURE 7.8	Representative Grain-Size Distribution for Facies D	138
FIGURE 7.9	Sketch of X-Radiograph of Subfacies D <sub>2</sub>	139
FIGURE 7.10	Representative Grain-Size Distribution for Facies E	141
FIGURE 8.1	Acoustic Profile to Core Correlation: Core 78-020-003	145
FIGURE 8.2	Acoustic Profile to Core Correlation: Core 78-020-004	147
FIGURE 8.3	Tentative Lithologic Correlation of Piston Core Units	149
FIGURE 8.4	Chronology of Piston Cores and Conformable Cover Unit	152
FIGURE 8.5	Chronologic Correlation of Piston Cores and Conformable Cover Unit	154
FIGURE 8.6	Stratigraphic Correlation of Piston Core Facies	155
FIGURE 9.1	Ternary Plot of Illite-Feldspar-Chlorite for Relict and Contemporary Sedimentary Units	162
FIGURE 9.2	Ternary Plot of Illite-Chlorite-Montmorillonite Plus Kaolinite of the Relict and Contemporary Sedimentary Units	163
FIGURE 9.3	Areal Distribution of the Relative Percent of Illite in the Relict, Grey, Clayey Silt	164
FIGURE 9.4	Up-core Variations in the Relative Percent of Clay and Clay-size Minerals: Core 78-020-003	166



FIGURE 9.5	Upcore Variations in the Relative Percent of Clay and Clay-size Minerals: Core 78-020-004	168
FIGURE 9.6	Ternary Plot of Illite-Chlorite-Montmorillonite Plus Kaolinite from Piston Core Facies Samples	171
FIGURE 9.7	Ternary Plot of Illite-Feldspar-Chlorite from Piston Core Facies Samples	172
FIGURE 9.8	Sample Frequency Histograms of Montmorillonite Content	173
FIGURE 9.9	Sample Frequency Histograms of Kaolinite Content	174
FIGURE 9.10	Surficial Distribution of the Relative Percent of Chlorite Samples from the Basinal Olive Mud and Coarse Olive Mud	176
FIGURE 9.11	Averaged Percents of Feldspar and Illite Progressing from Proximal to Distal Localities	186
FIGURE 9.12	Hypothesis for the Deposition of Clay Minerals	188
FIGURE 10.1	Areal Distribution of Benthonic Foraminifera	191
FIGURE 10.2	Distribution of Foraminifera in Piston Core 78-020-003	199
FIGURE 10.3	Distribution of Foraminifera in Piston Core 78-020-004	200
FIGURE 10.4	Tentative Downcore Estimates of Salinity, Temperature and Sedimentation Rate Based on Foraminiferal Distributions	210
FIGURE 11.1	Longitudinal Profile of Makkovik Bay Showing the Distribution of Contemporary Basinal Olive Mud and the Relict Conformable Cover Unit	214
FIGURE 11.2	Simple Model of Estuarine Circulation of a Partially Mixed Estuary	217

FIGURE 11.3	Model of Primary Controlling Factors of Postglacial Development	219
FIGURE 11.4	Schematic Illustration of Contrasting Deep Water Runoff Dominated Deposition in a Highly Stratified Estuary and Shallow Water, Wave Dominated Deposition in a Partially Mixed Estuary	222
FIGURE 11.5	Stratigraphic Model of Deposition	224
FIGURE 11.6	Hypothesis for Landward Migration of Glacio-isostatic Coastal Readjustment	228

LIST OF PLATES

		<u>Page</u>
PLATE 2.1 (a)	Aerial View of Ranger Bight	12
PLATE 2.1 (b)	Exposed Section of Ranger Bight	13
PLATE 2.1 (c)	Ice Crevasse Filling; Ranger Bight	14
PLATE 2.2	View of Burntwood Point Raised Delta	16
PLATE 2.3 (a)	Side View of Raised Makkovik Harbour Delta	17
PLATE 2.3 (b)	Close-up of Basal, Steep Sandy Foresets	19
PLATE 2.3 (c)	Close-up of Diamictite	19
PLATE 2.4	View of Boulder Strewn Intertidal Plat- form at Head of Ranger Bight	22
PLATE 4.1	Basin A: 3.5 kHz Profile	63
PLATE 4.2	Basin B: 3.5 kHz Profile	65
PLATE 4.3	Basin C: 3.5 kHz Profile	67
PLATE 4.4	Basin D: 3.5 kHz Profile	68
PLATE 4.5	Basin E: 3.5 kHz Profile	70
PLATE 4.6	Basin F: 3.5 kHz Profile	72
PLATE 4.7	Basin G: 3.5 kHz Profile	74
PLATE 4.8	Basin H: 3.5 kHz Profile	75
PLATE 4.9	Basin I: 3.5 kHz Profile	77
PLATE 4.10	Basin J: 3.5 kHz Profile	78
PLATE 4.11	Basin K: 3.5 kHz Profile	80
PLATE 4.12	Basin L: 3.5 kHz Profile	82

PLATE 4.13	Basin M: 3.5 kHz Profile	84
PLATE 6.1	X-Radiographs of Three Representative Short Cores of Unit III	108

LIST OF TABLES

		<u>Page</u>
TABLE 3.1	Table of Comparative Suspended Particulate Matter from other Localities	40
TABLE 3.2	Relationships Between Sediment Trap and Suspended Sediment Data	45
TABLE 3.3	Comparison of Sedimentation Rates from other Localities	47
TABLE 9.1	Average Percentage of Total Clay-size Minerals for the Piston Core Facies	169
TABLE 9.2	Average Percentage of Total Clay-size Minerals for the Major Lithologic Units	178
TABLE 9.3	Average Percentage of Clay Minerals from Makkovik Bay and Surrounding Areas	179
TABLE 10.1 (a)	Surficial Distribution of Foraminifera According to Lithology	192
TABLE 10.1 (b)	Total Foraminifera per gram and Percentage of Agglutinated Types from Samples of Surficial Olive Sediment	193
TABLE 10.2	Percentage of Foraminifera in Piston Core 78-020-003	197
TABLE 10.3	Percentage of Foraminifera in Piston Core 78-020-004	198
TABLE 11.1	Summary of Major Factors and Depositional Events since 19,000 years B.P.	226

ABSTRACT

Located on the east coast of Labrador, Makkovik Bay is a low relief, 35 km-long, complex fjord. Oceanographically, it is a nonstagnant, well stratified, partially-mixed-type estuary during the summer, probably with moderate sea water exchange. The degree of stratification appears to be related to fluvial flux and tidal mixing which is attenuated by sills and bay mouth constrictions. Low values of suspended sediment and high rates of sediment accumulation by sediment traps suggest that the contemporary environment is wave-dominated, resuspending marginal sediments with deposition in the deeper basins.

An original technique using morphology and character of reflection is capable of synthesizing 3.5 kHz acoustic analogue data. Three major acoustic units are recognizable within Makkovik Bay: lower basin-fill, conformable cover and upper basin-fill units. The lower basin-fill unit underlies the conformable cover unit in the deeper, quieter basins and is thought to be composed of coarse to muddy clastics deposited under relatively high energy conditions, probably during the early stages of postglacial transgression. The age of the oldest sediments is extrapolated to be approximately 19,000 years B.P.

The conformable cover unit is an acoustically well stratified unit found mantling the entire bay. It outcrops along topographic highs and flanks of high energy bays and along the nearshore in moderate energy bays. Short cores and grab samples penetrate an upper unit of stiff, homogeneous, olive gray, clayey silt and a lower unit of alternating brownish gray and olive gray beds with thin basal silt laminae. The distribution of benthonic

foraminifera suggests a high rate of sedimentation in a cold, open bay type environment. Detailed analyses of the clay and clay-size minerals show prominent differential sedimentation, concentrating illite proximally and feldspar distally. The conformable cover unit is interpreted to have had runoff-dominated deposition, occurring during the last major transgression and terminating at approximately 10,000 years B.P. Glacial detritus was transported fluviially northwards along the Makkovik Brook Valley and distributed across Makkovik Bay within the upper fresher water layer of a well stratified two-layer type estuary. Rapid deposition occurred through the lower, more saline water layer.

The upper basin-fill unit is characterized by poor acoustic reflectivity and a ponded morphology with a variable degree of flank-onlap which is inversely related to wave energy. The surficial sediments include a nearshore coarse veneer (unit I), a basinal, organic rich, grayish-olive clayey silt (unit II), a lower-flank, coarse grayish-olive mud (unit III), and a stiff, gray clayey silt (unit IV) which corresponds to the conformable cover unit. Two piston cores penetrate 4 major facies that represent a transition from runoff-dominated to contemporary wave-dominated deposition during regression and a decreasing fluvial flux. The lithologies change upwards from alternating olive gray and yellow brown through gray brown to dark grayish olive coloured muds. The sedimentation rate decreases from approximately 0.3 to 0.07 cm/year. The brackish to open marine type foraminifera are followed by agglutinated, cold water estuarine types. The dominant clay trend shows an upward decreasing illite-feldspar ratio suggesting further nearshore concentration of illite during resuspension. The transition to wave-dominated deposition occurs earlier in

the Approaches than the Outer Bay; it is controlled primarily by runoff and relative sea level.

An erosional unconformity occurs above the base of the upper basin-fill unit, approximately at 6,000 years B.P. This event is chronologically correlatable with a resurgence in runoff.



#### ACKNOWLEDGEMENTS

I am sincerely grateful to Drs. David Piper and Basil Cooke for supervising this research and for critical reading of the manuscript. Sincere thanks are also due to the other members of the supervisory committee, Drs. David Huntley and Gerry Reinson.

Throughout the course of this work a great deal of scientific stimulation has been generated from colleagues at Dalhousie, especially Ali Aksu, Phil Hill, John Letson and Peta Mudie. I would also like to acknowledge the useful advice offered by Drs. Kate Kranck and Barry Hargrave of Bedford Institute of Oceanography.

Thanks are due to Bob Iuliucci for his competent field expertise and to Dr. Charlotte Keen for the recovery of the piston cores during C.S.S. Hudson cruise 78-020. Clo Leone kindly did the typing of the manuscript.

The field and laboratory work was supported through an Energy Mines and Resources agreement grant to Dr. Piper (number 113-4-78). The Faculty of Graduate Studies, Dalhousie University provided financial support over the period of research.

Finally, I would like to express my warm appreciation to Olenka for her help, encouragement and enduring patience throughout the duration of this research.

## CHAPTER I

### INTRODUCTION

Makkovik Bay is a glacially excavated, low profile fjord located on the isostatically rising, eastern central Labrador coast at 55°10' North (Fig. 1.1). It is approximately 35 km long and about 2 km wide with a broad, poorly defined sill merging with an Approach area containing two major islands. The bay is subdivided into the Outer Bay, Eastern Inner Bay, Central Inner Bay and the Western Inner Bay (Fig. 1.2).

#### 1.1 Scientific Objectives

The study of recent marine sediments in an inlet such as Makkovik Bay on the central Labrador coast is scientifically important for the following reasons:

- (1) to produce a model of sedimentation of an inlet characterized by a relative fall in sea level;
- (2) to describe the nature of deglaciation of the central Labrador coastline.

Sedimentary processes within glaciated coastal inlets have been studied in Nova Scotia (Stanley, 1968; Barnes, 1976; Piper and Keen, 1976; Amos, 1978; Barnes and Piper, 1978) and Newfoundland (Slatt, 1974, 1975). Both areas are characterized by a relative rise in sea level, reworking and redistribution of glacial drift deposited during periods of lower sea level. In Labrador the glacio-isostatic rebound has been greater than eustatic sea

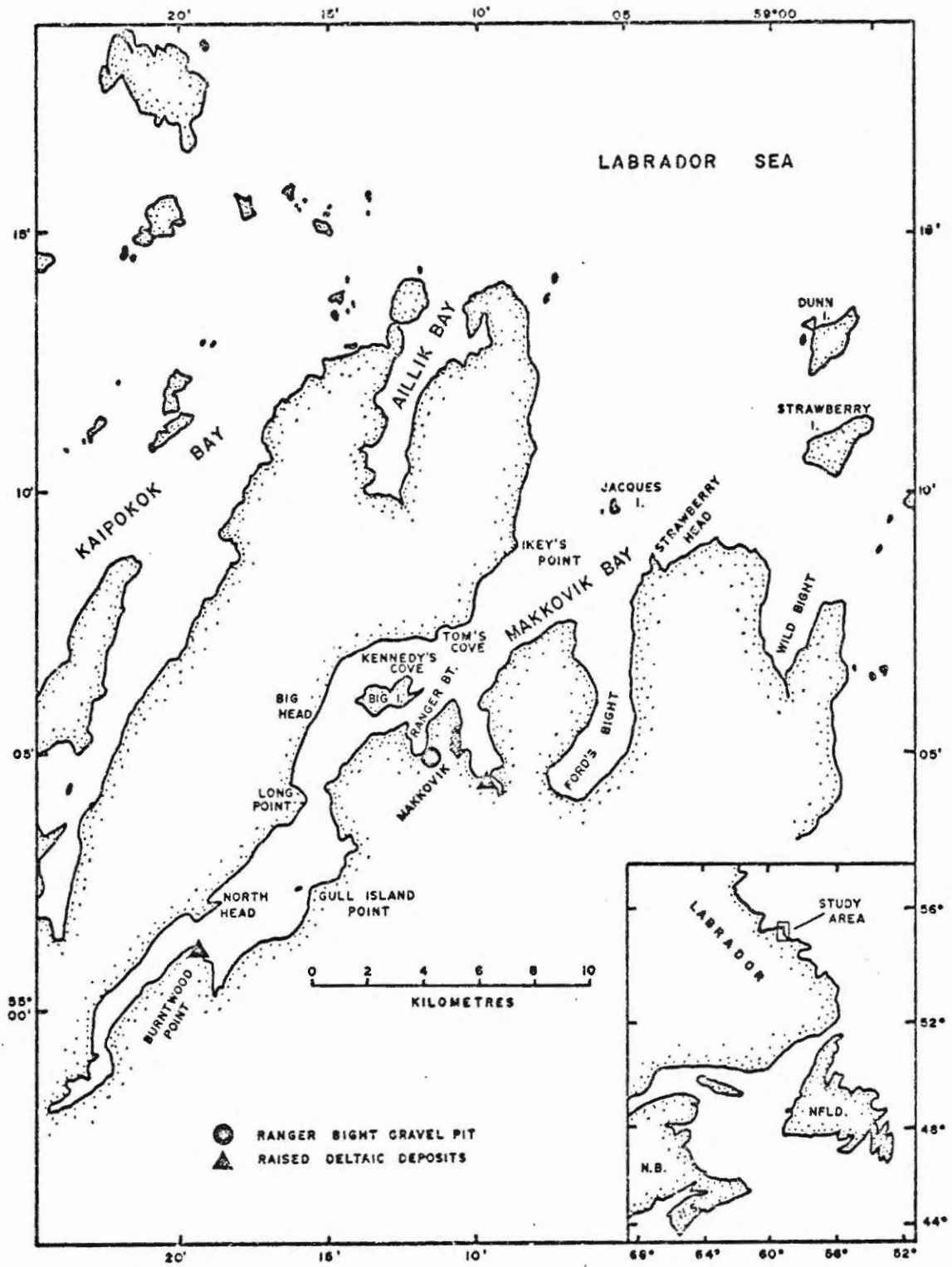


Figure 1.1: Location map of Makkovik Bay

level fluctuations creating a shoreline that has been emerging during the Holocene transgression resulting from the retreat of a late Wisconsinan ice sheet (e.g., Daly, 1902; Ives, 1958; Loken, 1962; Andrews, 1969, Johnson, 1969; Amos, 1978). The inlet sediments of Labrador have not previously been studied in detail. In a reconnaissance survey of Makkovik Bay, Piper and Iuliucci (1978) delineated 6 sediment types derived primarily from marginally exposed marine sediments. They suggested that during deglaciation the sea level stood 35 to 40 m above present, with proglacial deltas having silt and clay bottomsets extending across the bay. Since then, the falling sea level has reworked the coarse clastics into a near-shore sandy prism and the fine portion into the basins with an intermediate zone of no net deposition. One of the objectives of the present study is to examine these processes in greater detail, both sedimentologically and oceanographically, to describe the depositional processes and to clarify their mechanisms.

The glacial history of the Makkovik region has only been interpreted by one earlier worker. Because of the bare, glacially polished hilltops surrounding Makkovik Bay, Ives (1958) proposed a relatively thick ice sheet extending well out onto the continental shelf. Elsewhere, Prest (1970) speculated a 14,000 year B.P. deglaciation of the Labrador coastal area based on interpolations between widely spaced  $^{14}\text{C}$  dated marine deposits. Northwest Atlantic foraminiferal assemblages (McIntyre et al., 1976), Labrador Shelf geomorphic evidence (Fillon, 1976) and Labrador peat deposits (Wenner, 1947) suggest an even later deglaciation, possibly as late as 9,000 years B.P.

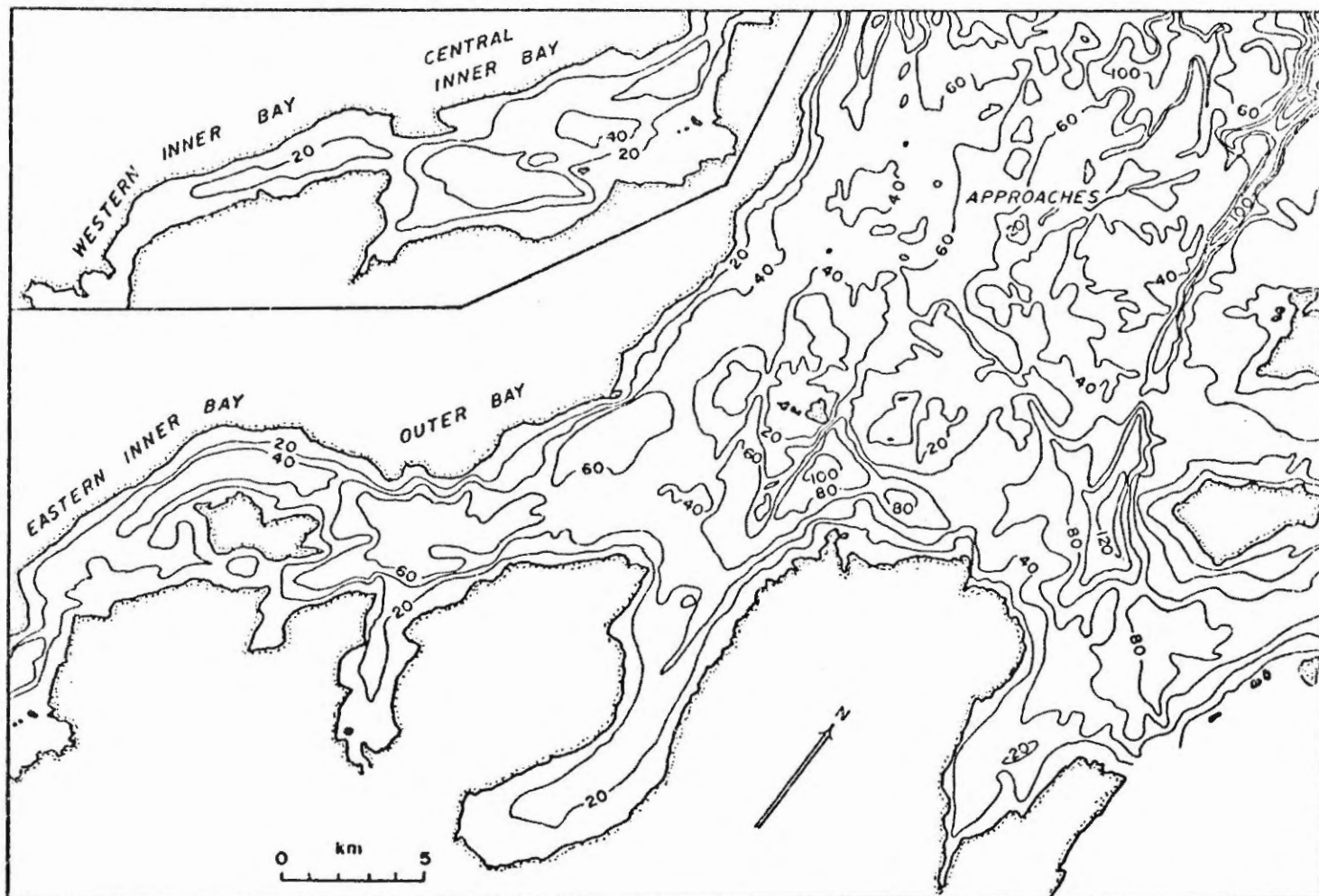


Figure 1.2: Bathymetry of Makkovik Bay. Contours at 20-m intervals based on Canadian Hydrographic Services field sheets. (Piper and Iuliucci, 1978; Barrie, 1978)

However, more recently, Vilks and Mudie (1978) found open water foraminiferal assemblages and sedge-shrub tundra pollen in shelf sediment cores off central Labrador, which suggest open water shelf conditions and at least the presence of some coastal refuges or nunataks as early as 21,000 years B.P.

Correlation of pollen lake stratigraphies to the north (Short et al., 1977; Short, 1978) and south (Jordan, 1976) suggest that glacial retreat from the coast commenced as early as 10,300 years B.P. and disappeared in the interior by about 5,500 years B.P. (Short, 1978). Pollen assemblages suggest that cold conditions continued after deglaciation until the hypsithermal climatic optimum between approximately 7,000 and 4,500 years B.P., followed again by a cooling period commencing at about 3,000 years B.P. (Short, 1978; Mudie, 1980).

Fjordic sediments of Labrador have been strategically selected in this study to help the decipherment of deglacial events because they concurrently monitor terrestrial and marine processes. The terrestrial input should record deglaciation directly, with hopefully minor marine influence, while the marine conditions themselves act as a chronostratigraphic control.

## 1.2 Practical Applications

Studies of the marine sediments and their depositional and erosional environment in central Labrador are immediately applicable to the research needs of industry. Knowledge of the contemporary erosional and depositional processes will aid expanding industries to locate waste disposal sites with efficient dispersal mechanisms. Environmental and lithologic investigations

of unconsolidated sediments are necessary for route selection of seabed cables and pipelines.

### 1.3 Approaches

Approximately 285 km of 3.5 kHz seismic reflection profiles, over 150 gravity cores, 13 temperature-salinity profiles, 6 suspended sediment samples and data from 4 sediment traps were collected from Makkovik Bay during August 1978, using a 35-foot fishing boat, the "Cathy Ford". Brief notes were made on surficial land deposits during boat down-time.

C. Keen of Bedford Institute of Oceanography collected 2 ten-metre Benthos piston cores in July 1978, cruise HU78-020.

This is an interdisciplinary study, stressing primarily geophysics and sedimentology. Working from basic principles of acoustic profiling, the geomorphic and reflective characteristics of 13 typical basins are described and compiled in Chapter IV to determine the general acoustic stratigraphy. This is combined with minor geological field observations (Chapter II) to produce an acoustic model of deposition (Chapter IV). The physical oceanography (Chapter III) and the distribution of foraminifera (Chapter IX) are studied in order to specify the nature of the contemporary estuarine processes. The surficial sediment distribution (Chapter VI) furnishes an insight to the relationship of the sediment deposition and the contemporary environment. Combined, this information provides a framework for the interpretation of the past depositional environments (Chapter X) as evidenced by the clay mineralogy (Chapter VIII), foraminifera (Chapter IX) and lithology (Chapters VII and VIII) of two piston cores. Finally,

the major depositional mechanisms are outlined and correlated with concepts of postglacial development in adjacent areas (Chapter XI).



CHAPTER II

GEOLOGY OF MAKKOVIK AREA

2.1 Bedrock Geology

Reconnaissance surveys of the bedrock geology of the Makkovik area have been published by Packard (1891), Daly (1902), Kranck (1939, 1953) and Douglas (1953), and there are unpublished Masters theses by Cooper (1951), Moore (1951), Riley (1951) and King (1963). Beavan (1958) assessed the economic value of uranium in the area. Gandhi et al. (1969) presented a detailed geochronology of the Makkovik area. A brief summary of the bedrock and structural geology is presented here (Fig. 2.1) taken primarily from Gandhi et al. (1969).

The Hopedale banded gneiss is Archean and is considered to be the migmatized basement on which the Aillik Series was laid down. The gneiss contains numerous mafic amphibolitic inclusions and is rich in granitic material occurring as dikelets and small irregular bodies. It outcrops extensively to the west of Kaipokok Bay and higher up the Makkovik River Valley.

The Proterozoic Aillik Series is exposed in two north trending anticlines, one south of Makkovik Bay (Round Pond Anticline) and one from Monkey Hill across Makkovik Bay to Aillik Bay (Makkovik Bay Anticline). It is estimated to be 7,620 metres thick and is composed of 9 lithologies. In chronological order these are: a granoblastic feldspathic quartzite, a banded, varicoloured quartzite often interbedded with a conglomerate, a

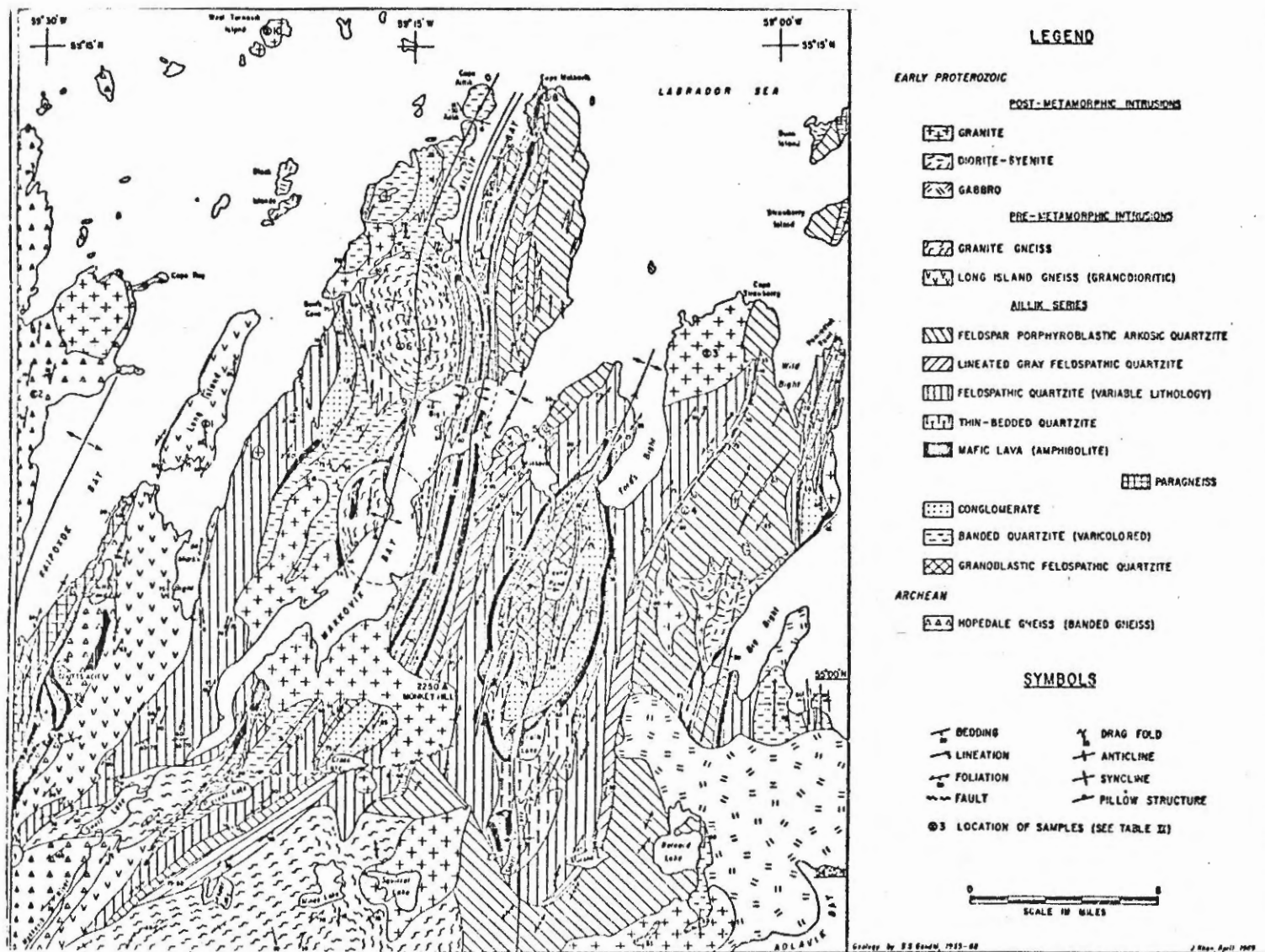


Figure 2.1: Geological map of the Makkovik Bay area, Labrador. (From Gandhi et al., 1969)

paragneiss (on the east shore of Kaipokok Bay), a thin amphibolitic mafic lava, a thin-bedded quartzite, a feldspathic quartzite of variable lithology, a lineated gray feldspathic quartzite, and a feldspar porphyroblastic arkosic quartzite.

Two early Proterozoic gneiss units are intruded into the Hopedale gneiss and Aillik Series. The Long Island Gneiss is an orthogneiss of granodiorite composition found on Long Island in Kaipokok Bay and extends as a wide belt subparallel to the Makkovik River Valley. The second gneiss, the synkinematic Granite Gneiss, occurs primarily as two large resistant domes along the west shore of Makkovik Bay and as a large mass south of the Bay.

Three post-kinematic intrusive types, also of early Proterozoic age, occur in the Makkovik area. A medium- to coarse-grained gabbro with dioritic to syenitic intrusions occurs along the coastal areas primarily south of Makkovik Bay. Post-kinematic intrusions of granite of variable composition occur widely as resistant stocks and related offshoots. The Monkey Hill type is a medium- to coarse-grained rock with a hypidiomorphic granular texture and is exposed from Monkey Hill northwest across Makkovik Bay. The Cape Strawberry type granite occurs as a large stock and, in comparison, is coarser grained and contains more potassic feldspar.

The dominant structural character is outlined by the two north-northeast trending anticlines of the Aillik Series. These folds are considered to be a consequence of synkinematically-emplaced granite gneiss domes, the intrusive gradually deforming the surrounding formations. For this reason, it is postulated that more granite gneiss domes may exist,

one beneath Cape Aillik and one forming the core of the Round Pond Anticline. The general pattern of the folds and the attitudes of foliations and lineations point to a single cycle of orogenic deformation for the Aillik Series. Furthermore, this deformation period corresponds with the Hudsonian orogeny in the Canadian Shield, approximately 1,600 million years ago.

## 2.2 Surficial Land Geology

There is a dearth of till deposits in the immediate area of Makkovik Bay. Hill tops are bare with abundant inclinational glacial polishing suggesting that, at one time (probably during the last glaciation) the ice was very thick and extended well past the present-day coastline (Ives, 1958, 1978). Small till deposits are found in the protected valleys (e.g., King, 1963) but in most cases have been overgrown by vegetation. Three sandy- to gravelly-raised deltaic-type deposits were studied briefly.

The Ranger Bight gravel pit (Plate 2.1, a-c) is located on the north side of a bedrock hill just west of Makkovik Settlement (Fig. 1.1) at an approximate elevation of 40 m (Plate 2.1 a). The gravel and sandy gravel strata dip obliquely toward the hillside (ca. 15/100 E) throughout most of the gravel pit exposure, except on the west side where the strata level then dips slightly in a downbay direction (ca. 05/280 W) (Plate 2.1 b). A possible ice crevasse filling occurs in the middle of the gravel pit (Fig. 2.1 c). The gravel deposit is unconformably overlain by a veneer comprised of basal boulders and well sorted, laminated sand. This veneer also occurs in the saddle west of Makkovik settlement (in foreground, Fig. 2.1 a).

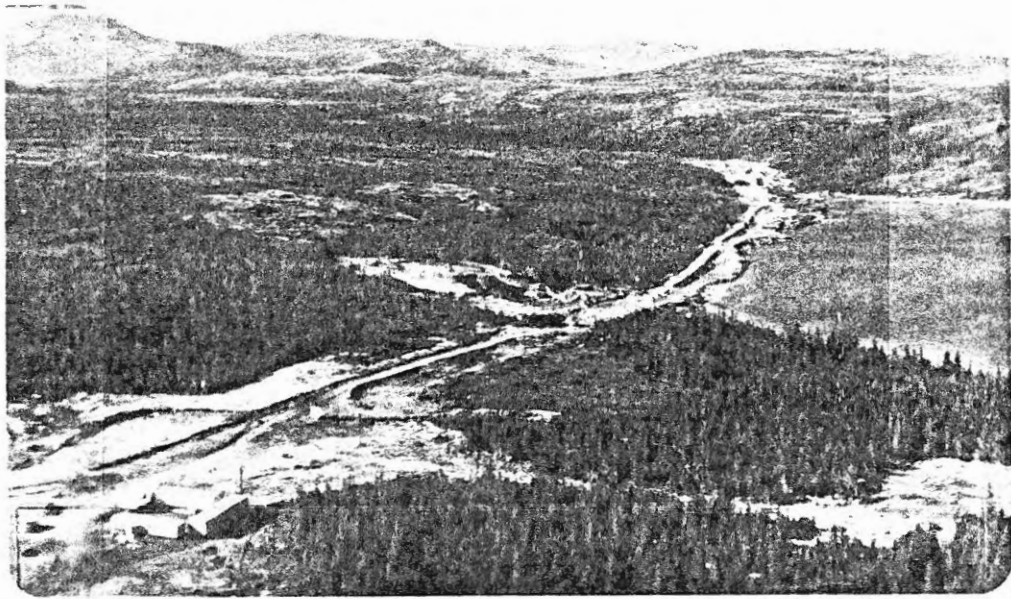


Plate 2.1(a) An oblique aerial view from the northeast showing the gravel pit at the head of Ranger Bight.

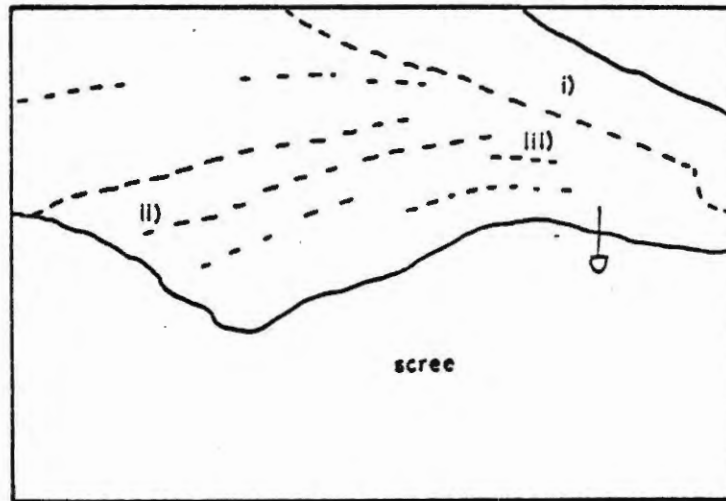
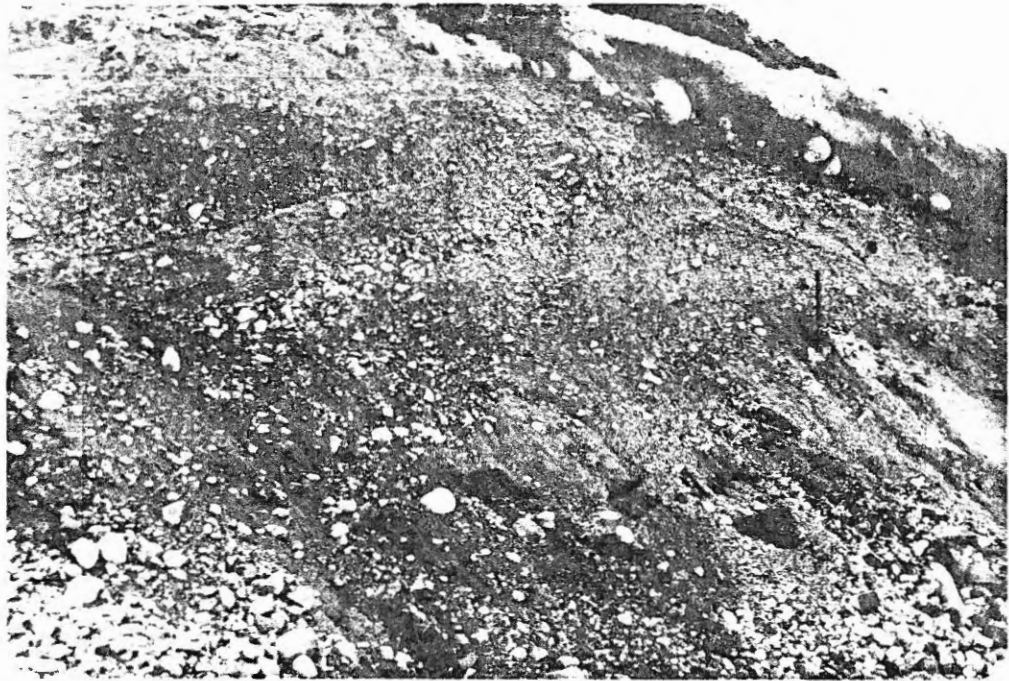


Plate 2.1(b) Exposed section of Ranger Bight gravel pit at west end showing i) well sorted, laminated sand veneer, ii) gravel and sandy gravel strata with dominant eastward dip and iii) with a shallow westward dip

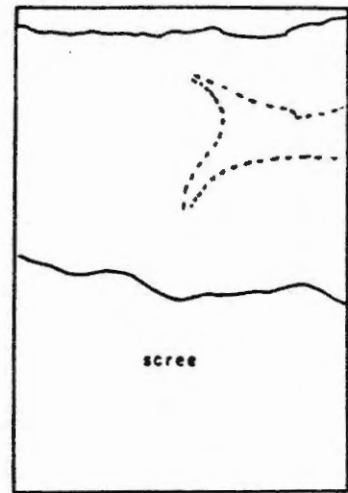
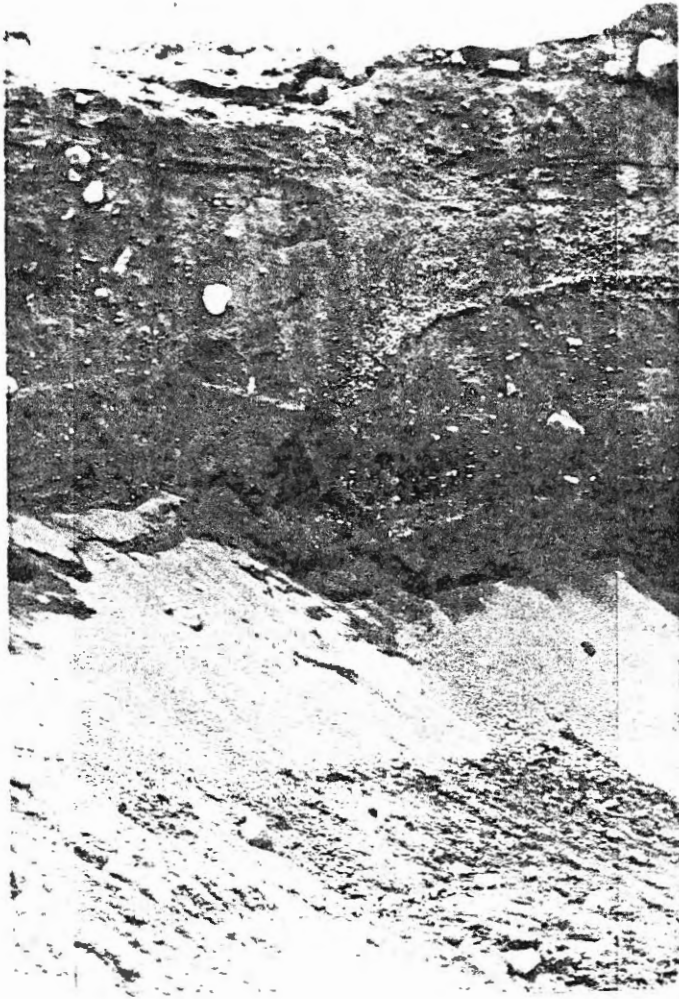


Plate 2.1(c): Ranger Bight kame deposit showing possible ice crevasse filling

The gravelly strata and their highly variable dips suggest that the deposit is a kame delta formed between the bedrock and glacial ice filling the valley. This interpretation is at variance with that of Piper (Piper and Iuliucci, 1978) who interpreted it as a marine delta and subsequently used the topset present position to demarcate the relative sea level. However, the unconformable veneer of laminated sand is probably a nearshore deposit reworked by a relatively long fetch, suggesting marginal marine influence. Therefore it is suggested that the proglacial marine transgression was at least 40 metres above present sea level in Ranger Bight.

A second raised deltaic deposit, located at Burntwood Point, was studied briefly. Plate 2.2 is a view looking southwards showing sandy foresets dipping ( $\sim 20^\circ$ ) down bay. Two earlier wave cut terraces are clearly observable and, upon close inspection, are covered with an armouring veneer of well-rounded cobbles, similar to the armour of eroded drumlins of Nova Scotia (Barnes, 1976; Letson, 1980). A contemporary wave cut terrace is eroding and destroying former wave cut terraces.

These terraces suggest at least three relative sea level stillstands, the contemporary one probably being the longest in duration, judging by the extent of the platform and the relative proportion of cobble armament.

The third major deltaic deposit is located at the head of Makkovik Harbour (Fig. 1.1). It is exposed as a downbay facing bluff with a basal-armoured platform (Plate 2.3 a). A stiff grey marine clay exists in the intertidal zone along the outer finges of the delta and presumably underlies it. The delta is composed of downbay dipping (ca.  $025^\circ/08-17^\circ N$ ) sandy foresets with well laminated sandy to clayey horizons and occasional small





Plate 2.2: View of Burntwood Point raised delta showing at least 2 older wave-cut terraces, one presently being obliterated by the contemporary wave action



Plate 2.3(a): Side view of raised Makkovik Harbour delta displaying a basal armoured platform, steep sandy foresets and a coarse upper horizon with a veneering vegetated mat

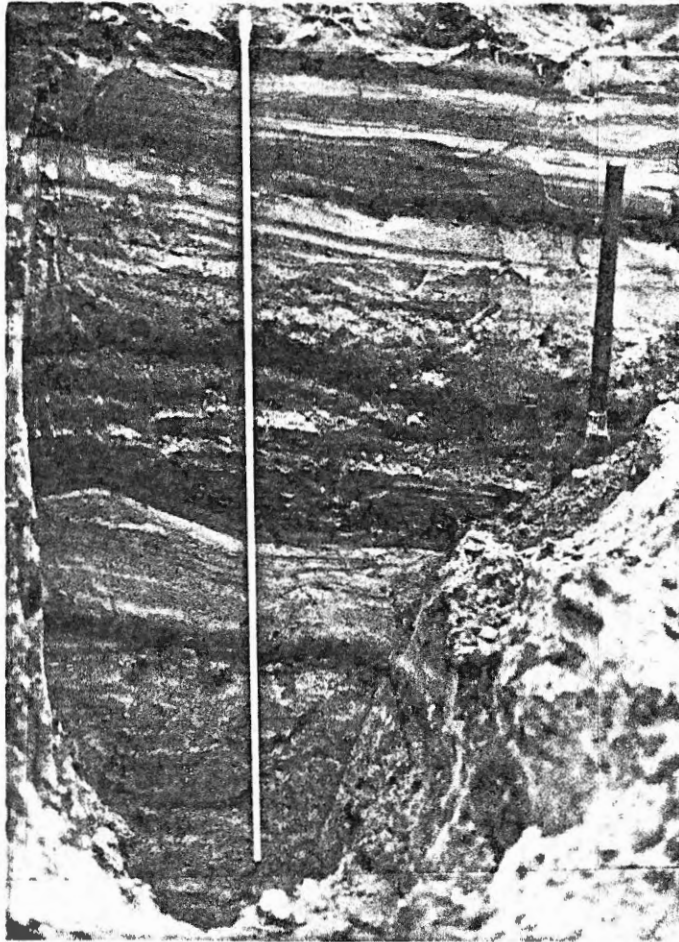


Plate 2.3(b): Close-up of basal steep sandy foresets



Plate 2.3(c): Close-up of diamictite, upper unit resting abruptly on sandy foresets *resting*

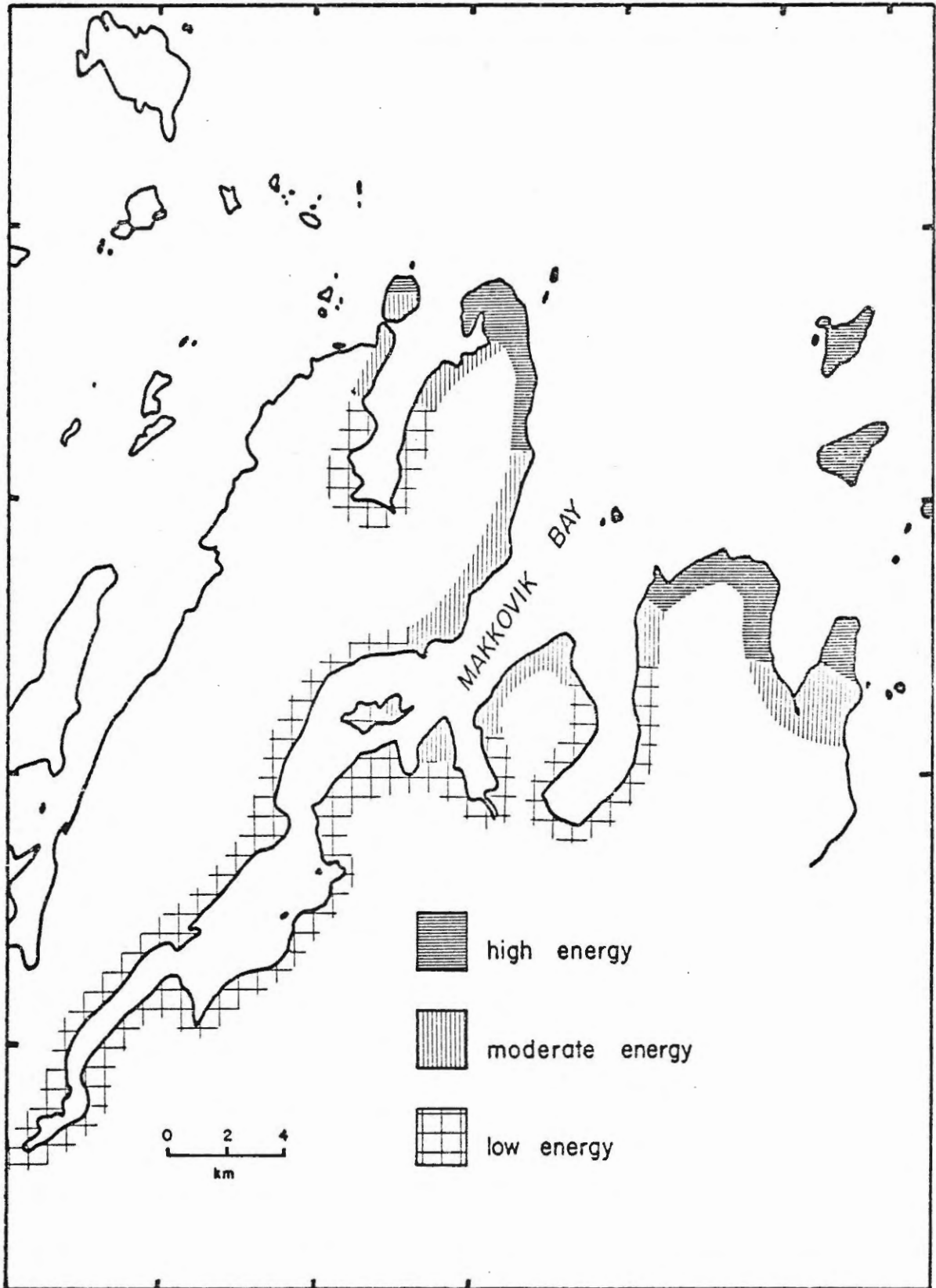


Figure 2.2: Classification of contemporary shoreline energy levels according to height of the wave wash zone. (Rosen, 1979a)

and isolated cobble beaches at the heads of structural embayments.

Low-energy shorelines have a wave-wash zone of less than 2 metres, occur in the protected inner bays, and are characterized by narrow sandy beaches or fringe marshes and a nearly continuous intertidal platform.

The moderate energy shorelines are transitional, consisting of rocky headlands, with pocket cobble or sandy beaches and occasional intertidal platforms.

Five intertidal platforms were examined during this study, all within protected areas of the Outer Bay. In each case, a stiff grey clay was overlain by an inner sandy beach at the high tide level and by scattered boulders across the platform, often piled into a boulder barricade at the low tide level. The origin of these barricades has been the topic of long debate (Lyell, 1862; Daly, 1902; Tanner, 1939; Ward, 1959; Liken, 1962; Bird, 1964; Rosen, 1979 a, 1979 b). The boulders are generally thought to have been derived from glacial till within eroding headlands, transported by ice rafting, and deposited strategically at the edge of the intertidal platform where ice cakes were grounded.

The nature of the platform veneer depends upon the energy of the shoreline, and the availability and type of sediment. In general, the sand veneer tends to increase in thickness in the protected bays. The completely sand-covered intertidal zones of the Inner Bays are presumed to be underlain by the same grey clay. Streams emptying into the Outer Bay debouch sandy, fan-shaped prisms over the platform. Plate 2.4 shows the intertidal flat at the head of Rangers Bight with a muddy veneer derived from fines



Plate 2.4: View of boulder strewn intertidal platform at the head of Ranger Bight at low tide (c.f. Plate 2.1a) with gravel pit in background

washed down from the gravel pit and Ranger Brook.

The genesis of the intertidal platforms is discussed in Chapter VI.

CHAPTER III

PHYSICAL OCEANOGRAPHY

3.1 Previous Work

There has been no previous work on the physical oceanography of Makkovik Bay; this study was at a reconnaissance level only and by itself has limited oceanographic value. However, by applying oceanographic interpretations from other fjords in Labrador, it is capable of providing a physical oceanographic framework for the construction of sedimentological and paleontological hypotheses. Extensive work has been done on six other fjords along the coast of Labrador by Nutt (1952, 1963) and Nutt and Coachman (1956).

The coastline of Labrador experiences a maximum tidal amplitude of approximately 2 metres, although this can be significantly dampened by the presence of sills and side constrictions. The shallow sill and narrow channel separating Hamilton Inlet from Lake Melville reduce the rise and fall of the tide there, by approximately 75%. Although the tidal amplitude may be quite small in the inner bays of Makkovik, there are often sufficiently strong tidal currents at sill depths to provide energy for vertical mixing of the water column.

Temperature and salinity profiles indicate pronounced annual variations in the structure of the water mass. During the winter there is reduced runoff and generally complete ice cover for up to 6 months of the year. Extensive mixing with the Labrador Current establishes isothermal and



isohaline conditions within the bay. The contributing portion of the Labrador Current is the inner component which is true Arctic water from Baffin Bay and Hudson Strait. Hence, the fjord water is cold ( $< 1^{\circ}\text{C}$ ) and relatively saline (32-33‰) during the winter.

The high runoff in the spring establishes a partially mixed, two-layer, stratified system composed of a warmer, fresh water veneer over a basal pocket of Arctic water. The degree of stratification is directly proportional to the volume of runoff which decreases throughout the summer, and to the restriction of water exchange with the Labrador Current which depends on the sill depth and channel width. Although a unique pocket of cold, saline water remains below the sill depth, it may be replenished by limited exchange with the marine source, especially during high tide. For this reason these fjords do not attain stagnant bottom water conditions during the summer, like the fjords of Norway. Dissolved oxygen contents of 60 to 90% saturation have been measured in Lake Melville, one of the more restricted basins.

During the autumn the intense summer stratification dissipates as the runoff decreases, and with the advent of winter ice cover, well mixed, isohaline, isothermal conditions prevail.

### 3.2 Bathymetry

The bathymetry of Makkovik Bay, as shown on the base map (Fig. 3.1, in pocket), was contoured (Piper and Iuliucci, 1978; Barrie, 1978) from Canadian Hydrographic Services fieldsheets (Makkovik Bay and Approaches, 1958-59). The coastal outline and the bathymetry define three main areas: the

Approaches, the Outer Bay and the Inner Bay (Fig. 1.2).

The Approaches is a broad zone well exposed to the Labrador Sea, except for local protection behind islands. Three prominent elongated basins up to 120 metres deep strike obliquely across the main axis of the fjord, traversing the sill and deeper parts of the Approaches.

The Outer Bay has three major basins and is separated from the Approaches by a wide sill of variable depth, ranging generally from 55 to 15 metres. Three smaller bays are situated on the south coast, parallel to the axes of the elongated basins of the Approaches. These bays and basins have probably been gouged and elongated by glacial action.

The Inner Bay is well protected both by its outline and by the presence of inner sills. It is subdivided into three bays: the Eastern, Central and Western Inner Bays with respective maximum depths of 40, 50 and 20 metres.

Maximum significant wave heights recorded seaward of Makkovik are 7.3 m with 16-second periods (Rosen, 1979a). During August 1978 the largest waves in the Outer Bay were estimated visually to be 2 metres. At that time only small waves (approximately 0.5 metres) were experienced in the Inner Bays (pers. comm., R. Iuliucci). In comparison, the annual, largest significant wave height for the coast of Labrador measured during 1976-1977 was 9 metres (Neu, 1979).

### 3.3 Physical Oceanographic Measurements

A tidal staff in Makkovik Harbour indicated a variation of tidal range from about 1.5 metres during early August 1978 to about 2.2 metres just past mid-month.

Crude drogue measurements were made on the western side of the constriction at Burntwood Point where the water is 25 to 30 metres deep during a strong westerly wind and a full ebb tide of normal range. These measurements indicate surface water outflow from the Western Inner Bay at approximately 10 cm/sec at 6-metres depth, and 6 cm/sec at 12-metres depth. Much lower values would be expected along the bottom. Under normal conditions, runoff and tidally-induced currents thus do not appear strong enough to sustain erosion in the Western Inner Bay basin. However, erosion may occur at the bay constrictions where the tidal flow is presumably funneled.

Temperature, conductivity, and hence salinity, were measured at 5-metre intervals at 7 stations (Fig. 3.1), from the Outer Bay to the Western Inner Bay using a Beckman RS-5 sensor. Temperature, salinity and density as  $\sigma_T$  (calculated according to Knudsen, 1901) for August 10th, 1978, are shown in Figure 3.2. All values are an average of up and down measurements.

The temperature profile (Fig. 3.2a) shows two major features: a stable stratification throughout the bay and a slight warming of the surface water at the head of the bay, reaching a maximum of approximately 10°C. Downbay this warming trend is partially obstructed by bay constrictions producing step-like gradients in the otherwise horizontal isotherms.

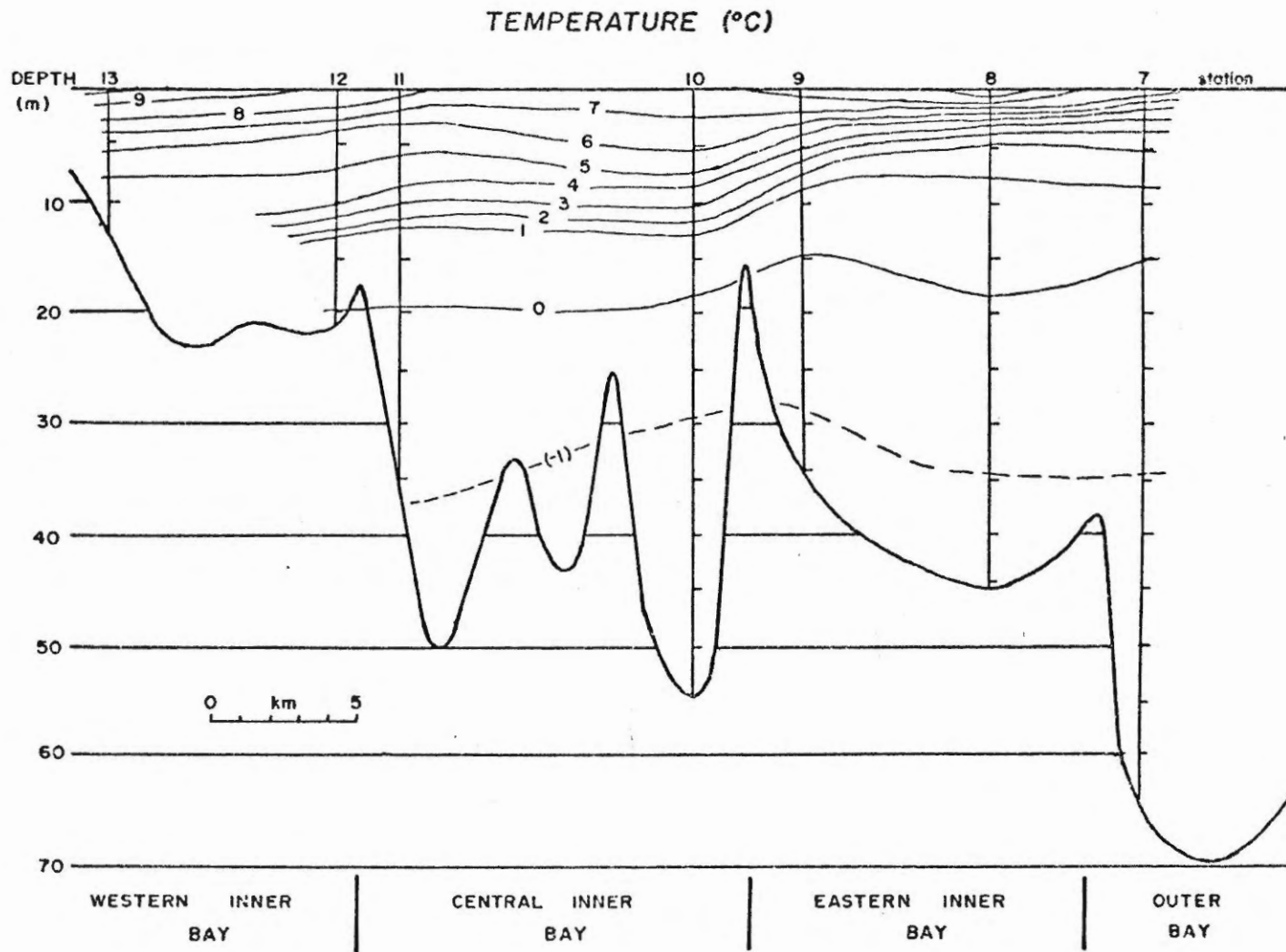


Figure 3.2(a): Downbay water temperature ( $^{\circ}\text{C}$ ) profile for August 10, 1978, during ebb tide. Parenthesized values are crude estimates since the sensor is not capable of detecting negative temperatures.

The sensor was not capable of measuring negative temperatures; however, from extrapolations of the temperature profile combined with estimates from salinity and conductivity trends, a temperature of approximately  $-1^{\circ}\text{C}$  is estimated for water depths of about 40 meters.

The salinity ( $\text{‰}$ ) profile in Figure 3.2b shows similar trends. The warm fresh water wedge of the Western Inner Bay dissipates primarily horizontally downbay in a step-like fashion. Vertical mixing is strongly impeded by the stable stratification.

The density ( $\sigma_{\text{T}}$ ) profile in Figure 3.2c shows similar stratification throughout the bay. The warm water at the head of the bay has a low density, veneering the Western Inner Bay with a sharp pycnocline. As with the temperature and salinity changes, the low density water dissipates primarily downbay in a step-like fashion. The changes in vertical gradient suggest that the zone of mixing between the upper fresh water and the lower isothermal, isohaline "marine" water occurs at about 5 metres depth in the Eastern Inner Bay and between 5-20 metres depth in the Central Inner Bay.

#### 3.4 Suspended Sediment

Six water samples were taken at a total of three stations during flood tide, using 12 l Niskin GO Flow bottles, then pressure filtered using a maximum of 5 p.s.i. onto 4.7 cm Nuclepore polycarbonate membranes (Sundby, 1974). The dried membranes were weighed on an electromicrobalance in a dust-free laboratory at Bedford Institute of Oceanography. Analytical error is conservatively estimated at approximately  $\pm 0.08 \text{ mg/l}$ . The

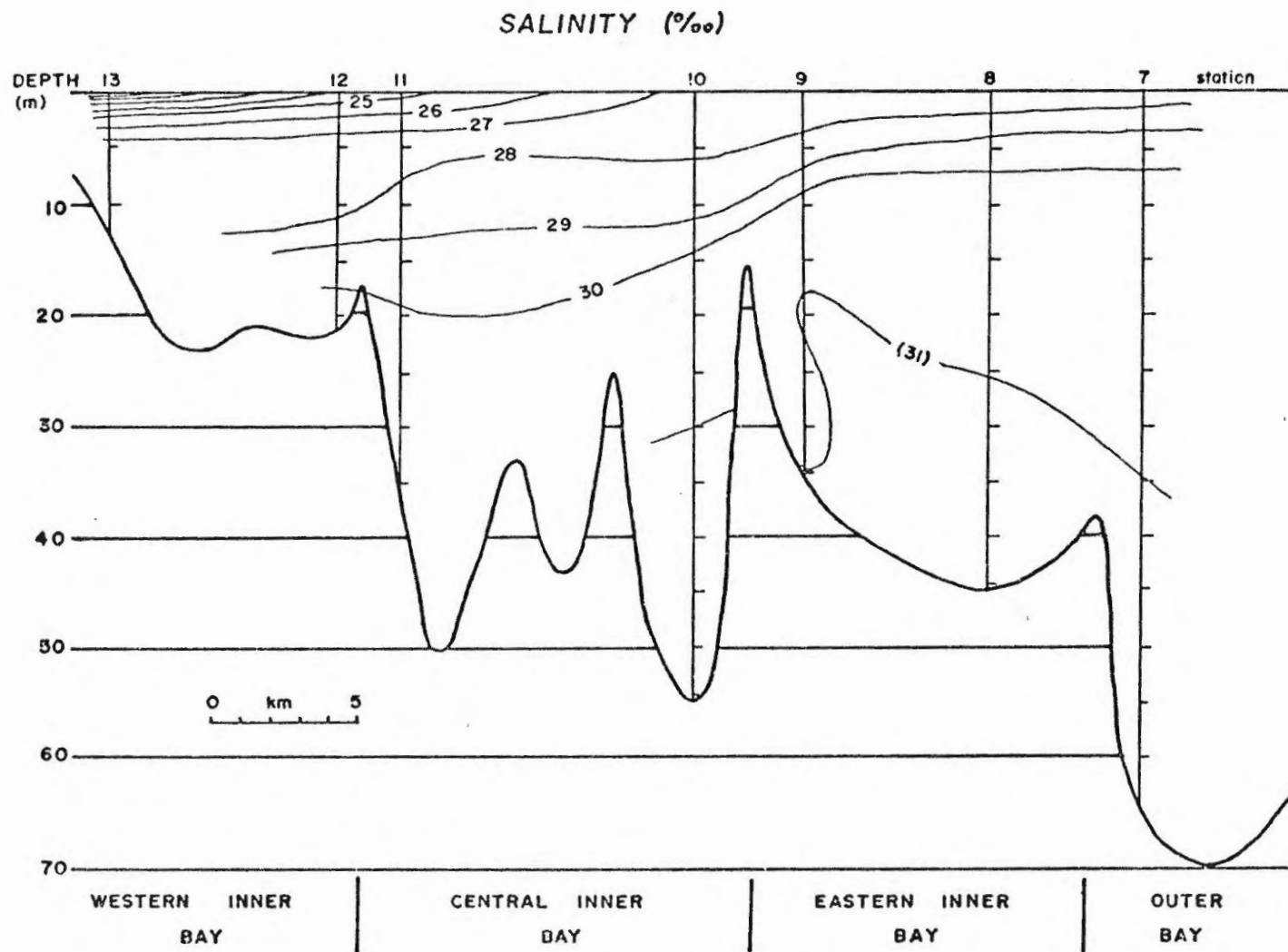


Figure 3.2(b): Downbay water salinity (‰) profile for August 10, 1978, during ebb tide. Parenthesized values are approximate since the sensor could not be adjusted to negative temperatures.

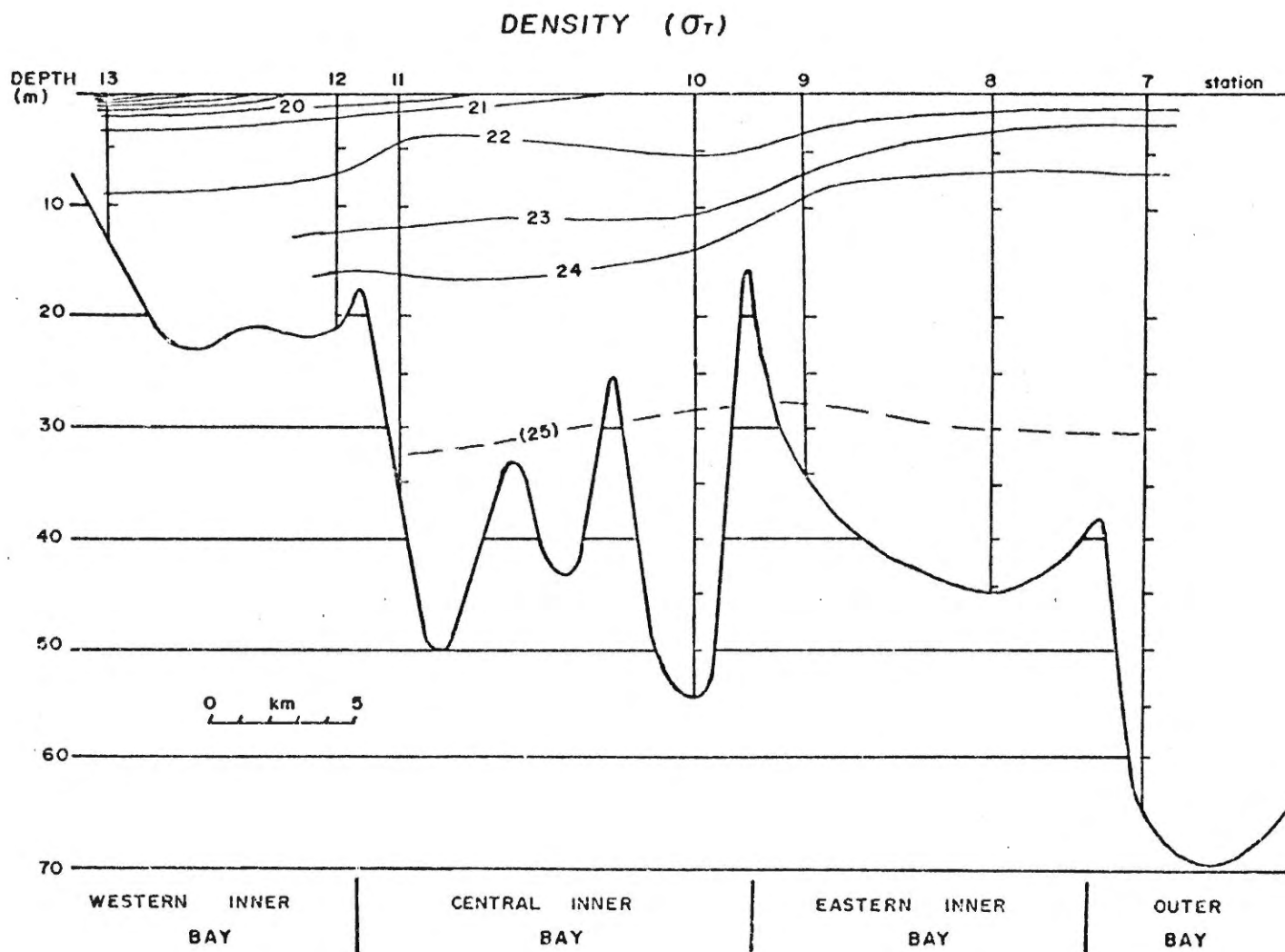


Figure 3.2(c): Downbay profile of density ( $\sigma_T$ ) profile for August 10, 1978, during ebb tide. Parenthesized values are approximate since negative temperatures are not available.

results are plotted in profile in Figure 3.3.

Microscopic examination of the Western Inner Bay samples revealed primarily organic material, buff-coloured "flocs" and clay-size material. The Outer Bay samples had dominant quartz and feldspar silt and minor floc material. The Central Inner Bay samples had an intermediate composition.

The concentration of suspended material normally varies directly with depth (e.g., Biggs, 1970). In the Outer Bay there is a 29% increase in weight from 40 to 60 metres depth. Extrapolating upwards gives 2.5 mg/l of suspended sediment at 20 metres depth.

In the Western Inner Bay there is an increase of 154% from 8 to 18 metres depth. There is significantly more suspended material in the Western Inner Bay than the Outer Bay at either the same depths or the same relative positions.

However, values from the Central Inner Bay indicate a reversed vertical situation, as there is a decrease of 42% from 30 to 50 metres. The suspended sediment value at the bottom is significantly less than the basal values from the Western Inner Bay and the Outer Bay.

### 3.5 Sediment Traps

There is general skepticism regarding the results of sediment traps. These include:

- (1) the presence of traps influences the adjacent currents, thereby affecting the rate of sediment deposition;



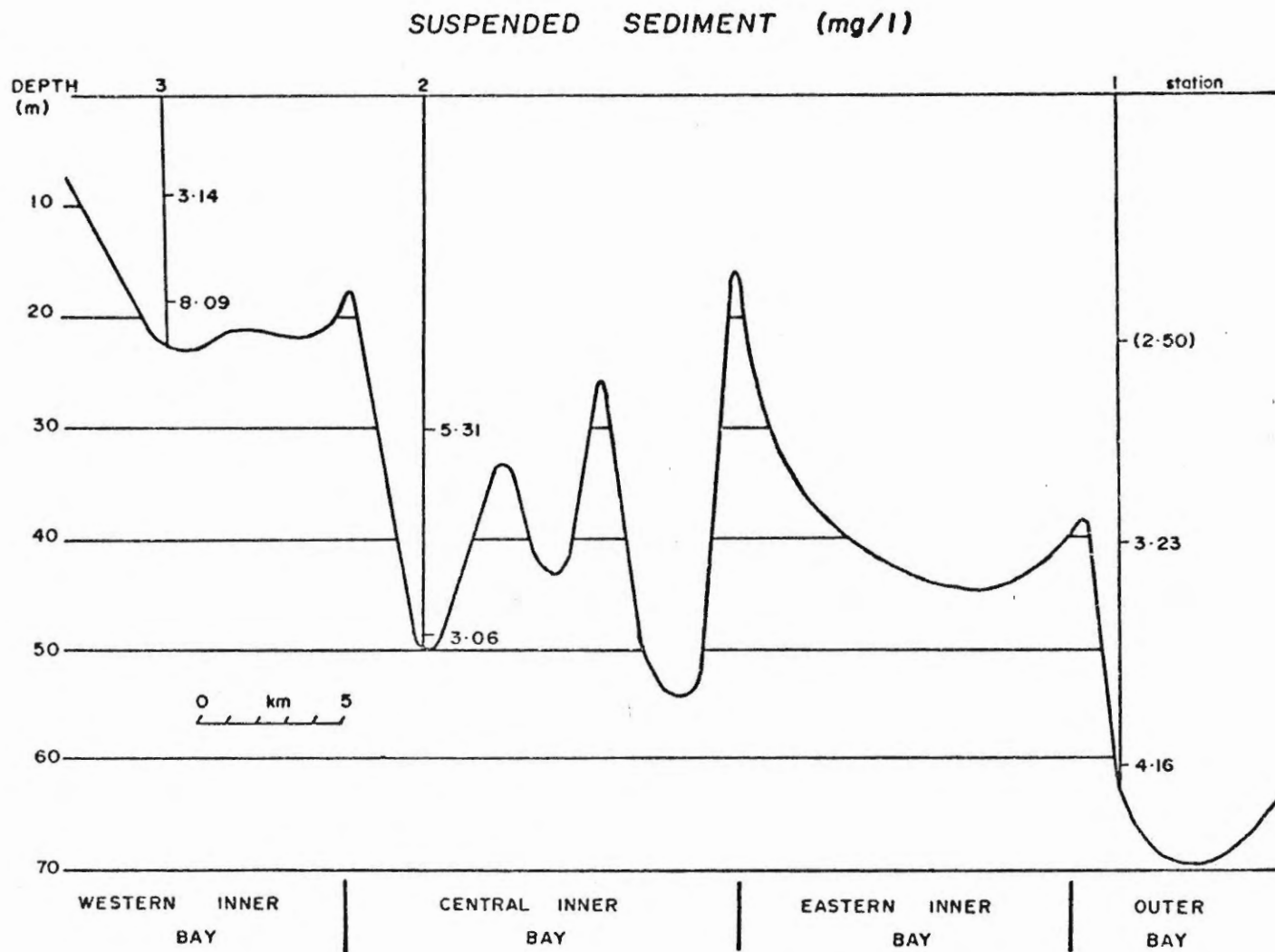


Figure 3.3: Downbay profile of suspended sediment as mg/l.  
 Parenthesized values are extrapolated.

- (2) particulate motion has vertical and horizontal components therefore a horizontal trap may not be representative of the sea floor;
- (3) suspended sediment may include resuspended sediment from the sea floor and therefore would not represent net deposition;
- (4) the quiet conditions within the trap would artificially increase the rate deposition of fine-grained sediments;
- (5) short-term results do not necessarily represent annual values.

In spite of these dynamic problems, meaningful estimates of net and gross sedimentation have been made in sheltered basins (e.g., Hargrave et al., 1976). Sediment traps are used in this study to provide a crude estimate of the sedimentation rate.

Twelve sediment traps were constructed (according to B. Hargrave, pers. comm.) and suspended on two mooring lines, one in the Outer Bay and one in the Western Inner Bay, for a period of 17 days. Each mooring had 2 sets of 3 traps, one set suspended 5 metres off the bottom and one set 10 metres below the thermocline. Because of the shallow depth in the Western Inner Bay, the upper trap was placed just above the base of the thermocline. The traps were constructed from a 10.7 cm I.D., 60 cm long plastic pipe held vertically by a holder clamped to a taut, vertical mooring line, as shown in Figure 3.4.

Immediately after retrieval, the upper two-thirds of the water column was decanted to remove the "suspended" sediments and the remaining sample

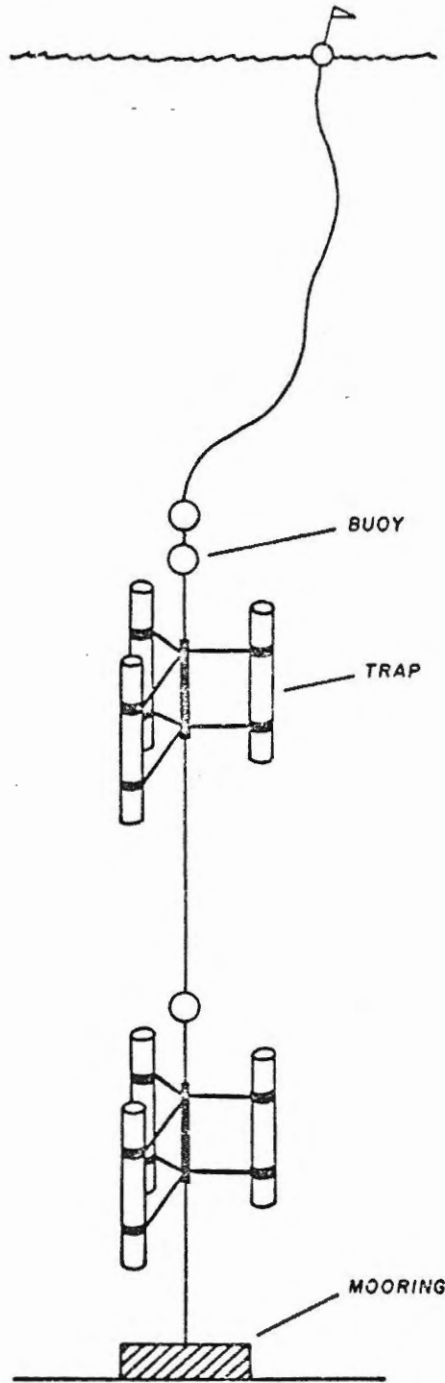


Figure 3.4: Sketch of sediment trap operation

was poisoned and bottled. These samples are desiccated and weighed in the laboratory. The dried sediment was calculated as the number of grams of sediment that would pass through one square metre per day (Hargrave et al., 1976). Two individual measurements were ignored, one due to contamination from the boat during retrieval and one due to an anomalously high standard deviation (see Appendix). The data are presented in Figure 3.5;  $2.5 \pm 4\%$  and  $8.0 \pm 15\%$  gm of sediment settled through 1 square metre per day in the basinal areas of the Western Inner Bay and the Outer Bay respectively during the period of measurement.

### 3.6 Discussion

The temperature, density and salinity profiles are very similar to those of Hebron fjord (latitude  $58^{\circ}10' N$ ) and other nearby fjords at the same time of the year (Nutt, 1952; Nutt and Coachman, 1956) and therefore similar oceanographic processes are suggested for Makkovik Bay. During the six months of ice cover virtually isohaline conditions should prevail within the fjord. With the melting of snow and ice in May, a large quantity of fresh water is introduced to the surface layers of the fjord. This spring freshet terminates the winter convections and establishes a stable density stratification. The fresh water wedge responds to the volume inflow of fresh water which decreases throughout the summer. The very bottom of the fjord essentially remains as an isolated pocket of cold, saline water (high Arctic type environment, c.f. Nutt, 1952) during the winter and summer as contrasted with the warmer (low Arctic) conditions that prevail outside the fjord in the summer.

### SEDIMENT TRAP ACCUMULATION ( $\text{g}/\text{m}^2/\text{day}$ )

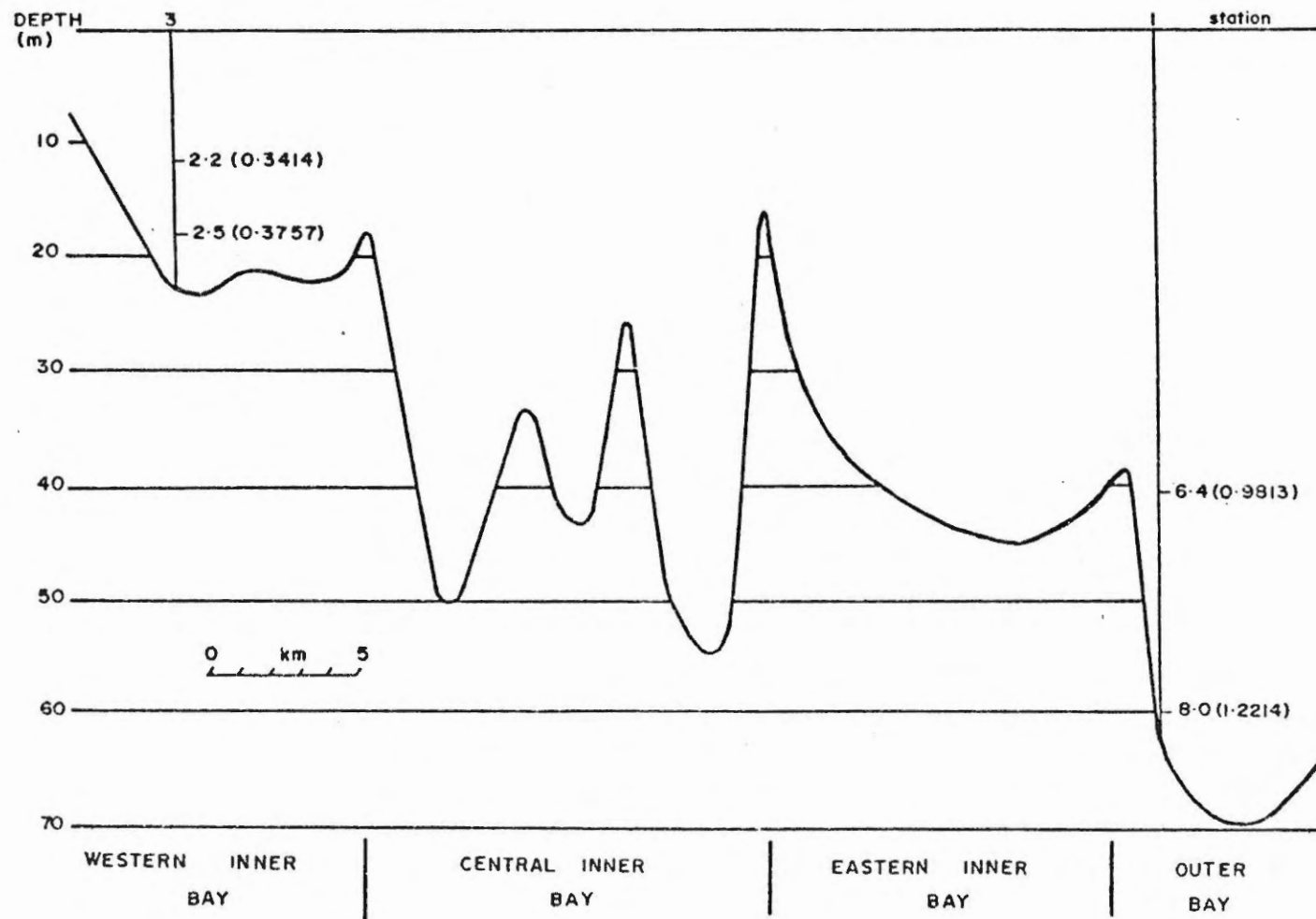


Figure 3.5: Downbay profile of sediment accumulation by sediment traps during 17 days expressed as grams of total dried mass and as  $\text{g}/\text{m}^2/\text{day}$

Key: (0.3414) - g, total mass; 2.2 -  $\text{g}/\text{m}^2/\text{day}$

The temperature and salinity distributions match those of dynamically active fjords in the sense that fresh water supply is sufficient to create an estuarine, circulation flow in the upper strata. The decreasing, step-like fashion of the stratification downbay is similar to types 1 and 2 active fjords according to Pickard (1961). Type 1 is a two-layer-type estuary with a fresh water veneer. Type 2 is a partially-mixed type estuary with a brackish veneer, similar to Makkovik Bay. According to Pederson (1978), a fjord has a tendency to change from type 1 to 2 when:

Geometry: Length/outlet depth increases (i.e. increases tidal-generated velocity and hence mixing). Width of outlet section increases (i.e. decreases critical depth and hence decreases the layer depth).

Hydrology: Fresh water discharge decreases (i.e. decreases the critical depth and hence decreases the layer depth).

Ocean. cond.: Tidal amplitude increases (i.e. increases tidal-generated velocities and hence mixing).

Wind field: Wind velocity increases (i.e. increases mixing).

All of these aspects appear to be applicable to the Makkovik Bay situation. Substantial reduction in tidal amplitude by side and sill constrictions has been recorded for other Labrador fjords (Nutt, 1963); hence it is suggested that the constriction at the Narrows, separating the Outer and Inner Bays, significantly dampens the tidal amplitude, reducing the degree of mixing in the Inner Bays.

As a consequence, there is a greater column of dense, saline water on the marine side of the sill, with a horizontal gradient decreasing

upbay at the sill depth. Therefore, the marine water was probably flowing inward over the sill into the Inner Bay, and may eventually flush the basin with cold, marine water. Although no data was collected out over the outer sill, the same processes are thought to occur from the Approaches to the Outer Bay.

In order to indicate the relative concentration of suspended particulate matter, the ranges from other localities are listed in Table 3.1. This brief comparison indicates that Makkovik Bay concentrations are well below the order of the high suspended sediment loads such as those found in the Fraser River Estuary but substantially above those values from open bays such as the Gulf of St. Lawrence. In general, these values suggest that Makkovik Bay, and hence Makkovik River have a low sediment yield similar to most other river-estuarine systems of the Atlantic Provinces.

The composition and distribution of the basal-suspended sediments of the three basins in Makkovik Bay suggest a simple explanatory hypothesis for the contemporary environment and the sediment source. The highest value (8.09 mg/l) was taken in the Western Inner Bay which is relatively shallow, well protected and close to the mouth of Makkovik River. Floccs form the dominant-suspended sediment component, presumably flocculated from fluvial-suspended matter. Probably, some proportion is composed of resuspended bottom sediments since the shallow depths effectively increase the influence of the wave disturbance.

The Central Inner Bay has the lowest basal value of suspended sediment while that of the Outer Bay is intermediate. Using the same reasoning as above, the Central Inner Bay low can be explained by the lack of influence both of

Table 3.1: Table of Comparative Suspended Particulate Matter (SPM) Values from Other Localities

Location	Time of Measurement	SPM (mg/l)	Reference
River Tay Estuary	2 tidal cycles	5-150	Sholkovitz, E.R, 1979
Fraser River Estuary	August	5-30	Grieve, D. and Fletcher, K., 1977
Northern Chesapeake Bay	"Upper" 2 1/2 years "Lower"	approx. > 20 approx. 0-20	Biggs, R.B., 1970
Miramichi Estuary	September	approx. 0.1-25	Winters, G. et al., 1978
Makkovik Bay	August	2-8	This study
La Have Estuary	September	1-5	Cranston, R.E. and Buckley, D.E., 1972
Gulf of St. Lawrence	April/May	0.1-3.3	Sundby, B., 1974
Gulf of Maine	Sept. 1966, March 1967, October 1967	0.1-1.1	Spencer, D.W. and Sachs, P.L., 1970



fluvial/marine flocculation and of a high-energy environment. The Outer Bay is considerably more exposed to waves and wells capable of resuspending bottom sediments along the flanks of the bay. These processes and their effects are illustrated in Figure 3.6.

Using estimates of wave size, it is possible to calculate theoretically the influence of wave action on the basinal muds (Komar and Miller, 1974). This calculation is shown graphically in Figure 3.7. An estimated maximum wave height of 2 metres ( $T = 15$  sec.) in the Outer Bay would mobilize mud at a depth of about 90 m, well within the station depth. Similarly an estimated 0.5 metre wave (with  $T = 15$  sec.) in the Western Inner Bay would influence mud to a depth of 20 metres, the approximate station depth. However, the waves of the Central Inner Bay are only marginally larger, approximately 0.75 m, and therefore would be able to influence sediments only down to about 30 metres. Therefore these crude estimates are consistent with the hypothesis offered by the suspended-sediment data.

These estimates can also explain the high value at 30 metres depth in the Central Inner Bay, since the estimated depth of wave influence on the bottom mud is approximately 30 metres. This suggests that the major portion of suspended sediment is resuspended from along the flanks. Presumably, entrainment into the mixing horizon between the two water masses or into the intense stratification prevented the suspended matter from settling to the bottom of the basin during the time of measurement. Within partially mixed estuaries the nontidal estuarine circulation operates to concentrate suspended sediment at the landward margin of the salt wedge and along the upper part of the halocline (Meade, 1972). In addition, some proportion

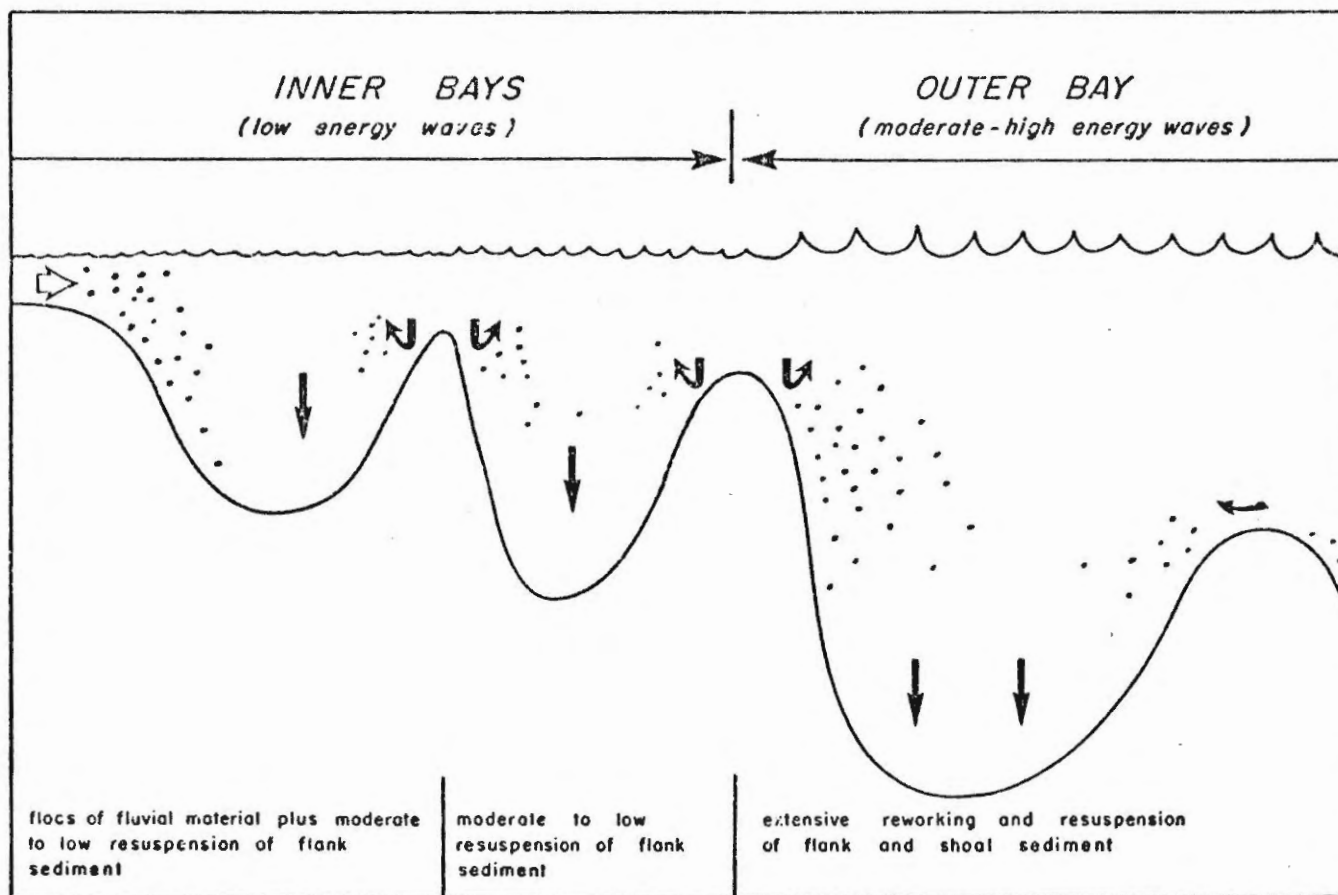


Figure 3.6: Hypothetical explanation for the distribution of near bottom suspended sediment concentration. (Not to scale.)

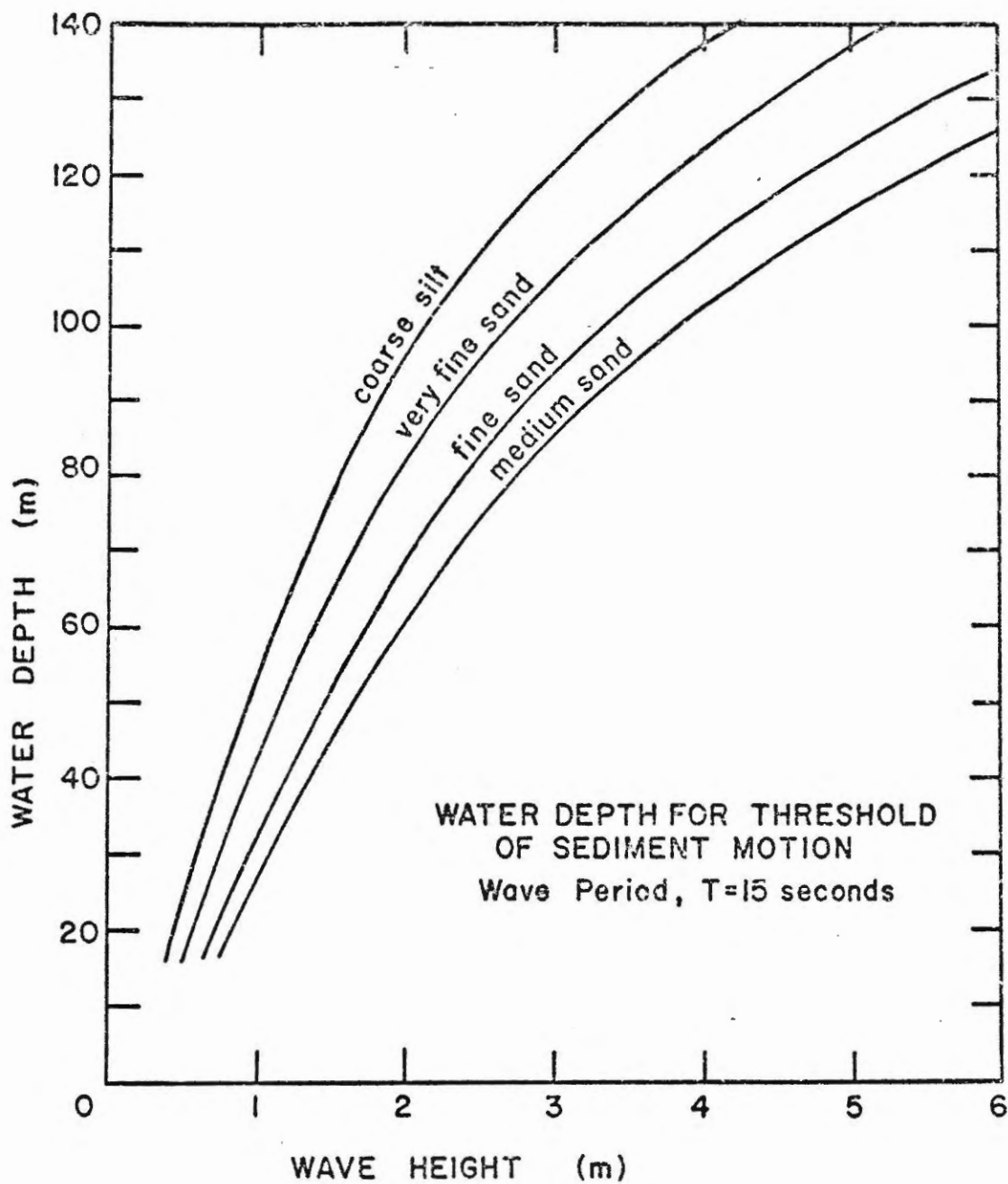


Figure 3.7: The water depth to which the sediment grain sizes shown can be placed in motion by waves of period 15 seconds. (From Komar and Miller, 1974.)

may be derived from the Western Inner Bay as spillover past the sill; however, such a process would have to act against the estuarine circulation and against the basal inflow of saline water.

Sediment trap data collected periodically over 2 years on Bedford Basin, Nova Scotia (Hargrave et al., 1976) indicate a range of  $1-3 \text{ g.m}^{-1} \text{ day}^{-1}$  with up to 35% organic content (phytoplankton, zooplankton) during August. The results from Makkovik Bay range from  $2-8 \text{ g.m}^{-1} \text{ day}^{-1}$ . Furthermore, presumably there is less primary production in the cooler waters of Makkovik Bay. This, combined with the suspended sediment distribution, suggest that resuspension of bottom flank sediments is an important source of sediments. The results of the Western Inner Bay are similar to those of Bedford Basin; however, those from the Outer Bay are higher by 12-40%, suggesting an increased influence of resuspended sediment.

The absolute values of an instantaneous measurement such as concentration of suspended material cannot be compared directly with a time lapse measurement such as sedimentation rate; however, their ratio may have some meaningful implications. Table 3.2 lists their values and their ratios. The similarity of the ratios within the Outer Bay profile suggest that the sediment traps may be measuring the suspended sediment, to a significant extent, which is interpreted to be primarily resuspended sediments from the flanks. However, with these data it is impossible to determine what proportion of the resuspended sediments is redistributed to the deep basins beyond the influence of further wave action.

Some information may be gleaned from a comparison of the relative values of these two types of measurements. Using the near bottom values

Table 3.2: Relationships Between Sediment Trap and  
Suspended Sediment Data

	Depth Density (m)	<u>A</u> Suspended Sediment (m g/l)	<u>B</u> Sediment Trap (g/m <sup>2</sup> /day)	B/A
Western Inner Bay	8*	3.2	2.2	0.7
	18	8.1	2.5	0.3
Outer Bay	40	3.2	6.4	2.0
	60	4.2	8.0	1.9

\*Taken above the thermocline

only, it can be seen that the Western Inner Basin has much greater suspended material but less deposited sediment than the Outer Bay. This reinforces the hypothesis that the suspended material is maintained at its equivalent water horizon at the head of the fjord.

Oceanographic data provide credence to the sediment trap data on two accounts. Firstly, the quiet, stable well-stratified condition of the fjord during the period of measurement minimizes some of the hydrodynamic problems and sedimentological variations associated with sediment trap measurements. Secondly, the period of measurement was during an intermediate stage, not during the spring freshet nor the winter isohaline conditions. This allows a better extrapolation to obtain an annual rate of sedimentation. These gross rates are  $913$  and  $2920 \text{ g.m}^{-2} \text{ yr}^{-1}$  for the Western Inner Bay and the Outer Bay respectively. Assuming an average density of  $1.7 \text{ g.cm}^{-3}$  for recent sediments the gross rate of sediment accumulation becomes  $53 \pm 2$  and  $172 \pm 32 \text{ cm } 1000 \text{ yr}^{-1}$  respectively. The error margins are estimated from the respective standard deviations (see Appendix).

These values are comparable to those of Nova Scotian bays (Table 3.3) where shoreline erosion of till (during the present relative rise in sea level) is the most important source of sediment (Piper and Keen, 1976).

Table 3.3: Comparison of Sedimentation Rates  
from Other Localities

Locality	cm/1000 years	Reference
Miramichi River Estuary	360-1200	Scott, D.B. et al., 1977
St. Margaret's Bay	150	Piper, D.J.W. and Keen, M.J., 1976
St. Margaret's Bay	104	Rashid, M.A. and Vilks, G., 1977
Grand Manan Basin	57-134	Rashid, M.A. and Vilks, G., 1977
Makkovik Bay	50-170	This study
Beaufort Shelf	3-30	Vilks et al., 1979
Mackenzie Canyon	100	Vilks et al., 1979
Beaufort Continental Margin	20-30	Vilks et al., 1979
Cartwright Saddle	36	Vilks, G., in press

CHAPTER IV

ACOUSTIC STRATIGRAPHY

4.1 Physical Guidelines for High Resolution Acoustic Stratigraphy

High resolution profiling is a commonly used method for obtaining a concept of the sedimentary strata. The physical aspects are well known and are described in textbooks (e.g. Dobrin, 1976; McQuillin and Ardu, 1977) and journals (e.g. van Overeem, 1978) but the actual method of interpretation is somewhat of an art and consequently very little has been written on the subject. King (1967) has correlated surficial samples with echograms to delineate the bottom textures plus some minimal stratigraphic relationships. Based on the correlation between high resolution seismology and piston core sedimentary lithologies, Dale and Haworth (1979) suggested that in general, the seismic character with limited core control can provide sound lithological mapping. Other studies have distinguished sedimentary units directly from acoustic reflection profiles, sometimes with surface samples (van Weering et al., 1973; Grant, 1975; van Weering, 1975; Bornhold, 1977; Howells and McKay, 1977).

An original technique of data synthesis is used here in order to reduce the inherent subjectivity of acoustic profile interpretation and mapping. This is preceded by a discussion of the physical aspects to act as guidelines in the interpretation of shallow water acoustic profiles.



### Equipment

The system used in this study consisted of an over the side Ocean Research Equipment (ORE) acoustic profiling unit coupled with an EPC nineteen inch analogue recorder. The controls were maintained at 3.5 kHz frequency, 10 kw power and, on the recorder, an 0.25 second sweep.

### Propagation of Sound

Propagation of sound in water is approximately 1500 m/sec; the variations with temperature, pressure and salinity are only a few percent and are considered negligible. Generally the speed of sound is faster in rocks and unconsolidated sediments; however, for loosely compacted sediments it may be slightly slower. In six cores of recent sediment measured by Dale (1979), four had velocities of 1500 m/sec throughout most of the core and an increase to over 1600 m/sec near the bottom. Two cores had initial sound velocities of approximately 1450 m/sec. The recorder is calibrated for an assumed velocity of 1500 m/sec, and so for a detailed study, velocity profiles of cores should be used to estimate sediment thicknesses accurately. Without knowledge of the actual velocity profiles it must be borne in mind that the recorded thickness of soupy sediments probably represent a maximum value and those of firm compacted sediments probably represent minimum values.

Propagation loss refers to the total decrease in intensity of sound at a given distance. It is comprised of spreading loss and absorption. Absorption loss in the water column is considered negligible due to the

relatively shallow depths and the high frequency used. Sound spreads in a roughly conical form such that the intensity decreases as the square of distance. Because the depths in Makkovik Bay range from 5 to 130 metres, spreading loss is highly variable throughout the bay.

#### Acoustic Reflection

Reflection of sound from a surface depends upon the specific acoustic impedance of a smooth surface. Smooth surface is taken to mean that the dimensions of roughness should be large compared with the wavelength of the sound pulse (which is approximately 0.4 metres). The specific acoustic impedance is defined as  $\rho c$  where  $\rho$  is the density of the acoustic medium and  $c$  is the speed of sound in that medium. The ratio of incident to reflected wave intensity is known as the reflection loss and characterizes the reflecting surface.

If the dimensions of roughness are of an order of magnitude less than the wavelength of the impinging sound, re-radiation occurs by backscattering in all directions. That portion which is picked up by the transceiver is called backscatter. Backscatter from such a surface is known as surface reverberation and the surface cannot be considered as a true reflector.

If the scatterer is distributed throughout the medium then volume reverberation occurs. Some examples of scatterers causing volume reverberation include local inhomogeneities in temperature and salinity, inorganic and organic particles suspended in the fluid, air bubbles and marine organisms including schools of fish (ORE manual).

In general, the properties of the reflector and the scatterer characterize the intensity of the return for a given sound frequency.

#### Horizontal Resolution and Side Effects

The beam width from the transducer is in the form of a cone projected downwards as a wave front with a beam angle of about  $55^\circ$  for 3.5 kHz. Only the central portion of the reflected ascending wave front will be picked up by the receiver. The part of the irradiated area that is detected is known as the Fresnel zone (Fig. 4a). Within this zone single small objects may be detected but no discrimination is possible; the reflections will be recorded in the form of a hyperbola with the arms pointing to the object. At a depth of 100 metres the Fresnel zone for a 3.5 kHz signal has a radius of 3.5 metres and thus, a horizontal resolution of approximately  $38.5 \text{ m}^2$  for a smooth and level seafloor.

If the bottom is rough some fraction of the energy will tend to be scattered back from the whole area illuminated by the beam (Fig. 4.1b), creating a recorder trace that is wider (longer in time) than the original pulse width. If the reflection is from an object outside the Fresnel area but within the irradiated area and is suitably oriented, it may produce a side reflector which may create an apparent increase or decrease in depth depending upon its location with respect to the signal front (Fig. 4.1c). If the transducer passes over a relatively uniform slope the Fresnel zone will effectively shift to that location where the descending wave front is tangential to the sea floor, thereby decreasing the apparent depth. For this reason slope gradients will tend to be exaggerated.

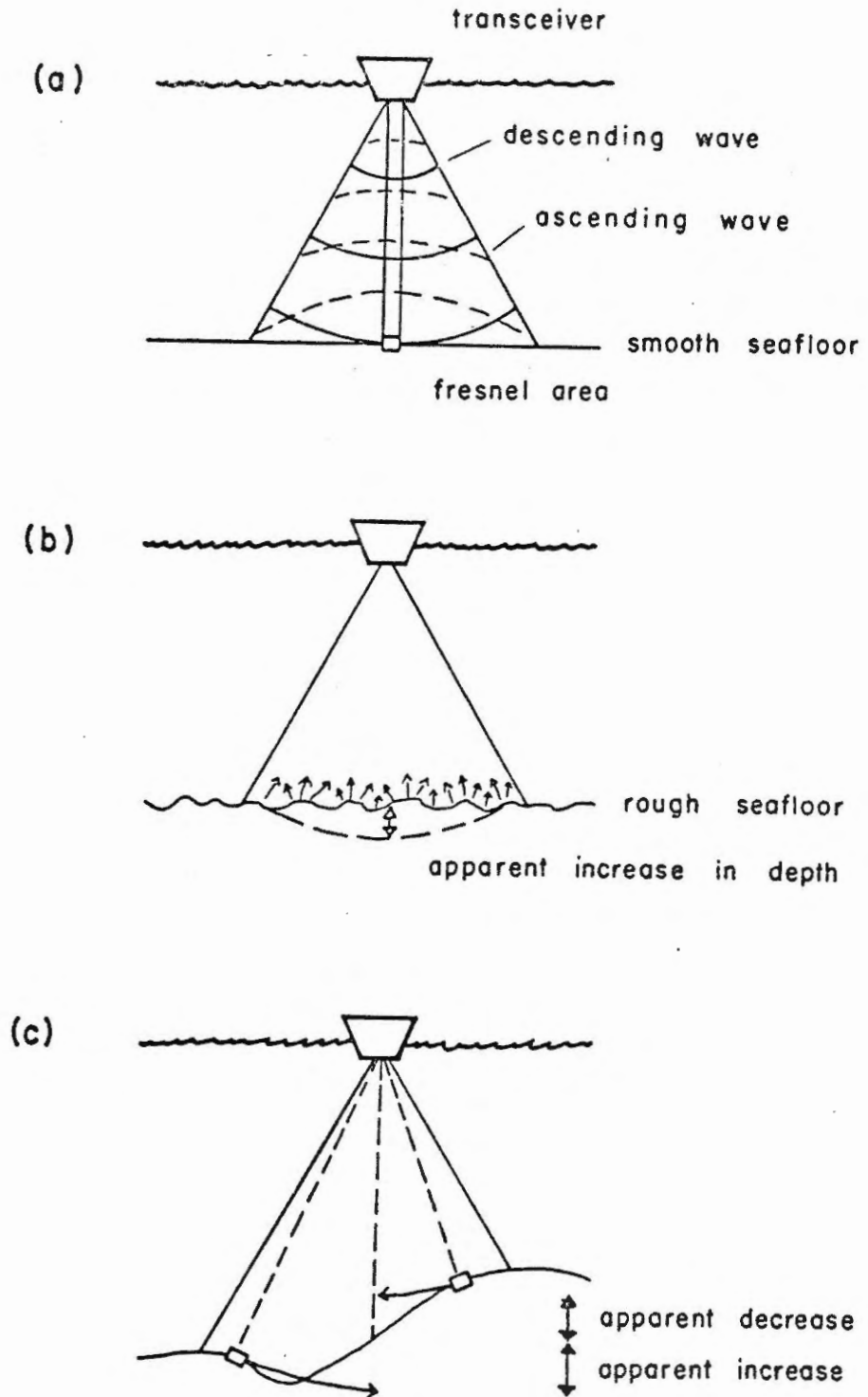


Figure 4.1: Relative effects of sea floor on recorder trace, (a) from a smooth floor, (b) from a rough floor and (c) from side effects

Side effects and slope exaggeration can seriously mislead an uninformed interpreter. Figure 4.2 shows a "terrace-like structure" which, once the user has gained familiarity with acoustic records, is interpreted as a sub-bottom side effect originating from the basement slope from 1149 to 1151/22. Similarly, the steep slope on the west side of the basin (1153 to 1155/22) inhibits any definitive observations regarding the sediment to basement interface.

Multiples occur when the signal bounces repeatedly between the water and bottom surfaces or between different reflectors. The former situation produces a first multiple of the bottom at twice the real depth plus the depth of the transducer. Second- and third-order multiples may occur where the signal strength and reflection are strong (e.g. Plate 4.2).

When the multiples originate between strata, internal multiples appear at successively increasing depths. These are difficult to distinguish from other strata, especially in the 3.5 kHz system where the pulse is long and poorly defined.

#### Vertical Resolution

Vertical resolution is controlled primarily by the length and shape of the acoustic pulse. The upper and lower interface of a bed can be determined until their separation decreases to approximately 1/8 of the wavelength (Widess, 1973). For the 3.5 kHz system this limit is approximately 5.4 cm. Beyond this, interference occurs and the two interfaces are seen as one.

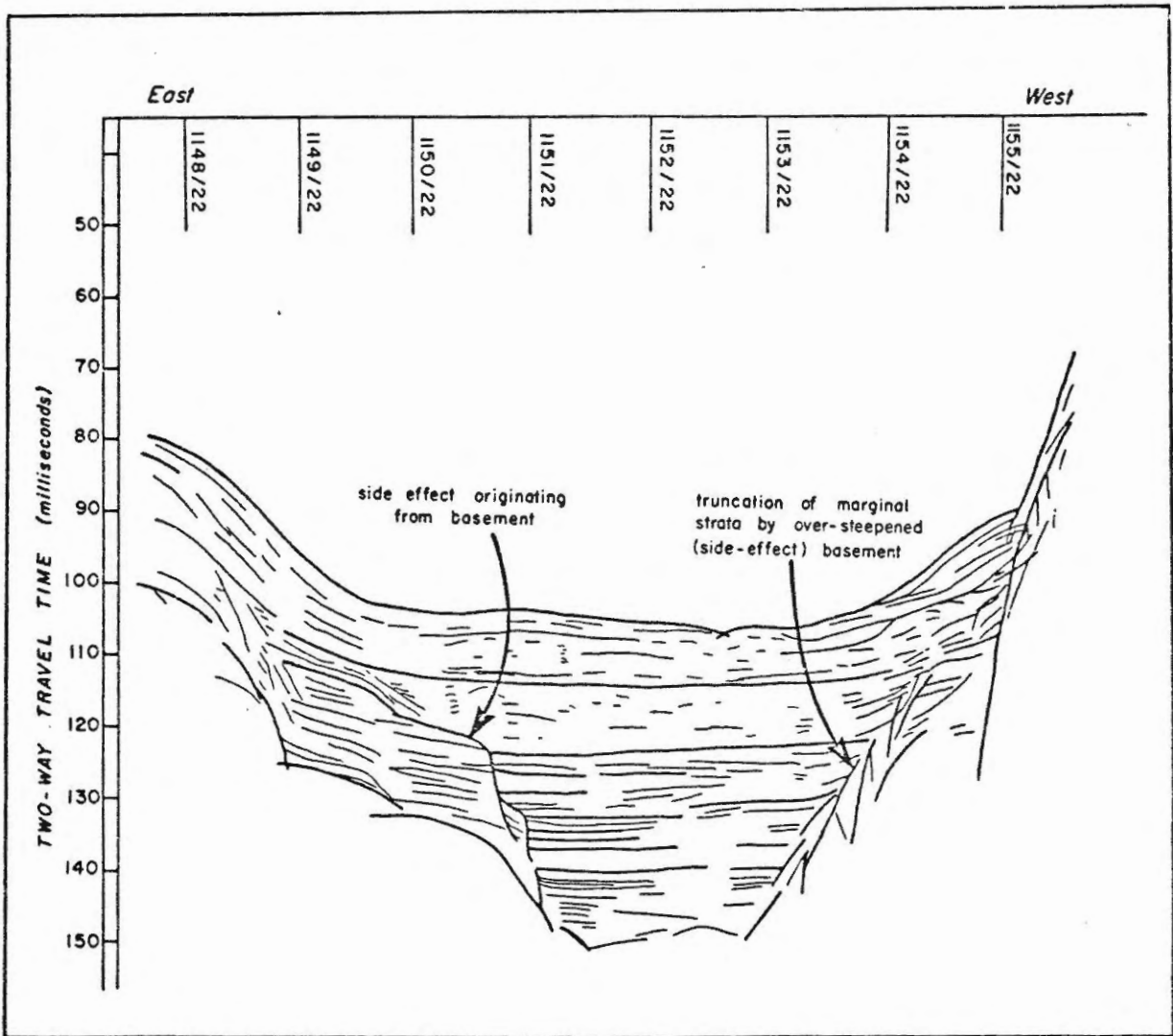


Figure 4.2: Profile 1148-1156/22 from the Outer Bay showing stratal reflections superimposed by side effects originating from the basement

Sub-bottom Compositon

The largest acoustic discontinuity is usually the transition from water to the seafloor. Some examples of reflective coefficients are:

	<u>van Overeem (1977)</u>	<u>Dale (1979)</u>
water to granite	R = 0.7	
water to sand	R = 0.3-0.4	
water to clay/silt	R = 0.2-0.1	R = 0.23
water to mud	R = 0.05-0.1	R = 0.25
mud to clay/silt	R = 0.1	R = 0.12
clay to sand	R = 0.1	R = 0.1
sand to granite	R = 0.4	

In this sedimentary profile the acoustical discontinuities are usually less pronounced and the reflection coefficients are not uniform. Interpretations are therefore based only on the relative reflection characteristics and cannot be conclusively defined. In general, muds, clays and silts possess a weaker record, often with volume reverberation. Coarse sands and gravels usually create an extremely strong reflection masking the presence of any lower strata. Fine sands, coarse silts and mixed sediment types tend to trace intermediate reflection characteristics.

#### 4.2 Acoustic Stratigraphy of Makkovik Bay

##### Evidence of Lithological Strata

Acoustic reflections often, but not always, correspond to a lithologic change at that level. Dale (1979) concluded that the offshore Late Quaternary sediments northeast of Newfoundland are poor approximations to a planar elastic stratified medium and this is probably the major cause of seismic to sediment incoherences. In this study there are two types of samples available that attempt to link acoustic reflections with lithologic changes: piston cores and short (25 cm) cores.

Piston core 78-020-003, taken in the Approaches, penetrated 9.2 metres of well stratified mud with less than 10% fine sand. Three 20 to 40 cm thick beds of gravelly mud occur at core depths of 3.4, 4.3 and 5.0 metres. These coarse layers appear to be correlatable with one or more strong reflectors observed in the 3.5 kHz profile (see Chapter VIII, Fig. 8.1).

Piston core 78-020-004, taken in the Outer Bay, penetrates a relatively uniform mud. This is comparable to the uppermost unit in the 3.5 kHz profile which appears relatively homogeneous and transparent with only weak reflectors. Correlation of these two piston cores with the 3.5 kHz profile will be considered in greater detail in Chapter VIII.

Numerous short cores were taken at the outcrops of sub-bottom reflectors throughout Makkovik Bay. Many cores contain lithologic contacts. Of special interest is a series of short cores near Gulf Island in the Central Inner Bay along an erosional surface that exposes strong reflectors. The



cores indicate contacts between olive-gray clayey mud and dark green to brown mud. Unfortunately, the resolution of these acoustic profiles is not sufficient to provide absolute correlation with individual reflectors.

#### Descriptive Techniques

Makkovik Bay is divided into five major physiographic bays, which in turn, can be subdivided into several basins. The entire sedimentary sequence is not usually traceable from one basin to the next so that individual basins must be studied before a synthesis can be compiled.

Thirteen representative basins were chosen, based on the amount and quality of the recorded data and their relative location. These are lettered A to M in an upbay direction, their positions shown in Figure 4.3. The data for each basin are presented respectively in Plates 4.1 through 4.13, each one in three portions: (a) a reproduction of the 3.5 kHz profile, (b) a line tracing of the profile and (c) a descriptive stratigraphic column which incorporates both vertical and lateral reflection descriptions.

The line tracings are intended to remove all the background noise to emphasize the salient features; however, no interpretation was used in their construction. Except for basement derived hyperbolas, all major lines were traced regardless of their apparent origin. Sediment derived hyperbolic reflectors are also included although they may originate from suitably oriented small objects.

The descriptive stratigraphic columns are compiled and subdivided into units on the basis of reflection characteristics and morphology.

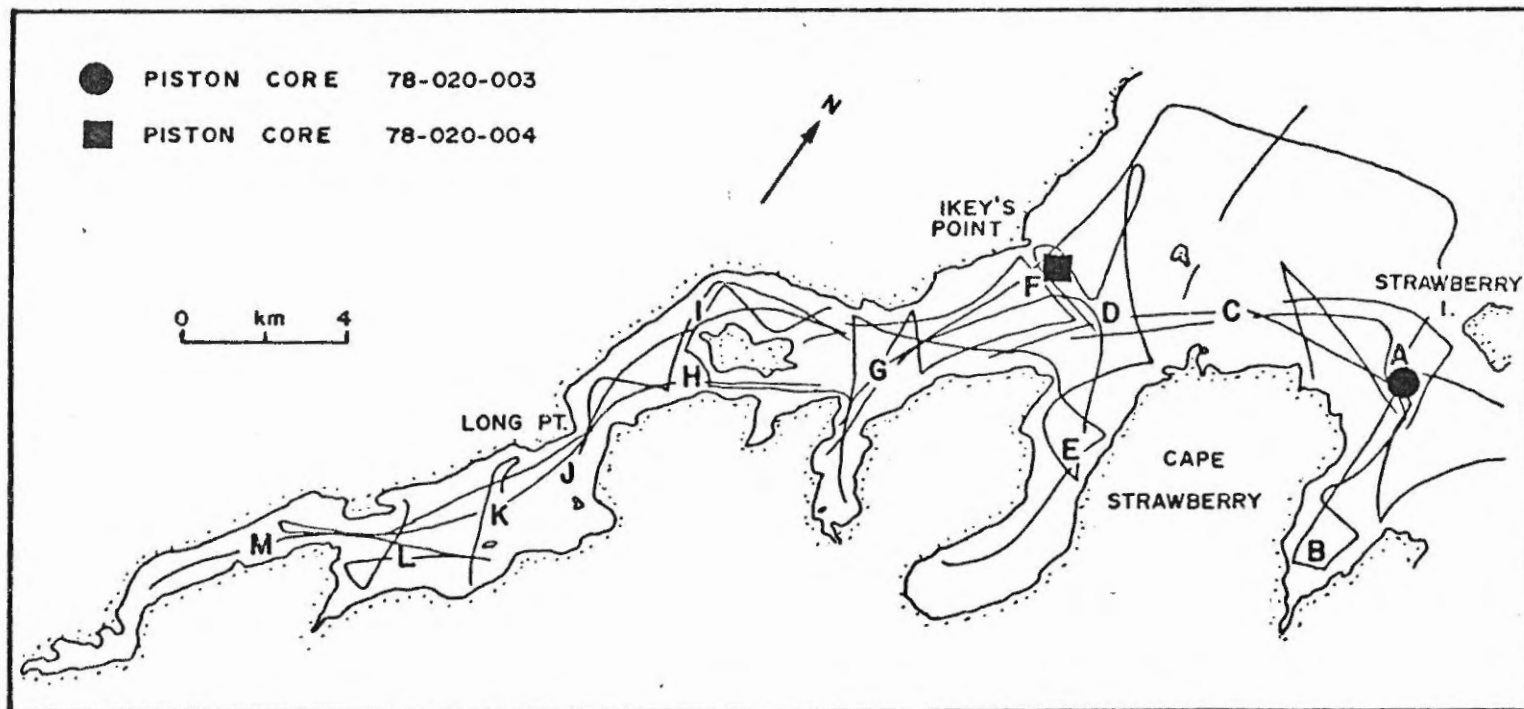


Figure 4.3: Smoothed track chart and the thirteen representative basins (lettered A to M) used for detailed acoustic reflection descriptions

Although subjective in nature, these columns are descriptive, not interpretational. The character of reflection incorporates the strength of reflection, continuity of reflection and the presence or absence of an erosional unconformity.

The relative strengths of reflection are classified as very weak, weak to moderate, and strong. They are evaluated separately for each profile such that criteria from one profile did not bias the determination in another profile. Therefore, when the two profiles are eventually correlated, the actual intensity of reflection may be different but the relative strengths will be comparable. This tends to overcome problems created by variations in instrument setting, water depth and acoustic velocities of different sediment types.

Continuity of reflection is regarded as being either continuous or noncontinuous. An erosional unconformity is based on evidence of truncated horizons, not just the likely representation of specific hyperbolic surfaces (Damuth and Hayes, 1977).

The strong, lowest, usually continuous reflection is considered to be basement. In the acoustic record it varies from a smooth solitary reflection, to broad overlapping hyperbolae, to irregular tightly overlapping hyperbolae with widely varying vertex elevations. The basement is thought to be predominantly bedrock, but might locally be till or coarse clastics.

Three types of morphology are distinguished: ponded, conformable cover and onlapping basin fill. Ponded forms possess horizontally strati-

fied reflectors such that the sediment is contained by the basin in a fluid-like manner. In general, the reflectors do not 'climb' the flanks of the depressions as shown in Figure 4.4.

The conformable cover type appears to have built up layer by layer in a blanketing habit with the reflectors usually traceable across sills into adjacent basins. There may be substantial thinning of individual reflectors on the basin slopes but in general the reflectors do not pinch out (Figure 4.4).

The onlapping basin-fill-type possesses the infill characteristic of the ponded forms plus the flank-climbing habit of the conformable type. For this reason many reflectors of questionable morphology have been assigned to the onlapping basin fill type. However, if the reflectors lack or have conflicting morphologic indicators, then they are classed as indeterminate. These morphologic characters are illustrated in Figure 4.4.

These different morphologic types are probably made possible by the confined environment of the inlet; the presence of interbasinal sills provide suitable basement variations to allow observation of different morphologic acoustic units. However, the slopes themselves often pose interpretational problems. Over steepening (side effect) of slopes may tend to obscure the nature of the sediment-bedrock interface, superimposing a ponded morphology on all types. In these areas they cannot be discriminated from a real lack of sediments. For this reason, morphologic type must be assessed only from the low gradient slopes, and preferentially on a driftline. Assessment of this critical slope must be done locally. For

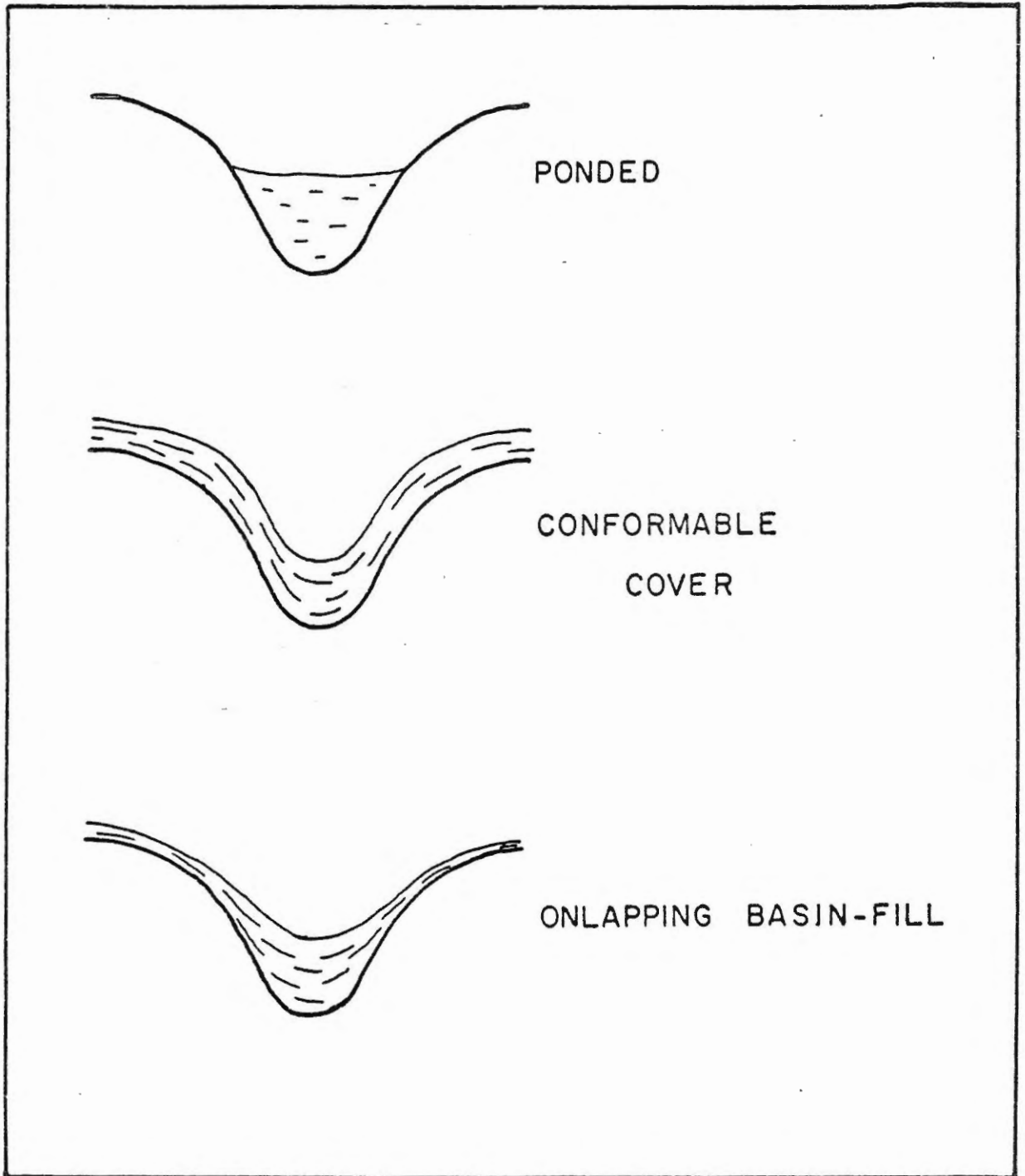


Figure 4.4: Illustration of 3 morphologic types of acoustic strata: ponded, conformable cover, and onlapping basin-fill

example, in Figure 4.2, the interpretation should be based on the left side of the basin only, neglecting the superimposed side effect.

#### Description of Basinal Acoustic Stratigraphy

##### (1) Basin A

Basin A, located between Strawberry Island and Cape Strawberry, is crisscrossed by five continuous profiles. Profile 1222-1233/13, which passes through the centre, was selected for detailed description (Plate 4.1).

The lowest unit above basement, A1, is characterized by strong, continuous conformable reflectors. Although total stratal thickness decreases rapidly from 1230 to 1224/13, the individual reflectors of unit A1 do not appear to thin out. At 1225/13 they seem to be truncated by an erosional unconformity. The basal strata extend the farthest, across the basin floor to the base of the steep slope off Strawberry Island (out of figure to north). Unit A1 reaches a maximum thickness of approximately 24 metres (assuming a velocity of 1500 m/sec).

Unit A2 has a maximum thickness of approximately 12 metres and is characterized by weak, noncontinuous, well spaced reflectors. The form is intermediate, between conformable and onlapping basin-fill. A2 does not extend to the deepest part of the basin, so that strata of A1 are exposed. The lower strata of A2 are clearly eroded while the upper reflectors either pinch out or are gradually truncated.

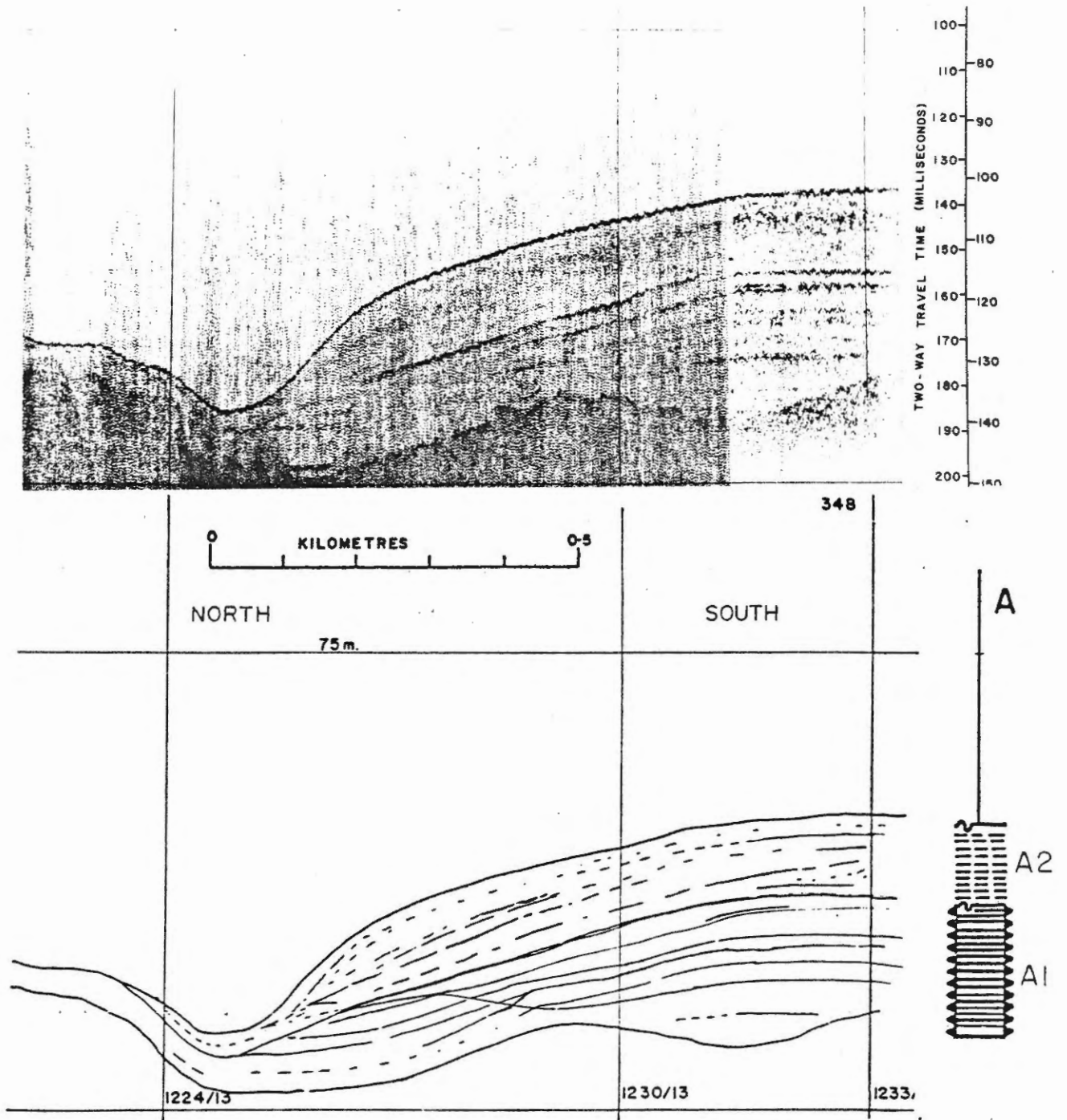


Plate 4.1: Basin A: 3.5 kHz profile (top), line tracing (bottom) and descriptive stratigraphic column (right) with acoustic units A1 and A2

(2) Basin B

Basin B, located at the head of Wild Bight, is represented by profile 1325-1344/13; the record is of good quality made during a drift line (Plate 4.2).

Unit B1 comprises the basal 10 metres of the basin. It is characterized by numerous, strong, continuous reflectors that are conformable with the basement. It may also show minor onlap. Some of the upper strata outcrop higher on the flanks at a water depth of 25 metres (not shown in figure).

The record shows large, somewhat circular areas that appear to rest on top of the basement within B1. These have relatively transparent to weak reflections and weak but obvious penetration in the basement. The poor intensity reflections tend to bow upwards suggesting a higher acoustic velocity either throughout the circular patches or along the crown. The estimated dimensions range from 5 to 10 metres in height and 30 to 60 metres in width. Their origin is discussed later.

Unit B2 contains predominantly moderate strength continuous reflectors. These are conformable with B1. Maximum thickness reaches 15 metres.

Unit B3 is approximately 5 metres thick and is characterized by non-parallel, noncontinuous and varying strength reflectors. The unit appears to be conformable with B2. The entire upper surface appears to be erosional.

The uppermost unit, B4, is approximately 2 metres thick and is characterized by its constant thickness across the basin and up the flanks. The lower interface is marked by a strong, continuous reflector that



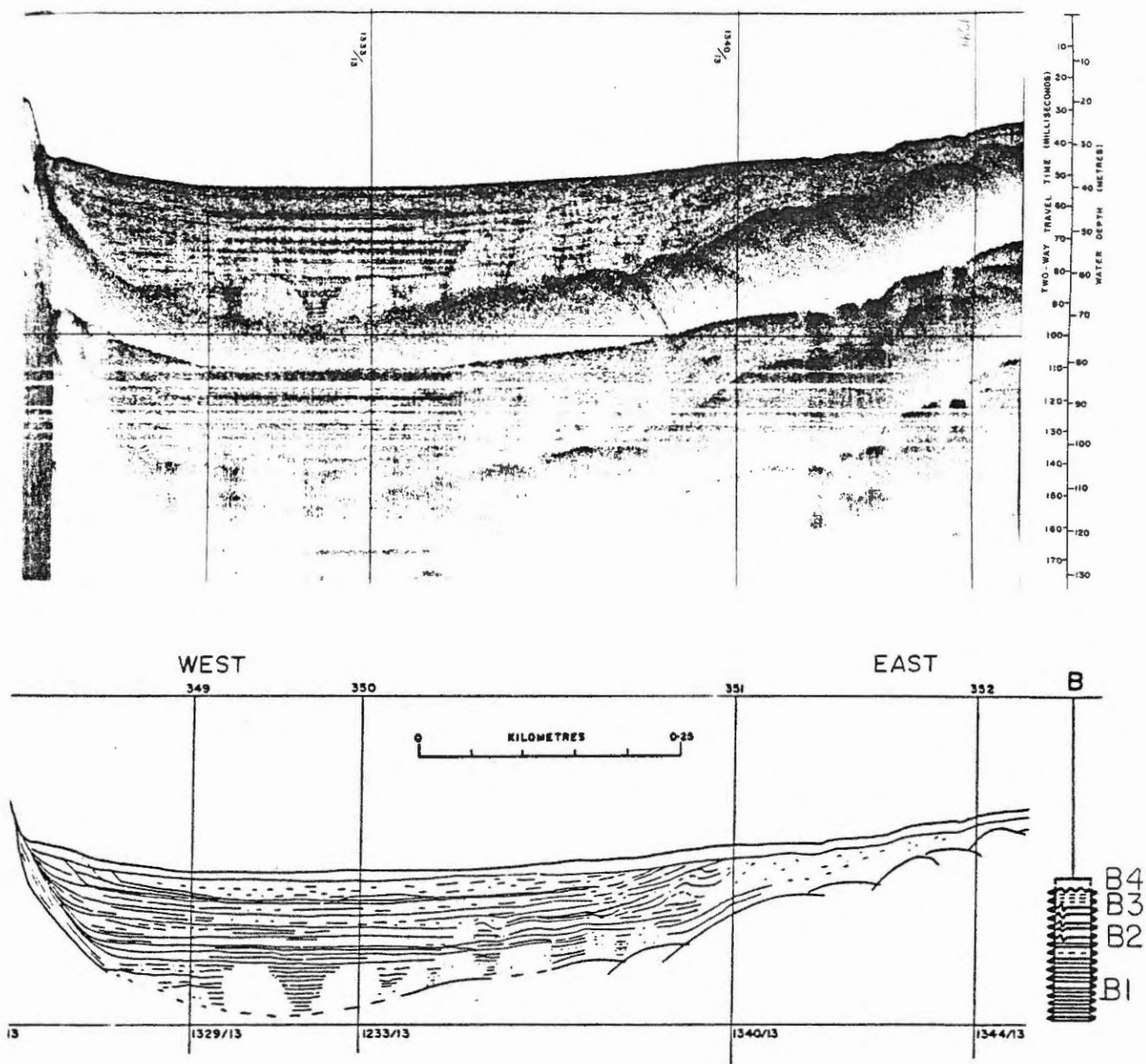


Plate 4.2: Basin B: 3.5 kHz profile (top), line tracing (bottom) and descriptive stratigraphic column (right) with acoustic units B1, B2, B3 and B4

appears to parallel the sea bed and truncate the upward curving reflectors of B2 and B3 on the flanks. The acoustic character of B4 is weak with noncontinuous reflectors.

(3) Basin C

Basin C is located between Jacques Island and Nipper Cove. Two profiles indicate relatively steep slopes and high background noise resulting in poor reflection records, especially with regard to morphology. Profile 1600-1610/13 was used for the unit type description (Plate 4.3).

The basal 8 metres comprise C1 and are characterized by several, well separated, discontinuous, strong reflectors. This is overlain by approximately 8 metres of weak reflectors making up unit C2. The uppermost 9 metres constitute C3, characterized by several very strong, non-continuous reflectors. These reflectors curve upwards and are truncated at the surface.

All three units have an indeterminate morphology.

(4) Basin D

Basin D is located south of Jacques Island, near the entrance to Ford's Bight. Of the two profiles made, 1632-1650/13 (Plate 4.4) was chosen for detailed analysis.

Unit D1 is conformable with the basement both in the basin and over most basement highs. It is approximately 8 metres thick with very strong, continuous reflectors. The lowermost 2 metres exhibit decreasing reflection intensity with depth.

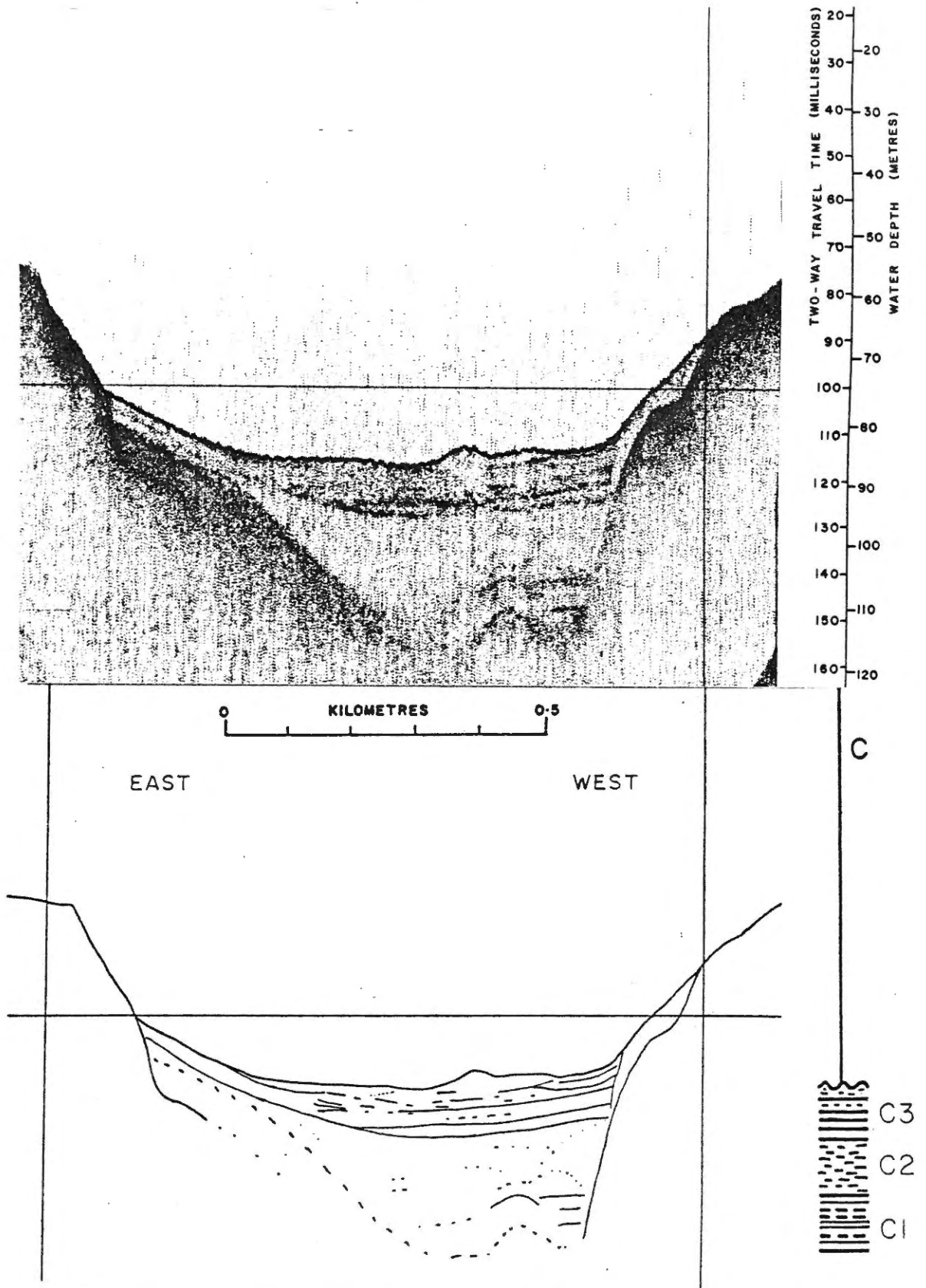


Plate 4.3: Basin C: 3.5 kHz profile (top), line tracing (bottom) and descriptive stratigraphic column (right) with acoustic units C1, C2 and C3

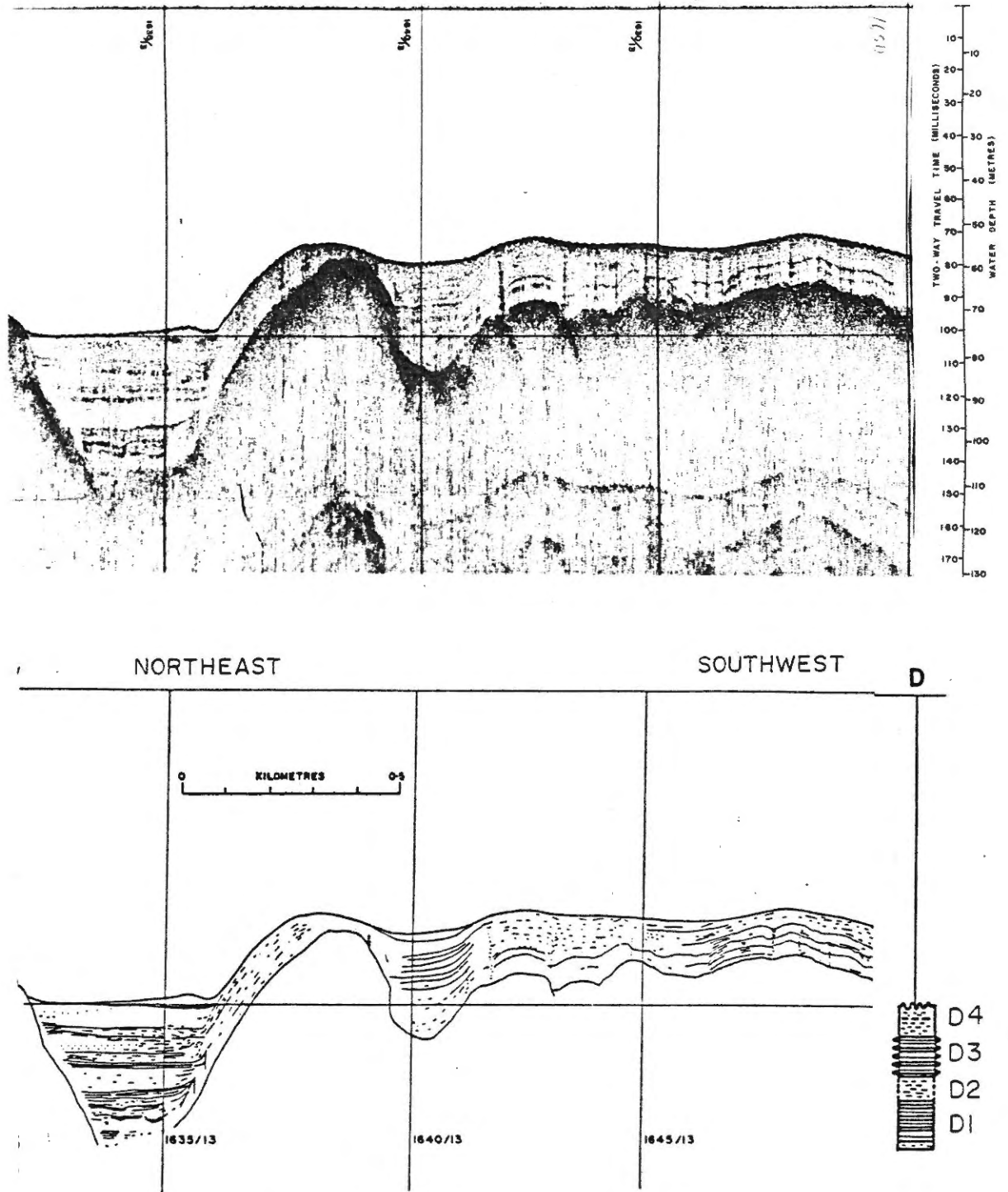


Plate 4.4: Basin D: 3.5 kHz profile (top), line tracing (bottom) and descriptive stratigraphic column (right) with acoustic units D1, D2, D3 and D4

Unit D1 is overlain in the basin by 6 metres of unit D2. This has very weak, noncontinuous reflectors and an onlapping basin-fill morphology.

Unit D3 is conformable with D2 in the basins and with D1 on the arches. In this profile it is acoustically similar to D1, but in the adjacent basin to the south, the strength of reflection appears to increase gradually with depth. D3 reaches a maximum thickness of 10 metres.

Unit D4 is 7 metres thick and overlies D3 in the basins. It has continuous, weak to moderate reflectors and appears to be provided with slight onlap. The upper surface is erosional.

(5) Basin E

The profile 1407-1419/7 (Plate 4.5) across Ford's Bight illustrates the acoustic stratigraphy of Basin E.

Unit E1 is ponded to a thickness of 12 metres with moderate continuous and strong noncontinuous reflectors. The basal section has very low intensity reflections, which in places, coalesce with rounded patches similar to those in B1.

Unit E2 is ponded to a thickness of 14 metres with predominantly strong, continuous reflectors.

Unit E3 is a 7 metre thick, onlapping basin-fill unit with weak to moderate, noncontinuous reflectors.

Unit E4 is up to 6 metres thick with continuous, moderate to strong reflectors. The upper surface is at least partially erosional. There is not sufficient horizontal exposure to determine the morphology.

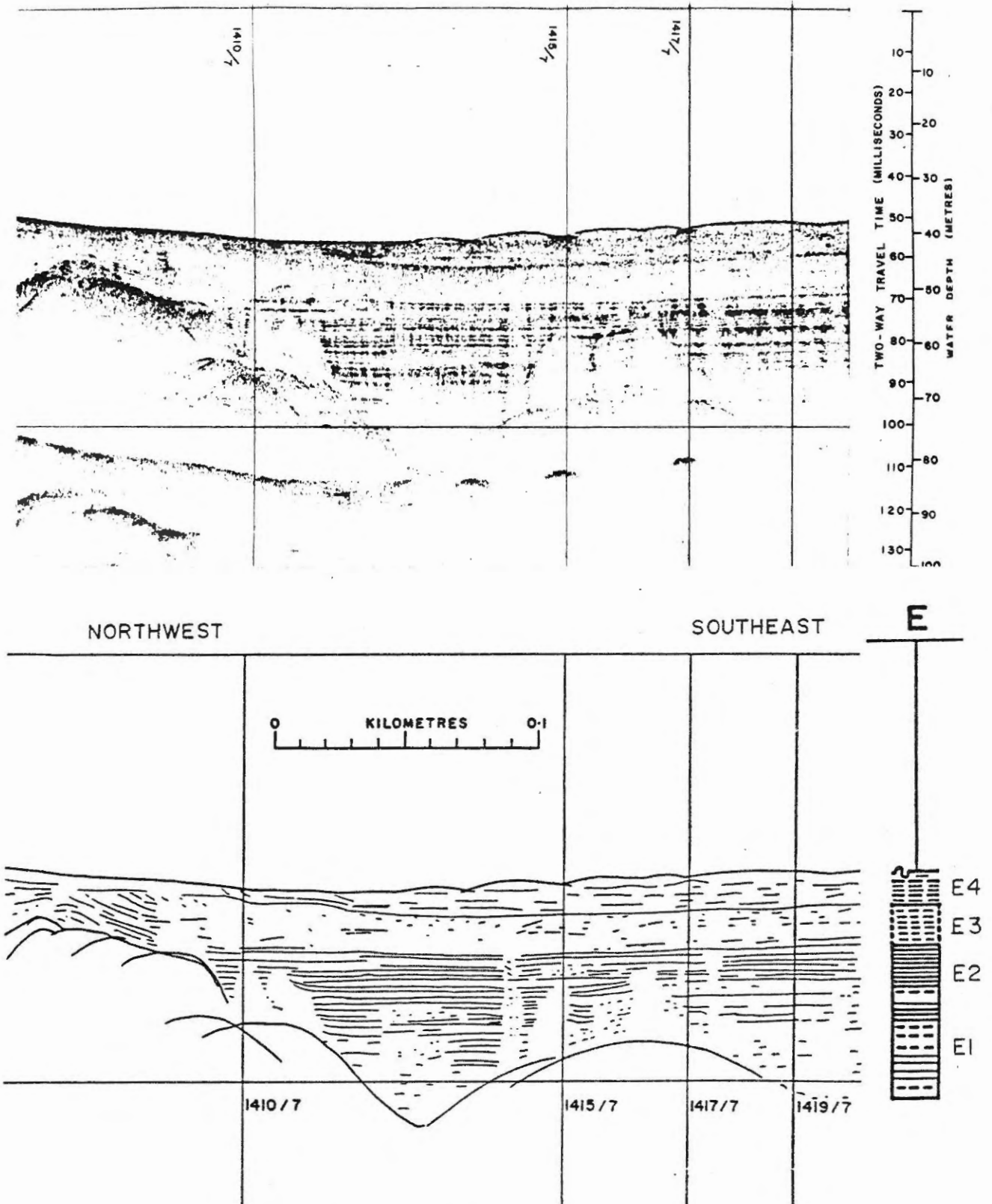


Plate 4.5: Basin E: 3.5 kHz profile (top), line tracing (bottom) and descriptive stratigraphic column (right) with acoustic units E1, E2, E3 and E4

(6) Basin F

Five profiles were made across basin F which is located in the Outer Bay adjacent to Ikey's Point. The type section is based on profile 0942-1002/21 (Plate 4.6).

The basal 4 metres, F1, have ponded to onlapping, very weak reflectors. This unit is not discernible in the other four profiles.

Unit F2 is 12 metres thick and has numerous strong, continuous reflectors that are conformable with the basement into surrounding basins. Surficial erosion plus thinning of individual horizons occur in shallower depths. The erosion extends from 40 metres down to almost 60 metres suggesting that F2 is relatively resistant. A buried erosional contact is also evident along the upper edge of F2 at the base of the steep slope off Ikey's Point (0959-1001/21).

Unit F3 is 6 metres thick, has a very weak to transparent reflection and exhibits an overall ponded morphology. Less reliable internal reflections suggest a possible onlap morphology. Very faint traces of possible reflectors appear to be truncated at the upper surface which is characterized by a strong reflection.

This is overlain by 8 metres of F4 which is characterized by an onlapping basin-fill morphology and very weak reflectors and minor, moderate strength, noncontinuous reflectors. Rapid thinning of F4 proximal to the steep slope is suggestive of a low net depositional zone; however, possible truncations of reflectors also suggest erosion.

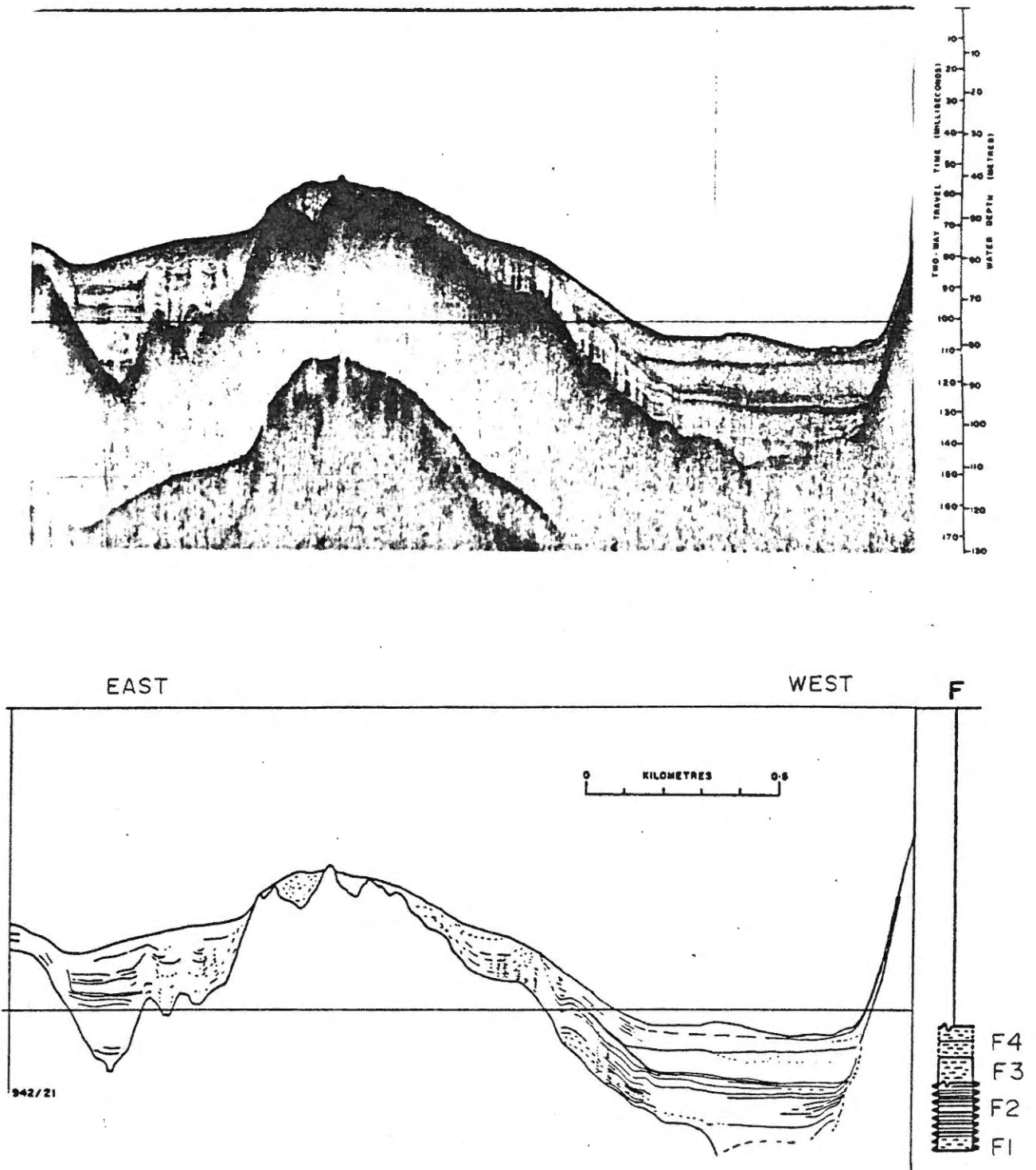


Plate 4.6: Basin F: 3.5 kHz profile (top), line tracing (bottom) and descriptive stratigraphic column (right) with acoustic units F1, F2, F3 and F4



(7) Basin G

Seven profiles were recorded from basin G, which is located down bay from Big Island. Profile 1044-100/7 (Plate 4.7), which recorded the thickest sequence of sediments, was selected for the type section.

The basal 10 metres comprise G1. It is characterized by strong and moderate strength reflectors that are usually continuous. The lowermost 4 metres are poorly defined and partially obscured by basement derived, irregular hyperbolae. Unit G1 appears to be ponded at the base and slightly onlapped at the top.

Unit G2 has primarily weak to moderate strength, noncontinuous reflectors. It is approximately 13 metres thick and is ponded with slight onlapping tendencies. A few hyperbolic reflections with vertices of equal elevation occur in the upper parts of the unit (1055-1102/7).

Unit G3 is approximately 13 metres thick and is conformable with the basement. The reflectors are strong at the base of the unit with decreasing upward intensity. They are predominantly continuous throughout the basin and can tentatively be traced up the flanks into Makkovik Harbour (not shown in Figure).

The uppermost unit, G4, has a maximum thickness of approximately 16 metres and appears to have an onlapping basin-fill morphology. The reflections are usually weak with secondary noncontinuous, moderate types..

(8) Basin H

Basin H, located upbay of Big Island, is represented by profile 1636-1647/8 (Plate 4.8).

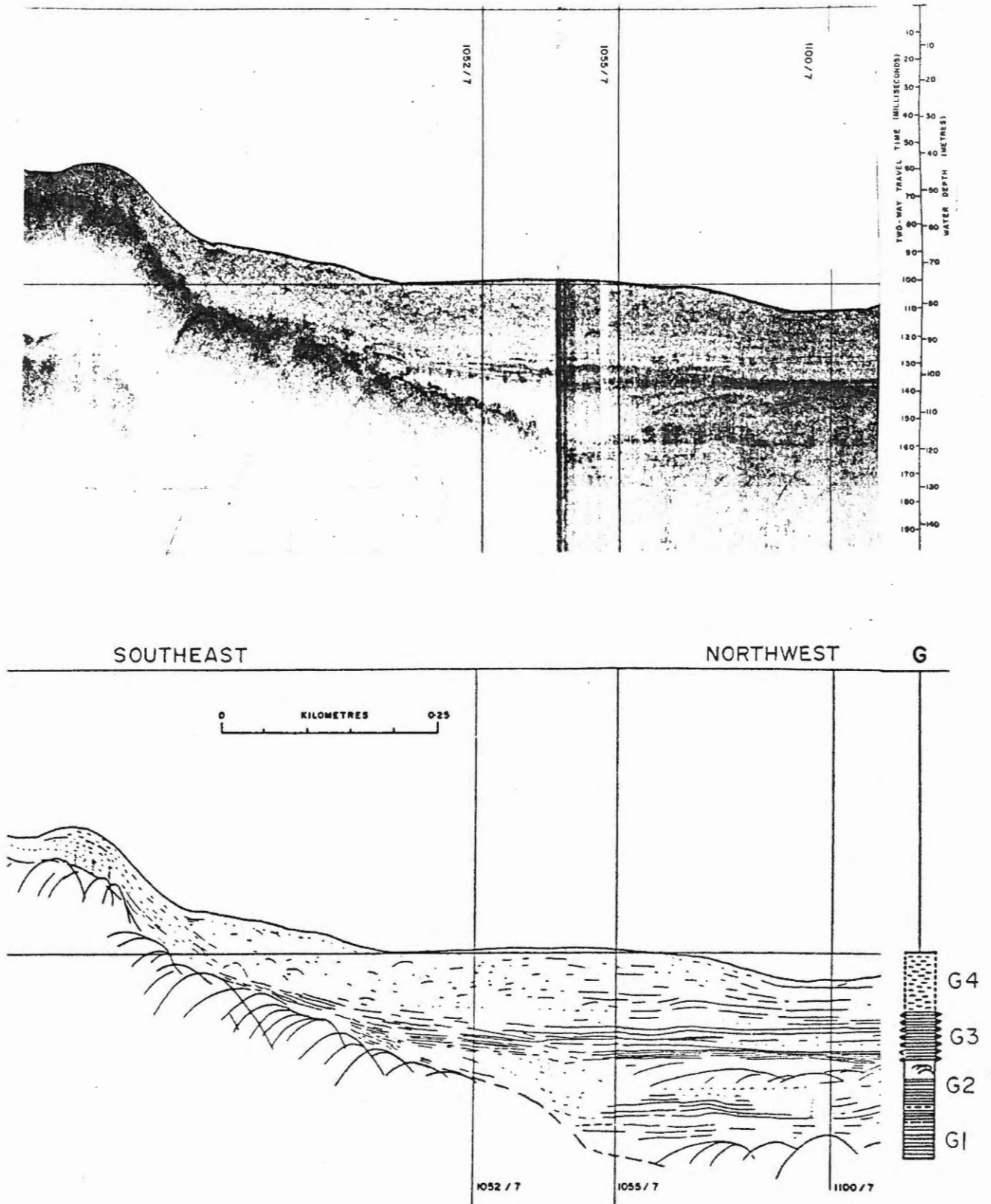


Plate 4.7: Basin G: 3.5 kHz profile (top), line tracing (bottom) and descriptive stratigraphic column (right) with acoustic units G1, G2, G3 and G4

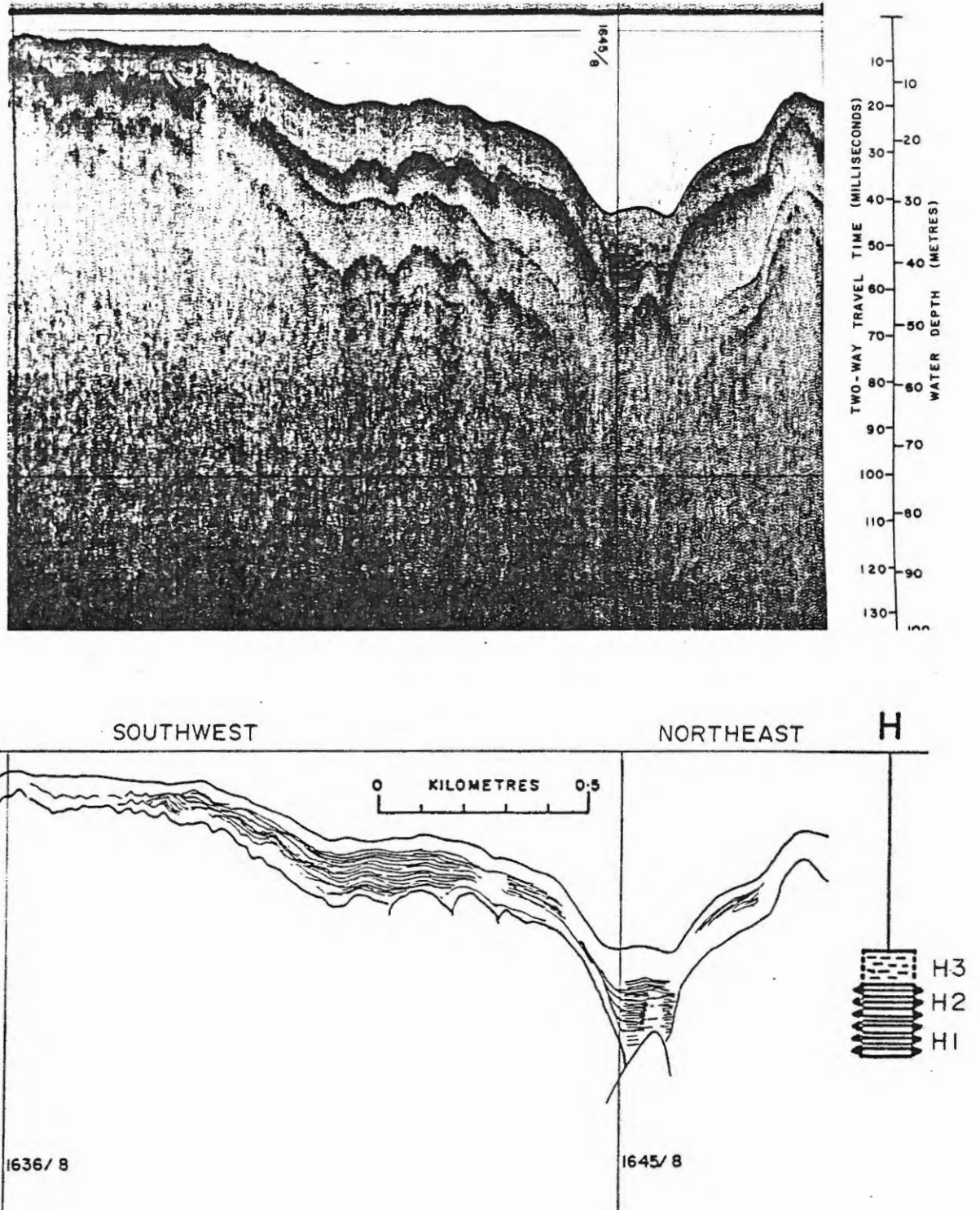


Plate 4.8: Basin H: 3.5 kHz profile (top), line tracing (bottom) and descriptive stratigraphic column (right) with acoustic units H1, H2 and H3

The basal 2 metres, H1, have moderate reflectors and, judging by the overlying form of H2, appear to be ponded.

Unit H2 is approximately 10 metres thick and has strong, continuous and conformable reflectors.

Unit H3 is approximately 5 metres thick and has weak reflectors and an onlapping basin-fill morphology.

(9) Basin I

Basin I is located between Big Island and Big Head. In the profile illustrated (1537-1556/22, Plate 4.9) there is a right-angle course change at 1551/21.

Unit I1 comprises the basal 14 metres and is composed of conformable, primarily noncontinuous reflectors. The reflectors become very weak in the lowest 2 metres but as they retain the same character, they are included in the same unit.

Unit I2 is 3 metres thick and has noncontinuous but conformable reflectors with weak to moderate intensity. The upper and lower interfaces are marked by continuous, strong reflectors.

Unit I3 comprises the uppermost 6 metres and has an onlapping basin-fill morphology and noncontinuous, weak to moderate reflectors.

(10) Basin J

Basin J, located immediately upbay from Grassy Point, is typified by profile 1620-1630/8 shown in Plate 4.10.

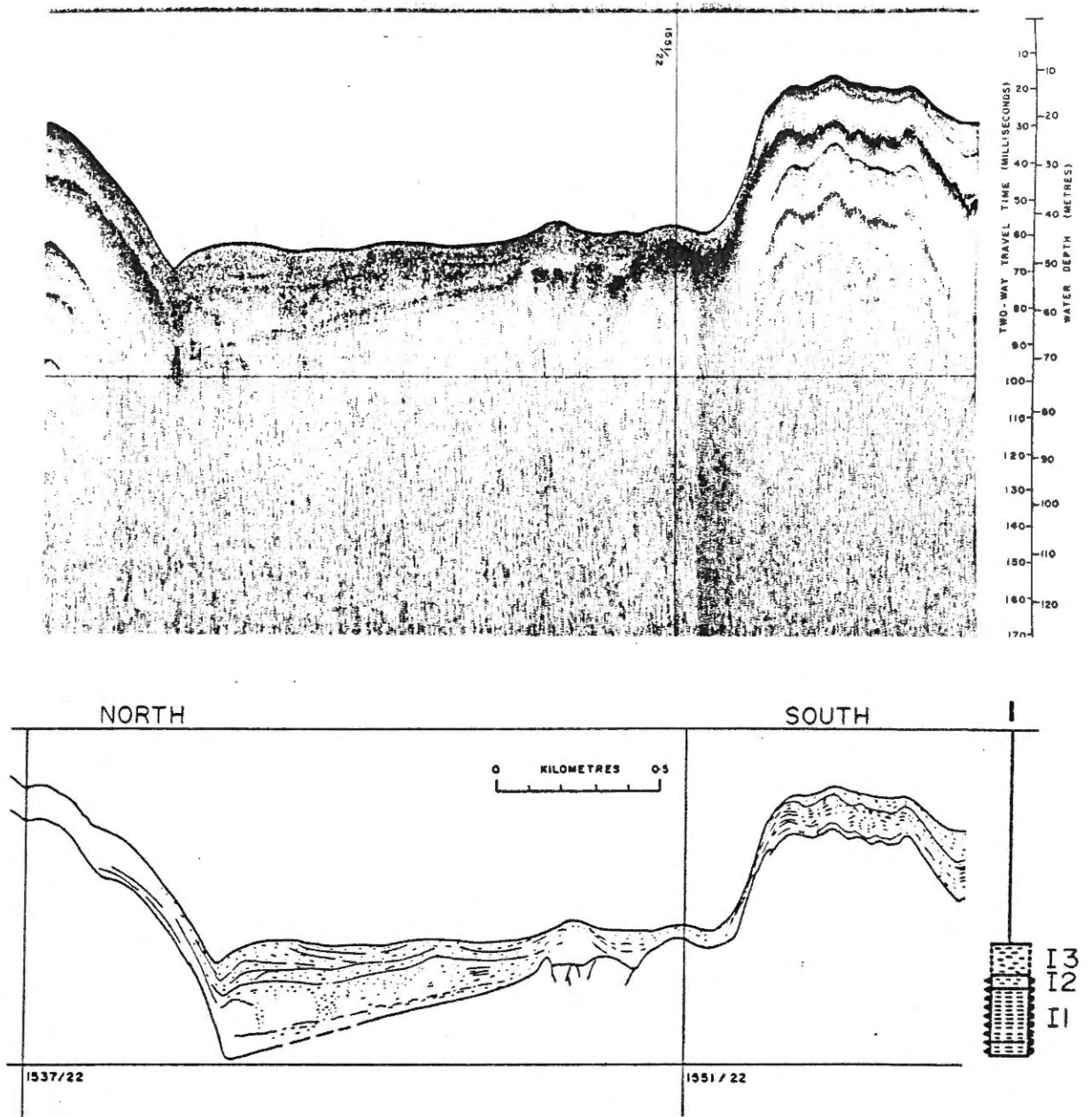


Plate 4.9: Basin I: 3.5 kHz profile (top), line tracing (bottom) and descriptive stratigraphic column (right) with acoustic units I1, I2 and I3

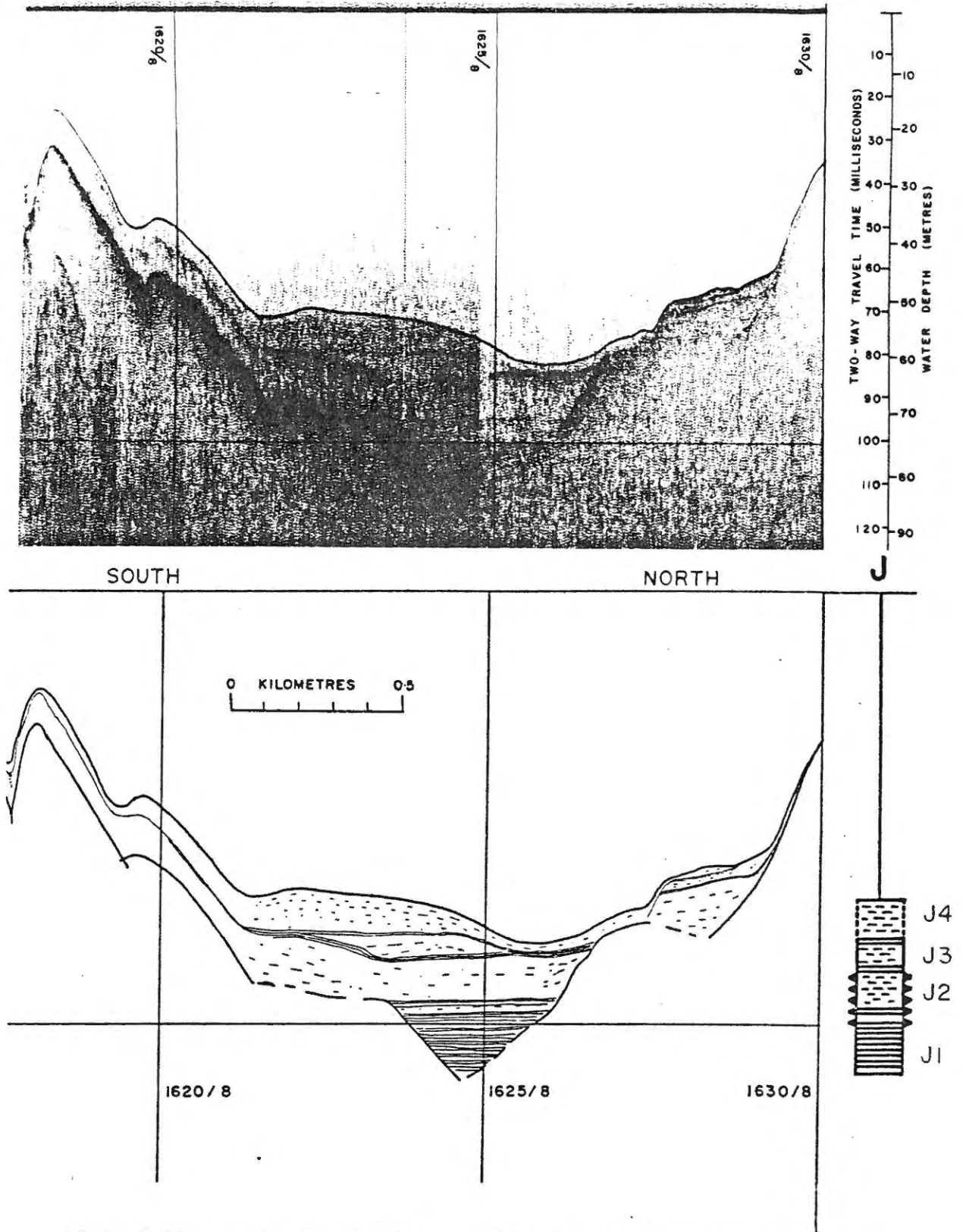


Plate 4.10: Basin J: 3.5 kHz profile (top), line tracing (bottom) and descriptive stratigraphic column (right) with acoustic units J1, J2, J3 and J4

Background noise has obliterated most of the basal 8 metres. Unit J1 appears to have strong, continuous, ponded reflectors.

Unit J2 is approximately 9 metres thick and has weak to moderate, non-continuous, conformable reflectors. The upper edge is very strong and continuous.

Unit J3 is a 4 metre thick ponded wedge found only in the centre of the basin (1622-1625/8) and has moderate, noncontinuous reflectors. While ponded on the upbay side (1622/8) the individual reflectors pinch out rapidly downwards at 1625/8. The upper surface is strong and continuous and appears to be nonerosional.

The uppermost 6 metres comprise J4. It is characterized by onlapping basin-fill strata with weak to moderate, noncontinuous reflectors. Unit J4 thins rapidly at 1625/8 where J3 pinches out. There does not appear to be an unconformity at the interface but an internal unconformity may exist within J4.

(11) Basin K

Four profiles were made of basin K, which is located north of Gull Island. The thickest stratigraphic thickness is illustrated by profile 1448-1458/16 in plate 4.11.

The basal 2 metres comprise K1. Obscured by poor resolution, it appears to have onlapping, strong, continuous reflectors.

Unit K2 is a 10 metre thick unit with moderate and strong, continuous, conformable reflectors.

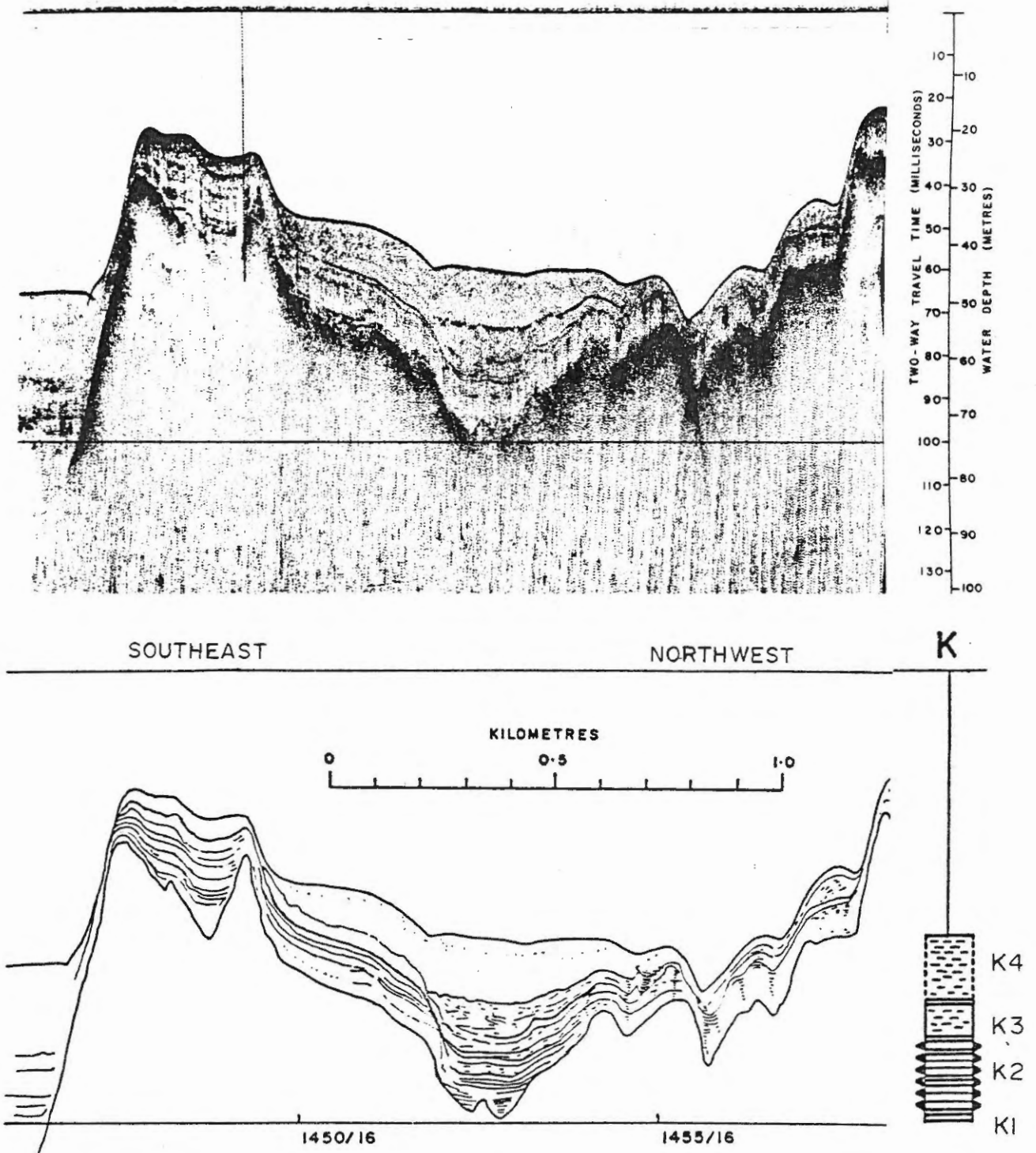


Plate 4.11: Basin K: 3.5 kHz profile (top), line tracing (bottom) and descriptive stratigraphic column (right) with acoustic units K1, K2, K3 and K4



Unit K3 is a 6 metre thick ponded unit with weak, noncontinuous reflectors and an intense upper boundary. The other three profiles and the left side of this profile (1452/16) suggest ponding and therefore it has been reported as such in the descriptive stratigraphic column. However, the reflectors show slight onlap on the left side of the profile (1454,1457/16) plus a few, faint traces of possible truncation of reflectors at the upper edge (1452-1453/16).

Unit K4 is 10 metres thick and has an onlapping basin-fill with weak, noncontinuous reflectors.

(12) Basin L

Located between Burntwood Point and Gull Island, basin L is recorded by five profiles; profile 1322-1340/20 (Plate 4.12) is used to typify the acoustic stratigraphy.

The lower 20 metres comprise L1 and are characterized by strong and moderate, continuous reflectors that are conformable with the basement. All the individual horizons exhibit pronounced thinning downbay. Two other profiles of basin L suggest the presence of a thin, continuous, onlapping unit adjacent to the basement.

Unit L2 is approximately 18 metres thick and is characterized by onlapping basin-fill strata with weak to moderate, noncontinuous reflectors. L2 onlaps the downbay flank up to a water depth of 30 metres where L1 is exposed (1323/20).

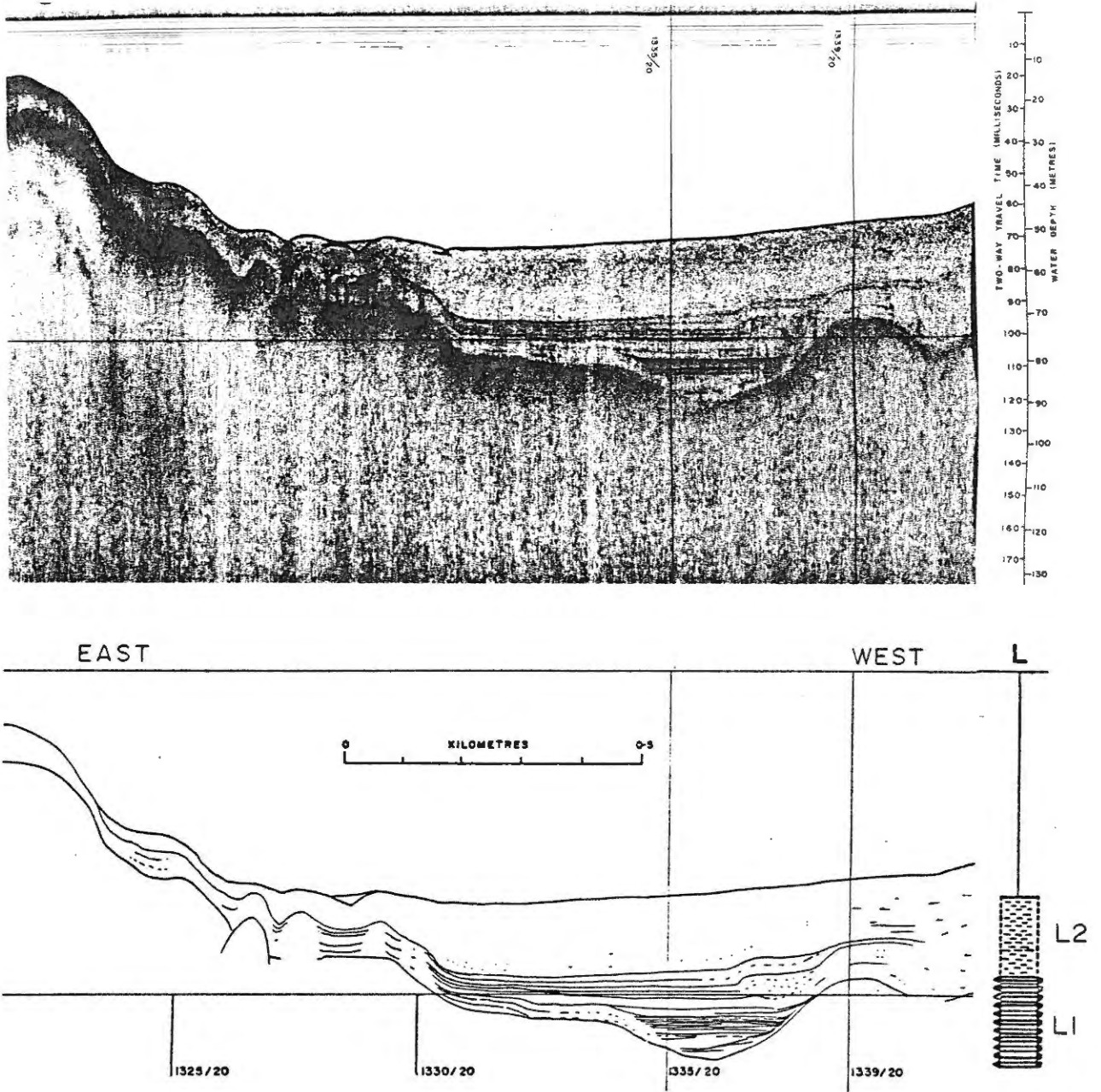


Plate 4.12: Basin L: 3.5 kHz profile (top), line tracing (bottom) and descriptive stratigraphic column (right) with acoustic units L1 and L2

(13) Basin M

Four profiles were made of basin M, west of Burntwood Point. The clearest profile (1453-1505/8) is shown in Plate 4.13.

The lower unit, M1, is 14 metres thick and has strong, continuous and conformable reflectors. As in the other Inner Bay basins, the acoustic nature adjacent to the basement is poorly defined, although the actual depth and thickness of overlying sediment is relatively low.

The upper unit, M2, is a 5-metre thick, onlapping basin-fill unit with weak, noncontinuous reflectors.

Specific Interpretational Problems

Two conspicuous but poorly understood features occur in the Makkovik Bay acoustic profiles. Basin M has a ridge-like structure at 1455/8 (Plate 4.13) which might be interpreted as a constructional feature such as an end moraine with a slight drape of marine sediments. However, repeated passes in the same general area failed to reveal a significant 3-dimensional aspect, and so it is tentatively interpreted either as some unknown technical artefact or as a small feature in the uppermost, strongly reflective layer characterized by high sound velocity and absorption.

Rounded features with similar acoustic properties were recorded north and south of Gull Island, at the mouth of Fords Bight and in Wild Bight (Plate 4.2), all during drift lines. The expanded horizontal scale allows better observation, although their interpretation remains problematic. Possible suggestions include dispersed gas bubbles, pockets or layers of

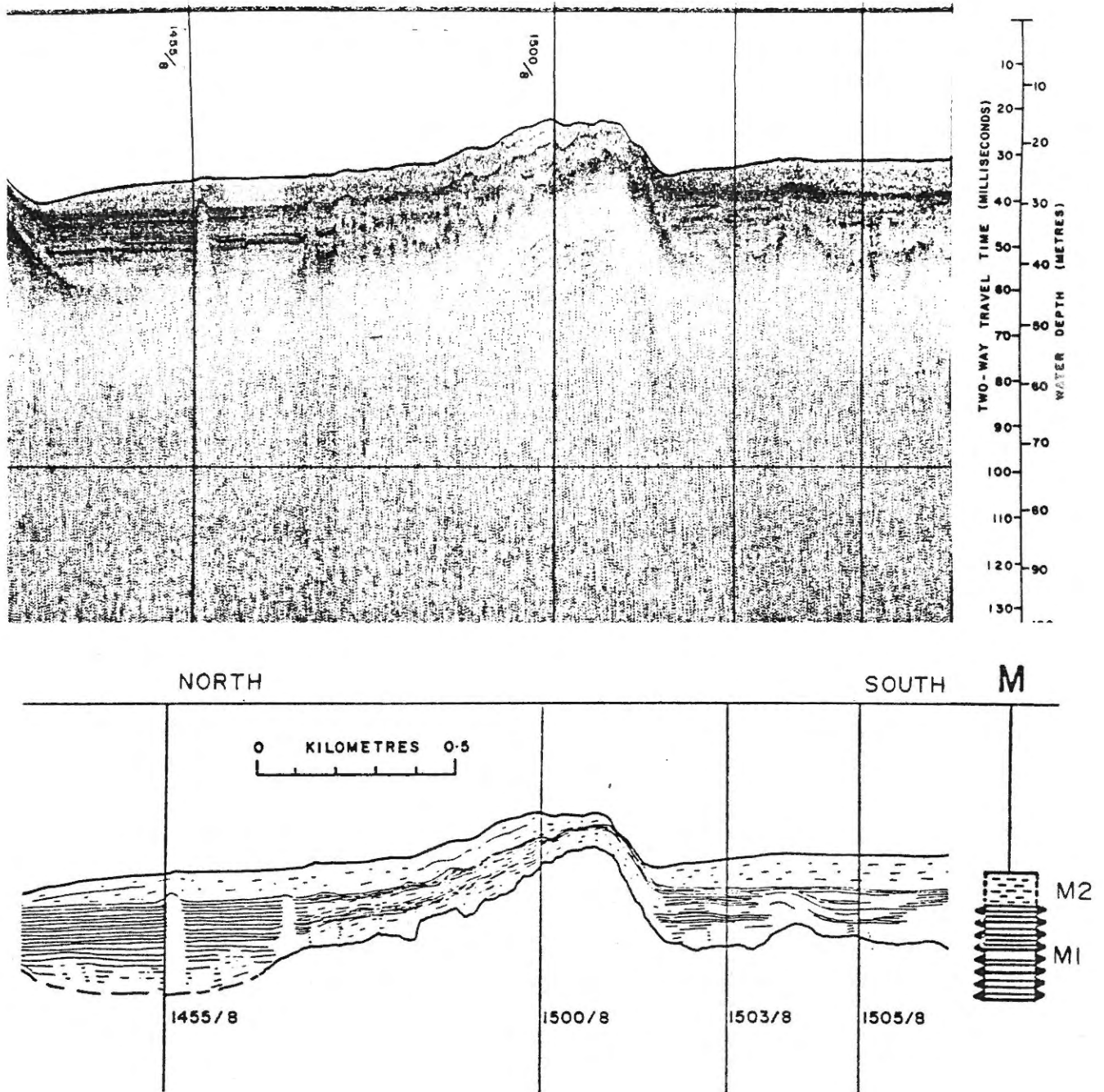


Plate 4.13: Basin M: 3.5 kHz profile (top), line tracing (bottom) and descriptive stratigraphic column (right) with acoustic units M1 and M2

ice or frozen sediment, organic material, or perhaps mixed sediment types. Grant (1975) suggested that 'bright spots' observed in seismic profile of Lake Melville were a consequence of gas formed through rapid burial of partly oxidized organic matter by fine clastics.

#### 4.3 Interbasin Correlation of Acoustic Stratigraphy

Correlation of the thirteen descriptive stratigraphic columns is made in Figure 4.5. All columns, except B, E and H, are drawn with their respective positions along the axis of the bay using the present-day sea level as a datum. Because basins B, E and H are not adjacent to the axis, their datum level is offset below the others to resemble their relative geographic position.

In general, three major acoustic units are present: the upper, weakly reflective, onlapping basin-fill unit, a middle, strongly reflective, conformable cover unit and a lower, basin-fill unit with variable strength reflections.

##### (1) Upper Basin-Fill Unit

Correlation of the upper basin-fill unit is excellent throughout the Inner and Outer Bays but highly speculative for basins in the Approaches.

As shown in the interbasin correlation chart (Figure 4.5), the upper basin-fill unit is represented by M2, L2, K4, J4, I3, G4, H3, F4, D4 and possibly E4. Units F3, J3, K3 and possibly E3 are also considered to be included because:

- (a) the acoustic reflectivity is similar,

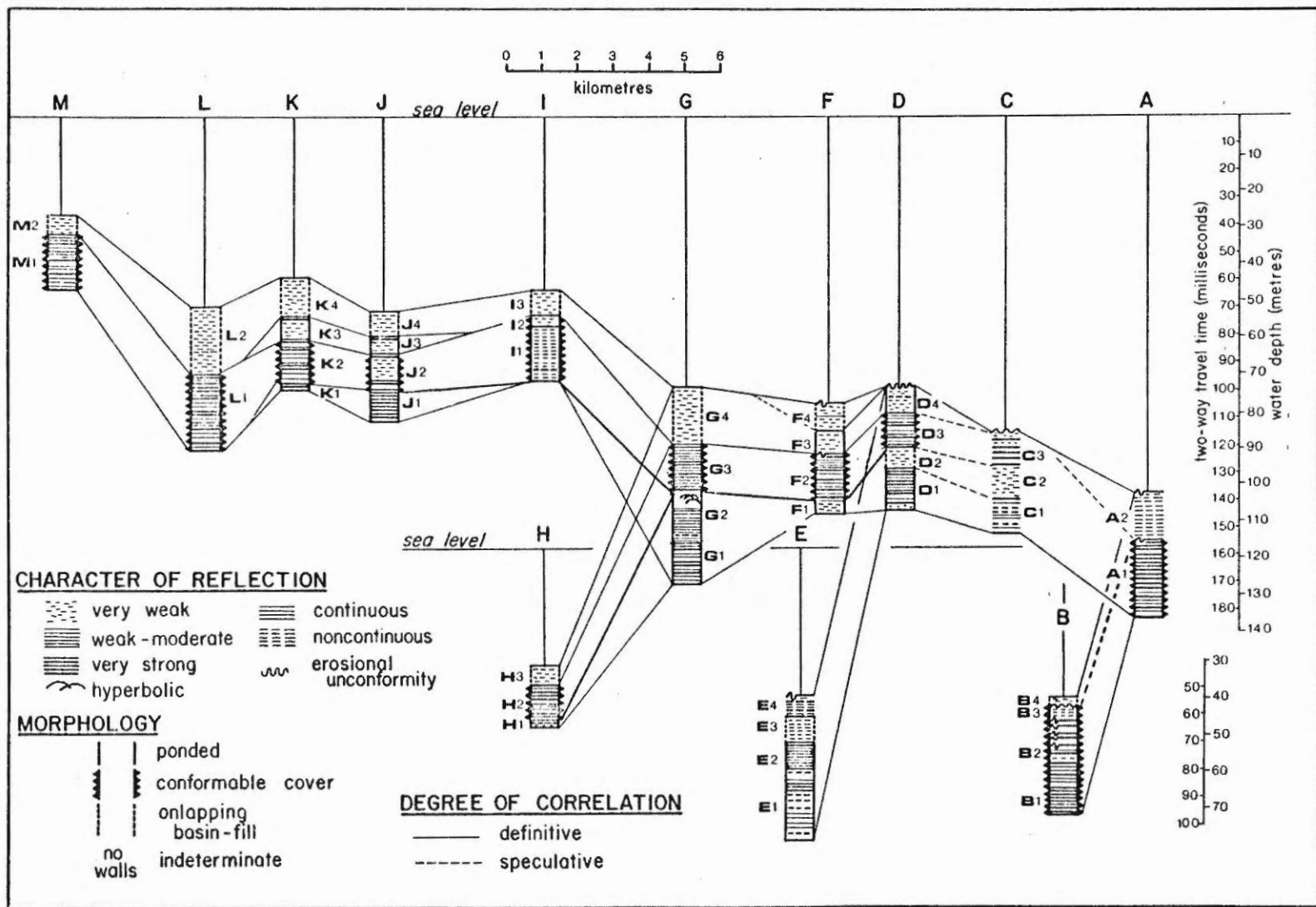


Figure 4.5: Interbasin correlation chart of the acoustic, descriptive stratigraphic columns showing three major units: (a) upper basin-fill unit, (b) conformable cover unit and (c) the lower basin-fill unit

- (b) truncation of faint reflectors at the upper surface suggest an onlapping, basin-fill morphology rather than a ponded morphology, and
- (c) the upper surfaces have strong, continuous reflections which, along with the truncation of interval, faint reflectors, suggest erosion. For these reasons, where ponded units occur on top of the conformable cover unit, they are thought to be eroded remnants of basin-fill type sediment.

Correlation of the upper basin-fill unit in the Approaches is problematic. Although A2 has weak reflectors, it also appears conformable in places; this unit occurs throughout the Approaches. In basin B there is a thin veneer with a weak reflection and a conformable outline, possibly representing remnants of eroding upper basin-fill type sediments as observed in the Outer Bay.

The distribution of the upper basin-fill unit is shown in an isopach map (Figure 4.6), interpolated between more than 800 measurements from the 3.5 kHz records and contoured in metres, assuming that velocity equals 1500 m/sec. There are four major features:

- (1) sediment thickness increases rapidly with depth for any basin;
- (2) maximum sediment thickness for each bay varies, in order of decreasing thickness: the Outer Bay, Central Inner Bay, Approaches, and the Eastern and Western Inner Bay;

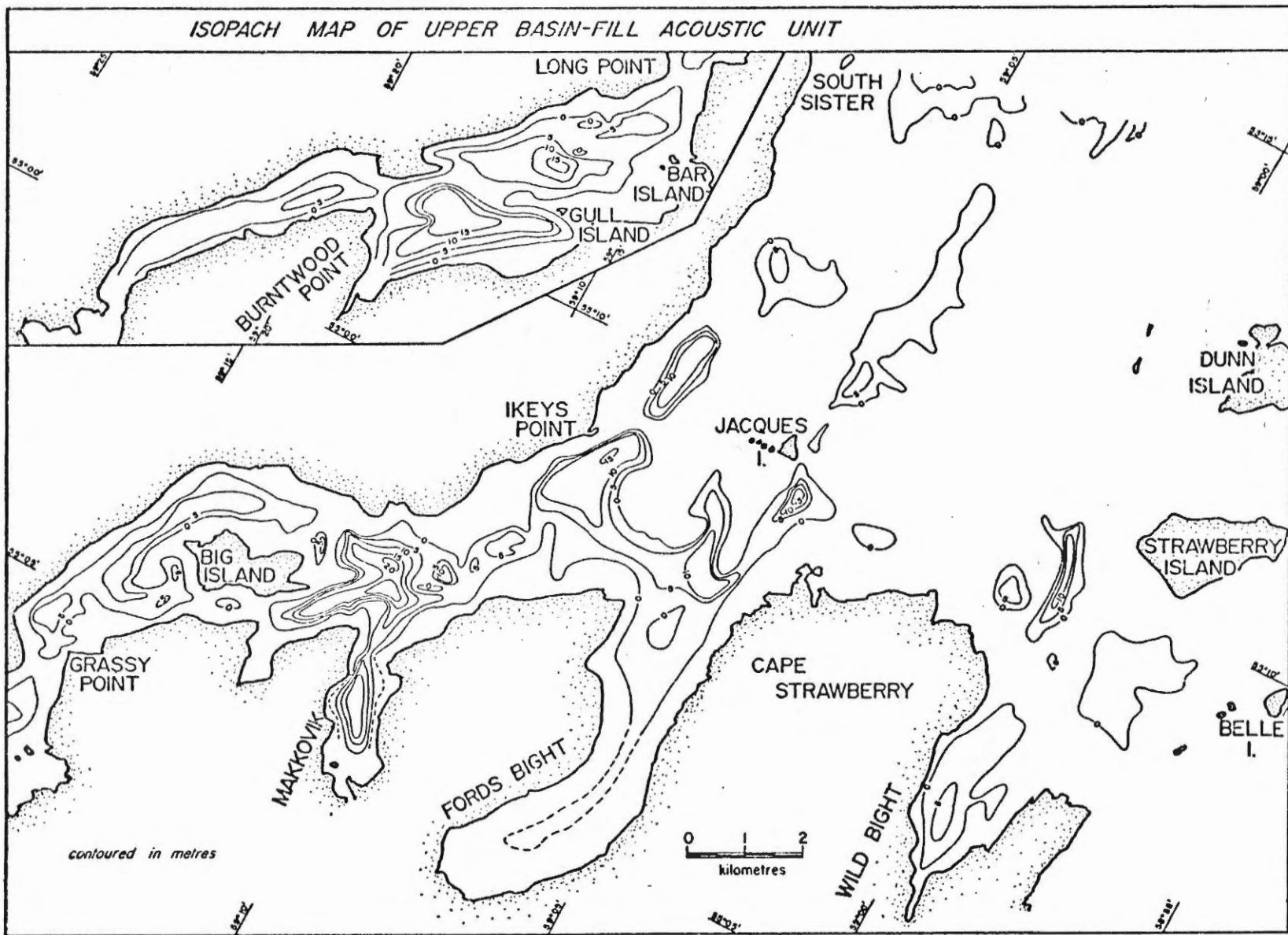


Figure 4.6: Isopach map of upper basin-fill acoustic unit, contoured in metres

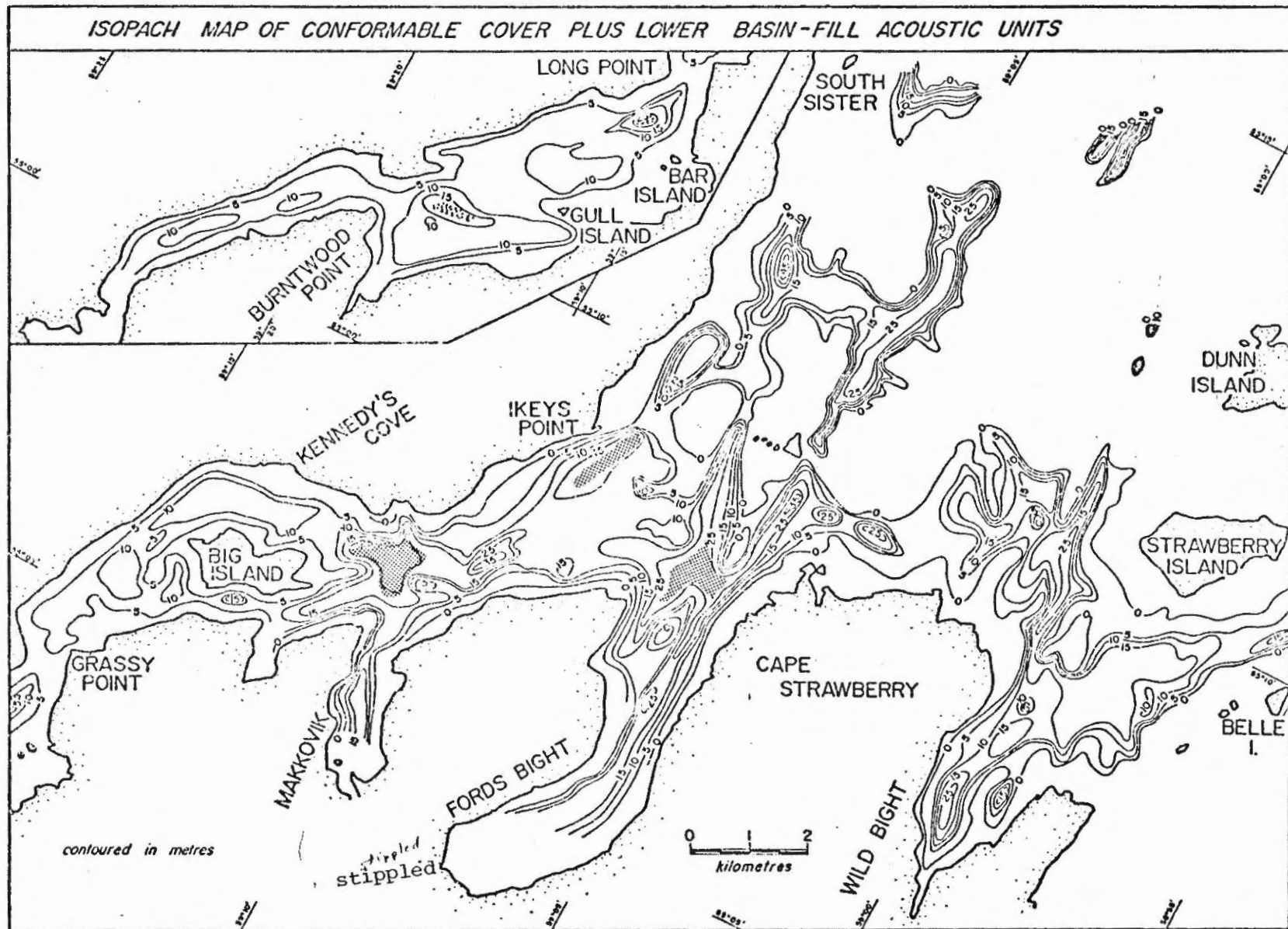


- (3) the outer end of the Outer Bay has almost half the sediment thickness of the inner end;
- (4) the distance of the zero contour from the shoreline increases downbay.

(2) Conformable Cover Unit

The conformable cover unit can be clearly correlated with the Inner and Outer Bays and in places, individual reflectors can tentatively be traced from one basin to the next. In Figure 4.5, the correlable, conformable cover unit is represented by M1, L1, K2, J2, I1, H1 and 2, G3, F2, and D3. These correlations can be extended speculatively to A1, B1 and 2, C3 and E2, but in three basal sections in the Approaches it is difficult to differentiate the conformable cover unit from the lower basin-fill unit (described below). Therefore, the isopach map includes both of these units. The lower basin-fill unit is distinguished in the isopach map by shading for the Inner and Outer Bays (Fig. 4.7).

The conformable nature of the unit is emphasized in the isopach map: the thickness increases only slightly with depth. Abrupt thickness changes are generally confined to the nearshore zone where the unit is being eroded. The maximum thickness varies by less than 5 metres from the Western Inner Bay to the Outer Bay. Although the average basinal thickness of the conformable cover unit is constant from the Inner Bays to the outer fringes of the Approaches, the larger basins display a conspicuous downbay pinching. This can be observed both in the profiles (e.g. Plate 4.12) and the isopach map (Figure 4.7). The distance of the zero contour from the shoreline increases downbay, similar to the trend seen in the upper basin-fill unit.



**Figure 4.7:** Isopach map of the conformable cover unit plus the lower basin-fill unit. The lower basin-fill unit occurs beneath the conformable cover unit in the deeper basin; the portion that exceeds approximately 20 metres thickness is contributed by the lower basin-fill unit.

However, the zero contour is always closer to the shoreline at any location than the zero contour of the upper basin-fill unit. Upbay from Big Island, it was impossible to locate the zero contour either because the conformable unit extended to the intertidal zone as at Kennedy's Cove area (see Chapter 6) or because a nearshore sandy prism masked deeper sediments.

(3) Lower Basin-Fill Unit

This unit is observed primarily in the Outer Bay, where the sedimentary sequence is the thickest. It is represented by G1 and 2, F1, and D1 and 2. Units D2, F1 and the upper portion of G2 have weak reflectors, ponded to onlapping basin-fill morphology and are situated directly beneath the conformable cover unit. Tentative correlation is made to E1 and C1 and 2 solely on the basis of reflection intensity.

This unit may also correlate with units H1, J1 and K1 in the Inner Bay. In J1, the extension of the reflectors into the basement flanks suggests that they might be internal multiples generated in J2; thus J1 may be characterized by acoustic transparency. Similarly the 'ponded' unit K1 and the basal few metres of the other Inner Bay basins may be correlatable with G2. Alternatively, the ponded nature of these units may be an artifact of slope or side effects, and they may in reality be conformable. Interpolations are severely limited by a poor data base.

An additional areal zone is defined by its acoustic character. A strong, non-penetrable reflector from bedrock, coarse clastics and possibly till occurs in high energy shoal areas. Although these zones do not

possess any acoustically determinable thickness and, hence, cannot be defined as a sedimentary unit, they are designated as the 'shoal non-penetrable unit' for mapping purposes.

(4) Erosional Unconformities

Erosion of sedimentary strata occurs in shallow water, at the base of steep slopes and in places across the entire basin.

The conformable unit and, in slightly deeper water, the upper basin-fill unit are at present eroded by waves. The greatest depth of erosion extends from at least 50 metres down the flanks in the Approaches to the intertidal zone in the Inner bays.

Shallow moats and truncated reflectors at the bases of steep slopes suggest areas of low net deposition and, in places, erosion. Moats are observed along all the steep slopes in Makkovik Bay; basin F serves as a noteworthy example (Plate 4.6). A surficial moat (0958-1001/21) and truncation of deeper reflectors (125 msec) indicate that these processes have been operational to varying degrees throughout the depositional history.

Basin F also displays an example of basin wide erosion. At 112 msec (0956-1001/12, Plate 4.6) a strong, continuous reflector truncates upward curving strata of F3. Other examples can be observed in profiles D (Plate 4.4, 1633-1635/15, at 100 msec), E (Plate 4.5, 1410-1420/7, at 60 msec) and at the upper boundaries of K3 (Plate 4.11) and J3 (Plate 4.10). All examples observed were in the upper-basin fill unit.

#### 4.4 Surficial Distribution of Acoustic Units

By superimposing the two isopach maps it is possible to produce a map of the surficial distribution of the acoustic units, as shown in Figure 4.8. This reinforces the concepts shown by the individual isopach maps. The upper basin-fill unit occurs in the protected basins, at shallower depths upbay. The conformable cover unit is exposed along the upper flanks of the Inner bays and the middle to lower flanks of the Outer Bay and Approaches. The erosion of the conformable cover unit has concentrated coarse lag sediments and in places, has exposed the bedrock, which together comprise the shoal non-penetrable unit.

#### 4.5 Depositional Interpretation

Because the acoustic reflections are laterally persistent and some samples from acoustic-reflection-outcrops indicate a different lithologies, it is suggested that the acoustic stratigraphic units, as defined by the relative strength of reflection and their morphology are, in most cases, representative of different lithologies and hence, different depositional environments.

##### (1) Upper Basin-Fill Environment

The acoustical transparency and homogeneity of the upper basin-fill unit suggest that the sediments are relatively homogeneous and fine grained. The morphology implies that the currents or wave base energy retards sedimentation on the flanks and topographical highs while fine grained sediments are deposited relatively uniformly in the basins.

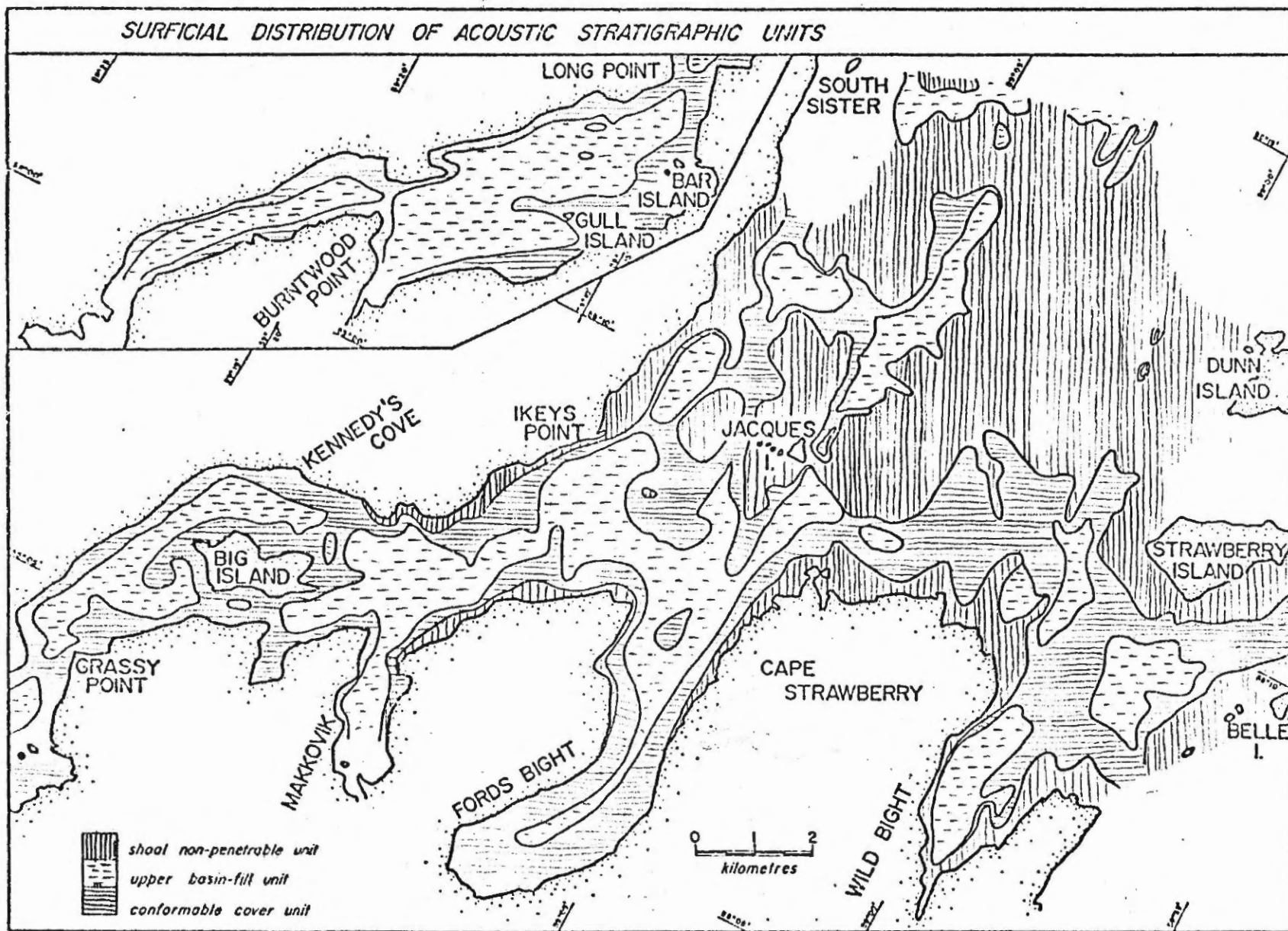


Figure 4.8: Surficial distribution of the acoustic stratigraphic units: the upper basin-fill, conformable cover and the shoal, non-penetrable unit

The erosion of flank sediments and the basin-fill morphology suggest a dominant marginal source area as older sediments are exposed by a falling sea level. The isopach map (Fig. 4.6) and the bathymetry (Fig. 3.1, in pocket) suggest that there is also a preferential deposition at the head of the Outer Bay. Basin G has a thick sequence of upper basin-fill unit while basin F has almost 10 metres less, even though it has a greater shoreline and hence, source area. The Approaches have even less sediment. From this it is suggested that a certain proportion of marginally disturbed sediments and/or possible basin sediments from the mouth of the Outer Bay are deposited at the head of the bay.

Assuming that the present rate of sedimentation (estimated from sediment traps, Chapter III) has persisted throughout the deposition of the upper basin-fill unit, the thicknesses can be used to determine the age of the base of the unit. A sedimentation rate of  $.053 \pm .002$  cm/yr in the Western Inner Bay (Chapter III) producing 5 m of sediment (measured from seismic profile) would take approximately  $9,430 \pm 360$  years. Similarly, a sedimentation rate of  $0.172 \pm .026$  cm/yr in the Outer Bay (Chapter III), producing 16 metres of sediment would require  $9,300 \pm 1300$  years. (The error margins are based on the standard deviations of the original data.)

The precision of these ages suggests that the upper basin-fill unit is time concordant and, given the foregoing assumptions, has been deposited in approximately the last 9,400 years. The acoustical homogeneity suggests an undisturbed sedimentary sequence, thereby adding credence to these age estimates.

The shallow moats at the bases of steep slopes are a function of the topographic increase of current velocities (Kögler and Larsen, 1979); hence, these localized zones represent areas of low net deposition or erosion.

Contemporary basin-wide erosion occurs in the outer half of the Outer Bay and throughout most of the Approaches. The relative level of erosion is proportional to the shoreline energy transitions (Fig. 2.2) from high to moderate to low (Rosen, 1979a), suggesting that basin-wide erosive energy is surface derived. It does not appear to be augmented by tidally-induced or base currents.

(2) Conformable Cover Environment

The acoustic character of the conformable unit suggests that it is composed of fine grained sediments that contain thin, laterally persistent reflectors. These reflections may be produced by just a few reflecting surfaces, the other reflections possibly being internal multiples. Because the acoustic intensity does not appear to be significantly reduced by these reflectors, their interpretation as sand or gravel strata is not favoured. Instead, it is suggested that they may be silt strata, or sand or gravel disseminated in a muddy matrix (c.f. Dale, 1979).

The reflectors are interpreted to have been deposited without significant winnowing or erosion because:

- (1) the acoustic nature suggests that they are composed of coarse material in a fine matrix;
- (2) the reflectors are persistent at variable depths throughout the same basin;



- (3) the entire unit and the reflectors pinch together on steep slopes while maintaining the conformable habit.

The coarser clasts would probably be ice rafted. Alternatively, if the coarse components are not coarser than silt, they could conceivably have been transported and deposited from a turbulent near surface current. Two examples of downbay pinching strata within the upper region of the conformable cover unit suggest a local sediment source, presumably from the adjacent raised deltas.

The conformable nature and the lack of moats or basin-wide erosion suggest that this unit was deposited during substantially quieter conditions. Furthermore, the presence of the 5 metre isopach in 5 metres of present day water depth in the Western Inner Bay (Fig. 4.7) suggests that the quiet water environment was created by a substantial increase in water depth. The quiet conditions may have been augmented by increased ice cover.

### (3) Lower Basin-Fill Environment

On account of the poor data base only tentative environmental conditions can be proposed. The overlapping basin fill morphology suggests that it is similar to the upper basin-fill environment, but the strong reflectors and lack of obvious erosional features suggest that it had a depositional environment similar to that of the conformable unit. If it is correlatable with deeper sediments of the Approaches (where the morphologic character possibly loses its importance), it is indistinguishable from the conformable cover unit. However, in general, the acoustic character sug-

gests rapid sedimentation of coarse clastics. The distribution a high energy environment, preventing deposition in all but the deepest basins. Furthermore, the upward increasing degree of onlap observed in basin G suggests that the sea level was rising.

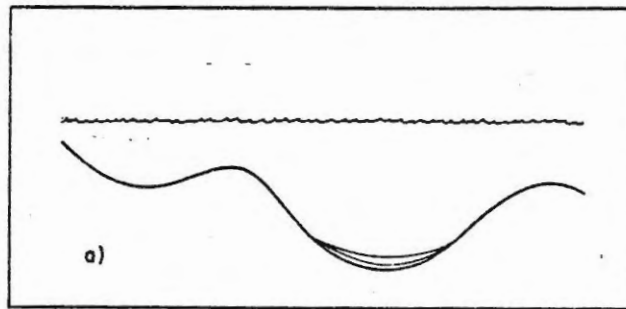
#### 4.6 Model of Acoustic Stratigraphy

The series of sketches in Figure 4.9 outlines the depositional history as interpreted from the 3.5 kHz stratigraphy. Initially, sedimentation was prevented by relatively deep influence of wave energy, possibly following glacial scouring. As the relative sea level rose, sedimentation of coarse clastics comprising the basin-fill unit was permitted in the deepest, well sheltered basins (Fig. 4.9a).

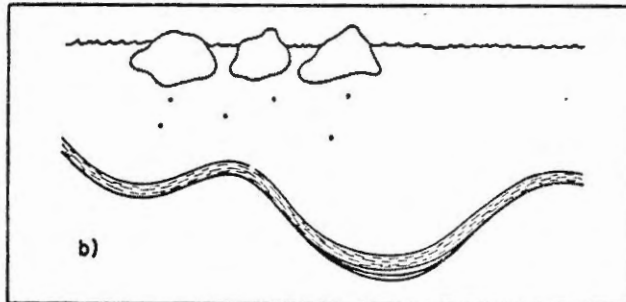
The conformable cover unit was deposited during the highest relative sea level (Fig. 4.9b) with very little influence of wave energy. This may have been augmented by increased ice cover. It is suggested that the extensive, stratified reflectors represent periodic proglacial or relict glacial material. The sedimentation probably had a relatively high rate, terminating at approximately 9,400 years B.P.

The transition to basin-fill sedimentation (Fig. 4.9c) was gradual, both in terms of morphology and acoustic character. The transition is marked by a relative decrease in sea level and a corresponding increasing influence of wave base energy.

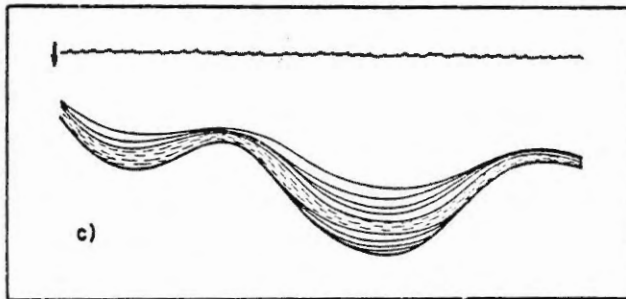
The period of increased basin-wide erosion (Fig. 4.9d) which planed off the upper basin-fill unit in shallow and exposed basins occurred at



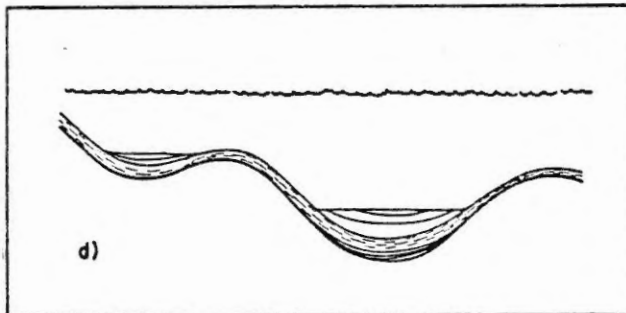
a) Lower basin-fill environment: deposition only in the deeps; influence of wave or current energy, probably with a low relative sea level.



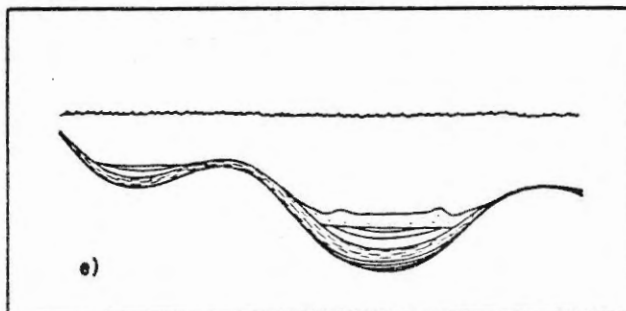
b) Conformable cover environment: wide-spread deposition during high relative sea level with little influence of wave energy terminating at approximately 9,400 years B.P.



c) Transition to basin-fill environment: major deposition in the basins during a decreasing relative sea level and an increasing influence of wave energy on the flanks.



d) Period of basin-wide erosion: basin wide erosion in shallow and exposed basins at approximately 6,000 years B.P.



e) Basin-fill environment (contemporary): continued decrease in relative sea level and subsequent erosion of sediment along the upper flanks and deposition in the basins; moats form at the bases of steep slopes.

Figure 4.9: Model of postglacial development as determined primarily from the acoustic stratigraphy

about 6,000 years B.P. The energy is thought to be wave energy, perhaps increased by a decrease in winter ice cover, exposing the bay to greater storm reworking or by increased runoff and surface circulation.

Normal upper basin-fill conditions (Fig. 4.9e) resumed with normal winter ice cover and a slowly decreasing relative sea level. Wave base energy is augmented by tidal currents and constrictions to form shallow, water, moat and minor basin-wide erosion.

CHAPTER V

LABORATORY TECHNIQUES

Samples from Makkovik Bay include 257 grabs, 15 short gravity cores and 14 land samples collected during 1977 (Piper and Iuliucci, 1978), and 134 short cores, 56 grabs, 44 land samples and two 10 m long piston cores (Barrie, 1978). These were kept at 4°C at Dalhousie University.

The two piston cores and 136 short cores were split, x-radiographed and described in detail. Sediment colours were estimated by A.E. Aksu in fluorescent light using a Munsell rock colour chart. From the piston cores 80 smear slides were made to provide a preliminary analysis of the texture and the relative abundances of microfossils.

Detailed grain size analyses were performed by standard seive and pipette techniques (Piper, 1977) between -1 and 8 phi intervals on 78 grab samples, 58 short core samples (both as class projects), and on 80 piston core samples.

Semi-quantitative x-ray diffraction analyses of the less than 2 $\mu$  fraction from 31 piston cores and 34 surficial samples were performed according to the methods of Piper and Slatt (1977) using the intensity factors and calcium carbonate and iron removal procedures of Piper (1977). Although slow scans were made over the chlorite-kaolinite peaks (24.5° to 25.5° 2 $\theta$ ), the kaolinite peak was frequently difficult to resolve. In addition, the "montorillonite peak" represents all minerals with montmorillonite-like structure, probably including mixed layer clays. Two

representative x-ray diffractograms are shown in Figure 5.1. The results of three Labrador till samples were obtained from Piper and Slatt (1977), one of their samples (L-20) being taken approximately 35 km inland from Makkovik Bay.

Analyses of foraminiferal assemblages were made on 26 piston core and 23 surficial samples. The samples were taken in 10 cm aliquots, dried at 40°C, weighed and dispersed in distilled water. They were wet sieved between 250 and 63  $\mu$  sieves, dried at 40°C and separated by sprinkling carefully on a 3:1 solution of carbon tetrachloride:tetrabromoethane. Large samples were split with a microsplitter and counted, counting between 300 to 500 individuals where possible. Entire samples were examined in fossil-poor sediments. Identification was primarily based on plates and descriptions given by Gregory (1971), Scott (1973, 1977), Hume (1972) and Feyling-Hanssen et al. (1971). Only total populations were examined and these do not necessarily correspond with the living population.

In addition, 15 surficial samples were counted for foraminifera by students as class projects; however, these were separated using only carbon tetrachloride. Both the picked and the sieved portions of these student samples were checked microscopically to verify, and if necessary, adjust the counts or identifications. If any inconsistency remains, it would most likely be dependent on different flotation techniques and therefore would tend to under-represent the agglutinated proportions. Only the actual calcareous/agglutinated ratio from these samples is used in this study.

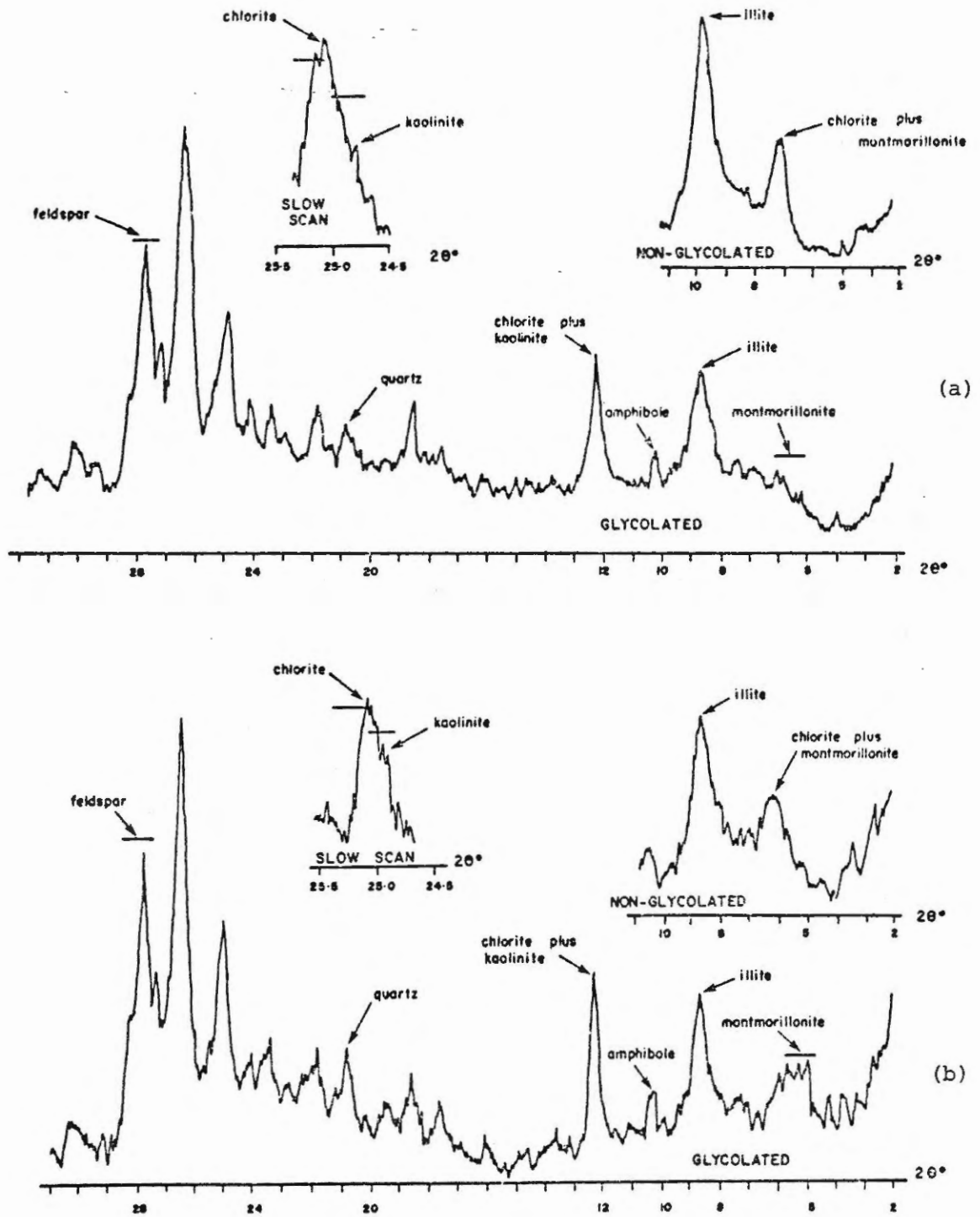


Figure 5.1: Representative x-ray diffractograms of oriented mounts of the less than 2 micron fraction of (a) gray clayey silt and (b) basinal olive mud

During the piston core analysis, it became evident that both piston cores had been labelled incorrectly onboard ship. The cores were recovered in three sections, the identification of the first and third sections being transposed. Although this mistake was confirmed (see Appendix) after subsampling, all the diagrams and sample numbers used in this study are based on the corrected core intervals.



CHAPTER VI

SURFICIAL SEDIMENT DISTRIBUTION

6.1 Purpose

It is important to compare the acoustic stratigraphy with both the piston core sediments and the surficial sediment distribution in order to develop a comprehensive stratigraphic model of basinal deposition. This is the primary mandate of the study of the surficial sediments. In addition, such a study should provide an opportunity for understanding the dominant contemporary processes. In particular, it is necessary to gain tangible surficial evidence of the marginal reworking and redistribution of older sediments, as proposed by Piper and Iuliucci (1978) and suggested by the acoustic stratigraphic model.

6.2 Short Core Sediment Types

Visual and x-radiographic examination of 130 short gravity cores provide the basis for the discrimination of 4 major sediment types, similar to those of Piper and Iuliucci (1978):

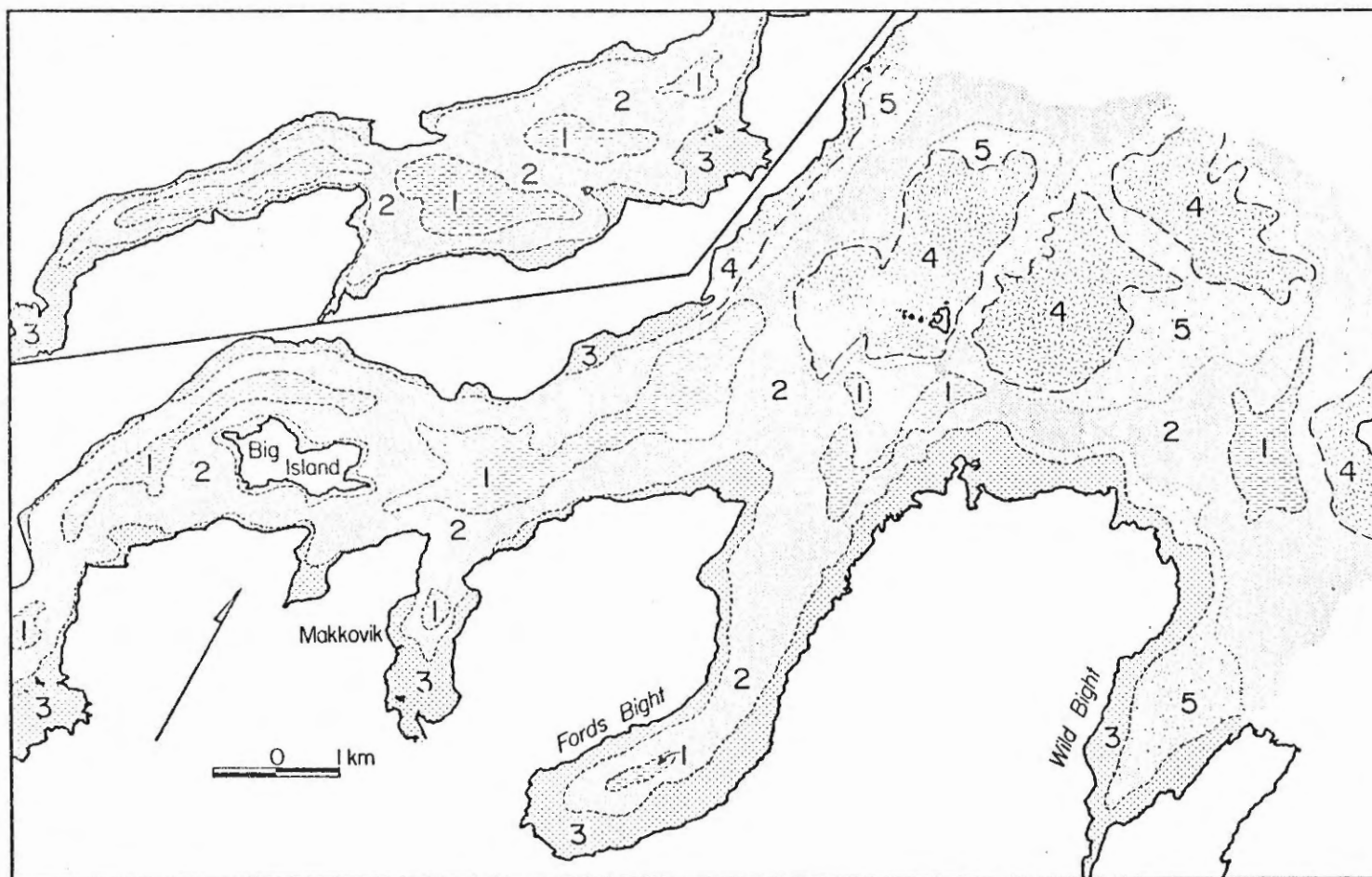
<u>This study</u>	<u>Piper and Iuliucci (1978)</u>
(I) coarse veneer	(3) nearshore sand prism
	(4) coarse sands and gravels among rocky shoals
	(5) veneer of sand and gravel
(II) olive mud	(1) dark mud
(III) coarse olive mud	(2) veneer of gravelly sandy mud
(IV) stiff gray clayey silt	(6) light gray clay

Unit I, the coarse veneer, is equivalent to units 3, 4 and 5 of Piper and Iuliucci (1978), which have been consolidated here as they all represent a contemporary reworked veneer. Unit I varies from a well sorted, medium and coarse sand, to pebble and cobble gravel, sometimes with comminuted shell material on high energy rocky shoals. Gravelly and poorly sorted sands occur at the margins of rocky shoals. The distribution of unit I is indicated in Figure 6.1 as units 3, 4 and 5 of Piper and Iuliucci (1978). These sediments were not examined in detail during the present study.

Unit II is a highly organic, bioturbated olive mud that is ponded in quiet basinal areas. This unit corresponds to unit 1 of Piper and Iuliucci (1978).

Unit III, the coarse olive mud (Unit 2 of Piper and Iuliucci, 1978) was identified primarily by the presence of sandy to gravelly mud horizons found on top and throughout the short cores (Plate 6.1). It occurs along the flanks of the bay. At the top of the flanks the coarse olive mud unit III is abruptly overlain by the coarse veneer unit I, whereas at the basin margins, unit III appears to grade upward into the overlying olive mud unit II.

Unit IV is a stiff, gray clayey silt and corresponds to unit 6 of Piper and Iuliucci (1978). It outcrops and is overlain by the coarse veneer (Unit I) in intertidal and shoal areas, and by the coarse olive mud (Unit III) and possibly the basinal olive mud (Unit II) along the flanks. Solitary and consecutive short cores taken along zones of differential



**Figure 6.1:** Surficial distribution of sediment types according to Piper and Iuliucci (1978).  
 1: dark mud; 2: veneer of gravelly sandy mud; 3: nearshore sand prism; 4: coarse sands and gravels among rocky shoals; 5: veneer of sand and gravel

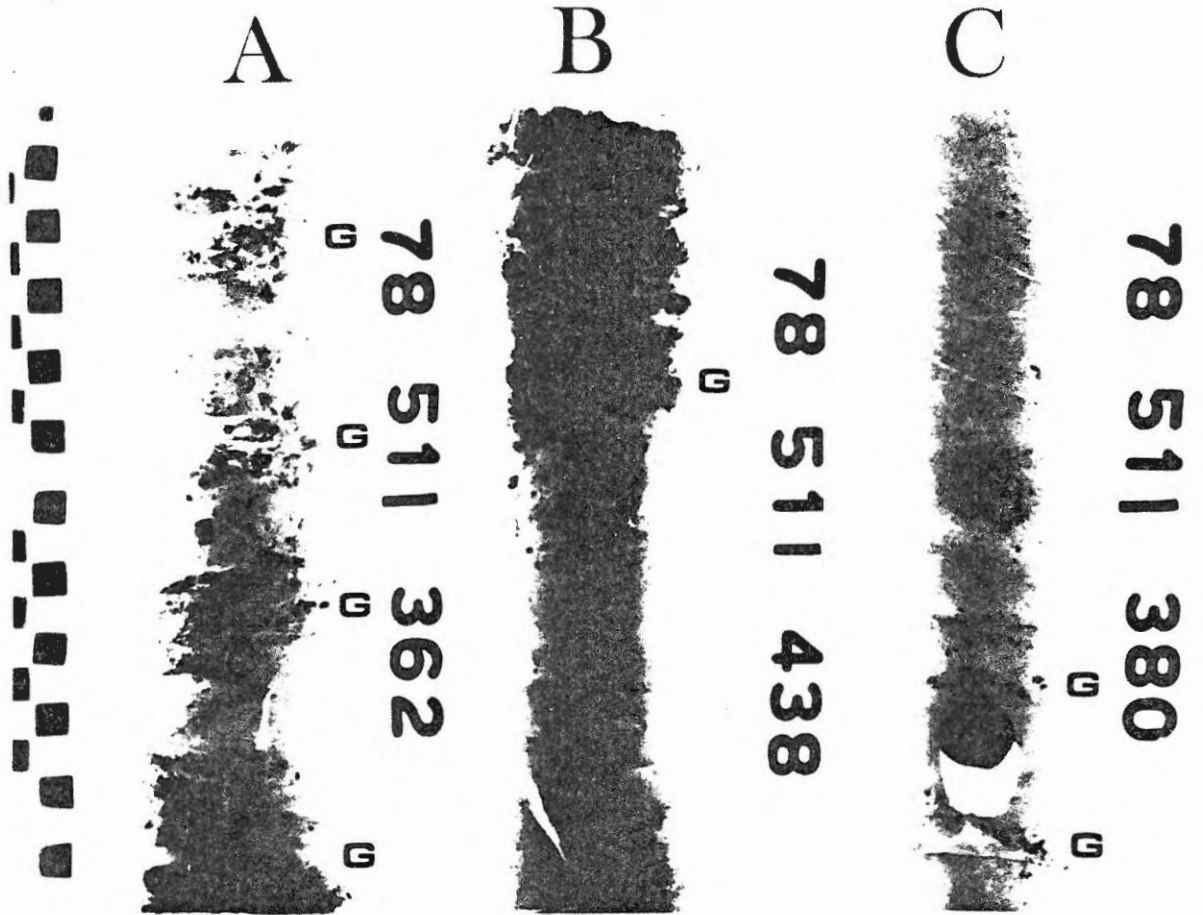


Plate 6.1: X-radiographs of three representative short cores of unit III, the coarse olive mud, showing (a) characteristic gravelly horizons G, (b) unit I, the coarse veneer sharply overlying unit III, and (c) unit III, grading upwards into unit II, the basinal olive mud

erosion (as revealed by the acoustic profiles) suggest an increasing grain size towards the base of the unit. Generally, unit IV is relatively homogeneous, but cores 78-511-525, 531 and 532, located near the base of the unit, have alternating brownish gray and olive-gray beds. Each bed is several centimetres thick with thin basal silt laminae rapidly transitional upwards to mud. Unfortunately the corer did not fully penetrate the gray clayey silt unit. The foraminifera from an exposure of homogeneous gray clayey silt at the head of Makkovik Harbour have been  $^{14}\text{C}$  dated at  $10,275 \pm 225$  years B.P. (GX-6345, Krueger Enterprises Inc., 1979).

### 6.3 Detailed Grain Size Distribution

From a total of 133 detailed grain size analyses of grab samples and core-tops from the short cores (see Appendix) representing all facies, it is apparent that the major trend in surficial sediment texture can be described by the percentage of sand. This is shown in Figure 6.2 as a ternary plot of percent sand plus gravel, silt and clay. Generally the gravel is insignificant. All the data follow a dominant trend from sand to clayey silt with only slight variations in the silt to clay ratio.

However, a surficial map of percent sand is unable to improve the sediment distribution map of Piper and Iulicucci (Fig. 6.1), primarily due to the local variability. Nevertheless, reasonable trends can be resolved if the data are examined in individual profiles from shallow to deep water. Plots of water depth versus percent sand are presented for the major physiographic areas, labelled (a) to (e) in Figure 6.3. Lines joining data points represent individual profiles, usually in order of sampling.

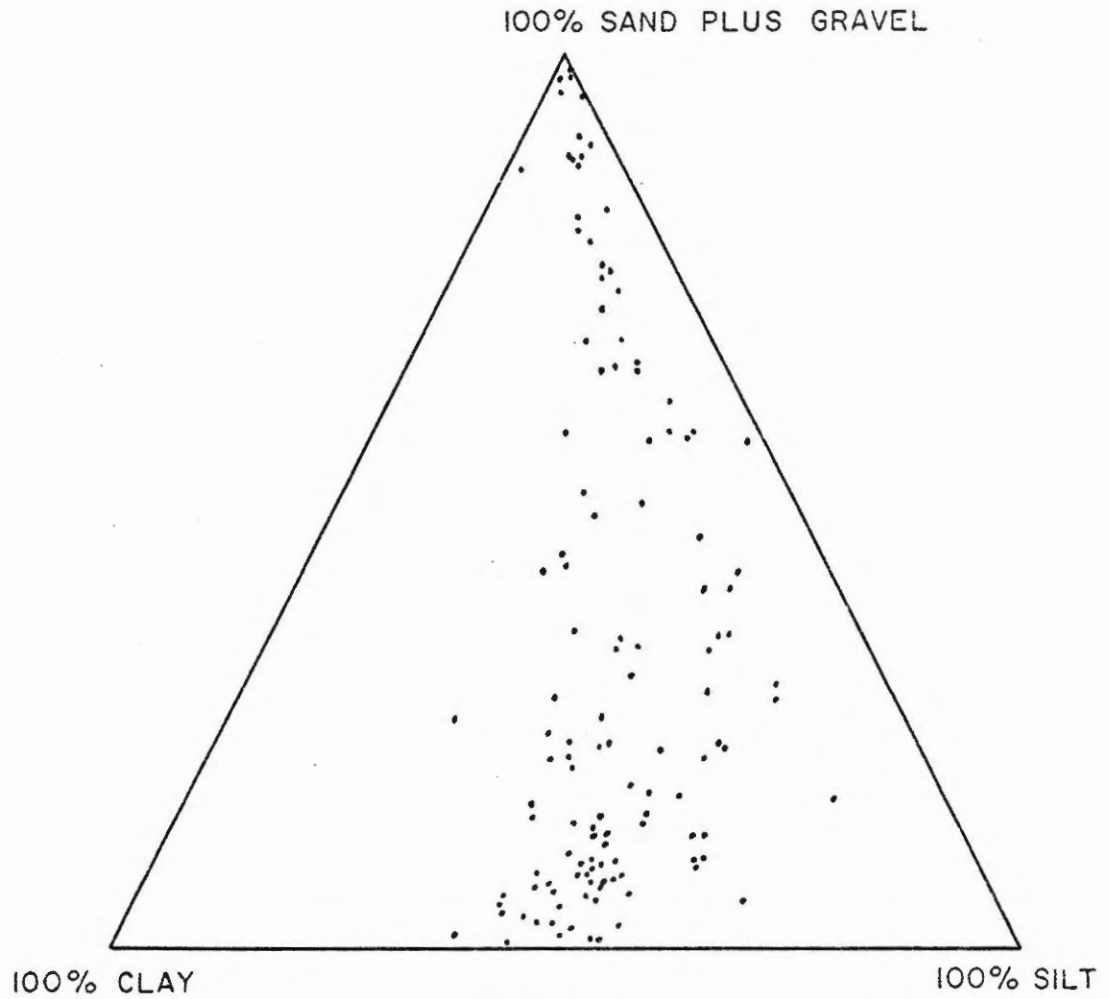


Figure 6.2: Ternary plot of grain-size distributions from all surficial sedimentary units showing the dominant trend from sand to clayey-silt

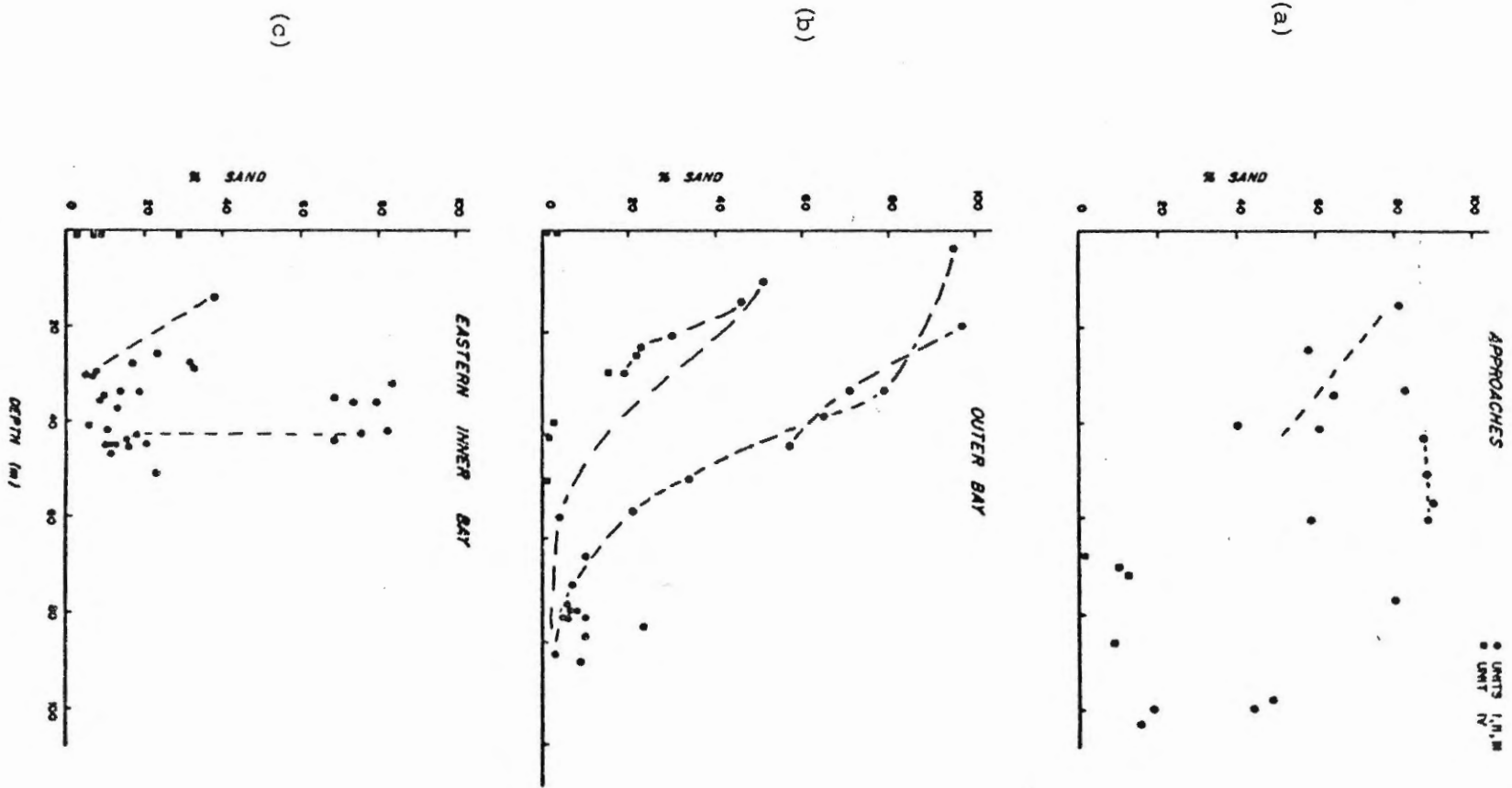


Figure 6.3: Plots of percent sand versus depth for the surficial samples showing an overall upbay fining: (a) the Approaches, (b) Outer Bay, (c) Eastern Inner Bay (e) the Central Inner Bay and (e) Western Inner Bay. Lines joining data points represent individual profiles, usually in order of sampling

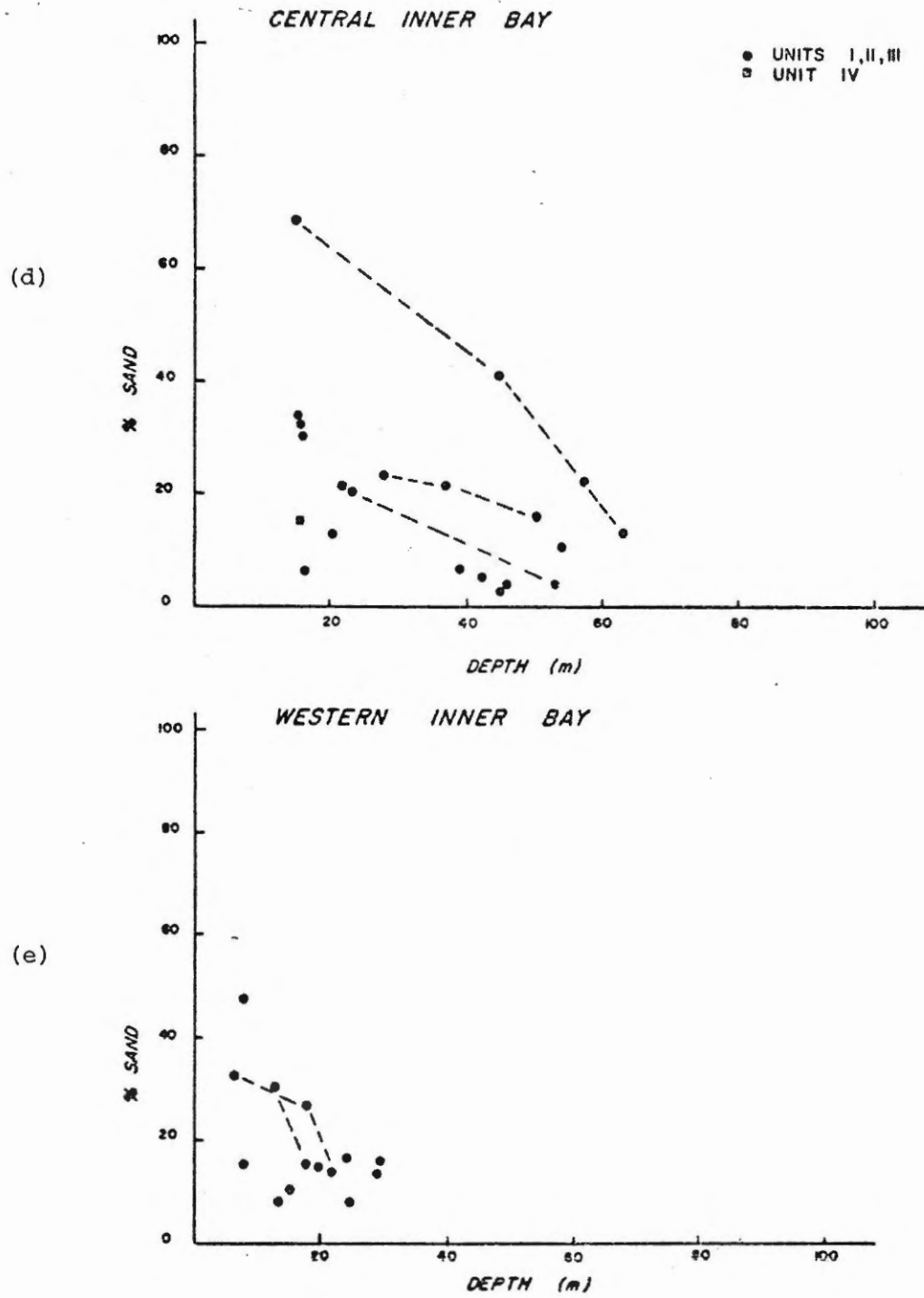


Figure 6.3: Continued



There is an overall fining in an upbay direction with a variable relationship with water depth. In the Approaches the percent sand ranges from over 50% in shallow water to 15-45% at 100 metres depth, whereas in the Outer Bay the 15-40% range is attained by 40 metres depth. The Western Inner Bay has generally less than 35% sand in shallow (< 8 m) water and a range of 5-15% in the basins.

The most complete line of sampling, the Tom's Cove profile in the Outer Bay (Figs. 6.3b and 6.4) best describe an individual profile. A medium sand (unit I) predominates to a depth of 35 metres, decreasing rapidly to coarse silt (unit III) which fines gradually to clayey silt (unit II) by 55 to 60 metres depth. The shapes of other individual profiles are quite variable even though they may be proximal geographically, but profiles with similar geomorphology and degree of exposure do tend to be similar.

An exception to the trend of decreasing grain size with depth occurs in the Eastern Inner Bay where some samples appear abnormally coarse for their relative depth (65-85% sand at 30-40 metre depth, Fig. 6.3c). These particular samples all occur in areas of bay mouth constriction. Also, most of the bays and the Approaches possess a few uncharacteristically fine data points in shoal to intertidal areas. These samples all belong to the stiff gray clayey silt unit (see acoustic stratigraphy, Fig. 4.7).

The silt/clay ratio along the depth profile shows an anomalous increase with depth. If an increasing silt/clay ratio is regarded as an increasing grain size within the silt and clay proportions, then the shallow

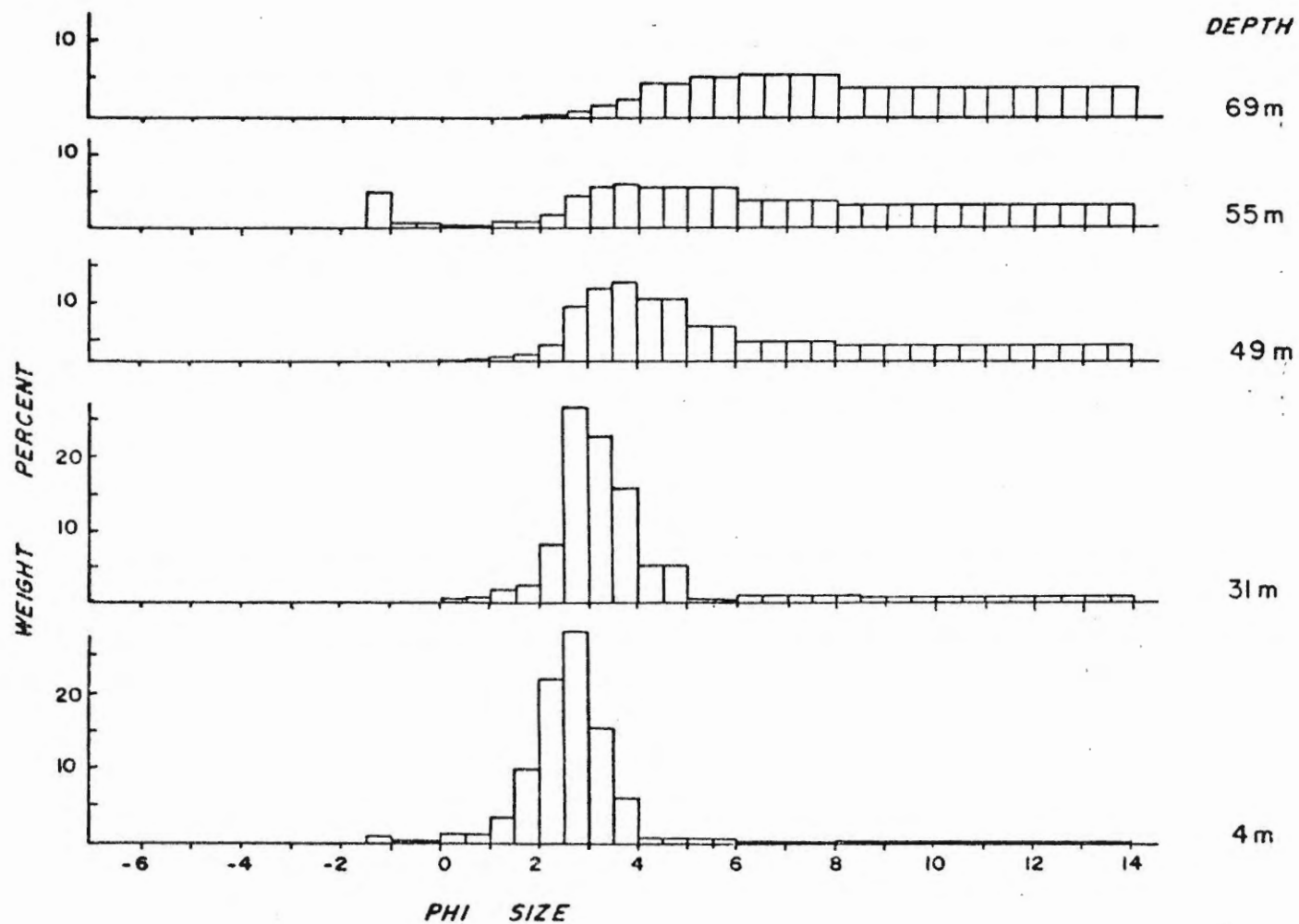


Figure 6.4: Six detailed grain size frequency histograms taken along the Tom's Cove Profile showing the abrupt change from sorted sands down the flanks to very poorly sorted, clayey silt in the basins

water samples of the Outer Bay profiles possess an increasing grain size with depth (Fig. 6.5). (However, it must be noted that this trend is secondary to the dominant decreasing grain size with depth shown by the percentage of sand.) This increase occurs throughout the sandy zone until the coarse silt zone where the silt/clay trend shows a decreasing grain size with depth. For example, in the Tom's Cove profile the silt/clay doubles between 5 and 35 metres depth in the sandy zone then abruptly decreases by more than half between 35 and 55 metres depth throughout the coarse silt zone.

#### 6.4 Discussion

##### Distribution and Stratigraphy

A comparison can be made of the areal distributions of the surficial sediment units (Fig. 6.1) and the acoustic, stratigraphic units (Fig. 4.8) as follows:

<u>Surficial Sediment Units</u>	<u>Acoustic Stratigraphic Unit</u>
I. coarse veneer	shoal non-penetrable unit
II. basinal olive mud	upper basin-fill unit
III. coarse olive mud	conformable cover unit
IV. gray clayey silt	

The best correlation exists between the basinal olive mud and the upper basin-fill both in terms of distribution and character. However, the equivalent unit of Piper and Iulicci (1978), the dark mud, has a less extensive areal distribution. They defined this unit according to

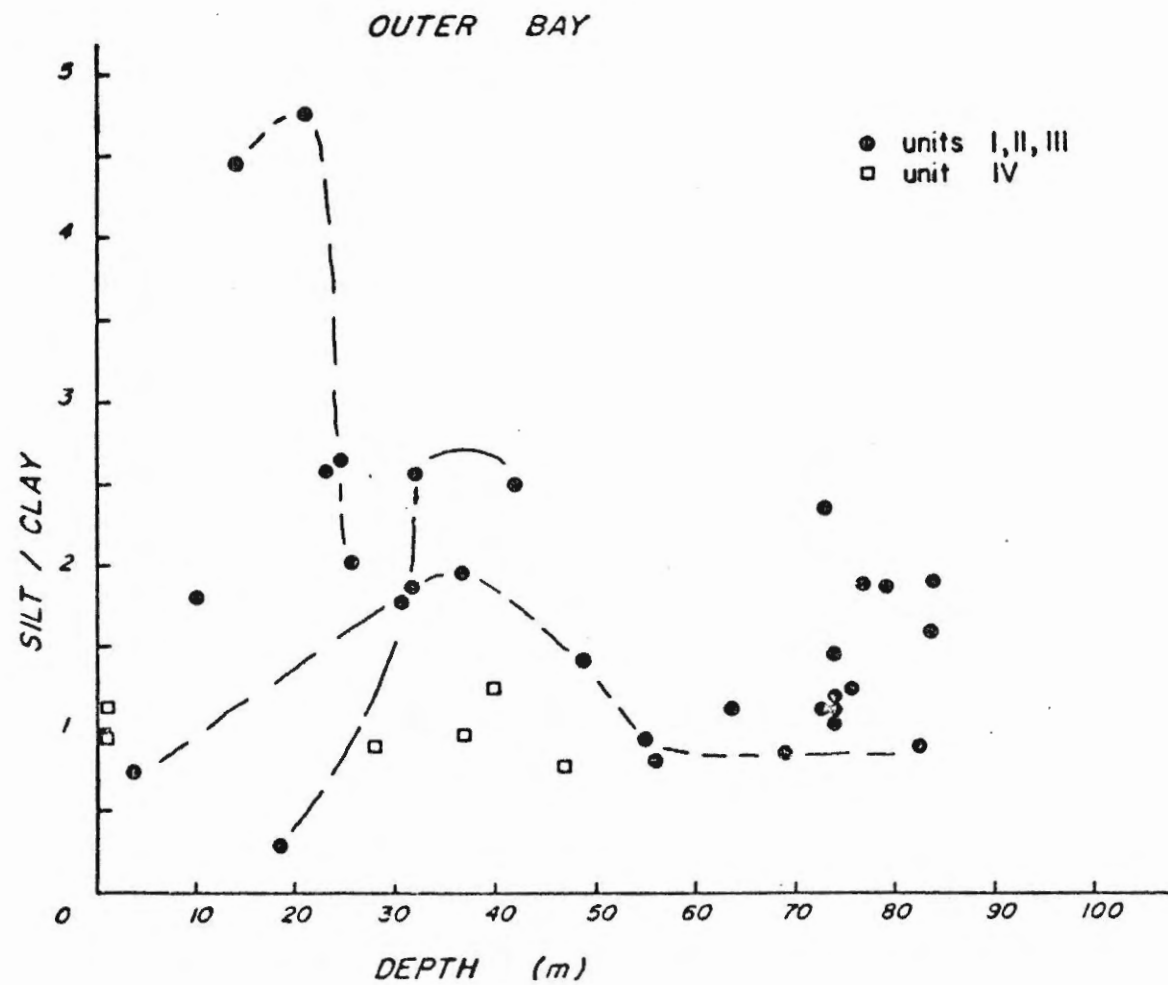


Figure 6.5: Plot of the silt-clay ratio versus depth for the Outer Bay surficial sediments showing an initial increase with depth followed by a decrease to the basin floor. Lines represent individual profiles.

the textural analysis of grab samples and the relatively flat, smooth upper surface as indicated by 14 kHz acoustic profiles. The present study uses the sub-bottom-reflection morphology recorded by the deeper-penetrating 3.5 kHz analogues to identify the basinal muds, allowing observation of the distinct onlapping habit of the basin-fill unit along the lower flanks. This onlapping habit may also be detected in the short gravity cores where the olive mud (unit II) overlies the coarse olive mud (unit III) (Plate 6.1c). Therefore, the acoustic basin-fill unit has a greater surficial distribution than the basinal sediments of Piper and Iuliucci (1978).

The coarse veneer, unit I, corresponds to the shoal non-penetrable unit defined by the 3.5 kHz acoustic stratigraphy (Fig. 4.7). The surficial distributions of these two units have conspicuous similarity. The non-penetrable unit is defined only by reflective character and therefore may be bedrock, till or coarse sediments. The surficial sediment distribution has indicated that a coarse clastic veneer occurs in these areas. In addition, the upflank erosion of sediments observed in the acoustic profile suggests that this reflector is often bedrock with only marginal clastic veneers in the high energy areas. In places such as the Tom's Cove Profile (Fig. 6.3b), the coarse veneer (unit I) fines gradually downflank in the form of a reworked veneer of the coarse olive mud (unit III). The fine portions of this veneer are resolvable only by detailed grain size analysis (discussed later).

The surficial distribution of the conformable cover acoustic unit corresponds to both unit III, the coarse olive mud, and unit IV, the gray

clayey silt. Only gray clayey silt was sampled by short cores along erosionally truncated strata of the conformable cover unit. The suggested upward transition from bedded silts and clayey silt to homogeneous clayey silt within unit (IV) suggests a decrease in depositional energy.

Because (1) the basinal olive mud (unit II) overlies the coarse olive mud (unit III) in some cores, (2) the coarse olive mud overlies the gray clayey silt (unit IV) in other cores, and (3) the coarse olive mud occurs near the top of the conformable cover unit, the coarse olive mud (unit III) is interpreted to lie stratigraphically between the basinal olive mud (unit II) and the gray clayey silt (unit IV). This is at variance with Piper and Iuliucci (1978) who interpreted this unit as a veneer of gravelly sandy mud deposited slowly in a zone of sediment bypassing. This difference in interpretation can be explained by the fact that the 3.5 kHz sounder affords significantly greater depth of penetration, thereby providing improved stratigraphic interpretation. Also, numerous short cores taken during this study provide direct stratigraphic evidence. The gravelly horizons observed in the short cores are generally matrix supported, suggesting that they were deposited rapidly by episodic ice-rafting.

The possibility that the coarse olive mud of unit III occurs only at the upper boundary of the conformable cover unit cannot be precluded. It is conceivable that the coarse olive mud and the gray clayey silt are bedded alternately throughout the conformable cover unit. The prominent acoustic stratification may be a summation of the effects of (1) bedding within the gray clayey silt, (2) alternation of coarse olive mud and gray clayey silt, and (3) the gravelly horizons within the coarse olive mud.

Furthermore, in some basins (e.g. Plates 4.3, 4.4, 4.5) the prominent acoustic strata are separated by more acoustically transparent sediments, often possessing basin-fill-like morphology. The stiff, resistant nature of the gray clayey silt would explain why it is the only sediment sampled along zones of erosionally truncated strata of the conformable cover unit. Unfortunately, none of the short cores fully penetrated the gray clayey silt and, therefore, there is no direct evidence for this hypothesis.

The grain size distribution of the gray clayey silt of unit IV in the Outer Bay is similar to the sediments presently found below the 50 metre isobath (Fig. 6.3b), suggesting that the gray clayey silt was deposited when the relative sea level was at least 50 metres higher than at present.

#### 6.5 Clay Intertidal Platforms

All the intertidal platforms studied (Chapter II) were composed of the stiff gray clayey silt (unit IV). Burrowing clams augment erosion of this unit; however, its stiff nature and the protective coarse veneers make the outcrops relatively resistant. The surficial distribution of acoustic units (Fig. 4.8), individual acoustic profiles (e.g. Plates 4.6, 4.7, 4.9, 4.10), and the texture of the gray clayey silt all suggest that the intertidal platforms are outcrops of the conformable cover unit (Fig. 6.6). The model envisages a falling sea level that erodes the overlying marine muds leaving the resistant, gray clayey silt unit, eroded only by direct wave action. The platforms exist by virtue of the stiff, resistant nature of the clayey unit, and thereby provide a collecting site for the coarse clastics, including the boulder barricade. The boulder barricades

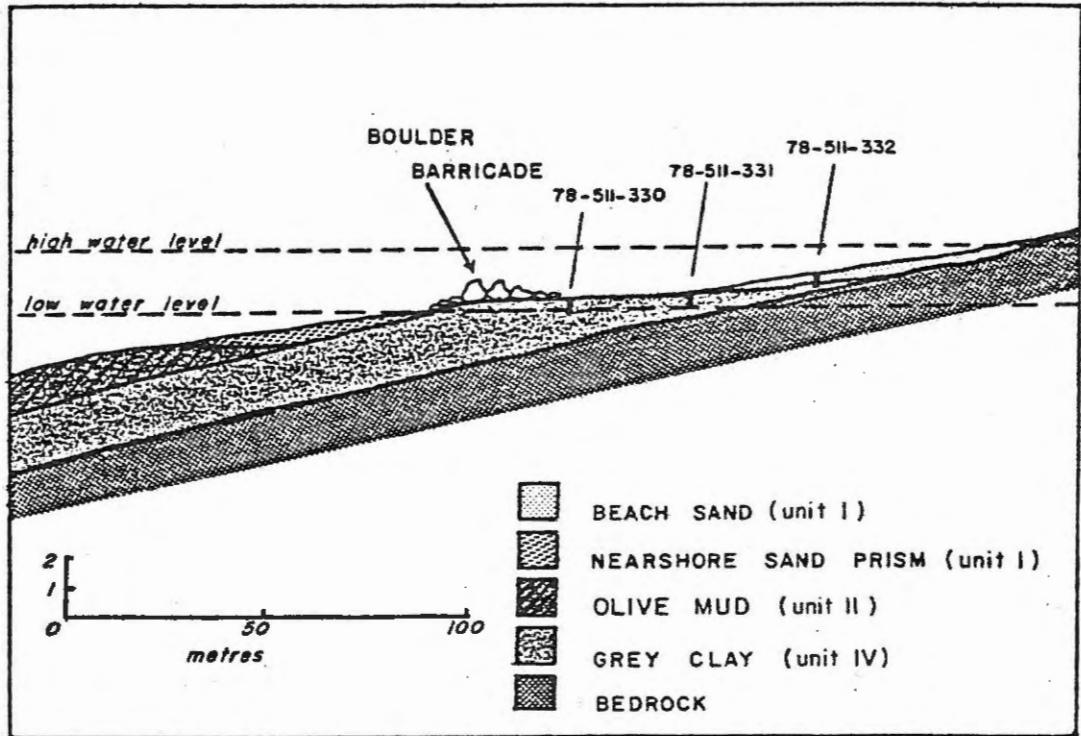


Figure 6.6: Cross-sectional profile of the clay intertidal platform west of Kennedy's Cove showing the veneer of coarse clastics (unit I) over relict gray clayey silt (unit IV) and the locations of three hand cores



and platforms require the presence of the gray clayey silt unit and hence it is proposed that these platforms be termed "clay intertidal platforms".

These clayey outcrops also exist at depth in more energetic environments. Examples are shown in Plates 4.7 and 4.8. However, because they are not directly controlled by the waves and tide, they do not usually occur as extensive, relatively horizontal platforms.

#### 6.6 Interpretation of Grain-Size Trends

The systematic variation of surficial grain size with depth from the nearshore to basinal zones (e.g. Tom's Cove Profile, Fig. 6.3b) suggests that the coarse veneer (unit I) extends down the flanks as a thin, fine-grained veneer overlying the coarse olive mud. The sandy nearshore sediments (unit I) represent the coarse residue remaining from wave-reworked sediments. The basinal olive muds (unit II) represent the fines that are winnowed out and distributed in suspension throughout the bay, eventually being deposited in the quiet, deep basins. The flanks are intermediate in that there appears to be some winnowing of the coarse olive mud (unit III) and possibly minor deposition from the coarser, suspended fraction of the reworked coarse veneer (unit I). Although the Tom's Cove Profile transcends different outcropping units, the grain size trends indicate a relatively uniform, depth-related change. Therefore, the contemporary environment can be regarded as wave-dominated (Fig. 6.7).

The relative depth of the reworked, sandy nearshore zone depends upon the general energy of the environment and specifically, on the variability of the wave climate. The lower limit of reworking is approximately 80

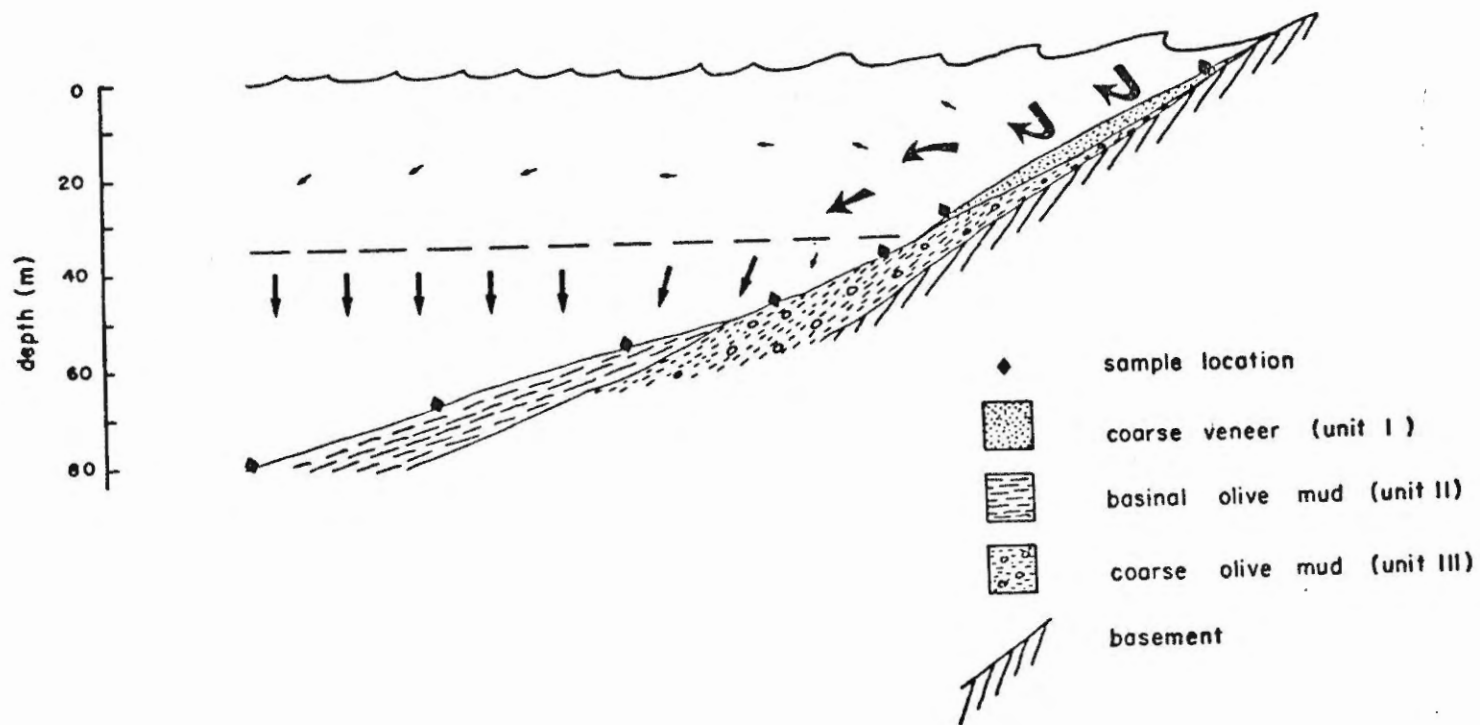


Figure 6.7: Schematic description of the mode of deposition along Tom's Cove Profile showing winnowing, transportation and deposition as controlled by the relative depth of wave disturbance

metres water depth for the Approaches, 30 to 50 metres for the Outer Bay, and 10 to 20 metres for the Inner Bays. These are proportional to the shoreline energy levels according to the height of the wave wash zone (Fig. 2.2). This depth limit is a relative measure of the degree of exposure for a given basin where the total exposure is a summation of current, wave and swell effects, all of which may be locally augmented by the confined nature of the inlet.

The trends of silt/clay ratio with depth, as observed in Makkovik Bay, possibly allow observation and interpretation of secondary trends. In general, an increase in the silt/clay ratio can be caused by an increasing silt fraction with respect to the clay, or a decreasing clay fraction with respect to the silt. The dominant textural trend is one of decreasing grain size with depth. As the mode passes from sand to silt there will be an overall increase in the silt content and therefore the silt/clay ratio will increase. As the sediment fines further, the mode remains in the silt range but the clay proportion increases; therefore the silt/clay ratio will decrease. According to this mechanism, as the mode decreases down-slope from sand through silt to clayey silt, the silt/clay ratio will increase from the sandy to silty modes, and decrease from the silty to clayey silt modes. These trends can be observed in Figures 6.4 and 6.5.

However, another interpretation is also possible. If the silt/clay ratio increases in shallow water and is regarded as a decrease of clay with respect to silt, then a fine grained source or deposition of fines is required in the nearshore zone. High tide deposition of muds is not favoured because the total clay percent increases with depth in the sandy

nearshore zone. Alternatively, the fine grained source could be a marginally eroding, muddy sediment, eroding beneath a thin, active nearshore sand or higher, along the upper unconsolidated sediment. The presence of the gray clayey silt unit is consistent with this model. Unfortunately there is no direct textural evidence in the contemporary sediments that supports any hypothesis, nor even confirms the premise that there is an actual decrease in the proportion of clay with depth. The decreasing grain size with depth is the dominant trend and may obscure such secondary trends. On the other hand, acoustic evidence can be found that clearly indicates outcropping fine sediment located high on the flanks above coarser sediments. Figure 6.8 shows the textural facies superimposed on a line tracing of an acoustic profile made near Big Island. This is directly analogous to the clay intertidal outcrops. The marginally eroding sediments are reworked down the steep flanks to form the coarse clastic veneer. However, this does not necessarily indicate that there is a secondary trend of decreasing clay content with depth throughout the coarse veneer.

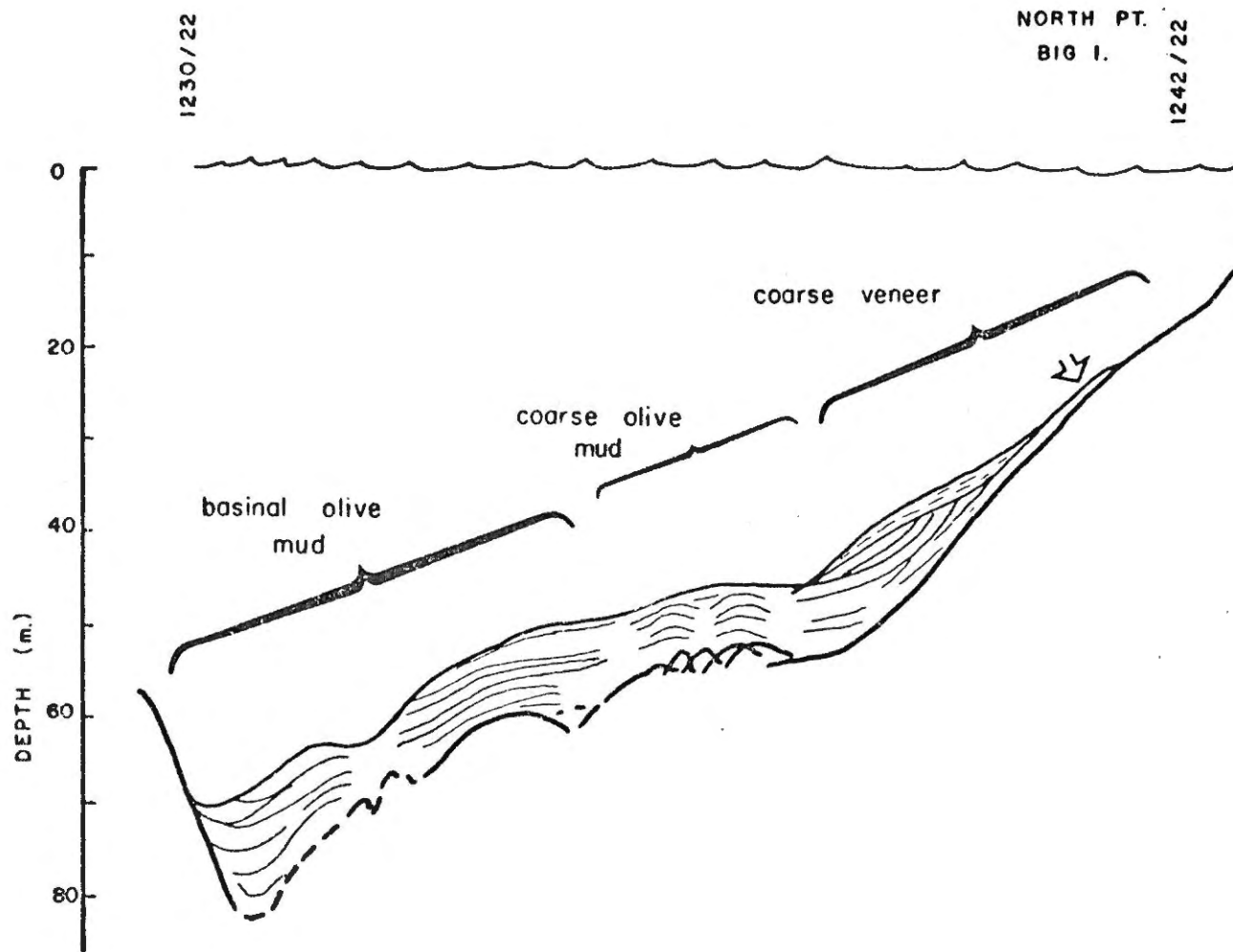


Figure 6.8: Superposition of the Tom's Cove Profile grain-size distributions on the 3.5 kHz seismic profile 1230-1242/22, taken on the north side of Big Island

CHAPTER VII

PISTON CORE FACIES DESCRIPTIONS

7.1 Introduction

The primary objective of the piston core stratigraphy is to identify and describe the lithologic facies with the hope that they can eventually be correlated with the acoustic stratigraphic and surficial sedimentologic units. Such a compilation would refine previous depositional interpretations.

One piston core (78-020-003) was taken from the Approaches, southwest of Strawberry Island, and one (78-020-004) from the mouth of the Outer Bay, adjacent to Ikey's Point. These locations are shown on the base map, Figure 3.1 (in pocket). Site locations were determined by Loran C navigation and adjusted according to bathymetry.

7.2 Facies Descriptions


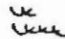



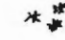
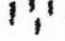


The following facies and subfacies are identified on the basis of detailed core description, x-radiographs, smear slide examination and detailed grain size analysis:

FACIES A	Diatom-rich, olive mud
FACIES B	Dark olive mud
FACIES C	Gray-brown mud
FACIES D	Olive-gray mud

## COLOUR

	MEDIUM OLIVE GREY (5Y 4/2)
	GREYISH OLIVE (10Y 4/2)
	DARK GREYISH OLIVE (10Y 3/2)
	GREY-BROWN (5YR 3/2, 5YR 4/1)
	OLIVE GREY (5Y 4/1)
	DARK YELLOWISH BROWN (10YR 4/2)
	YELLOWISH OLIVE GREEN (5GY 4/2)

## LITHOLOGY - XRADIOGRAPH

	MUD
	FAINT WISPY LAMINATION
	SILTY LAMINATION
	NORMALLY GRADED BED
	PEBBLES, GRANULES
	SHELLS AND FRAGMENTS
	BIOTURBATION
	IRON SULPHIDE-FILLED BURROWS
	GAS EXPANSION CRACKS

Key for Figures 2.1 and 2.2

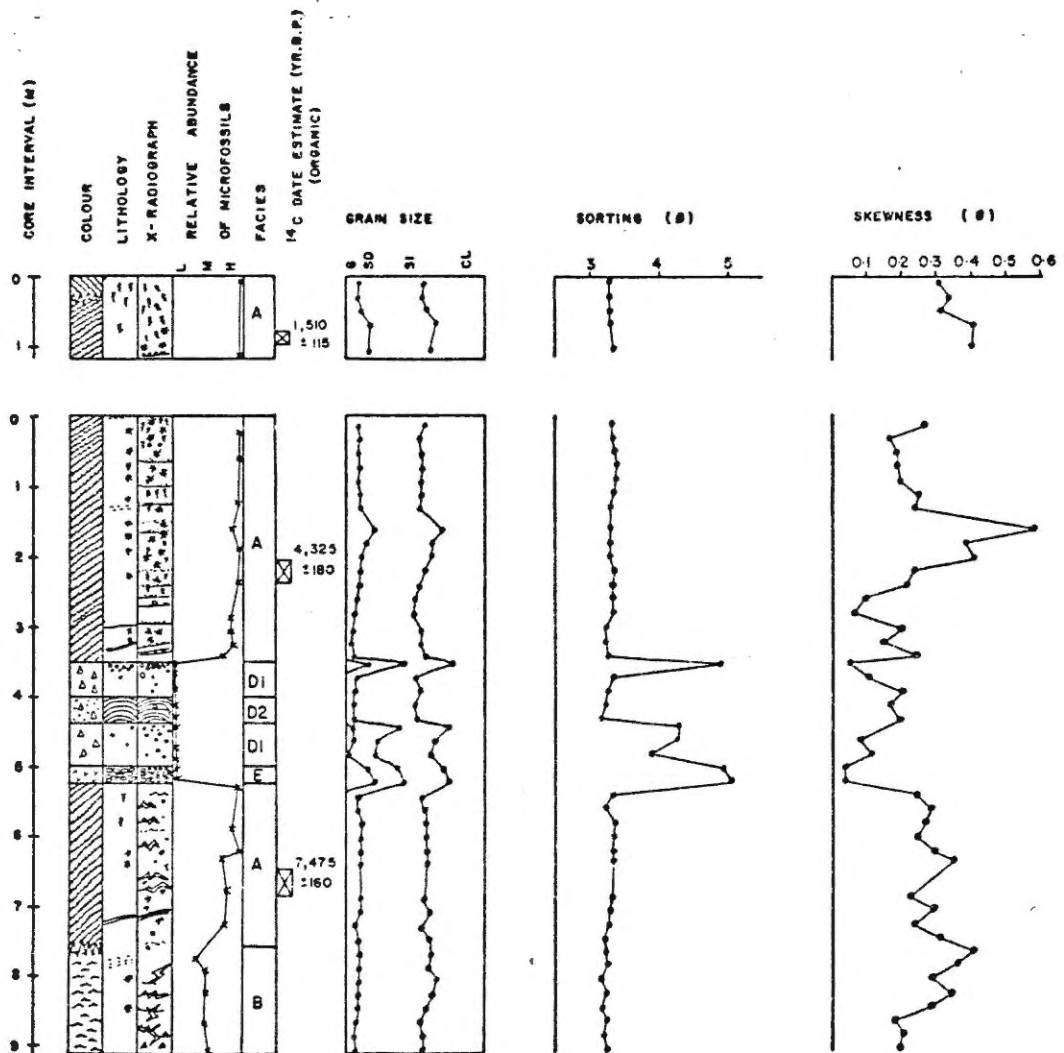


Figure 7.1: Colour, lithology, x-radiography, relative abundance of microfossils and granulometry of piston core 78-020-003



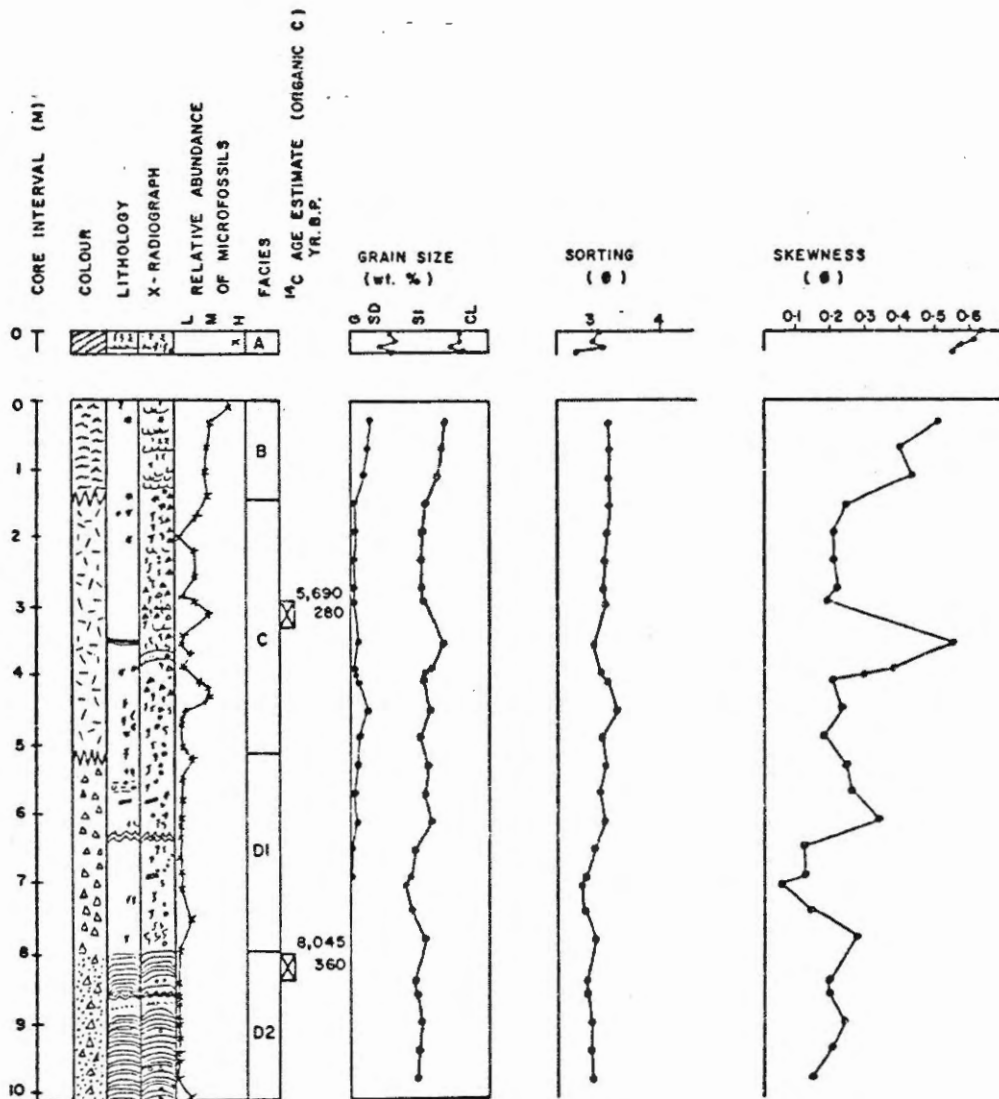


Figure 7.2: Colour, lithology, x-radiography, relative abundance of microfossils and granulometry of piston core 78-020-004

D-1	Massive bedded
D-2	Graded silt and mud
FACIES E	Yellow-green, gravelly mud

The sections shown in Figures 7.1 and 7.2 illustrate the nature and distribution of these facies.

#### Facies A

Facies A is usually grayish olive (10 Y 4/2) except when located at the tops of cores where it is medium olive gray (5 Y 4/2). It is a poorly sorted clayey silt with approximately 10% fine sand. There is a high relative abundance (greater than 5%) of microfossils, principally well preserved, discoid diatoms.

The x-radiographs show distinct small cycles of sediment types a few centimetres thick. At the base is found a continuous laminae of silt to fine sand (Fig. 7.3). Such laminae contain slightly less relative abundance of microfossils and grade upward into a poorly stratified bed of clayey silt containing abundant shells and shelly fragments. This grades upward into a highly bioturbated and homogenized bed of clayey silt. This upper unit is not always present.

Facies A has a generally uniform grain size distribution with a broad mode around 5 phi. Changes in skewness indicate minor variations within this sediment distribution (Figure 7.4). The laminae possess the most prominent mode, with the dominant shoulder on the coarse side, at 4 phi. The overlying shelly horizon has a reduced peak (still at 5 phi) with the dominant shoulder on the coarse side, at 6 phi. The bioturbated clayey

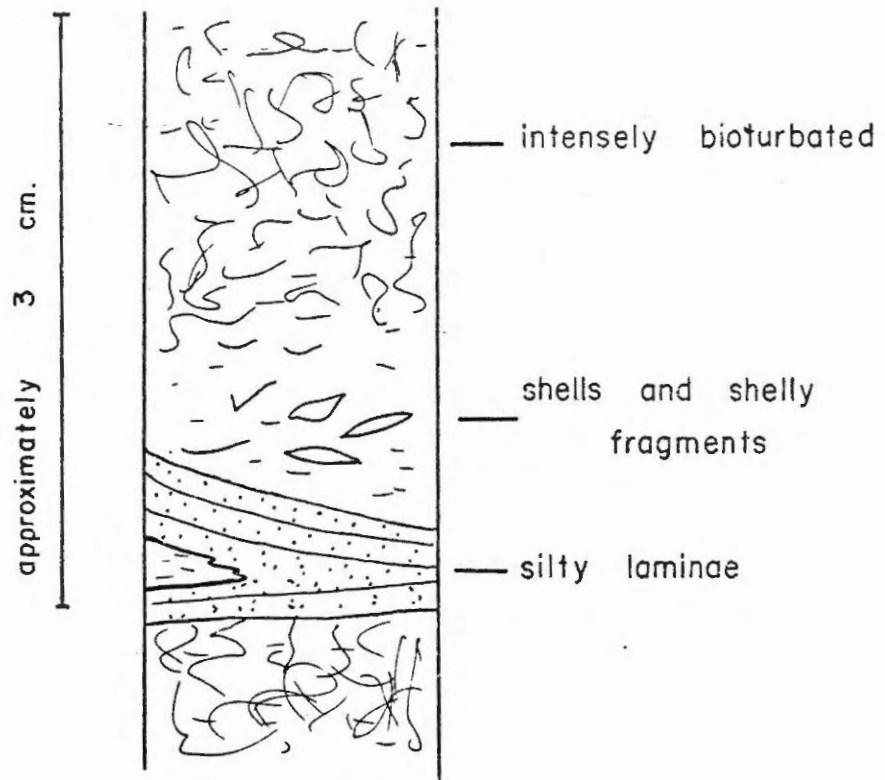


Figure 7.3: Sketch of x-radiograph of core 78-020-003 at the 160 cm. interval showing the flat based silty laminae, shelly fragments and the upper intensely bioturbated mud of facies A

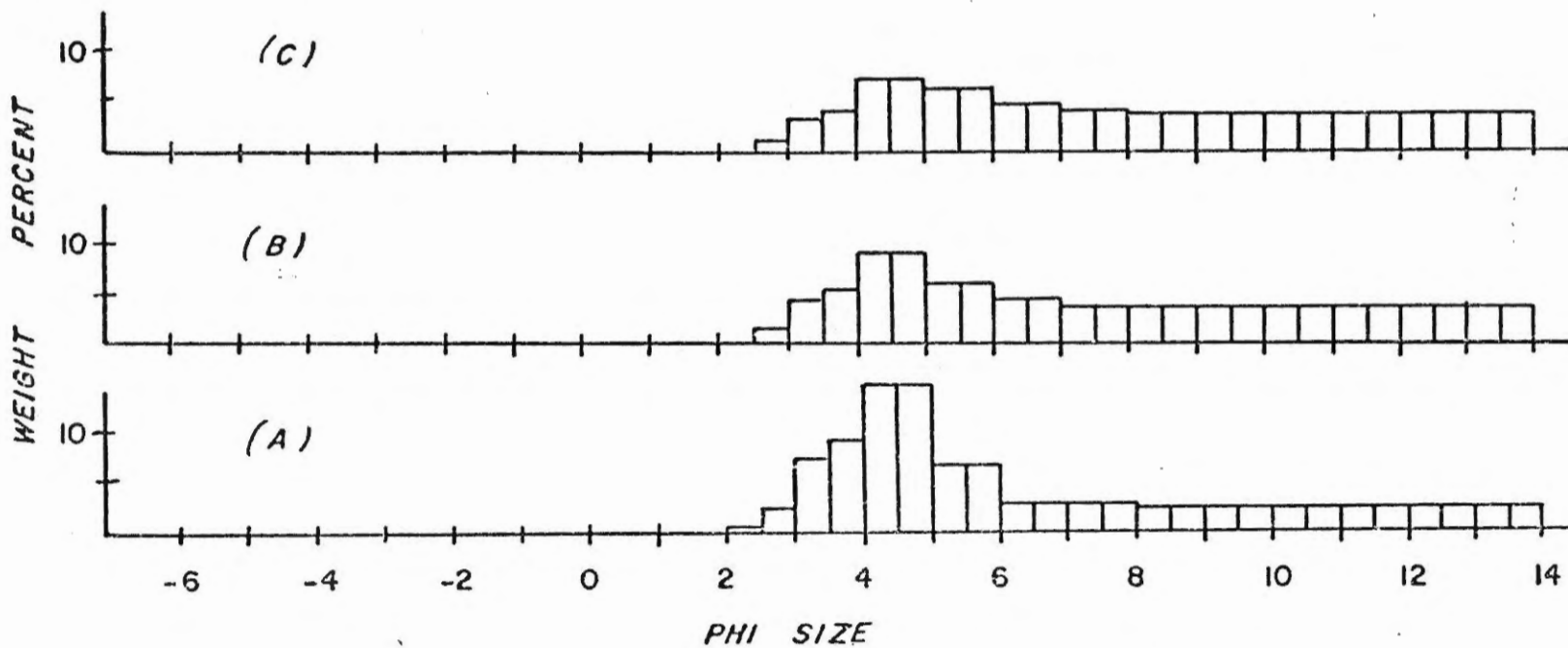


Figure 7.4: Modal analysis of facies A shows a decreasing primary mode, a shift of the dominant shoulder from 3 1/2 to 6 phi, and an increasing fine tail proceeding from (a) silty laminations through (b) shell and shelly fragment beds, to (c) bioturbated clayey silt

silt has the least prominent mode (still at 5 phi) and the highest silt and clay proportions. These upward transitions are consistent with a decreasing skewness. The decreasing primary mode and the shift of the dominant shoulder indicate a progressive decrease in the energy of deposition above the silt laminae.

Where facies A is located near the bottom of the core it contains slightly fewer micro- and macrofossils but has numerous gas expansion cracks tentatively attributed to methane production.

#### Facies B

This is a dark grayish olive (10 Y 3/2), very poorly sorted clayey silt with a moderate abundance of microfossils, fewer macrofossils than facies A and variable bioturbation. Small, isolated dark mottles, tentatively identified as iron sulphide mottles (Stow, 1977; Berner, 1974) occur throughout facies B. Faint, wispy laminae are observed in the x-radiographs (Fig. 7.5).

Facies B is present in both cores forming a unit slightly more than 2 cm thick. In both instances the sand content increases upwards from 5% to 10% at the tops of the units. Similarly the skewness increases from approximately 0.2 to over 0.4. This is related to the increasing 5φ mode, primarily at the expense of the 6φ fraction (Fig. 7.6).

#### Facies C

Facies C is a gray brown (5 YR 3/2, 5 YR 4/1), clayey silt with less than 10% fine sand. It is characterized by a positively skewed, coarse

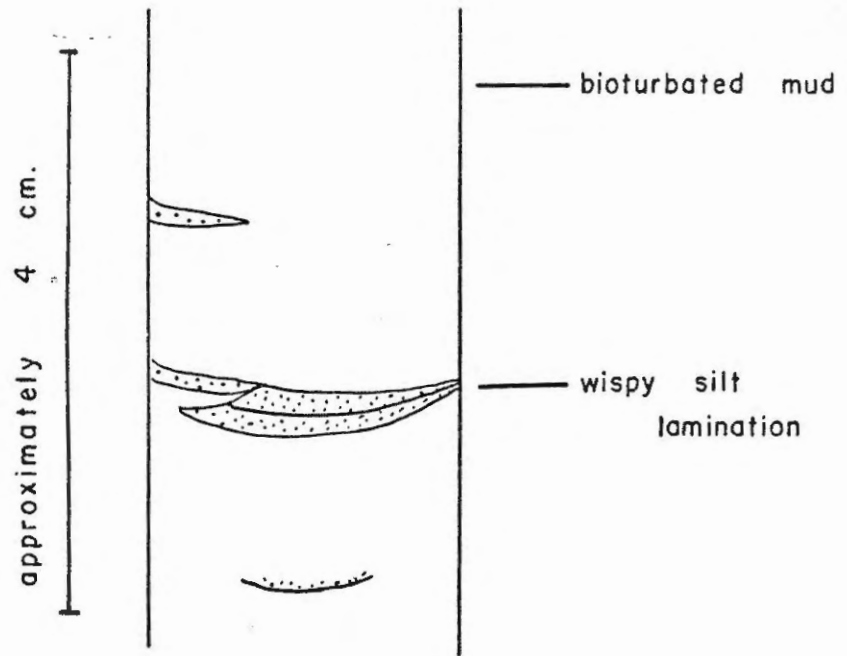


Figure 7.5: Sketch of the x-radiograph of core 78-020-004 at the 115 cm core interval showing the wispy silt laminae of facies B

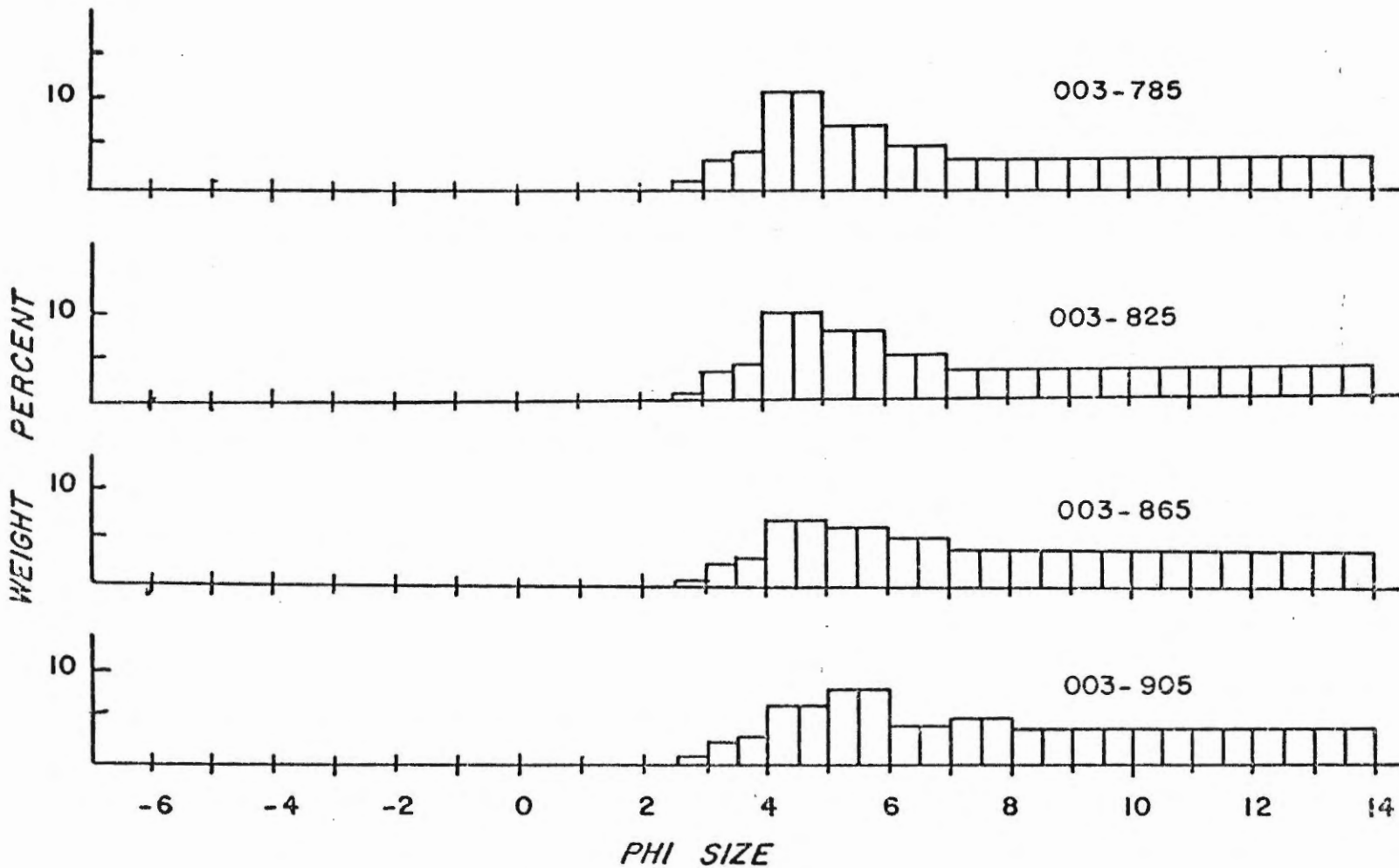


Figure 7.6: Modal analysis of facies B from core 78-020-003 shows an upward increasing primary mode at 5 phi primarily at the expense of the 6 phi portion; the fine (clay) tail remains constant

silt mode with a fine silt to clay soil (Fig. 7.7) and occasional silty, wispy laminations. The relative abundance of microfossils varies from trace to moderate. Shell material is infrequent. Bioturbation and worm-tube-shaped solid pyritic growths are very common and in places form the most conspicuous feature.

#### Facies D

Facies D is an olive gray (5 Y 4/1), poorly sorted, clayey silt (Fig. 7.8) with generally less than 6% sand, and variable bioturbation and dispersed pebbles. Only trace amounts of microfossils are present, mostly as finely comminuted particles (observed under the scintillation microscope). In core 004 facies D has two prominent gas cracks, presumably indicating the anerobic bacterial production of methane.

#### Subfacies D-1

Subfacies D-1 is a massive unit with minor to moderate bioturbation and shelly fragments. Dispersed pebbles are generally rare except in the two units of the Approaches core where the gravel content increases upward to 10-30%. Horizontal stratification occurs in both gravelly areas whereas steeply inclined, faint strata occur in the mud. The x-radiographs suggest that the internal structures in the muddy portion have been deformed during coring, probably without changing the original unit thickness.

#### Subfacies D-2

Subfacies D-2 has bedded couplets (Figure 7.9) of thin (< 1 cm) olive gray (5 Y 4/1) silt alternating with thicker (0.5-3 cm) dark yellowish



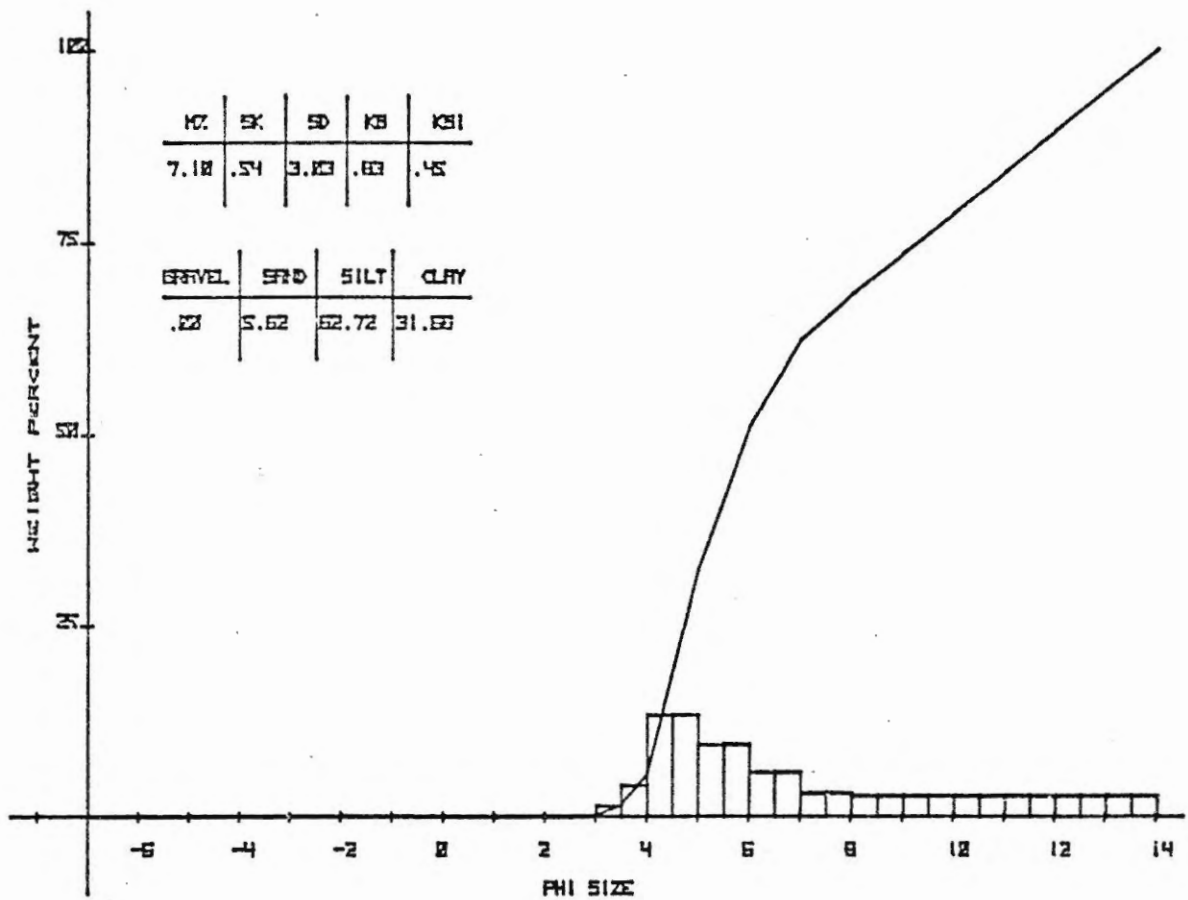


Figure 7.7: Representative grain-size analysis of facies C (78-020-004) indicates a strong primary mode at 5 phi with a reduced fine tail

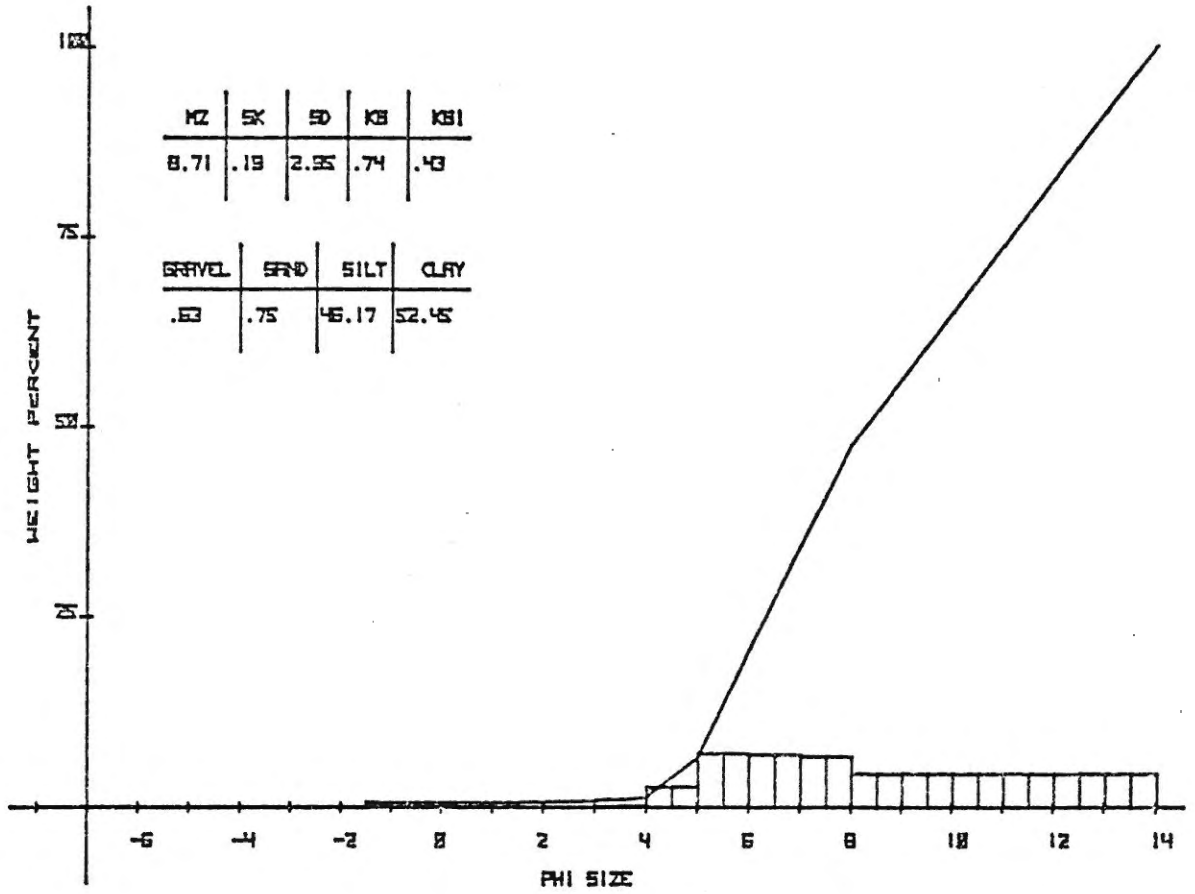


Figure 7.8: Representative grain-size distribution for facies D (78-020-003) showing a broad primary mode from 6 to 8 phi

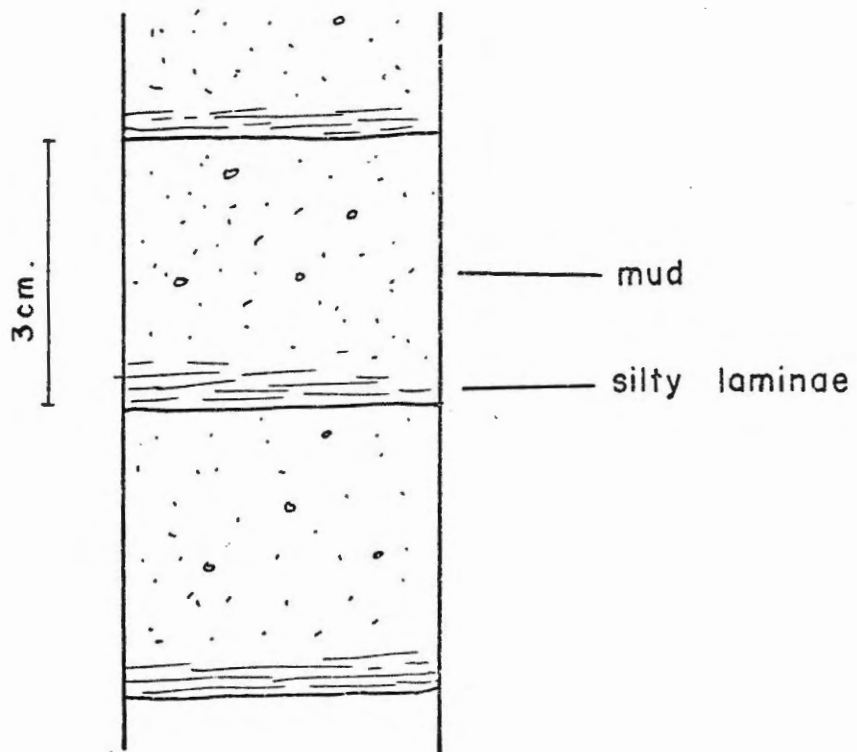


Figure 7.9: Sketch of x-radiograph of subfacies D2 (78-020-004-910) showing the silt-mud couplets

brown (10 YR 4/2) mud with minor sand and pebbles toward the top. The silt appears to be finely laminated in the x-radiographs, and in places, is abruptly transitional to mud. There are a total of 6 relatively coarse couplets in 78-020-003, all dipping 21° within the core liner. Core 78-020-004 contains over 75 couplets with the ratio of silty laminations/mud decreasing upwards, eventually obliterated by the bioturbation of sub-facies D-1.

#### Facies E

Facies E is a yellowish olive green (5 GY 4/2), extremely poorly sorted, gravelly mud. The gravel content ranges from 30-40% and is presumably ice rafted. The muddy fraction has a mode at 5 $\phi$ , similar to the other facies (Fig. 7.10).

No internal bedding traces, macrofossil shell material or bioturbation was observed. Facies E has only trace amounts of microfossils. The basal contact is perpendicular to the core liner whereas the upper contact has an apparent dip of 20° and appears to be disturbed during coring.

### 7.3 Facies Distribution

The distribution of the lithofacies is shown in Figures 7.1 and 7.2. Facies A occurs throughout both trigger weight cores and throughout most of core 003 (the Approaches core). The x-radiographs, percent grain size and skewness all indicate a continuous trend in sediment properties passing upwards from piston core 004 to its trigger weight. This suggests that there is negligible core-top loss between the trigger weight and the

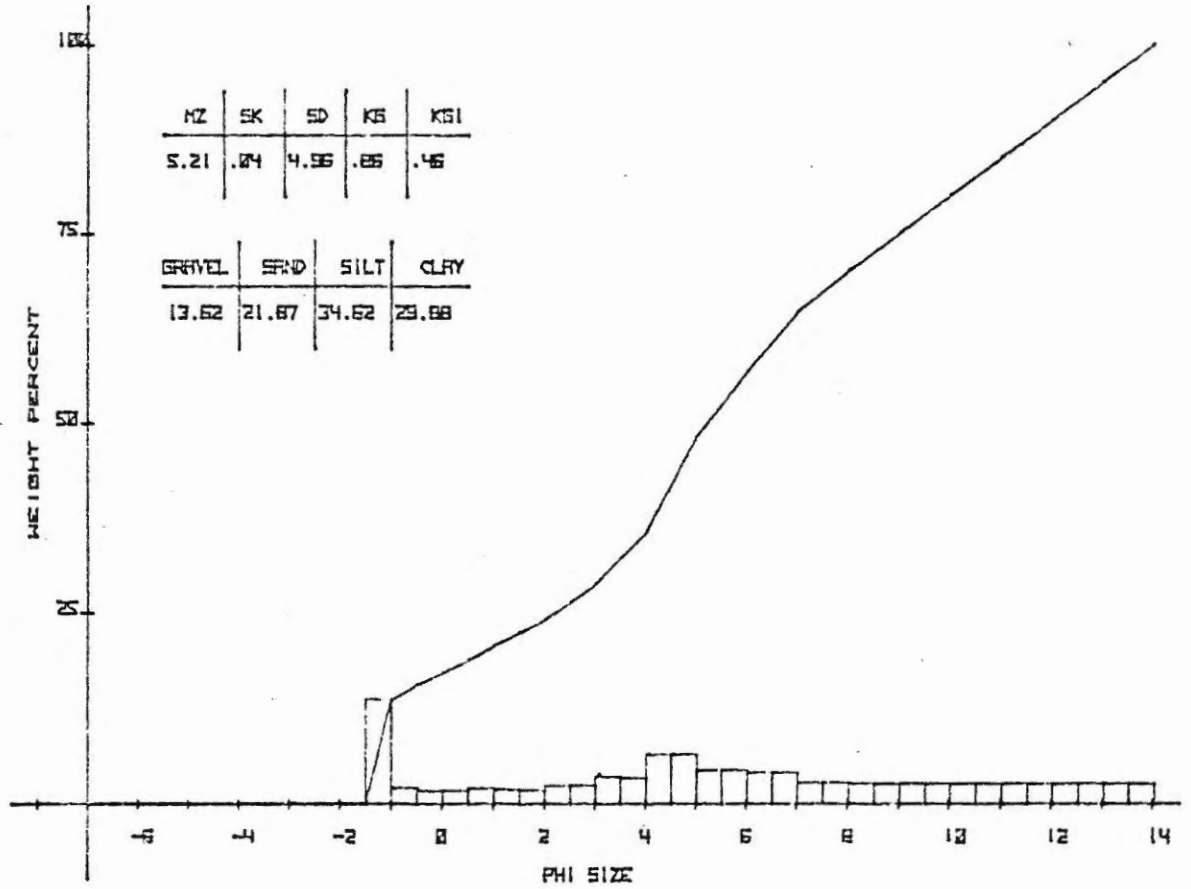


Figure 7.10: Representative grain-size distribution for facies E (78-020-003) shows the extremely poor degree of sorting

piston. The presence of a distinctive silt lamina in both the trigger weight and piston cores suggests a 5-10 cm overlap.

Facies B is present as two 2 m thick units. In core 003 it occurs at the bottom of the core grading upwards into facies A. In core 004 it occurs at the top of the core, not extending to the trigger weight core. Nevertheless, upcore trends of relative abundance of microfossils, percent grain size and skewness all suggest minimal core-top loss in core 004.

Facies C occurs only in core 004, as a 3.5 m thick unit, grading upward into facies B and downward in subfacies D1.

Facies D occurs in both piston cores. At the base of core 004, 2 m of D1 overlie 3 m of D2. In the middle of core 003, a 40 cm thick unit of D2 is found between two 55 cm thick units of D1. All lithologic boundaries are sharp, emphasized in part by the highly variable gravel content.

Facies E occurs only in core 003 as a 30 cm unit beneath facies D and above facies A. Both contacts are sharp.

CHAPTER VIII

PISTON CORE CORRELATION AND FACIES INTERPRETATION

8.1 Introduction

The lithological facies in the piston cores have been described in detail but it is necessary to inter-relate these facies with the acoustic profiles as a first step in the overall interpretation of the stratigraphy. Individual piston cores can be correlated with the nearest acoustic profile and absolute dates from the piston cores can be used to extrapolate ages for the acoustically detected units. Amalgamation of these sources of data should provide a sound basis for a detailed interpretation of the lithologic stratigraphy.

8.2 Piston Core - Acoustic Correlation Techniques

Recent studies (e.g. Dale, 1979) using a short, well defined pulse signal have been unable to correlate with certainty the actual recorded acoustic profile with the geotechnical properties of the cored sediments, although knowledge of the down core acoustic profile is considered to be an asset. The state of the art for core to profile correlation, especially for 3.5 kHz profiles, utilizes equivalent depths within the core and profile, plus the matching of strong reflections with obvious core features such as gravelly or sandy beds.

### 8.3 Piston Core 78-020-003

Piston core 78-020-003 of the Approaches was taken at approximately 55° 09.77'N, 59° 00.17' (Loran C); its location has been adjusted on the base map (Fig. 3.1) according to the sounder depth of 102 metres. Tentative correlation is made in Figure 8.1 with two profiles, 1129/19 and 1212/15 which are approximately 0.6 kilometres apart and probably within 0.4 kilometres of the core site.

The core only samples the upper basin-fill acoustic unit. The strongest reflections presumably correlate with the gravelly unit, facies C and D, since these offer the greatest reflectivity contrast. The reflections clearly suggest the presence of several discrete coarse layers, especially in profile 1129/19. The other lithologic units also appear to be discriminable in the acoustic profile. Facies A has weak reflections that appear to correlate with sandy zones in the core. Facies B appears to possess a slightly enhanced reflection at the upper surface (perhaps as a consequence of upward coarsening, Chapter VII) and possibly an increased 'gray' area throughout. The apparent decrease in acoustic thickness of the lower sedimentary units may be a consequence of a higher acoustic velocity. The bottom of the piston core is approximately 3 metres ( $v = 1500$  m/sec) above the conformable cover unit.

### 8.4 Piston Core 78-020-004

The Outer Bay piston core was taken at approximately 55° 09.07'N, 59° 08.44' W (Loran C); its location has been adjusted on the base map



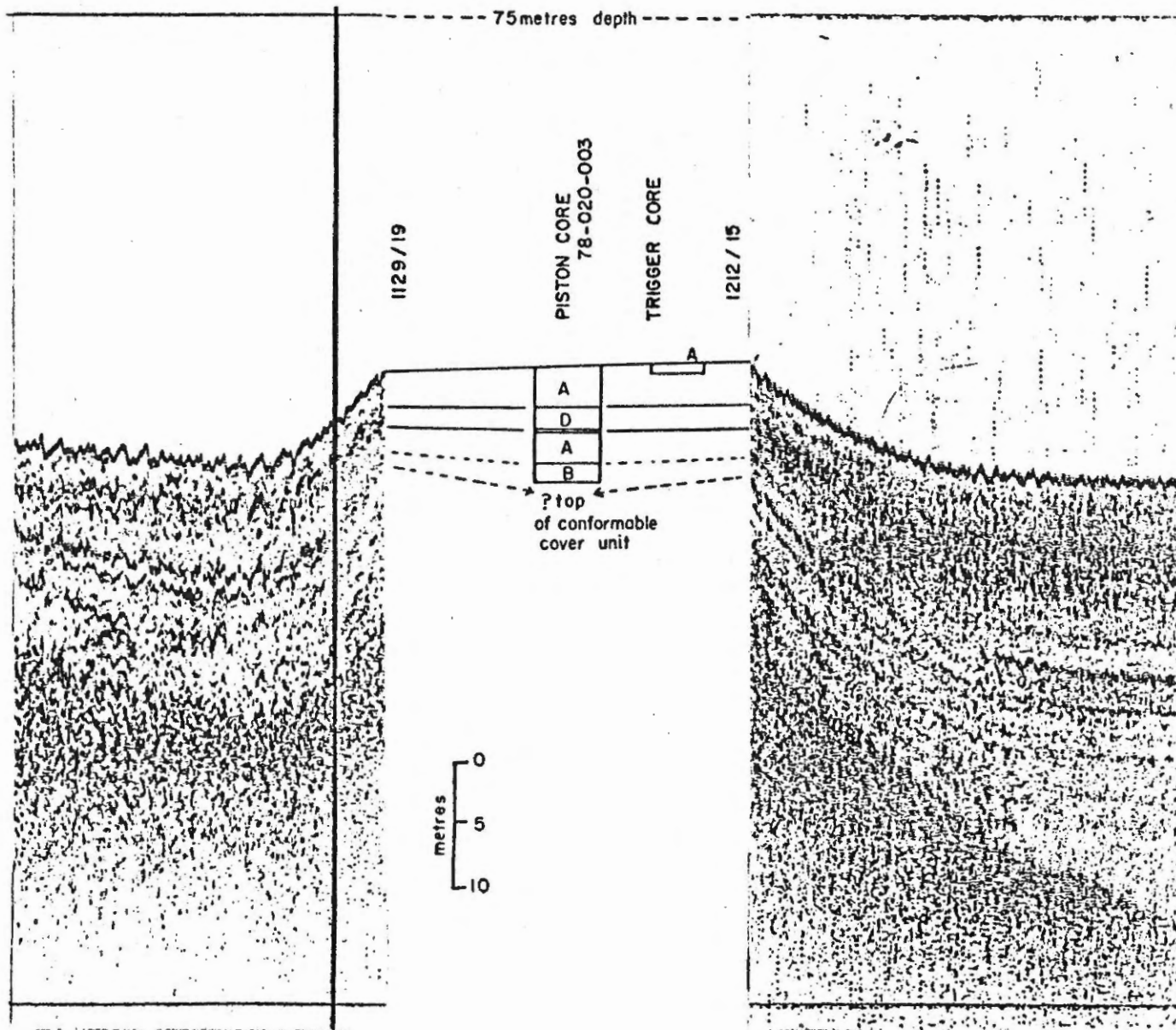


Figure 8.1: Acoustic profile to core correlation for core 78-020-003 (Approaches).

Core penetrates only upper basin-fill sediments.

(Fig. 3.1) according to the sounder depth of 81 metres. Tentative correlation is made in Figure 8.2 with profile 0959/21 about 0.2 km away.

Similar to the Approaches core, core 004 only samples the upper basin-fill acoustic unit. Two prominent acoustic reflections are depth correlated with the upper and lower boundaries of facies C. Generally, facies B and C have weak to transparent reflections. The upper portion of facies D, probably subfacies D1, possesses a weak acoustic record increasing downward to continuous, moderate strength reflectors, probably representing subfacies D2. This grades rapidly downward, through approximately 3 metres ( $v = 1500$  m/sec) of sediment, to the conformable cover unit. There are approximately 18 metres ( $v = 1500$  m/sec) of sediment below the top of the conformable cover unit.

#### 8.5 Lithologic Correlation

A tentative lithologic correlation is shown in Figure 8.3. It is suggested that the top units of facies in the two cores are correlable, although this requires that some of A is missing in core 004. This is consistent with the acoustic stratigraphy and correlation. In both cores A is found somewhere above D. In core 004 facies B and C lie between A and D, and are transitional in colour from facies D to A. However, A abruptly overlies D in core 003, with a substantial change in colour from D to A. Therefore it is suggested that facies B and C may be missing from core 003.

This interpretation predicts that facies E presumably would be found below core 004 (hence the lower correlation line) and that C lies below B in core 003. Thus the interpreted, full sequence would be ABCDE.

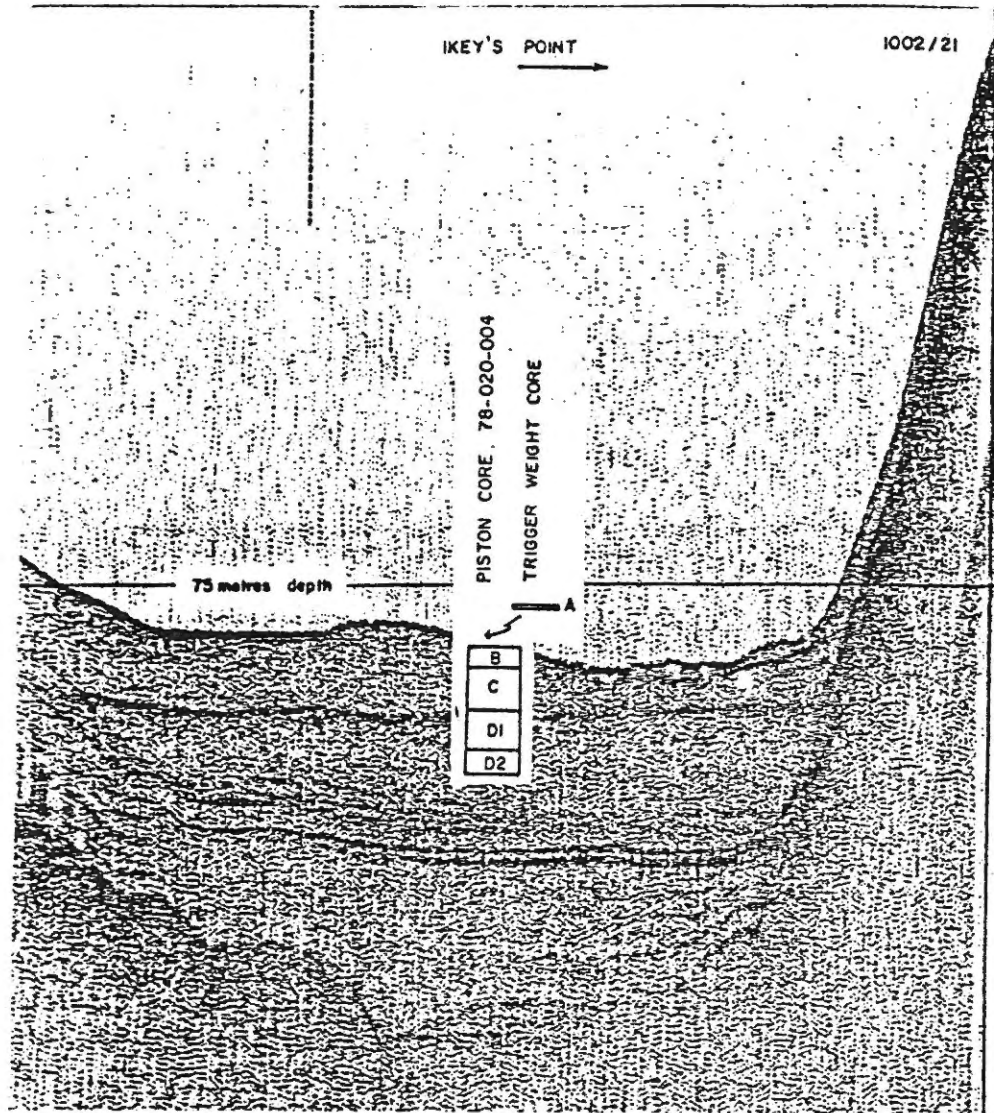


Figure 8.2: Acoustic profile (0959/21) to piston core correlation, 78-020-004, Outer Bay. Core penetrates only upper basin-fill sediments.

The foregoing is based on the assumption that all the facies units, as observed in the piston cores, are in situ deposits. However, the variable colours and textures, the inclined strata, and the abrupt lithological boundaries of facies D and E in core 003 suggest a possible allochthonous origin. It is possible that these sediments occur as a slide deposit, originating from higher up the flanks. This would imply that the A-B facies contact which is observed only once in each core, may be lithologically correlatable. However, this interpretation is not favoured because:

- (1) nowhere in the acoustic record was there evidence for a slide or slump-process, either at this locality or anywhere in Makkovik Bay;
- (2) the lithologic correlation imposed by the slide hypothesis is not consistent with the overall acoustic stratigraphic correlation of Makkovik Bay (Figs. 4. and 8.1);
- (3) the inclined strata throughout facies D appear to be related to core deformation, not to inclined strata of an allochthonous unit.

The autochthonous sediment hypothesis is more convincing. The abrupt lithological changes may be explained by ice-rafting. Therefore, the only change in depositional environment required is a temporary return of conditions similar to that which deposited the bedded couplets of D-2 of core 004. While not totally conclusive, the lithological and acoustic evidences favour the in situ hypothesis for these sediments, presumably deposited

78-020-004

78-020-003

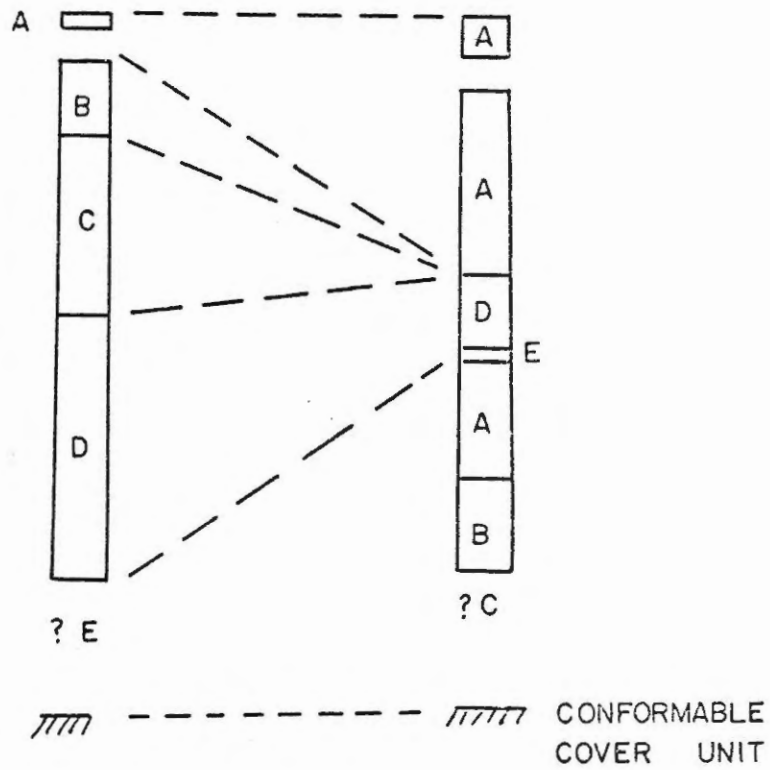


Figure 8.3: Tentative lithologic correlation of piston core units and conformable cover unit

during a fluctuating environment. This is discussed later according to foraminiferal and clay mineralogical evidences in Chapters IX and X.

### 8.6 Chronologic Correlation

Five organic carbon samples from the two piston cores have been  $^{14}\text{C}$  dated. In addition, a homogeneous sample of the gray clayey silt, interpreted to be from the upper zone of the acoustic conformable cover (Chapter VI), was  $^{14}\text{C}$  dated using the tests of calcareous foraminifera, primarily I. teretus and I. islandica. These dates are:

<u>FACIES</u>	<u>CORE</u>	<u>CORE INTERVAL (CM)</u>	<u><math>^{14}\text{C}</math> YRS B.P.</u>	<u>LABORATORY NUMBER</u> <u>KRUEGER ENTERPRISES</u> <u>INC.</u>
A	78-020-003	80-100	1,510 ± 115	GX-5810
A	78-020-003	205-235	4,325 ± 180	GX-6348
A	78-020-003	650-690	7,475 ± 160	GX-5811
C	78-020-004	290-330	5,690 ± 280	GX-6346
D	78-020-004	800-840	8,045 ± 360	GX-6347
Gray Clayey Silt	(surficial unit IV)	(conformable cover)	10,275 ± 225	GX-6345

The morphology of the acoustic conformable cover unit suggests that it was deposited under quiet conditions, probably deep water (Chapter IV). Therefore it is suggested that the conformable cover unit is time concordant, at least within Makkovik Bay. This is supported by the sediment trap data (Chapter III). Extrapolation of the two rates of sedimentation measured in different basins by the sediment traps suggest time concordant

deposition of the base of the upper basin-fill unit within Makkovik Bay.

The age estimates of the core samples are shown in Figure 8.4 along with the relative position of the upper boundary of the conformable cover unit. The upward extrapolation from the two age estimates near the top of core 003 terminate at the top of the core suggesting that there has been insignificant loss of depositional record. Similarly, a linear extrapolation downwards from these two age estimates suggests an age of approximately 6,500 years B.P. for the base of the upper unit of facies A in core 003. The lithology suggests that the lower units in core 003 have high rates of sedimentation, especially facies D and E. Therefore, it is suggested that the lower rates are, to the first order of approximation, linear. An extrapolation upwards from the two age estimates suggests that the top of facies D is approximately 6,500 years B.P., the same value as that suggested by the extrapolation from the upper dates. This suggests that there is not a significant loss of depositional record between facies D and A in core 003, but rather that facies C and B were not deposited.

Interpolation of the age estimates of core 004 suggest that the C-D contact is approximately 6,500 years B.P., coinciding with facies D of core 003. At the top of core 004, the lithology suggests a gradual decrease in rate of sedimentation but not as great as that in facies A of core 003. Therefore the rate is interpreted to decrease moderately throughout facies C and B, suggesting that the age of facies A in core 004 is approximately 2,000 years B.P. This assumes that either significant erosion has removed part of facies A or the net rate of sedimentation is very low. The grain size distribution (Chapters VI and VII) and the acoustic stratigraphy

core 78-020-004

core 78-020-003

$^{14}\text{C}$  YEARS B.P. ( $\times 10^3$ )

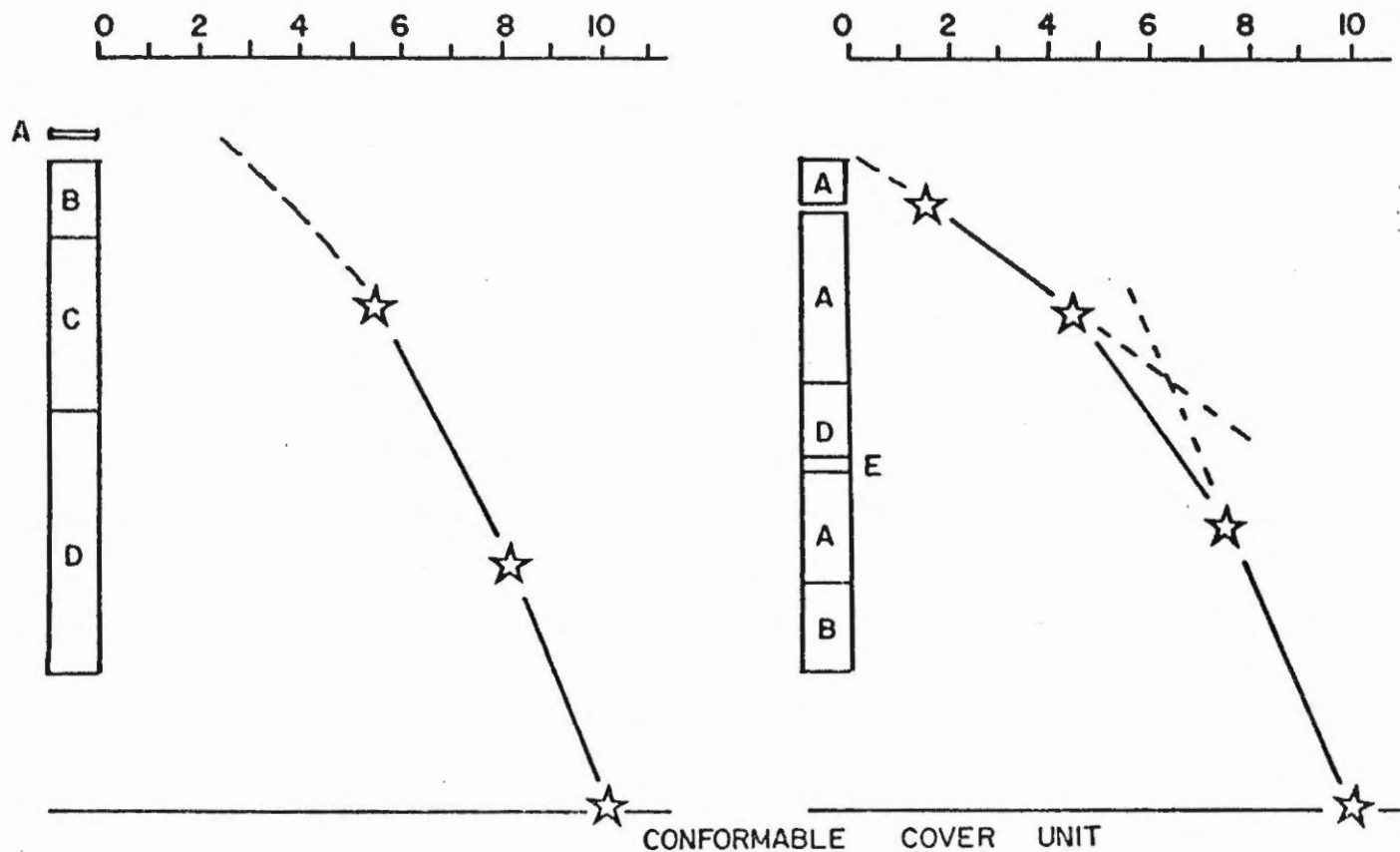


Figure 8.4: Chronology of piston cores and conformable cover unit



(Chapter IV) favour the presence of contemporary erosion or winnowing at the core location.

The chronologic correlation of the piston core units (Fig. 8.5) indicates that at certain periods the deposition of the facies units were diachronous from the Approaches to the Outer Bay. Approximately 8,000 years B.P., facies A and B were deposited in the Approaches while facies D was being deposited in the Outer Bay. By 6,500 years B.P., facies D extended out to the Approaches as well. Since then, facies C, B and A were deposited in the Outer Bay, whereas only facies A is thought to have been deposited in the Approaches.

#### 8.7 Stratigraphic Correlation

The acoustic correlation plus the similarity between the lithologic and chronologic correlations suggest a stratigraphic correlation that outlines facies changes from the Approaches core to the Outer Bay core (Fig. 8.6). This correlation is consistent with the facies sequence ABCDE. Presumably, facies B and C were not deposited during the upper sequence in the Approaches core, or perhaps have been removed by erosion although this is not suggested by the chronologic correlation. Instead, it appears that the deposition of facies A in the Approaches (observed as two units) (a) commenced prior to that of the Outer Bay and (b) was interrupted at approximately 7,000 years B.P. by the deposition of facies D and E.

Although the acoustic stratigraphy indicates that the various piston core facies should outcrop along zones of differential erosion, it was not

core 78-020-004                      core 78-020-003

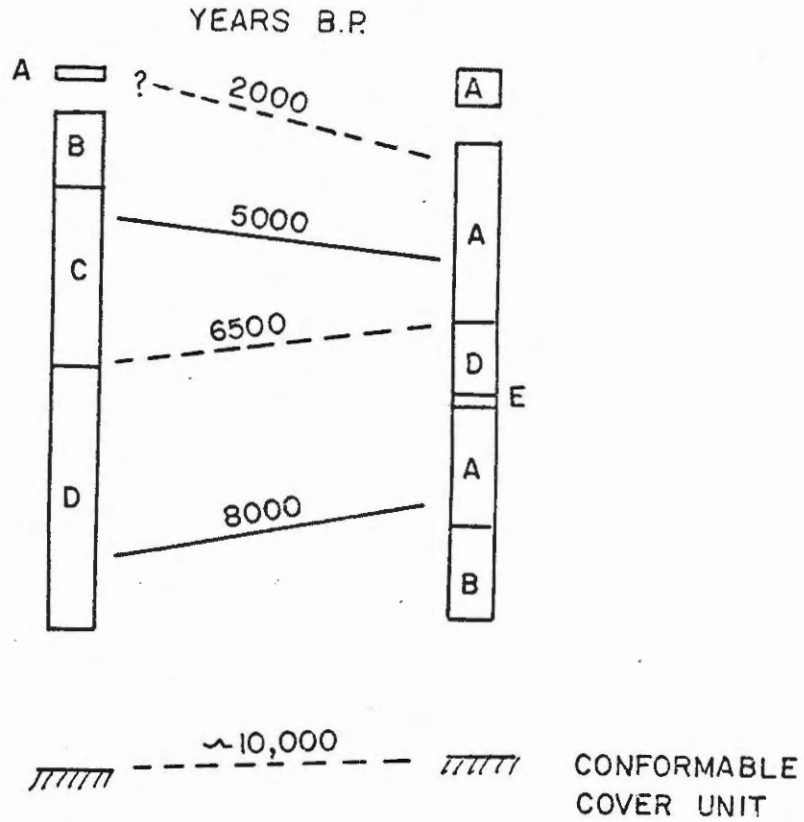


Figure 8.5: Chronologic correlation of piston cores and conformable cover unit. The solid correlation lines are based on absolute  $^{14}\text{C}$  dates whereas the dashed correlation lines are based on lithologically "weighed" extrapolations from  $^{14}\text{C}$  ages (see Figure 8.4).

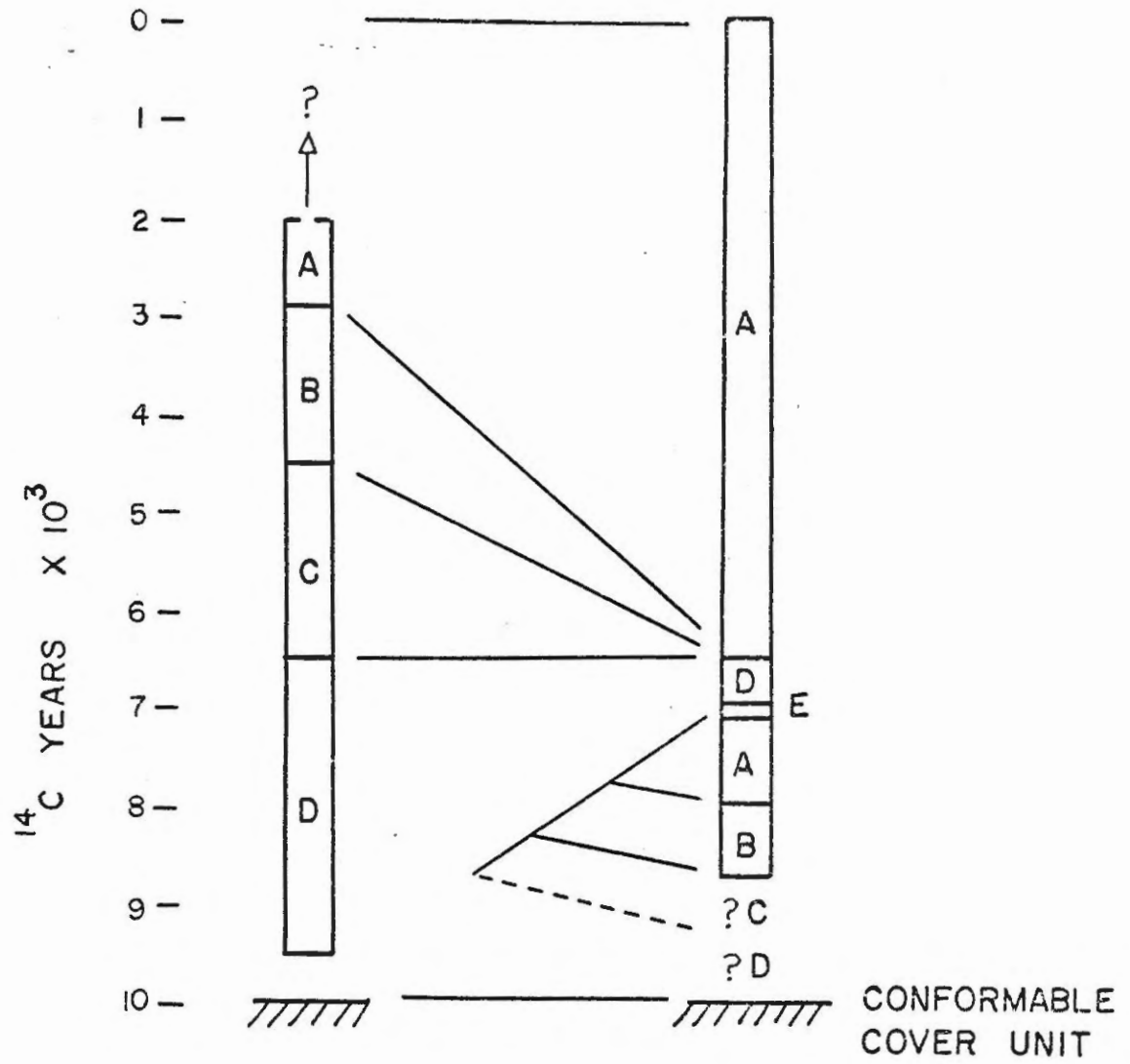


Figure 8.6: Stratigraphic correlation of piston core facies

possible to discriminate the vertical facies along the surface using the present sample distribution and analytical techniques.

### 8.8 Facies Interpretation

The interpreted facies sequence can be used to evaluate the upward transition of the characteristic aspects of the sediments. The microfauna, bioturbation, methane and pyrite production, sedimentary structures and  $^{14}\text{C}$  chronology suggest upward changes in the rate and nature of sedimentation.

The abundance of microfauna, primarily diatoms, is transitional from trace amounts in facies E and D, to meagre, moderate and abundant amounts in facies C, B and A respectively. Similarly, the degree of bioturbation varies from essentially non-existent in E and D2, gradually increasing to a hiatus by facies A. Both these trends suggest an upward decreasing rate of sedimentation between and throughout facies C, B and A.

The distributions of gas expansion cracks and replacement pyrite growths indicate changing conditions. Very small, noncontinuous cracks are observed in the base of core 003 and are considered to be insignificant. However, very large, continuous gas expansion cracks are found in facies D of core 003. These cracks are presumably caused by the anerobic bacterial production of methane, normally favoured by high sedimentation rates and terrestrially derived organic matter (Rashid and Vilks, 1977; Weber and Maximor, 1976). Generally, rapid rates of sedimentation create a depletion of soluble sulphates in the interstitial waters, thereby favouring the subsistence of methanogenic bacteria (Rashid and Vilks, 1977).

The overlying facies C is characterized by growths of burrow-like pyrite and an absence of gas expansion cracks. Generally the formation of pyrite in marine sediments is controlled by (1) the availability of iron minerals that are reactive with  $H_2S$ , (2) the availability of dissolved sulfate, and (3) the amount of organic matter available for bacterial decomposition (Berner, 1970). The pyrite in facies C can be explained by a decreased rate of sedimentation, allowing greater concentration of soluble sulphates in the interstitial waters. Simultaneously, in the zone of sulphate reduction, the bacterially produced hydrogen (from the fermentation of organic matter) becomes unavailable for the production of methane (Rashid and Vilks, 1977). In addition, the absence of methane may also suggest a reduction in the proportion of terrestrially derived organics.

The absence of substantial pyrite throughout facies B may be related to a decrease in salinity. Berner et al. (1974, 1979), studying both contemporary and ancient sediments, have suggested that the presence of authigenic iron sulphide may be used as a paleosalinity indicator. This is based on the fact that the abundance of sulphate in the marine environment favours pyrite as the dominant form of iron sulphide. Thus, it is possible that the lack of substantial pyrite in facies A and B may reflect the decreased sulphate concentration of brackish water, preventing sulphate reduction. This process may have been augmented by increased bioturbation which might effectively release  $H_2S$  from the sediment, arresting sulphate reduction. Although no quantitative measurements were made, the presence of small isolated mottles, tentatively identified as iron reduction centres (Stow, 1973; Berner, 1974) suggests that bioturbation was not effective in removing

all the  $H_2S$  from facies B. More conclusive interpretations would be possible if the cores had been analyzed for iron monosulphides, the corresponding sulphides characteristic of fresh or brackish environments (Berner et al., 1979). Upcore variation of paleosalinity is discussed further in Chapter X on the basis of foraminiferal evidence.

Variations in primary sedimentary structures also suggest changing depositional regimes. The lower facies, D and E, both contain high concentrations of dispersed gravel. These gravelly horizons are observed only in the Approaches and are interpreted to be ice-rafted deposits, deposited from an ablating iceberg. Subfacies D2 is characterized by bedded couplets of mud and laminated silt. The nature and deposition of these couplets is more problematic. The various mechanisms endorsed for the deposition of silt-laminated muds have reviewed by Stow and Bowen (1978); these include velocity fluctuations, turbulent boundary layers, migration of bed forms, reworking and placer concentrations, congregational sorting of like particles, differential settling, and diagenetic effects. Although no specific mechanism is postulated for these particular laminated muds, the repetitive nature and the internal, horizontal laminations suggest a relatively high rate of sedimentation. In contrast, the scour-like base and the frequent grading observed in the laminations of facies A, B and C suggest that the laminations are erosional or winnowed features. The wispy laminations increase in frequency from facies C to B but are almost absent in facies A, presumably destroyed by the intense bioturbation. The preserved laminations in facies A are well formed, graded and relatively continuous. The overall trend from facies C to A suggests an increase of physical energy

capable of reworking the sediments, whereas the primary structures of facies D and E suggest a high rate of deposition.

The relative rates of sedimentation, as proposed by the lithologies, are consistent with the interpreted rates obtained from extrapolated,  $^{14}\text{C}$  chronologies (Fig. 8.4). The absolute dates suggest the following rates of net sedimentation:

facies A	-	0.07 cm/year
facies B	-	ca. 0.1 cm/year
facies C	-	0.2 cm/year
facies D	-	0.3 cm/year
facies E	-	?

Note that the rate for facies A is similar to that obtained by the sediment trap in the Western Inner Bay.

The thickest sedimentary column is located in basin G of the Outer Bay and has approximately 27 metres of sediment below the upper basin-fill unit. The dates from the base of the upper basin-fill unit (core 004) and the top of the conformable cover unit suggest a sedimentation rate of 0.3 cm/year for the conformable cover unit. Extrapolating this rate down to the lowermost sediments suggests an age of approximately 19,000 years B.P. This extrapolation assumes a constant rate of sedimentation and a velocity of 1500 m/sec.

Facies E was sampled only in the Approaches area and it is thought to be primarily ice-rafted material. The colour of the muddy matrix suggests an exotic source. Therefore, facies E is not considered to be genetically related to the rest of the facies.

CHAPTER IX

CLAY MINERALOGY

9.1 Introduction

In this study, the determination of the clay mineralogy has two principal objectives: (1) to gain further understanding of the relationships between the sediment distribution and the depositional environment, and (2) to aid in the interpretation of the overall stratigraphy. The clay and clay-size fraction mineralogy has been determined by semi-quantitative XRD analyses on representative samples from land deposits, the conformable cover unit, the upper basin-fill unit and the surficial sediments. Laboratory techniques are discussed in Chapter V and the data are tabulated in the Appendices.

9.2 Distribution of Clay and Clay-Size Mineralogy

(a) Land Samples

Three samples of raised deltaic, grey sandy silt were taken between Ranger Bight and Makkovik Harbour. One of these samples was recovered from the base of the kame delta at the head of Ranger Bight (Chapter II). The overall ranges of clay and clay-size minerals from all three samples are listed in order of abundance:



	<u>Percentage Clay-Size Fraction</u>	<u>% Clay Minerals (recalculated to 100%)</u>
feldspar	50-75	
illite	5-25	45-65
quartz	7-16	
chlorite	3-13	25-35
amphibole	5	
kaolinite	1-4	5-13
montmorillonite	0-2	0-5

Till samples from adjacent areas in Labrador are also dominated strongly by feldspar and illite (Piper and Scott, 1977).

(b) Conformable Cover Unit

The conformable cover unit is exposed surficially as grey clayey silt, of which 14 samples were analyzed. There is a conspicuous variation of the illite content within these samples. Figures 9.1 and 9.2 indicate that the illite content responds inversely with the proportions of the other dominant minerals, feldspar and chlorite, suggesting that the illite content is the major controlling factor. Furthermore, Figure 9.3 shows that the samples with the highest proportion of illite are concentrated along the south shore of the Outer Bay. These particular samples are identified separately as the 'south shore grey clayey silt' samples in Figures 9.1 and 9.2.

A minor trend is also detected within the conformable cover unit.

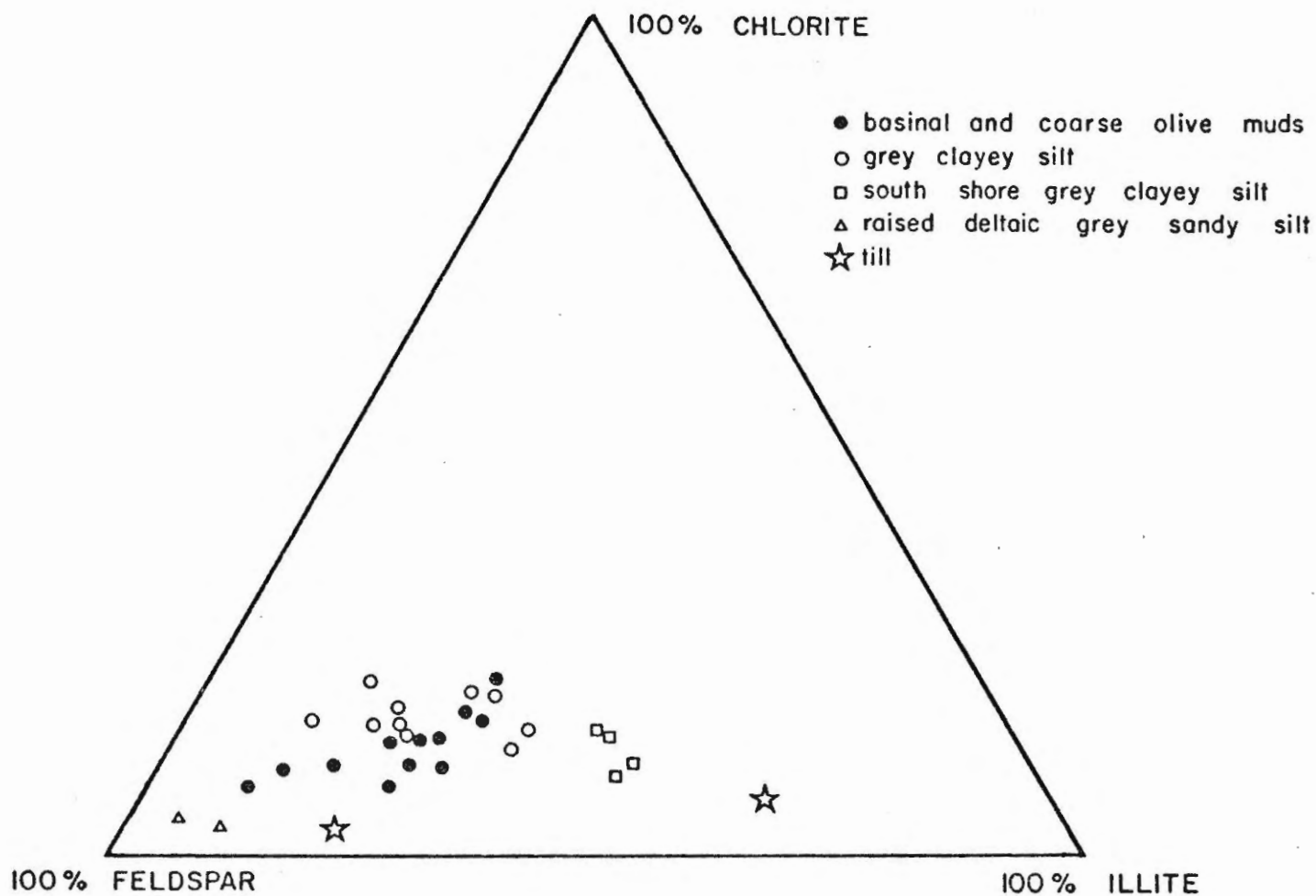


Figure 9.1: Ternary diagram of the  $< 2\mu$  fraction of illite, feldspar and chlorite for the major, relict and contemporary sedimentary units as exposed on land and along the sea floor

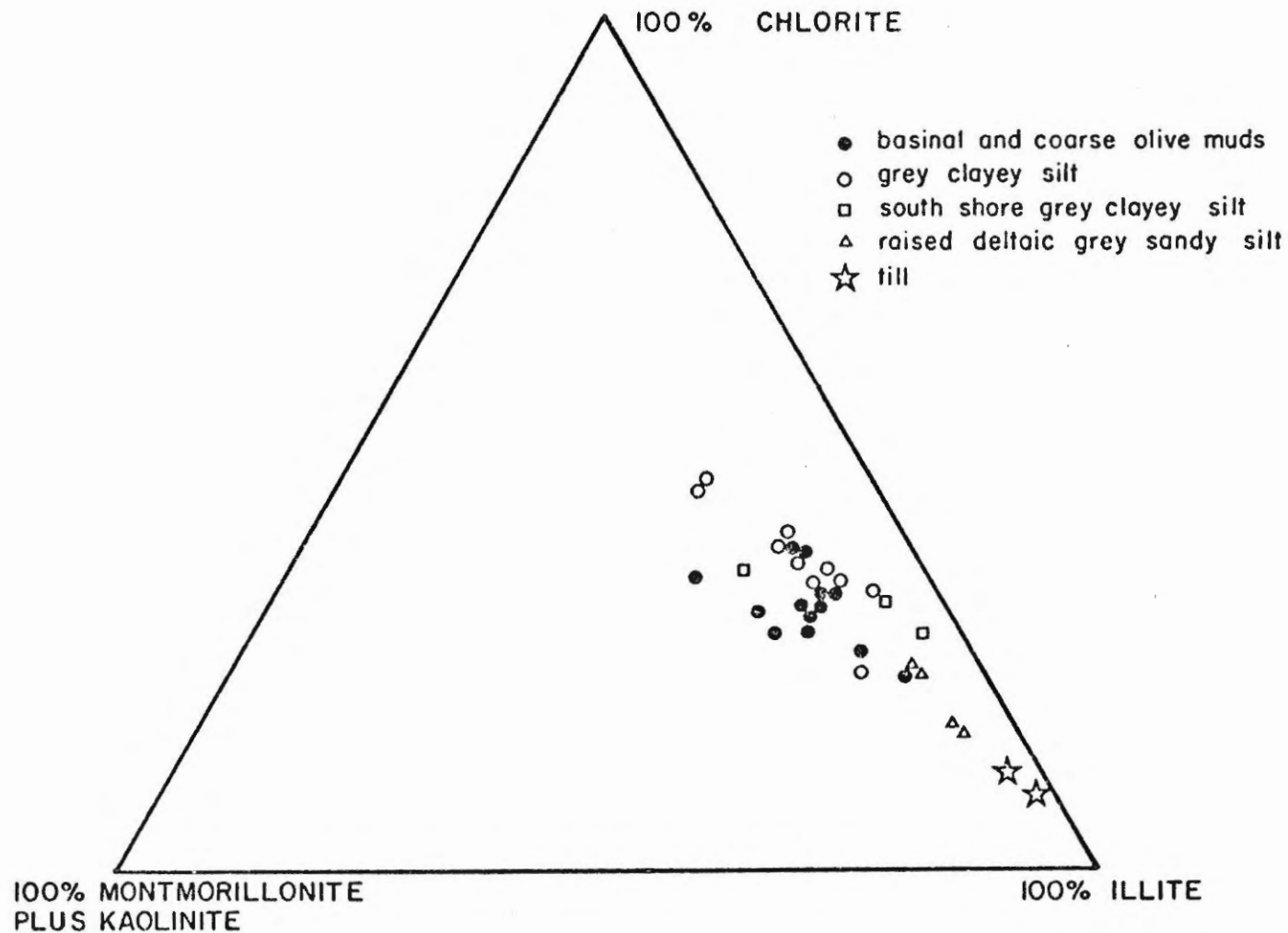


Figure 9.2: Ternary plot of illite, chlorite and montmorillonite plus kaolinite from the < 2 $\mu$  fraction of the major, contemporary and relict sedimentary units as exposed on land and along the sea floor

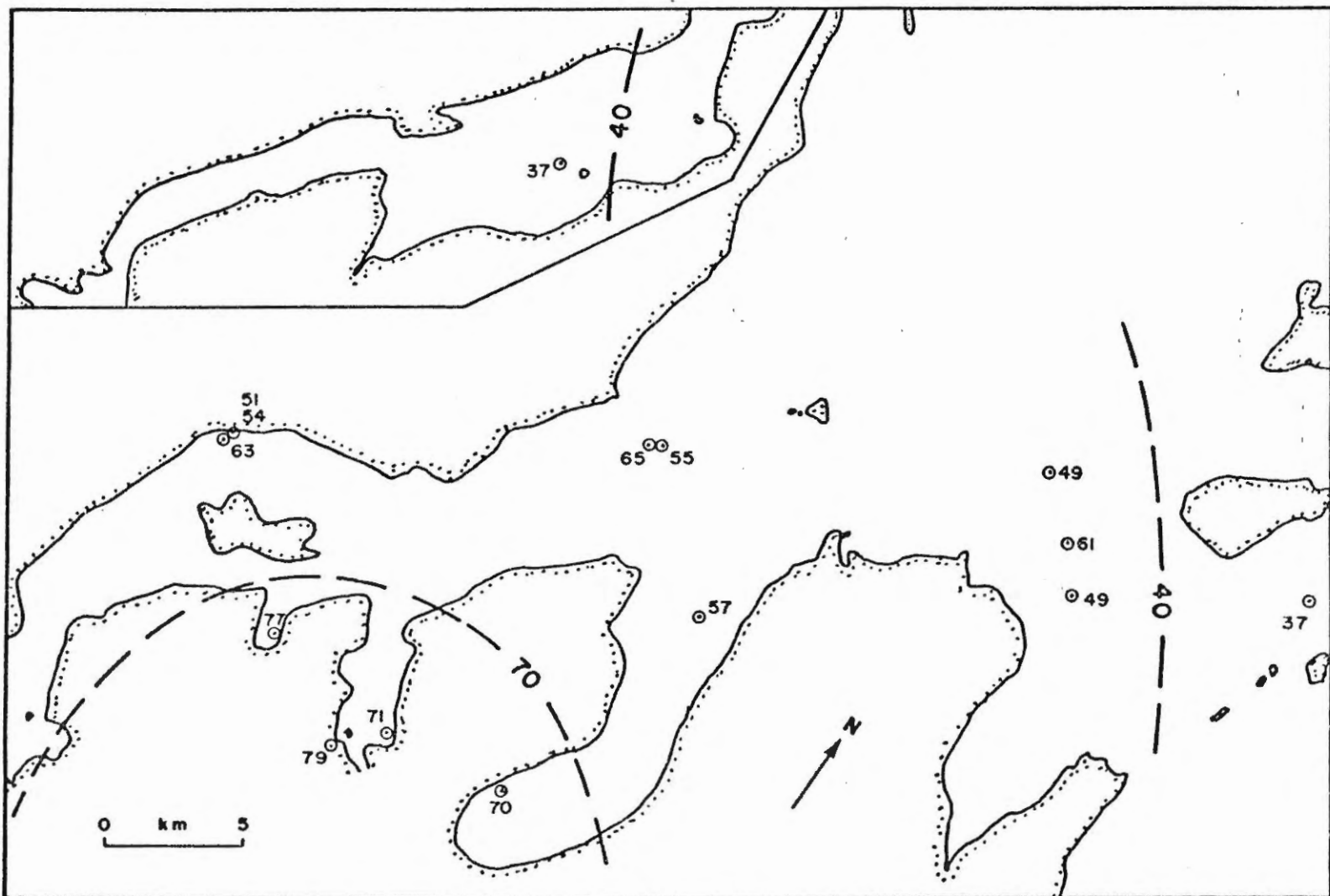


Figure 9.3: Areal distribution of the relative percent of illite (expressed as percent of clay minerals) of the < 2μ fraction of the relict, gray clayey silt (unit IV)

Figure 9.2 shows a slight increase in the proportion montmorillonite plus kaolinite away from the 'southshore' samples.

(c) Upper Basin-Fill Unit

Semi-quantitative XRD analyses of the <2 $\mu$  fraction of 30 upcore samples show the following minerals in order of abundance:

	<u>Percentage Clay-Size Minerals</u>	<u>% Clay Minerals (recalculated to 100%)</u>
feldspar	30-65	
illite	15-35	55-65
chlorite	5-15	20-35
quartz	5-15	
amphibole	3-10	
kaolinite	1-5	3-15
montmorillonite	0-3	1-10

The upcore variations in these mineral abundances are shown in Figures 9.4 and 9.5. Feldspar is the dominant mineral and shows the most pronounced variations in abundance.

Core 003

Within facies A of Core 003 (Fig. 9.4), the feldspar content increases upwards from 40 to 60 percent throughout both the upper and lower units. The proportion of feldspar in the rest of the core is as follows:

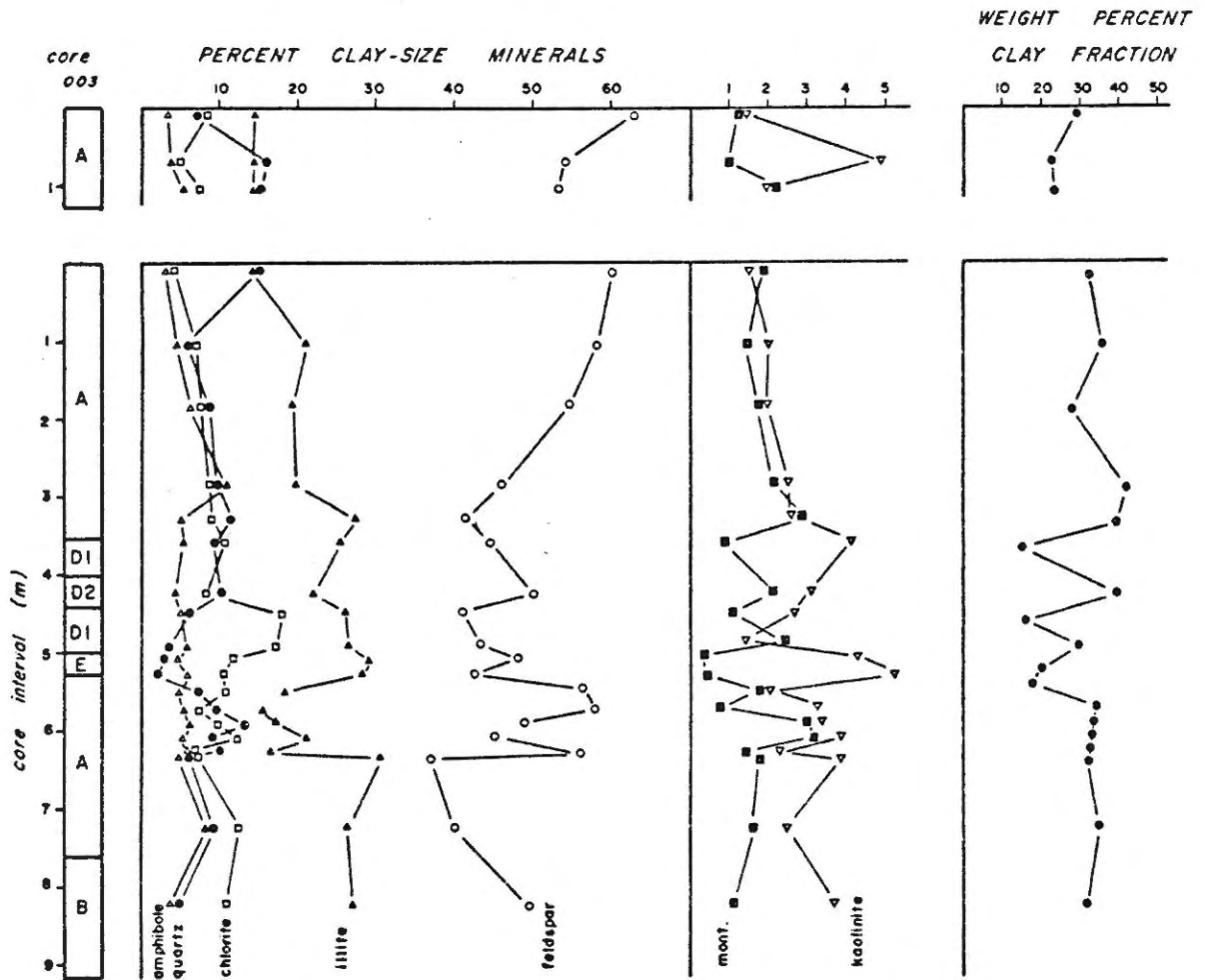


Figure 9.4: Upcore variations in the relative percent of clay and clay-size minerals (expressed as a percentage of clay-size minerals) from core 78-020-003

- 50% - facies B
- 50% - facies D<sub>2</sub>
- 45% - facies E
- 40-45% - facies D<sub>1</sub>

Throughout facies D and E, the feldspar content appears to vary proportionally with the weight percent of the clay size fraction (<4 $\mu$ ). The proportions of illite and chlorite respond inversely to the proportion of feldspar.

#### Core 004

In Core 004 (Fig. 9.5), the clay abundances are relatively uniform upcore. The approximate proportions of feldspar are:

- 40% - facies A
- 40% - facies B
- 40% - facies C
- 35% - facies D<sub>1</sub>
- 30-35% - facies D<sub>2</sub>

The abundance of illite responds inversely to feldspar and chlorite and directly with the weight percent of the clay fraction as determined in the grain size analysis. There is a slight but uniform increase in the abundances of kaolinite and montmorillonite upwards throughout the core.

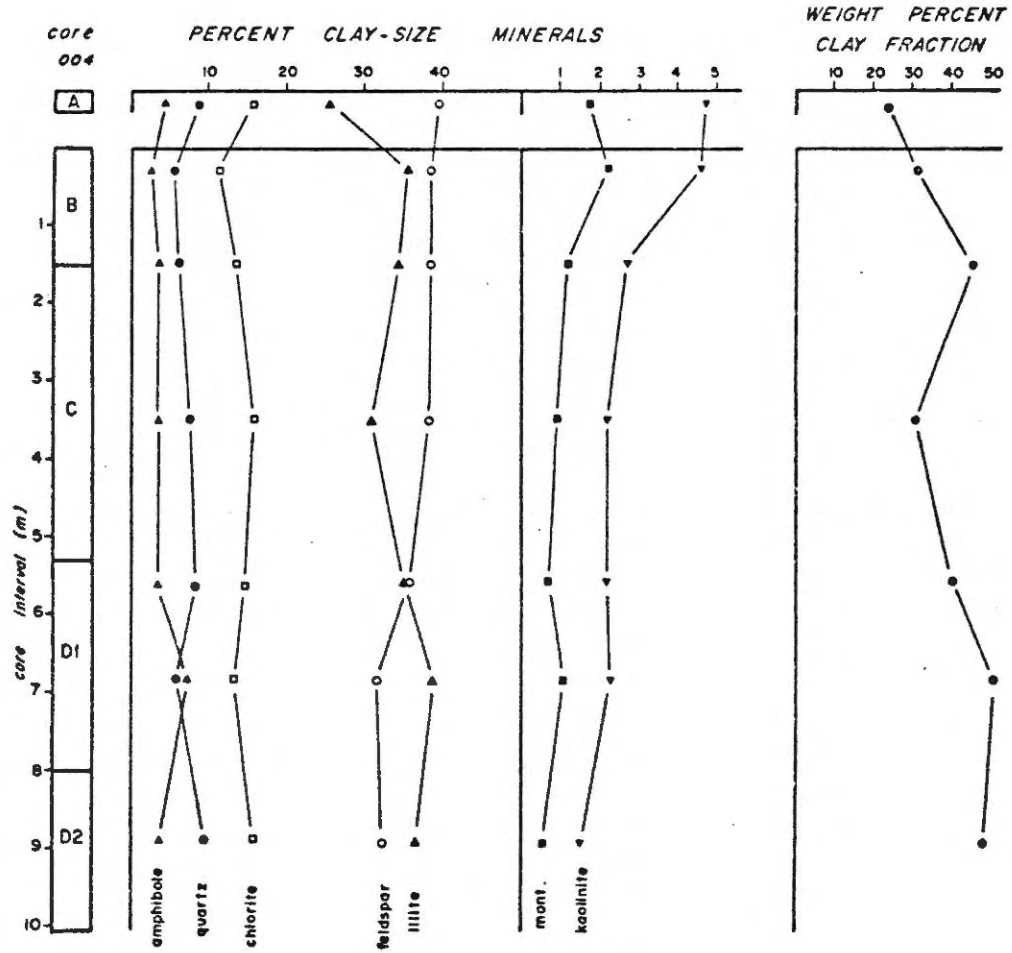


Figure 9.5: Up core variations in the relative percent of clay and clay-size minerals (expressed as a percentage of clay-size minerals) from core 78-020-004



TABLE 9.1 Average percentage of total clay-size minerals for the piston core facies sequence; x is less than 1%

FACIES		No. of Samples	Montmorillonite	Illite	Kaolinite	Chlorite	Quartz	Amphibole	Feldspar
Core 003	A	15	2	19	3	9	10	6	52
	B	1	1	27	4	11	5	4	49
	C	-							
	D1	1	2	22	3	9	10	4	50
	D2	3	1	26	3	15	6	6	43
	E	2	X	29	5	11	5	5	46
Core 004	A	1	2	25	5	16	9	4	39
	B	1	2	35	5	11	5	3	38
	C	2	1	33	3	14	7	4	38
	D1	3	1	33	2	13	7	6	37
	D2	1	1	36	2	16	9	4	32
	E	-							

### Piston Cores

The average percentage of the total clay-size minerals for the piston core facies sequence for both cores (Table 9.1) indicates that there is an up-facies decrease in the illite content and a proportional decrease in the abundance of feldspar. In addition, there is a smaller proportion of illite and a corresponding increase in feldspar content of the Approaches core (003) compared to the Outer Bay core (004).

The ternary plots of the clay minerals (Fig. 9.6) and the dominant clay-size minerals (Fig. 9.7) show graphically the decreasing illite and increasing feldspar contents both up-facies sequence and down-bay from core 004 to 003. In addition, a secondary trend can be observed in Figure 9.6, that of increasing abundance of montmorillonite plus kaolinite up the facies sequence. These data as presented in Figure 9.8 clearly suggest an up-facies increase in percent montmorillonite; this trend is within the error margin (approximately  $\pm 5\%$  montmorillonite) of the individual measurements. The data do not suggest a similar trend for the kaolinite content, although there is a slight upcore increase observed in core 004 (Fig. 9.9).

#### (d) Surficial Sediments

The surficial sediments constitute the veneer of the upper basin-fill unit and include the basinal olive mud (unit II) and the coarse olive mud (unit III) as described in Chapter VI. The overall ranges of clay and clay-size minerals are listed in order of abundance:

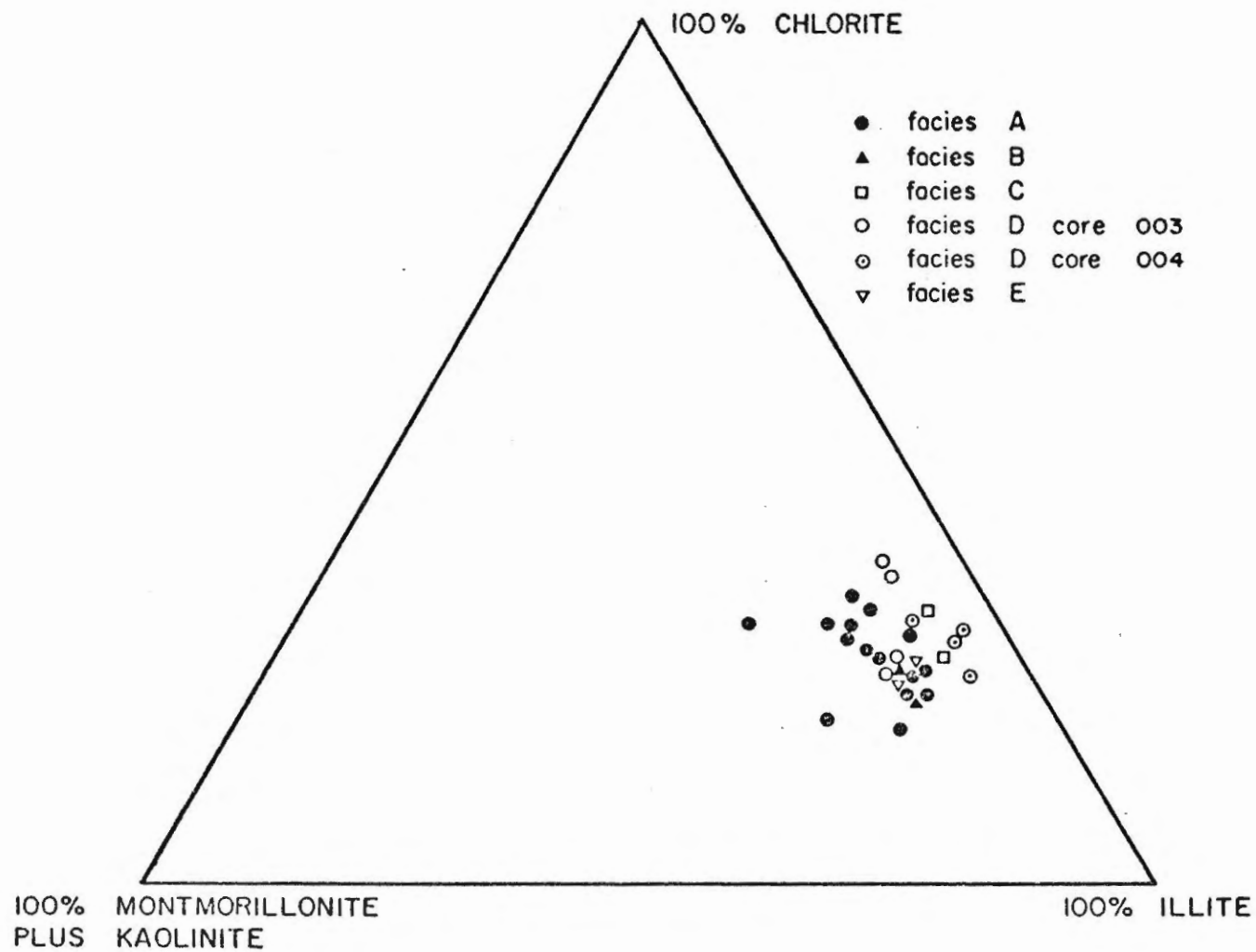


Figure 9.6: Ternary plot of illite, chlorite and montmorillonite plus kaolinite of the < 2 $\mu$  fraction of representative samples from the piston core facies

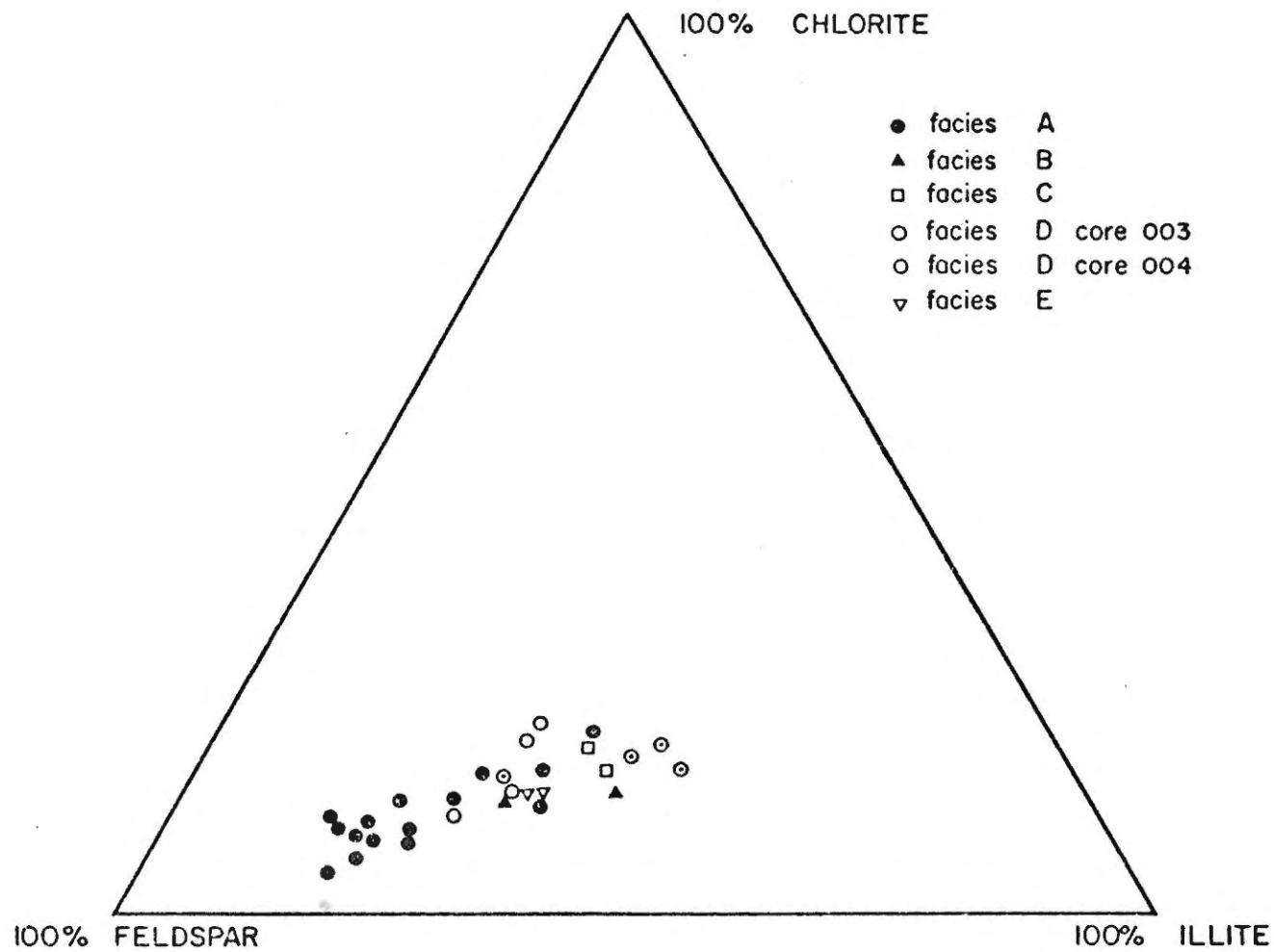


Figure 9.7: Ternary plot of illite, chlorite and feldspar of the  $< 2\mu$  fraction from representative samples of the piston core facies

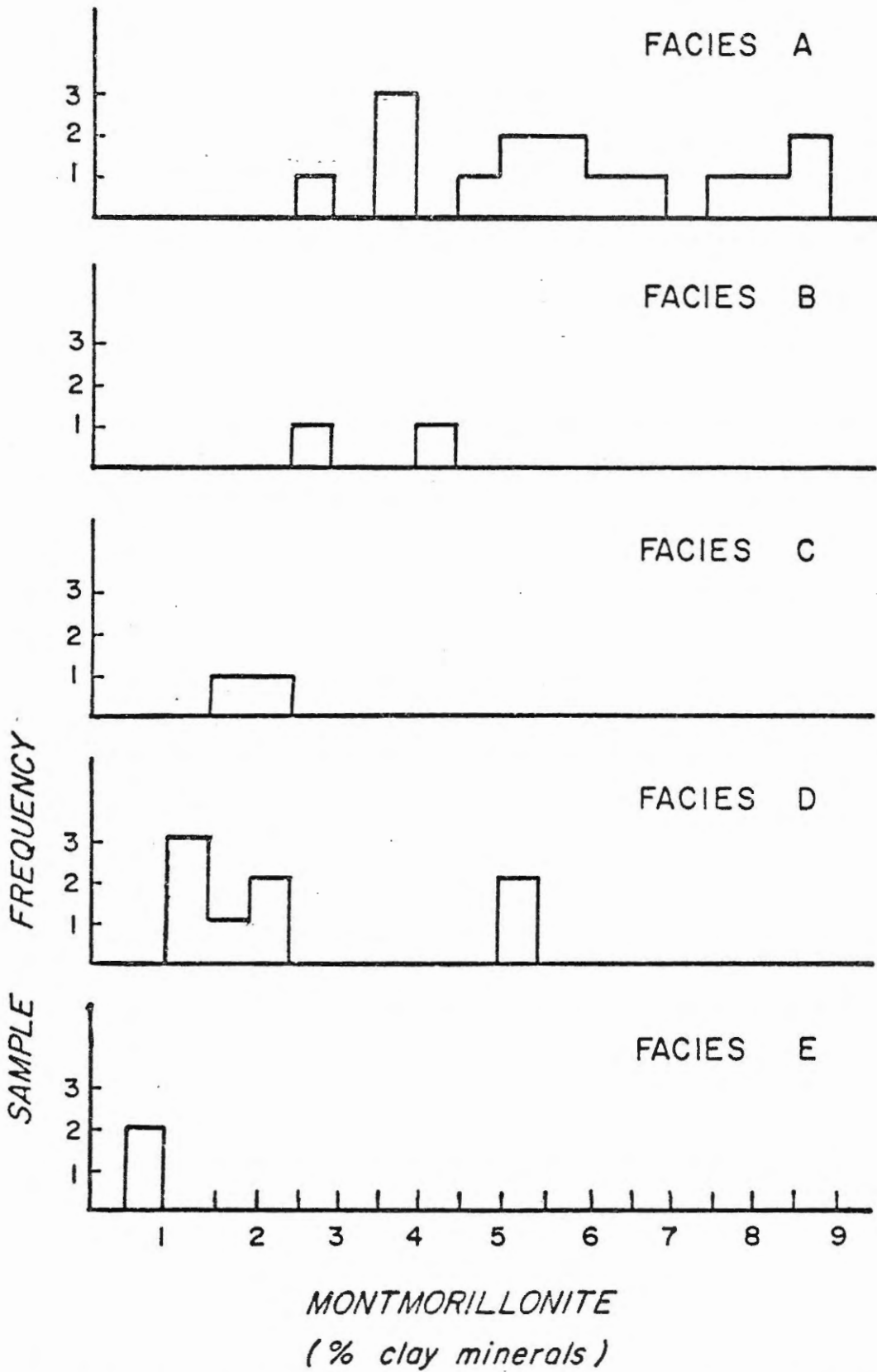


Figure 9.8: Sample frequency histograms of montmorillonite content (expressed as percent of clay minerals) from 30 piston core samples, showing the up-facies increase in montmorillonite content

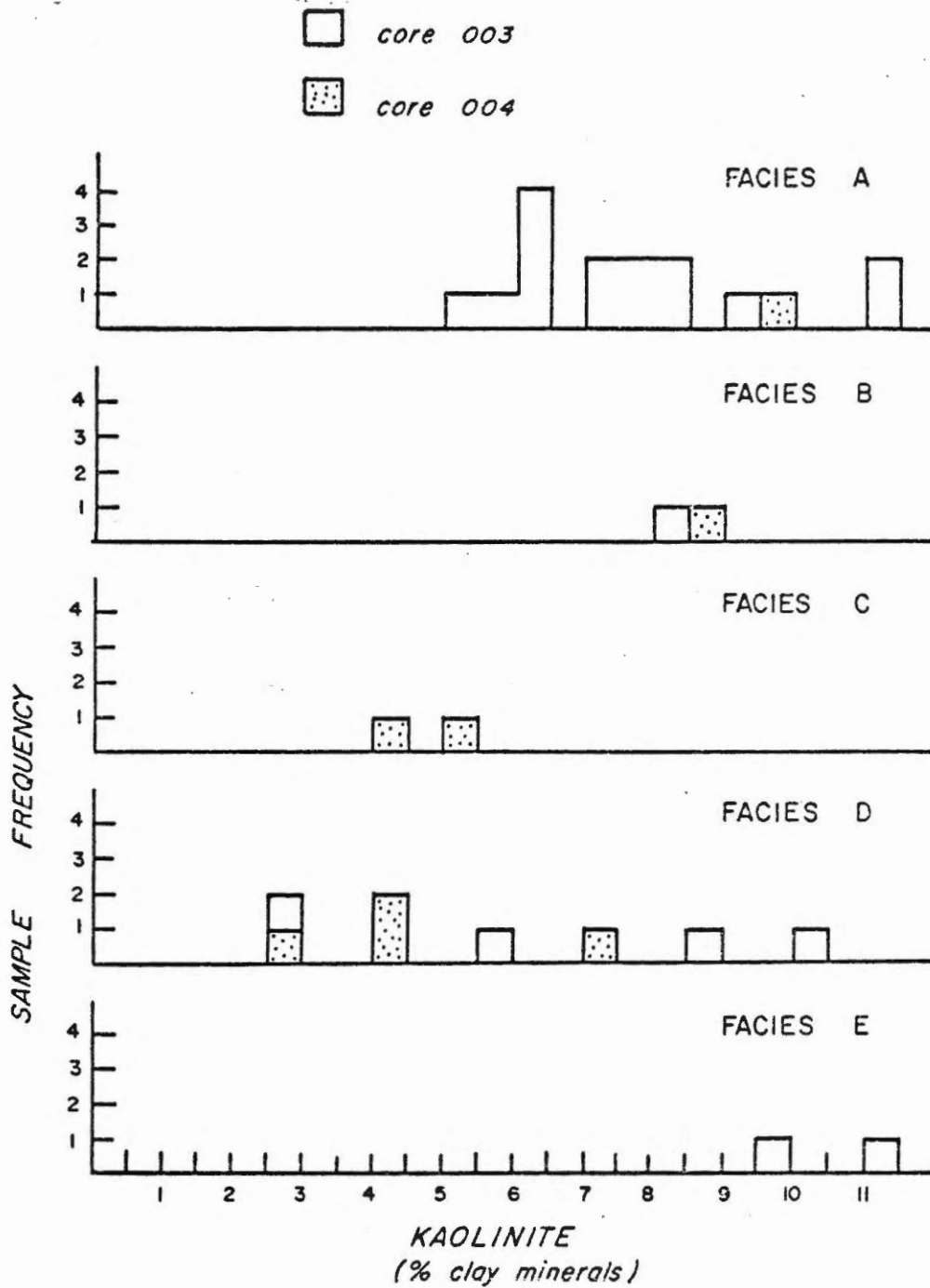


Figure 9.9: Sample frequency histograms of kaolinite content (expressed as percent of clay minerals) from 30 piston core samples, showing an up core increase in core 004 only

	<u>Percentage Clay-Size Fraction</u>	<u>% Clay Minerals (recalculated to 100%)</u>
feldspar	35-60	
illite	10-35	40-70
chlorite	7-20	20-35
quartz	4-12	
amphibole	3-6	
kaolinite	1-5	5-20
montmorillonite	0-3	1-7

The data as exhibited in Figures 9.1 and 9.2 do not show any major fluctuations throughout the bay. In general, the clay mineralogical distribution is uniform. Within the given sample distribution, the values for the coarse olive mud and the basinal olive mud are similar. However, there are two minor but significant downbay trends: (1) chlorite decreases from 18% (total clay size) in the Western Inner Bay to 8% in the Approaches (Fig. 9.10), and (2) the proportion of montmorillonite tends to be higher at the seaward edges of the individual Inner and Outer Bays.

### 9.3 General Interpretations

The dominant feldspar-illite-chlorite suite is common of northern latitudes (Biscaye, 1965; Lisitzin, 1972; Piper and Slatt, 1977) and indicates that detrital inheritance from mechanically weathered metamorphic rock is the major controlling factor (e.g., Millot, 1970). Furthermore, the similarity of these marine clays with those of a local

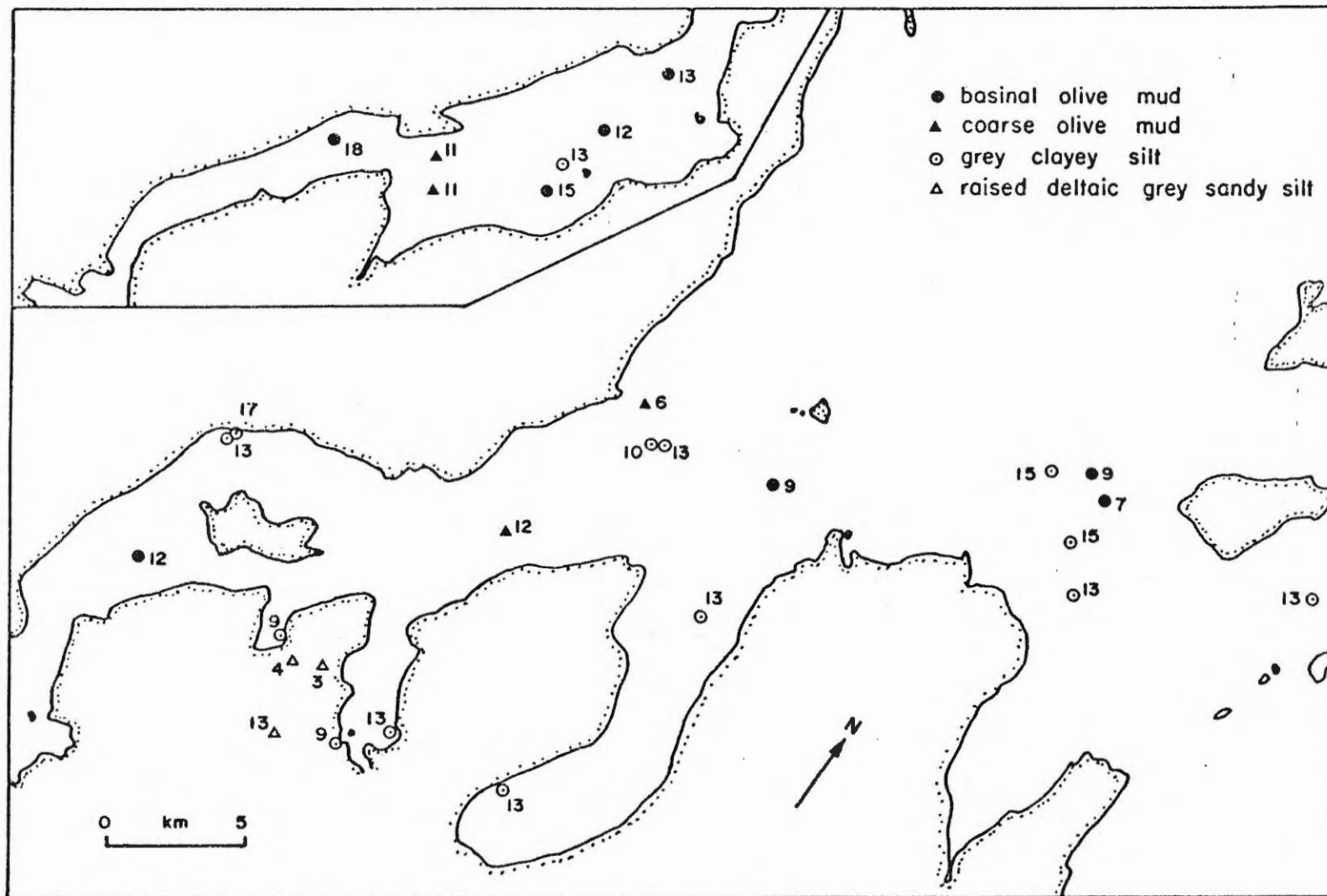


Figure 9.10: Surficial distribution of the relative percent of chlorite sampled from the basinal olive mud (unit II) and the coarse olive mud (unit III) (expressed as percentage of clay minerals)



kame deposit and three regional tills suggests that glacial detritus is probably the ultimate source.

In general, the sediments of estuaries may be derived from fluvial input, shoreline erosion or landward migration of shelf sediments (e.g., Pinet and Morgan, 1979). The nontidal circulation pattern of partially mixed estuaries has been used to explain the distribution of suspended sediments, suggesting that net landward migration of shelf suspensates occurs along the basal, saline inflow (Meade, 1972; Pevear, 1972). However, the clay mineralogy of the basinal olive mud is strikingly similar to that of the marginally eroding grey clayey silt and raised deltaic deposits (Table 9.2), suggesting that these are the primary source of the olive muds. This interpretation is consistent with the relatively small rivers and drainage basins, and the emergent coastline which has exposed marginal sediments to continued erosion.

Although the shelf sediments have significant amounts of montmorillonite and kaolinite and therefore could conceivably be a partial source, the lack of these minerals along the Labrador nearshore zone (Table 9.3) suggests that there is no significant net landward migration of shelf clays. Furthermore, of the three Labrador tills examined by Piper and Slatt (1977), two had significant amounts of montmorillonite and one had a relatively large proportion of kaolinite. Significant amounts of kaolinite found in Arctic marine sediments are thought to have been derived from kaolinite bearing Mesozoic sedimentary rocks (Naidu et al, 1971; Darby, 1975; Bjorlykke and Eleverhoi, 1975). Gandhi et al. (1969) have observed significant proportions of kaolin in 3 out of 10 rock samples

TABLE 9.2 Average percentage of total clay-size minerals for the  
major lithologic units; x is less than 1%

	No. of Samples	Montmoril- lonite	Illite	Kaolinite	Chlorite	Quartz	Amphibole	Feldspar
basinal olive mud	8	1	22	3	12	7	5	51
coarse olive mud	5	2	19	4	11	9	5	51
gray clayey silt	6	1	40	2	11	6	5	37
south shore gray clayey silt	8	1	22	4	14	7	4	49
raised deltaic sandy silt	2	x	7	1	4	13	5	72

TABLE 9.3 Average percentage of clay minerals from Makkovik Bay and surrounding areas

	No. of Samples	Montmorillonite	Illite	Kaolinite	Chlorite	Reference
basinal olive mud	8	3	58	8	32	this study
coarse olive mud	5	5	53	11	31	this study
gray clayey silt	6 8	2 3	74 52	4 9	20 36	this study
raised deltaic sandy silt	2	3	57	10	31	this study
Labrador Tills	3	7	76	2	12	Piper and Slatt (1977)
Labrador near-shore	2	0	>60	0	<25	
Labrador shelf	2	>10	>60	<10	>25	Piper and Slatt (1977)
Labrador shelf	?	<10	60-80	<10	10-30	Lisitzin (1972)

from the Makkovik Bay area (see Fig. 2.1). Therefore, it is suggested that, although the marine environment may have an influence by reworking and redistributing, most of the clays have an ultimate detrital inheritance from the surrounding terrain with an insignificant clay flux from ocean sources.

Lateral and vertical variations in the relative proportions of clay and clay-size minerals indicate that different processes have operated throughout different periods in Makkovik Bay. The 10,000 year B.P. conformable cover unit shows conspicuous mineral segregation; illite is concentrated along the south shore of the Outer Bay (Fig. 9.3). Feldspar responds inversely. In contrast, the contemporary basinal olive mud shows an overall random downbay distribution in the proportions of clay-size minerals. The change from the former depositional regime to the contemporary regime is shown by the piston core facies. Facies C and D are most similar to the conformable cover unit, showing a downbay decrease in the illite/feldspar ratio. This suggests that facies C and D represent the waning components of the conformable cover unit, as previously indicated by the stratigraphic correlation (Chapter VIII). Piston core facies A and B show an upward decrease in the illite-feldspar ratio for a given locality, indicating a change in source or nature of segregation.

The clay mineralogical trends and their depositional interpretations support the in situ depositional hypothesis for facies D and E of core 003 (see Chapter VIII). Both units of facies A indicate a characteristic upward increase in the percentage of illite. The fact that the abundance of illite has a gradational change upwards from facies D to A suggests that

these units may be in depositional continuity. Environmentally this suggests that the deposition of reworked marine clays has predominated in the Approaches since approximately 8,000 years B.P., except for a brief period at about 7,000 years B.P., during which time first generation, land-derived clays were deposited.

#### 9.4 Discussion: General Aspects of Clay Mineral Segregation

Variations in the relative abundances of clay minerals have been observed along the Atlantic coastal plain estuaries of the United States (e.g. Nelson, 1958; Postma, 1967; Pinet and Morgan, 1979; Feuillet and Fleischer, 1980). However, no detailed studies have been done on the higher latitude estuaries characterized by high proportions of feldspar and illite.

In general, three mechanisms have been endorsed that explain the lateral trends in the clay mineralogy of bottom sediments of estuaries:

- (1) chemical alteration
- (2) differential flocculation
- (3) physical sorting by sediment size

The mechanism of chemical alteration suggests that when a clay mineral enters seawater it is not in chemical equilibrium and in time will transform to a more stable phase. The transformation required by this study would be degradation of illite (Millot, 1970) in order to explain the increase in montmorillonite content up the facies sequence. However, degradation is a weathering process that occurs in solutions sufficiently

unsaturated in cations to dissolve the soluble elements of clay minerals. As such, it occurs primarily in terrestrial or fluvial environments, not in a cold, estuarine environment. Furthermore the increase in proportion of montmorillonite is very slight compared with the conspicuous decrease in illite. Therefore, chemical alteration by transformation is not considered to be a significant process within the marine-estuarine environment. Transformation may occur in the terrestrial or fluvial environments but is thought to be minimal here because (1) high latitude weathering is primarily mechanical, especially during deglaciation and (2) there is presently little terrestrial influx.

Flocculation is the aggradation of material into small lumps. Early workers (e.g. Whitehouse et al., 1960) proposed inorganic flocculation whereby positive ions from the sea water surround the cation reducing the repulsive forces between the ions and allowing the van der Waals forces of attraction to take over. Such a process depends upon salinity, turbulence, concentration and importantly, mineralogical structure, thereby providing a mechanism for differential flocculation. From extensive settling experiments, Whitehouse et al. (1960) recorded settling velocities in brackish water of 15.8, 11.8 and 1.3 m/day for pure illite, kaolinite and montmorillonite respectively. Montmorillonite requires higher relative salinities in order to flocculate and therefore will tend to be deposited last, both spatially and temporally.

Recent workers (Pfeister et al., 1969; Dugan et al., 1971; Neihof and Loeb, 1973; Gibbs, 1977) have indicated that flocculation may also result from adhesion by organic coating or extracellular polymer strands. These

organic coatings plus possible metallic coatings may give all clay minerals similar flocculating properties (Gibbs, 1977).

Finally, segregation may occur by differential flocculation according to grain size. Because flocculation depends upon surface area, smaller particles will tend to flocculate first (van Olphen, 1966) until their settling speed equals the speed of the largest single grain, producing a bimodal deposit (Pierce and Myers, 1974; Kranck, 1975). Note that specific clay minerals are often found concentrated in different components of the size distribution curve (Gibbs, 1977), thereby providing an indirect mechanism for mineralogical segregation. Alternatively, Gibbs (1977) has proposed that in some environments clay mineral segregation may occur by direct physical sorting, the coarser particles settling out first or redistributed by estuarine circulation (Postma, 1967; Feuillet and Fleischer, 1980). In such a mechanism flocculation would play a minor role presumably because (1) turbulence does not allow the flocs to persist, (2) a low concentration reduces the likelihood of a collision, or (3) a combination of both mechanisms.

The numerous and variable mechanisms endorsed for clay mineralogical segregation indicates the necessity for further research in this field. It is suggested that this type of research should be aimed at mineralogical studies within detailed grain size fractions for the entire sample.

The variability of estuarine circulation systems further enhances the complexity of the depositional processes. Estuarine circulation of a partially mixed fjord may sustain net landward transport of bottom sediments, concentrating sediments along the landward margin of the basal salt

layer (Postma, 1967). The upward and outward flow of the circulation pattern at this point may segregate the clay minerals, the coarser or heavier fraction being deposited nearshore and the finer or lighter fraction being carried out to the basins again in the upper water strata (Meade, 1972). Tidal mixing may occur along the interface of the water strata, especially in partially mixed estuaries, effectively dispersing the suspended sediment load (Nichols, 1972). In contrast, highly stratified type estuaries possess very weak landward transport along the bottom; the sedimentation is usually dominated by river floods (Pritchard, 1955; Dyer, 1972).

#### 9.5 Hypothesis for Deposition of Clay Minerals

Although the clay mineralogy of discrete grain size fractions has not been determined and consequently size segregation cannot be distinguished from mineralogical segregation, a hypothesis can be proposed based on the observed clay mineralogical distributions and the nature of this particular estuarine environment. The observations must be treated separately for the conformable cover and for the contemporary and basin-fill unit distributions.

The pertinent conditions regarding the 10,000 years B.P., conformable cover unit are:

- (1) regionally, this period was characterized by deglaciation (Short et al., 1977), presumably with relatively high proportions of sediment laden runoff



- (2) the freshwater runoff enters Makkovik Bay, an unspecified-type estuary, meeting brackish to marine water
- (3) illite is concentrated along the south shore of the Outer Bay; feldspar responds inversely
- (4) there is a minor concentration of montmorillonite in the basins
- (5) the poorly sorted grain size distributions of the conformable cover unit suggest possible deposition by flocculation (Kranck, 1975).

The regional environment and the distribution of illite (Fig. 9.3) suggest that at least locally, the source of the clay minerals is to the south. The ultimate source has been interpreted to be glacial detritus. Presumably it was transported by glacial meltwater northwards along the glacially enlarged, Makkovik Brook valley. It is speculated that upon entering Makkovik Bay, illite was preferentially deposited proximally, due to (1) size segregated flocculation, (2) mineralogically segregated flocculation, or (3) some combination of both mechanisms. The changes in the relative proportions of the major clay-size minerals are shown in Figure 9.11 assuming a southern source and that the average of till proportions obtained from Piper and Slatt (1977) represent the proportions of local tills. In addition, montmorillonite is concentrated distally, presumably because of its slower settling velocity or because it generally flocculates less readily than other minerals in waters of very low salinity (Whitehouse et al., 1960).

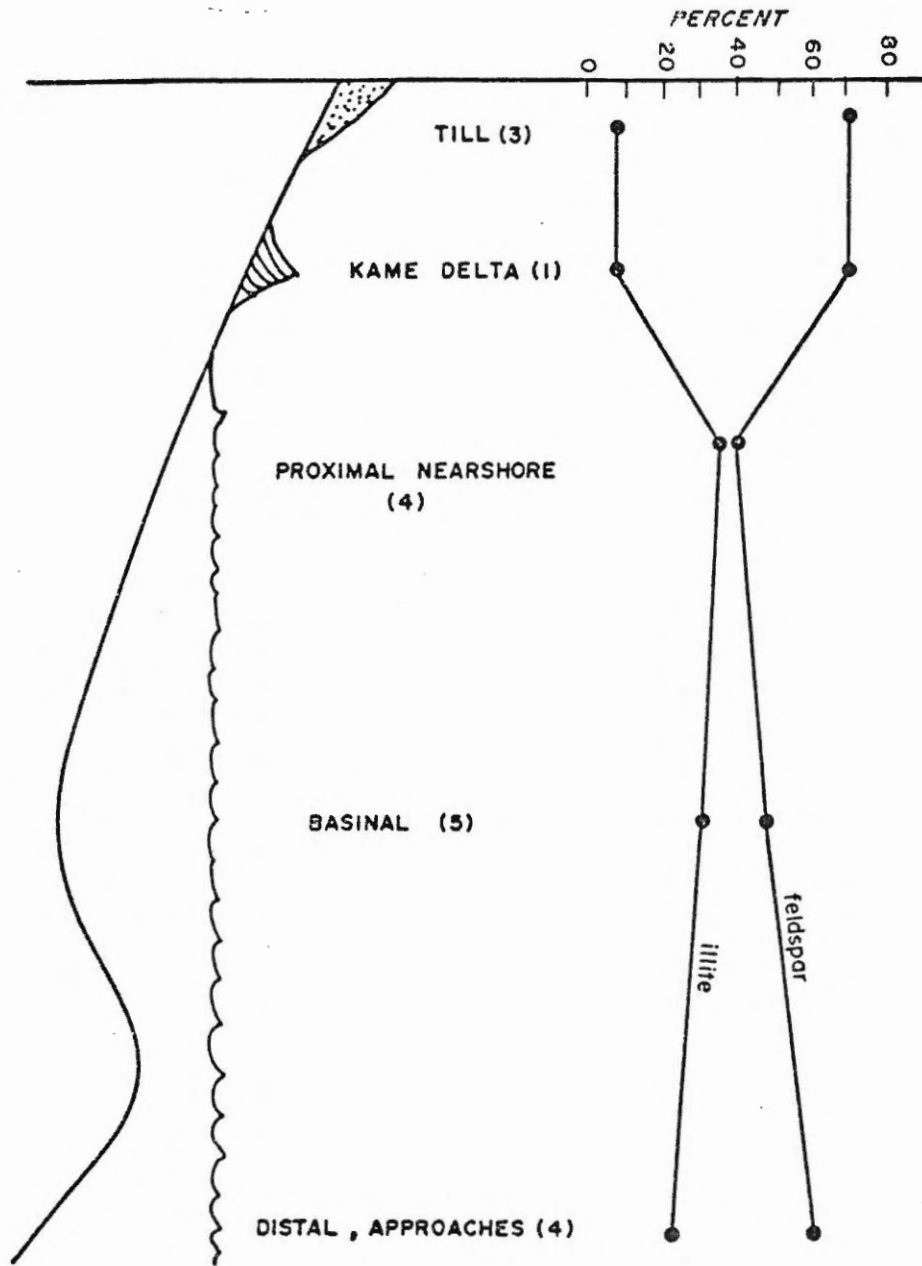


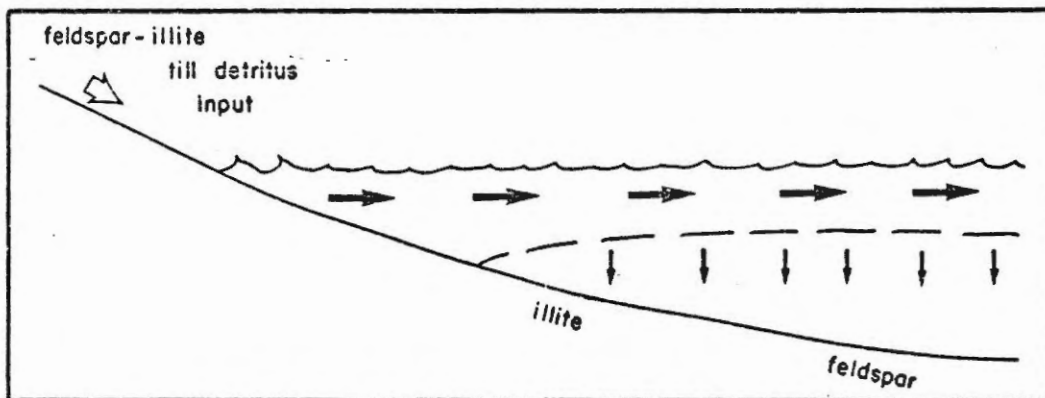
Figure 9.11: Averaged percents of feldspar and illite according to locality, progressions from terrestrial through proximal nearshore. Values in parentheses represent number of samples

It is speculated that Makkovik Bay was a highly stratified, two-layer type estuary during the deposition of the conformable cover unit (Fig. 9.12a). Suspended sediment of glacial detrital origin was transported by meltwater to the south shore of the Outer Bay and distributed across the fjord in a freshwater upper layer. The suspended material settles slowly until it reaches the lower, more saline bottom layer where it flocculates. Segregation of illite may have occurred during transport with the upper layer, concentrating illite proximally. The highly stratified, two-layer type estuary can therefore explain both the distribution of the clay minerals and the extensive lateral transport of sediment required by the acoustic morphology of the conformable cover unit. The runoff dominated deposition and the lack of estuarine circulation as suggested by the otherwise random clay mineralogy and the conformable morphology further indicate that the estuary may have been a highly stratified, two-layer type estuary.

The model for the contemporary distribution of clay-size minerals is based on the following observations:

- (1) generally, the clay mineralogy is random or well mixed throughout the bay; however, the illite/feldspar ratio decreases upwards throughout the piston core facies
- (2) there is minor concentration of chlorite at the head of the fjord and of montmorillonite at the seaward edges of individual Inner and Outer Bays.
- (3) the direct source of the basinal clays is the marginally eroding conformable cover unit

a) 10,000 years B.P. (conformable cover)



b) Contemporary (basinal olive mud)

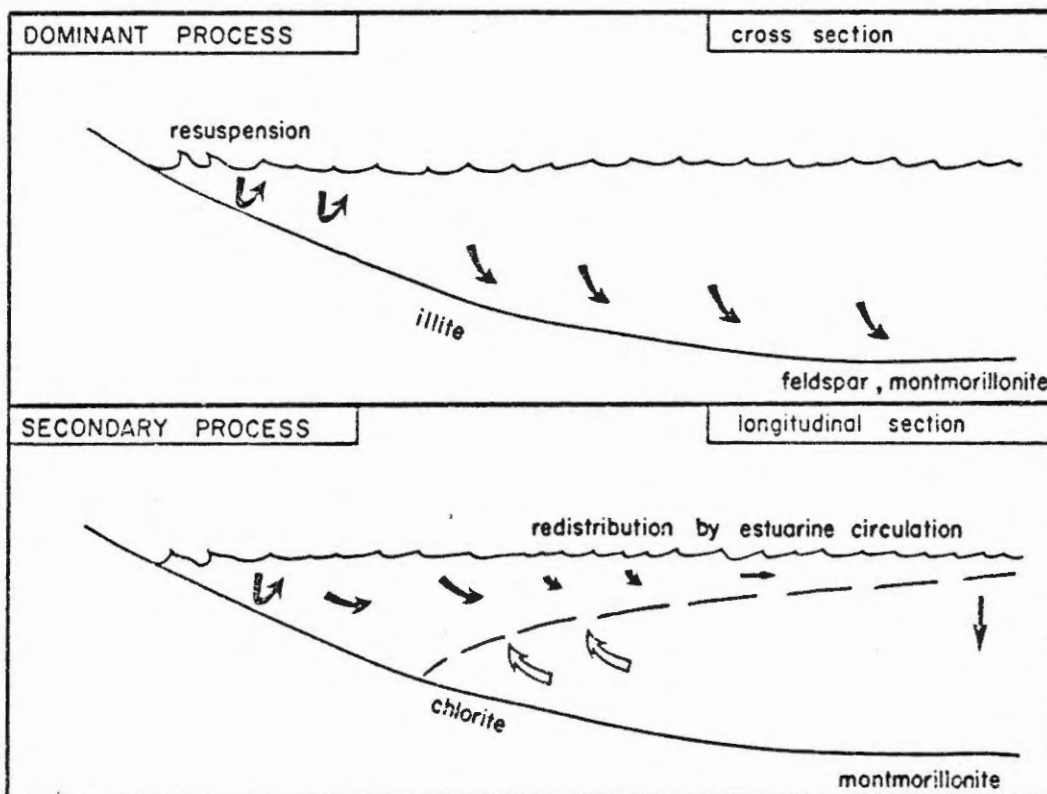


Figure 9.12: Hypotheses for the deposition of clay minerals for (a) the conformable cover unit in a highly stratified, 2-layer type estuary and (b) the basinal olive mud in a partially mixed type estuary

- (4) oceanographically, the fjord is a partially mixed estuary during the summer months.

Although the source is variable downbay, especially with respect to the dominant minerals, there is no major segregation observed in the contemporary environment. It is suggested that the first generation clays of the conformable cover unit are reworked and redistributed by a combination of wave energy, estuarine circulation and tidal mixing, effectively mixing the sediments to form the relatively homogeneous second-generation clays. This would explain the lack of downbay trends. However, illite may be further concentrated along the shoreline during resuspension (Whitehouse et al., 1960) thereby explaining the upward decreasing illite/feldspar ratio observed in the piston core facies. Presumably illite and feldspar are responding to the wave-dominated environment and are deposited relatively rapidly. In contrast, the distribution of chlorite and montmorillonite appear to be controlled by estuarine circulation. This is suggested by the minor concentration of chlorite at the head of the fjord and of montmorillonite both at the individual Bay mouths and upwards throughout the piston core facies.

CHAPTER X

FORAMINIFERA

10.1 Introduction

Variations in assemblages of benthonic foraminifera have been used elsewhere to demarcate major fluctuations in relative sea level and salinity (e.g. Fillon, 1974; Scott, 1977; Scott and Medioli, 1978, 1979). Consequently, the foraminiferal distributions were examined in the present study to help define the paleoenvironment of proglacial deposition as compared with the contemporary environment. A sampling program was carried out on the surficial and piston cores, ultimately to aid in the development and interpretation of a detailed stratigraphic-depositional model bridging postglacial and recent environments.

Sample processing and identification are discussed in Chapter V.

10.2 Surficial Distribution

The data are presented in Figure 10.1 and Table 10.1. In general, the foraminiferal distribution can be described according to 3 sediment types:

- (1) the surficial olive sediments including the basinal olive mud, the coarse olive mud and the coarse veneer units;
- (2) the relict, gray clayey silt and

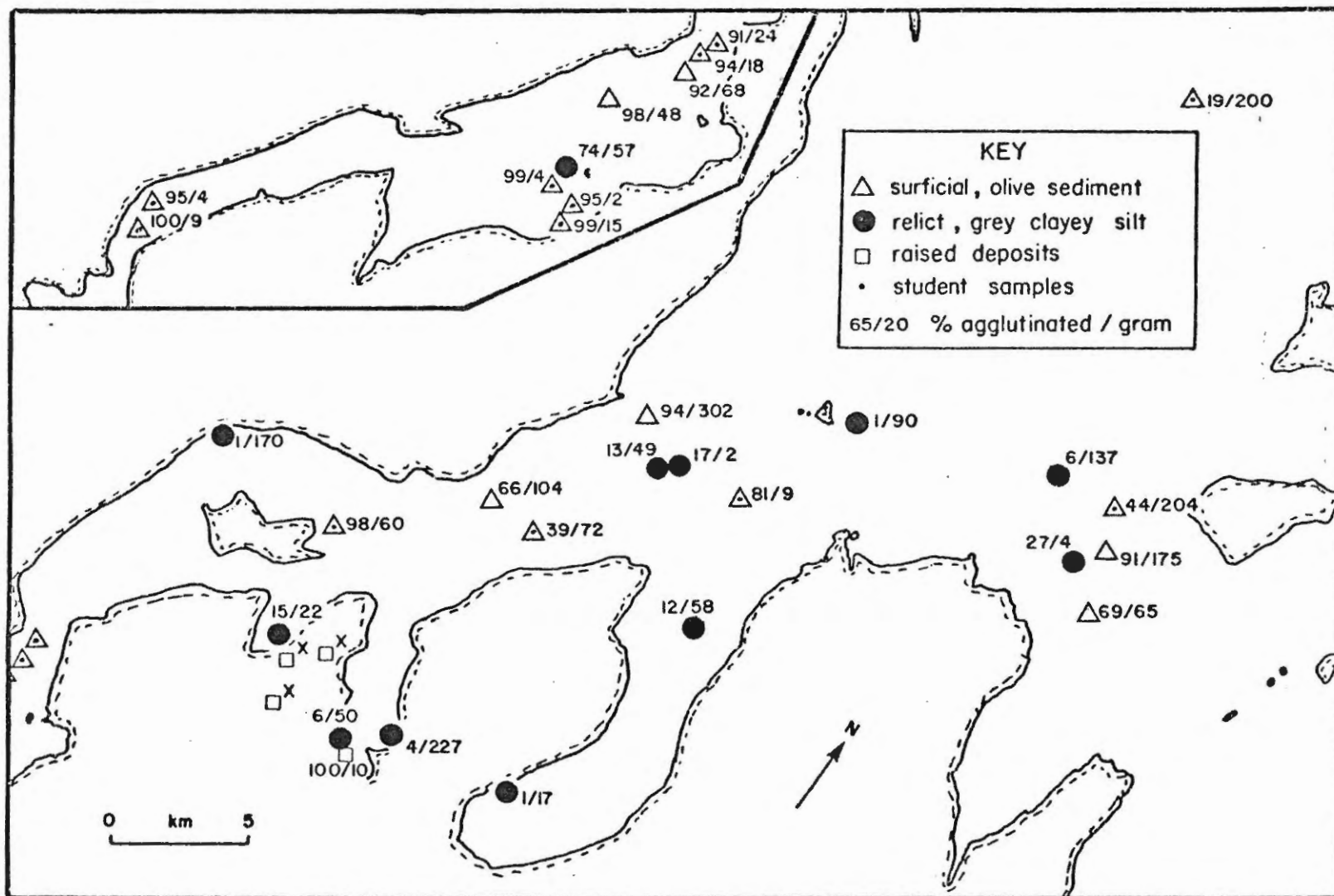


Figure 10.1: Areal distribution of benthonic foraminifera expressed as percent agglutinated and total number of individuals per gram for the surficial olive sediment (units II and III) and the relict gray clayey silt (unit IV); x is less than 1 percent

TABLE 10.1 (a) Surficial distribution of foraminifera according to lithology; individual species are expressed as a percentage, x being less than 1%

	SURFICIAL OLIVE MUD				RELICT GREY CLAYEY SILT										
Sample number	422	393	519	474	434	530	291	292	293	344	509	524	525	462	471
Lab number	M48	M47	M49	M30	M32	M31	M20	M21	M22	M23	M25	M26	M27	M28	M29
Total Foraminifera	129	172	632	128	358	343	230	671	163	217	262	361	38	306	67
Foraminifera per gram	48	68	104	65	57	170	17	227	22	50	58	49	2	137	4
Astrammina sp.	2	5	1	2	6	-	-	1	-	x	x	-	-	-	2
Annotium sp. (A. cassia)	-	-	-	-	-	-	-	-	-	-	-	x	-	-	-
Cribrostomoides sp. (C. crassinargo)	10	9	8	8	8	1	-	x	4	-	1	2	3	1	-
Eggerella advena	59	53	48	26	46	-	x	-	1	-	x	3	8	1	6
Reophax sp. (R. arctica)	22	23	5	29	17	1	1	2	7	5	6	2	3	1	8
Spiroplectammina biformis	3	-	x	-	x	-	-	x	1	-	x	4	-	2	6
Textularia sp.	2	-	3	2	1	x	-	-	1	x	2	1	-	1	-
Trochammina spp.	2	2	1	2	3	x	x	1	1	1	3	1	3	-	5
Other agglutinated	-	-	-	-	-	-	-	-	-	-	-	-	-	-	-
Astrononion gallowayi	-	-	3	-	-	x	-	-	-	-	x	-	-	x	-
Buccella frigida	-	-	-	1	1	4	1	1	1	1	2	x	-	1	-
Cibicides lobatulus	-	2	2	-	-	-	-	-	-	-	-	-	5	-	-
Elphidium excavatum group	2	-	4	4	2	38	x	40	10	9	34	8	3	16	-
Elphidium spp.	-	-	-	3	2	2	1	x	4	2	4	2	-	3	5
Fursenkoina sp.	-	-	-	2	-	4	-	15	1	-	5	-	8	1	2
Islandiella islandica	-	5	17	7	8	38	32	27	42	58	27	42	16	43	48
Islandiella toretus	-	1	7	-	5	6	57	5	21	11	2	27	11	24	6
Lagena sp.	-	-	-	-	-	-	-	-	-	x	-	-	-	-	-
Nonionellina labrad- dorca	-	2	1	5	3	1	x	2	-	-	-	2	8	4	3
Oolina sp.	-	-	-	-	1	1	1	-	1	-	1	-	-	-	-
Protelphidium sp.	-	-	-	2	1	1	-	2	2	3	2	1	8	1	-
Pseudopolymorphina sp.	-	-	-	-	1	1	-	2	-	-	-	1	3	1	-
Quinqueloculina sp.	-	-	-	-	-	-	-	-	1	-	-	1	-	1	-
Other calcareous	-	-	-	5	3	4	5	2	4	8	9	4	21	2	12
Other agglutinated	98	92	66	69	74	1	1	4	15	6	12	13	17	6	27



TABLE 10.1(b) Total Foraminifera per gram and percentage of agglutinated types from samples of surficial olive sediment, examined by students

Sample number	535	536	489	431	430	392	390	526	297	459	445	468	455
Lab number 78-511-	F59	F58	F82	F80	F79	F69	F70	F73	F65	F66	F84	F85	F87
Total foraminifera/g.	9	4	4	15	2	18	24	60	72	9	90	204	200
% Agglutinated	100	95	99	99	95	94	91	98	39	81	1	44	19

- (3) raised land deposits, including deltaic sands and sandy muds.

The surficial olive sediments are characterized by a primarily agglutinated assemblage, conspicuously dominated by Eggerella advena and Reophax arctica. Other species include Cribrostomoides sp., Spiroplectamina biformis, Astrammmina sp., Textularia sp. and Trochammina spp. The major calcareous forms are Islandiella islandica, I. teretus and Elphidium excavatum. The samples examined by the students (Table 10.1b) suggest an increase in the total population and the percentage of calcareous types in a downbay direction.

The relict, gray clayey silt is characterized by a calcareous assemblage, strongly dominated by Islandiella islandica, I. teretus and E. excavatum. The minor species include all those present in the surficial olive sediment plus Buccella frigida, Cibicides lobotulus, Elphidium sp., Fursenkoina sp., Nonionellina labradorica, Oolina sp., Protelphidium sp., Pseudopolymorphina sp. and Quinqueloculina sp.

From 8 raised land samples examined, all were barren except for one sample at the base of the Makkovik Harbour raised delta. This was a gray sandy sample with only 10 individual/gram of Eggerella advena.

No planktonic foraminifera were observed in any of the samples.

### 10.3 Discussion of Surficial Distribution

The downbay decrease in the agglutinated/calcareous ratio with the surficial olive sediments may be controlled by one or both of (1) the

transition from estuarine to open marine conditions, and (2) the contamination from the calcareous-dominated assemblage in the underlying gray, clayey silt. This can be determined conclusively only by studying the living fauna, although some insight can be obtained from the present oceanographic data. The temperature and salinity profiles indicate pronounced downbay changes, typical of other Labrador fjords. In addition, the highest proportion of agglutinated forms and the smallest total population occurs at the mouth of Makkovik River. This suggests that the oceanographic conditions may actively control the foraminiferal distribution.

On the other hand, the proximity of the surficial olive sediments to the calcareous dominated, gray clayey silt suggests at least some degree of contamination. This contamination may be contemporary in the erosional sense as the marginally reworked gray clayey silt is redistributed in the basins, or in the initial depositional sense with a gradational upward transition from the calcareous dominated assemblage of the gray clayey silt to the agglutinated dominated assemblage of the surficial olive sediments. The latter is the suggested circumstance for the low agglutinated/calcareous ratios observed in the centre of the Outer Bay. At these locations, the acoustic profiles suggest that erosion has removed almost all of the overlying, acoustically transparent olive sediment (Fig. 4.5). These samples are interjacent to less diverse, agglutinated assemblages in the contemporary ponded olive muds. Therefore, it is suggested that the foraminiferal distribution within the surficial olive sediments is controlled by at least the contemporary oceanographic environment and by the contamination from calcareous dominated, older sedimentary units.

Presumably, the calcareous-dominated fauna of the gray clayey silt unit was deposited in a more saline, possibly warmer environment (Greiner, 1970). This suggests that the Outer Bay, which is presently in the transitional estuarine regime (Scott et al., 1980), was in the "outer bay" estuarine-marine environment typified by close to normal marine salinities, during the deposition of the gray clayey silt unit. Note, however, that the foraminiferal distribution of the solitary sample of this unit from the Inner Bay (sample 78-511-434) suggests that this area remained estuarine to transitional-estuarine during this period.

The lack of foraminifera, even of agglutinated forms, in the land deposits suggests (1) that they may not be marine or estuarine sediments, (2) an extremely high sedimentation rate, (3) an environment of high energy or (4) a lack of fossil preservation.

#### 10.4 Distribution Within Piston Cores

The 26 samples were selected according to the lithological facies. The data are shown in tables 10.2 and 10.3 and graphically in Figures 10.2 and 10.3. The most prominent trends are shown by the abundance of benthonic foraminifera per gram of dried sediment, the proportion of the dominant species and by the agglutinated-calcareous ratio.

##### (i) Facies A

The total population in facies A varies from 50/g at the bottom of the core, increasing upcore to about 700/g at the 2 m core interval (approximately 4,000 years B.P., Chapter VIII), diminishing again to 180/g by the

TABLE 10.2 Percentage of Foraminifera in piston core 78-020-003 and trigger weight core from the Approaches; x is less than 1%

Sample number 78-020-003- Lab number	0T	100T	85	185	285	313	353	413	443	483	523	583	645	733	83
Total Foraminifera	459	432	364	352	172	517	127	87	74	190	35	321	267	357	106
Foraminifera per gram	175	397	288	687	131	410	33	8	19	36	5	122	64	49	17
Astrammina sp.	1	1	1	3	1	1	2	3	-	2	-	2	-	1	1
Ammotium sp. (A. cassis)	1	x	-	x	-	-	-	-	-	-	-	-	-	x	-
Cibrostomoides sp. (C. crassimargo)	7	6	2	1	3	2	3	9	-	-	3	1	2	1	3
Eggerella advena	32	23	32	22	56	29	8	15	8	9	9	43	43	69	60
Reophax spp. (R. arctica)	48	38	40	31	23	26	2	25	6	3	3	27	37	21	25
Spiroplectammina biformis	4	3	-	1	1	-	1	2	-	2	-	-	-	-	-
Textularia sp.	-	5	2	3	3	2	1	7	-	3	-	3	1	2	4
Trochammina spp.	x	5	6	5	2	3	1	5	1	-	3	4	4	5	8
Other Agglutinated	-	-	-	-	-	-	-	-	-	-	-	-	-	-	-
Astrononion gallowayi	-	1	x	1	1	-	-	-	-	-	-	1	-	-	-
Buccella frigida	x	1	-	1	1	x	-	-	2	-	3	1	1	-	-
Cibicides lobatulus	-	1	x	1	1	x	-	-	-	1	-	1	1	-	-
Elphidium excavatum group	3	2	5	9	1	9	24	5	20	16	23	3	4	-	-
Elphidium spp.	x	1	2	2	1	5	4	1	-	2	3	2	2	-	-
Fursenkoina sp.	3	2	x	1	-	3	2	-	-	8	-	1	1	-	-
Islandiella islandica	1	2	2	4	2	5	35	15	42	26	40	5	2	-	-
Islandiella teretus	-	1	1	4	-	2	13	-	14	24	14	1	1	-	-
Lagena sp.	1	x	x	-	1	x	-	-	-	2	-	1	-	-	-
Nonionellina labradorica	x	1	1	-	-	3	1	3	3	-	-	1	-	-	-
Oolina sp.	-	1	x	x	1	x	-	-	3	-	-	x	1	-	-
Protelphidium sp.	-	x	x	1	-	1	-	-	-	-	-	1	1	x	-
Pseudopolymorphina sp.	-	1	-	-	-	x	-	-	-	-	-	1	-	-	-
Quinqueloculina sp.	-	-	x	-	-	x	-	-	1	1	-	-	-	-	-
Other calcareous	x	7	4	11	-	7	5	9	-	2	-	-	1	x	-
Percent Agglutinated	91	79	83	65	91	63	18	67	15	19	18	81	85	99	100

TABLE 10.3 Percentage of Foraminifera in piston core 78-020-004 and trigger weight core from the Outer Bay; x is less than 1%

Sample number 78-020-004- Lab number	10T	70	190	360	443	483	613	693	705	735	895
Total Foraminifera	396	145	277	131	263	476	170	215	127	118	105
Foraminifera per gram	302	42	135	25	520	461	72	61	97	32	7
Astammina sp.	4	3	2	-	-	-	-	2	-	-	4
Ammotium sp. (A. cassia)	1	1	1	-	-	-	-	-	-	-	1
Cribrostomoides sp. (C. crassimargo)	8	6	-	2	-	x	2	-	1	3	-
Eggerella advena	51	82	24	16	-	-	3	-	-	3	9
Reophax spp. (R. arctica)	23	4	25	5	x	5	12	12	17	2	68
Spiroplectammina biformis	1	-	x	2	-	1	8	3	15	7	1
Textularia sp.	3	1	2	3	-	1	2	3	1	-	1
Trochammina spp.	5	1	2	2	-	1	-	1	2	1	17
Other Agglutinated	-	-	-	-	-	-	-	-	-	-	-
Astrononion gallo- wayi	-	-	-	5	2	1	2	-	2	-	-
Buccella frigida	x	-	3	5	2	2	-	1	2	-	-
Cibicides lobatulus	-	-	-	-	-	-	-	-	-	-	-
Elphidium excavatum group	1	-	7	26	55	48	2	8	7	3	-
Elphidium spp.	1	-	3	3	2	1	-	-	-	-	-
Fursenkoina sp.	-	-	-	-	1	x	1	2	-	-	-
Islandiella islandica	1	-	11	27	31	25	51	34	30	17	-
Islandiella teretus	x	-	1	2	7	4	14	14	9	54	-
Lagena sp.	-	-	x	-	-	-	-	-	-	-	-
Nonionellina labra- dorica	2	-	3	-	-	x	-	-	-	1	-
Oolina sp.	-	-	-	-	-	-	-	-	-	-	-
Protelphidium sp.	x	-	1	1	-	3	1	2	-	-	-
Pseudopolymorphina sp.	-	-	-	4	-	1	-	-	14	-	-
Quinqueloculina sp.	-	1	-	-	-	-	1	1	-	-	-
Other calcareous	-	-	15	-	3	7	1	17	1	11	-
Percent Agglutinated	94	99	56	30	x	8	25	21	36	16	100

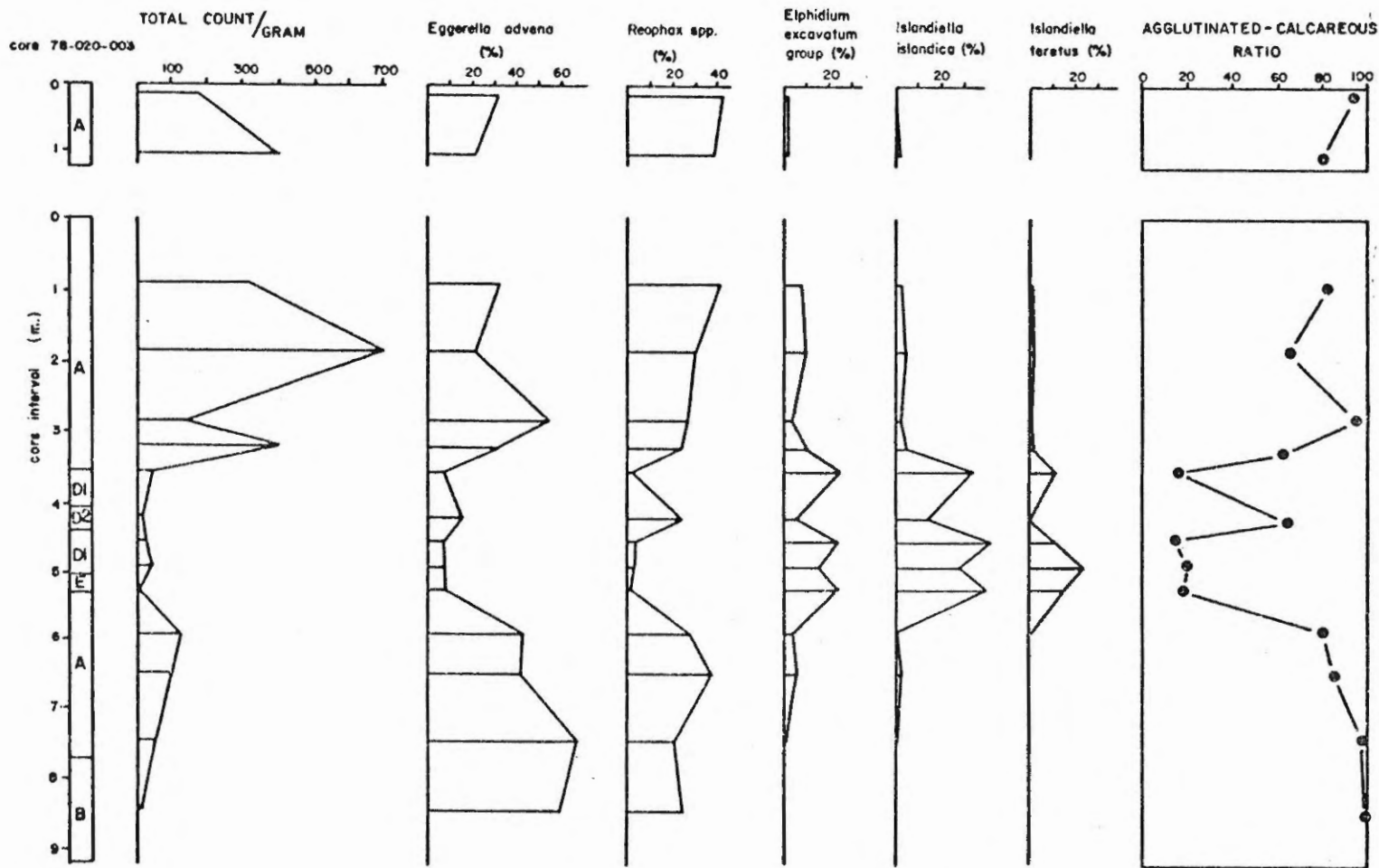


Figure 10.2: Distribution of foraminifera according to piston core lithofacies for core 003 plus the showing total populations and percentages of dominant species

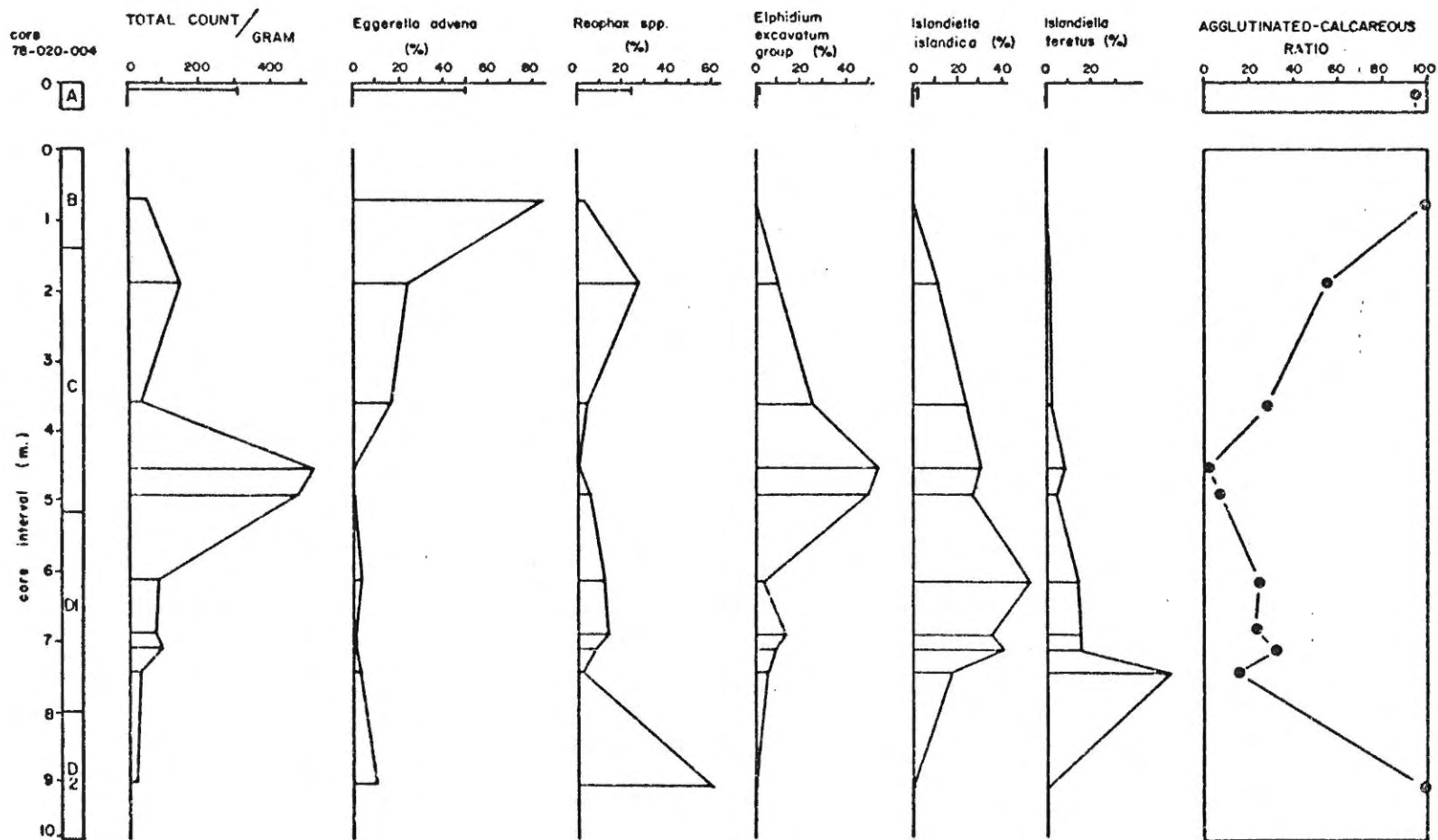


Figure 10.3: Distribution of foraminifera in piston core 004 according to lithofacies showing variations in the total population and percentages of dominant species



top of the trigger weight core and is then dominated by R. arctica. The proportion of agglutinated tests is high, ranging from 65 to 96%, generally varying inversely with the total population. E. advena and Reophax spp. (R. arctica) together form 55-85% of the total population. Other agglutinated species include Astrammia sp., Cribrostomoides sp. (C. crassimargo), Spiroplectammia biformis, Textularia sp. and Trochammia spp. The major calcareous fauna include E. excavatum, Fursenkoina sp., I. islandica and I. teretus.

(ii) Facies B

Facies B has a low absolute population, less than 75/g. E. advena is conspicuously dominant followed by R. arctica, and together they make up 85% of the total population (Figs. 10.2, 10.3).

(iii) Facies C

The total absolute population in facies C diminishes rapidly upcore from a peak of 500/g to 50/g, while there is a synchronous increase in the proportion of agglutinated tests from 5 to 60%. The basal peak has 40% E. excavatum, 30% I. islandica and minor I. teretus, Protelphidium sp., Pseudopolymorphina sp., Fursenkoina sp., B. frigida, A. gallowayi and C. lobatulus. The upper portion of facies C is dominated by E. advena and Reophax sp.

(iv) Facies D

The total absolute population of facies D is less than 75/g. Subfacies D2 has a faunal assemblage similar to facies B, except that E. advena and

Reophax sp. are equally abundant. In contrast, subfacies D1 has 80% calcareous tests dominated by I. islandica and I. teretus followed in abundance by E. excavatum, N. labradorica, Quinqueloculina sp. and Fursenkoina sp.

(v) Facies E

Facies E has the lowest absolute population (5/g), but otherwise is similar to subfacies D1.

10.5 Discussion of Ecology of Benthonic Foraminifera

Numerous environmental and biological parameters have been invoked to explain fluctuations or breaks in faunal distributions. These are discussed at length elsewhere (e.g. Ellison Jr., 1951; Bandy and Arnal, 1960; Phelger, 1960; Bartlett, 1966; Scott et al., 1977; Bergen and O'Neil, 1979; Osterman and Kellogg, 1979; Lagoe, 1979) and therefore only selected aspects will be considered here. Note that only total populations were examined in this study and these do not necessarily correspond with the living populations, although for some environments they have been demonstrated to be a reliable indicator (Scott and Medioli, 1980).

Bartlett (1965) identified three major faunal assemblages along the Atlantic nearshore from northern to southern latitudes according to general, climatic environments:

- (1) northern, subarctic to arctic environments have predominantly agglutinated foraminifera;

- (2) temperate to cool temperate environments are pre-  
dominated by hyaline calcareous tests, and
- (3) southern, warmer more saline environments have a  
strong miliolid assemblage.

In general, calcareous foraminifera require warm, saline conditions for the growth of calcareous shells, whereas most agglutinated foraminifera utilize organic cement for test construction and hence, do not depend upon the availability of calcium carbonate in the water (Greiner, 1970). Consequently, the restricted marine environments such as paralic and estuarine environments have predominately agglutinated forms whereas open marine environments have calcareous forms (e.g. Cockbain, 1963; Greiner, 1970; Vilks, 1976; Scott et al., 1980).

Carbonate dissolution in high latitudes has been well documented (e.g. Osterman and Kellogg, 1979) and with the presence of runoff from an acidic terrain, would appear to be an important influence. However, dissolution is not favoured as a major controlling factor in Makkovik Bay because:

- (1) the extremely low absolute populations of calcareous  
and agglutinated forms occur synchronously,
- (2) while macrofossil carbonate material was not observed  
in raised marine deposits exposed to runoff, it is  
observed in abundance without obvious dissolution  
textures in both whole and comminuted states in marine  
lithologies containing relatively few calcareous  
foraminifera and

- (3) the acidic runoff tends to be confined to the upper strata of the fjord, maintaining relatively consistent bottom water with important characteristics such as abundant dissolved oxygen (Nutt and Coachman, 1956)
- (4) the high sedimentation rate would tend to reduce dissolution effects.

Furthermore, the possibility of diagenetic dissolution of the cement in agglutinated tests (Fillon, 1974) is considered to be unlikely for these species because (1) they possess highly resistant, tough organic cements and (2) their relative proportions in the Approaches core are generally increasing a uniformly down to the bottom of the core.

From a synthesis of data from 16 estuarine areas in Maritime Canada, Scott et al. (1980) concluded that estuarine foraminiferal distributions can be used to map salinity distributions both in space and time. Therefore it is important to identify the ranges of the characteristic oceanographic parameters that are associated with individual species for present day environments.

Eggerella advena is a shallow water, cosmopolitan, agglutinated form found in water generally less than 90 m deep (Phleger, 1952). Significant amounts have been recorded from the Arctic by Phleger (1952), Cooper (1964), and Vilks (1975). Cockbain (1963), Cooper (1964) and Hooper (1975) have described E. advena dominated assemblages associated with a wide range of temperature (-1 to 8°C) and salinity (21 to 33‰) conditions from the Arctic, St. Lawrence estuary and Georgia Strait, British Columbia.

The other important agglutinated form, Reophax arctica, is widely distributed in all substrates and at all depths in the Arctic (Phleger, 1952), but tends to be more abundant in the basins with sediment in the silt range (Cooper, 1964). Osterman and Kellogg (1979) identified Reophax spp. in water depths greater than 400 m in the Ross Sea. Scott and Medioli (1978) observed minor proportions of R. arctica from Maritime lake cores of basinal estuarine sediments, just above reworked glacial material. E. advena, A. cassis, R. arctica, R. fusiformis plus an array of other species form the characteristic assemblage of the transitional zone of deep, subtidal estuaries in the Maritimes (Scott et al., 1980).

The calcareous form, Islandiella teretus, is presently found in abundance primarily in the Canadian Arctic (Leoblich and Tappan, 1953; Vilks, 1969), St. Lawrence estuary (Hooper, 1968) and in the Gulf of St. Lawrence (Vilks, 1968). The latter occurrences are largely restricted to water depths of 55 to 75 m, a constant annual temperature of about 0°C and a salinity of approximately 52‰ (Vilks, 1968). Using this information plus data from the Chuckchi Sea (Cooper, 1964) and other regions of the Arctic (Cushman, 1948; Phleger, 1952; Leoblich and Tappan, 1953), Fillon (1974) suggested that I. teretus may be limited to cold marine water that does not rise much above 3°C during any part of the year.

Islandiella islandica is common from 50 to 300 m water depth off eastern Canada (Hooper, 1968; Vilks, 1968). It is the dominant species of a faunal assemblage in the St. Lawrence estuary in water characterized by a temperature of 4 to 5°C and a salinity of 34.6‰ (Hooper, 1975). I. islandica was not observed in the Bras d'Or Lakes of Cape Breton where

the salinities are generally low at about 24‰ (Vilks, 1968). The probable range of salinities of coastal waters preferred by I. islandica is 30 to 33‰ (Cooper, 1964; Vilks, 1968).

Elphidium excavatum is common from 0 to 150 m water depth throughout the Arctic (Cushman, 1943; Phleger, 1952; Loeblich and Tappan, 1953; Cooper, 1964) and along the eastern continental shelf (Cushman, 1948; Parker, 1952; Phleger, 1952; Weiss, 1954; Hooper, 1968; Todd and Low, 1961; Slessor, 1970). However, the E. excavatum dominated occurrences are generally restricted to shallow, low salinity environments such as estuaries (Loeblich and Tappan, 1953; Cockbain, 1963). Slessor (1970) reports a depth of less than 4 m and a salinity range of 18 to 24‰ for an E. excavatum dominated fauna in Covehead Bay, Prince Edward Island. E. excavatum is generally considered to be an arctic to subarctic near-shore species that is found in waters free of summer ice and is able to tolerate wide temperature and salinity fluctuations (25-30‰) (Leslie, 1965; Vilks et al., 1979).

The transition from open marine fauna such as I. islandica to open bay fauna such as E. excavatum to inner bay fauna usually typified by a predominately agglutinated fauna has been widely recognized (e.g. Cockbain, 1964; Hooper, 1968; Scott et al., 1980). Furthermore, foraminiferal assemblages from core samples of the early Champlain Sea have been interpreted to reflect glacio-isostically induced shallowing and eventual warming and freshening (Fillon, 1974; Cronin, 1977). The five faunal zones in order of freshening or warming of the Champlain Sea are: I. teretus, I. teretus, I. teretus and I. islandica, P. orbiculare and E. bartletti, E. excavatum

and P. orbiculare, and E. clavatum. Scott and Medioli (1978) interpreted similar sequences from Maritime lake cores as gradual freshening from originally marine basin conditions.

#### 10.6 Interpretation

Using the ranges of oceanographic conditions for individual species and the fluctuations of foraminiferal assemblages both in contemporary estuarine systems and other analogous cores, it is possible to make some logical interpretations from the piston core faunal distributions. It should be noted that as the two piston cores are from different estuarine environments and their lithofacies are diachronous, the controlling factors themselves are probably diachronous.

From facies D1 to C in core 004 the dominant species are, in order, I. teretus, I. islandica, E. excavatum and E. advena. This sequence indicates upward decreasing salinity and possibly increasing temperature. From the approximate ranges of contemporary oceanographic conditions for these species the following changes are suggested:

	<u>Salinity</u>	<u>Temperature</u>
<u>E. advena</u>	21-33%	-1 to 8°C
<u>E. excavatum</u>	18-30	wide range
<u>I. islandica</u>	30-33%	< 3°C
<u>I. teretus</u>	32%	~ 0°C

E. excavatum appears to indicate the greatest transition from an open bay to a restricted marine environment. The abundance of R. arctica at the

top of the core suggests that the environment is still relatively deep and cool.

The overall increase in the total absolute population from the bottom of both piston cores to approximately 4,000 years B.P. is consistent with a decrease in the rate of sedimentation. The peak at the base of facies C in core 004 is dominated strongly by E. excavatum, presumably indicating that it is a rapid colonizer. The decrease in the total absolute population since 4,000 years B.P. (as observed at the top of core 003) is problematic, especially as the rate of sedimentation and salinity (which are both related to the relative sea level) are presumably still decreasing. A decrease in temperature of the bottom water would explain the decreased total population and the dominance of R. arctica. This is consistent with the subarctic bottom conditions presently observed within the fjord (Chapter III). If this is a major controlling factor, then the total population peak at about 4,000 years B.P., previously attributed to a decrease in the rate of sedimentation, may also be affected by an increasing temperature. This is consistent with the upward trend shown by the calcareous fauna in core 004.

The assemblage and trends within facies E and D suggest an open bay, estuarine marine environment. However, subfacies D2, the interbedded mud and laminated silt unit, is dominated by R. arctica, suggesting a period of cool, brackish water conditions.

While there are undoubtedly many factors that influence the distribution of foraminifera within these sediments, the following conditions outline the interpreted, major controlling factors up the facies sequence:



Facies E: high sedimentation rate in open marine environment

Facies D: high sedimentation rate in an open marine, cold environment with possible brackish fluctuations (subfacies D2)

Facies C: rapidly decreasing salinity, moderately decreasing rate of sedimentation

Facies B: slow rate of sedimentation, brackish estuarine conditions

Facies A: slow rate of sedimentation, brackish estuarine conditions, possibly decreasing temperature since 4,000 years B.P.

The conformable cover unit, sampled from surficial exposures, contains a dominant assemblage of I. islandica, E. excavatum and I. teretus. Reophax arctica is the main agglutinated species. This is the same assemblage associated with facies D and accordingly has a similar environment. Crude salinity, temperature and sedimentation rate trends are shown schematically in Figure 10.4.

The composite sequence, as sampled in core 003, does not show the expected facies sequence. This problem has been outlined in Chapter VIII, discussing two alternative explanations: the allochthonous and autochthonous hypotheses. In core 003 the open bay, estuarine fauna of facies D and E overlie the agglutinated, brackish fauna of facies A. However, the upward increase in the proportion of calcareous fauna in facies A suggest that it is in depositional continuum with facies D and E. Therefore, the

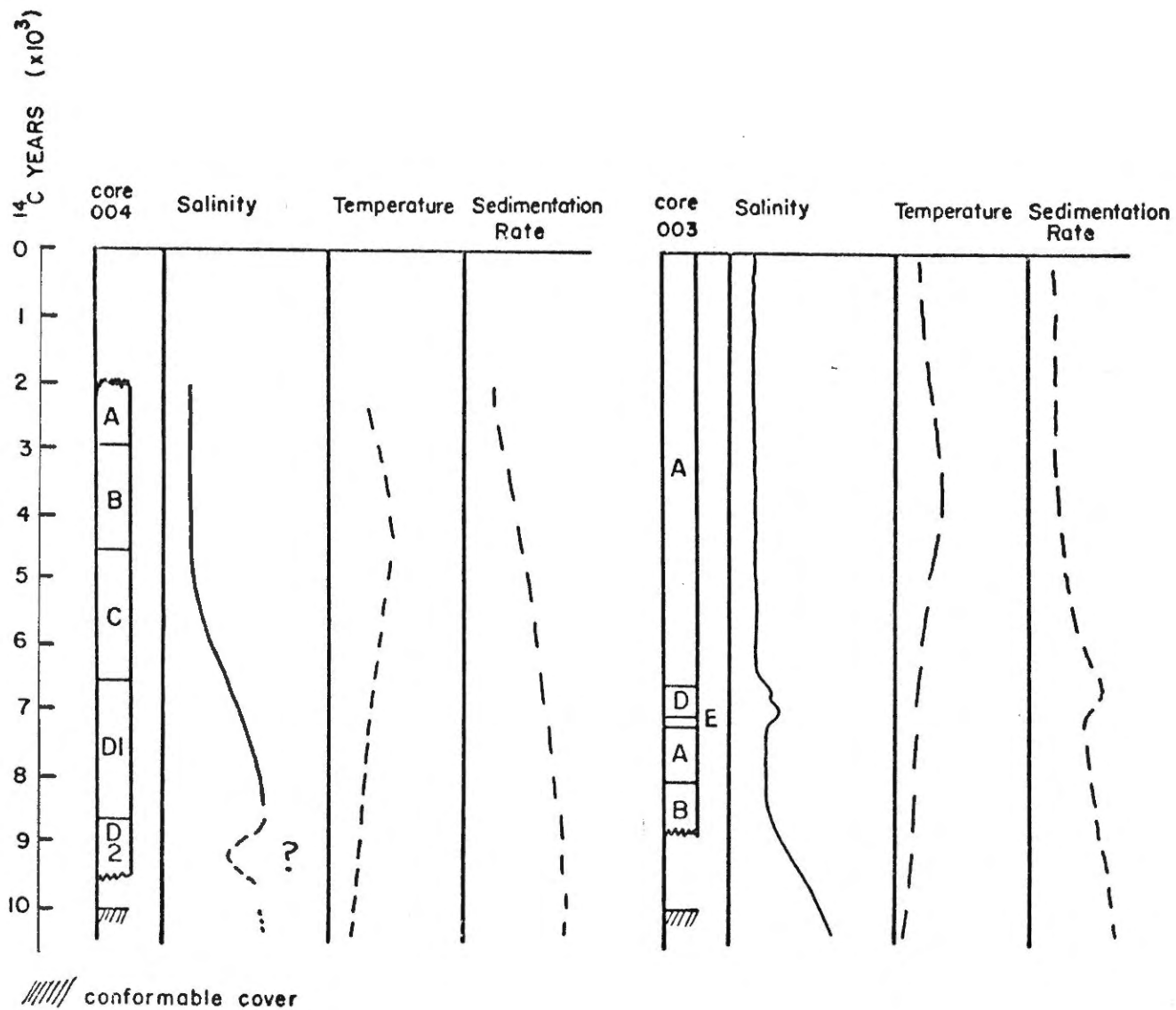


Figure 10.4: Tentative down core estimates of salinity, temperature and sedimentation rate based on foraminiferal distribution

distribution and interpretation of the foraminiferal trends add further support to the autochthonous hypothesis.

The acoustic profiles suggest differential erosion of the upper basin-fill unit throughout Makkovik Bay (Chapter IV) and therefore one would expect to observe successive piston core facies along the erosional zones. This has not been observed because:

- (1) the sample distribution and analytical detail of the surficial samples was not sufficient to allow positive identification of the facies changes
- (2) the vertical, piston core facies may not be laterally continuous or uniform
- (3) it is difficult to distinguish the veneering sediments from the outcropping sediments, especially at the margins of the basins where they grade into one another.

It is suggested that the foraminiferal assemblages would be the best indicator of individual facies that outcrop along the seafloor. However, it must be realized that (1) the present day estuarine foraminiferal facies have not been mapped in detail and that (2) older facies may not possess similar foraminiferal assemblage patterns.

CHAPTER XI

FACIES MODEL OF POSTGLACIAL DEPOSITION

11.1 Factors Controlling Deposition

It is apparent from the distributions of the clay mineralogy and the benthonic foraminifera that two dominant factors have controlled the depositional environment since deglaciation. These factors are: (1) the change in relative sea level and (2) the fluctuations in runoff from an ablating ice sheet and the surrounding drainage basins.

Changes in relative sea level have three major effects on the estuarine environment. Firstly, a high relative sea level will reduce the restrictive influence of sills allowing enhanced interchange of estuarine and marine water. These changes would be monitored by foraminiferal assemblages. Secondly, a transgressing or regressing shoreline would expose respectively terrestrial or marine sediments to wave erosion, thereby altering the source of sediments deposited in the basins. Thirdly, variations in the water depth would change the morphology and degree of preservation of the sedimentary unit; the blanket-like sediment morphologies are laid down without erosion along the topographic highs from relatively uniform water depths, achieved during a higher sea level. In Chapter IV, it was proposed that the water depth was sufficient to effect and maintain the blanket-like morphology of the conformable cover unit. Figure 11.1 demonstrates that the postulated 50 m higher sea level (inferred from land geology and surficial sediment textures) was capable of producing a conformable unit. The lower limit of erosion from wave and swell energy, as determined by the

contemporary distribution of basinal muds (and consistent with the crude wave-reworking-depths calculated in Chapter III), would be well above the sills and topographic highs if the depth were increased 50 metres.

Piper (1977) postulated elsewhere that a decreased annual ice cover would effectively depress the lower limit of wave erosion during the spring and fall storm periods. Conversely, an increased ice cover would dampen the activity of waves. Unfortunately, it is difficult to provide direct evidence for such a mechanism; rather, it logically explains a given set of observations.

McCave (1971) has pointed out that deposition of mud will result from a sediment-laden fluvial plume where the suspended sediment concentrations are on the order of 100 mg/l. or greater. This mode of deposition may also produce a blanket-like unit. Also, since the sediment rate of the lower piston core facies was high, this factor would appear to be important. However, it is not favoured as a primary controlling factor here because the thickness of the conformable cover unit is relatively uniform throughout the entire fjord and does not show attenuation away from the river mouths.

The other major controlling factor, the degree of runoff, has two influences on the estuarine environment. Firstly, large freshwater discharges are usually associated with high proportions of suspended and bed-load detrital matter which eventually are deposited in basinal areas. The nature and concentrations of these sediments would vary substantially if the original detrital source were an active or ablating glacier. Secondly, increased freshwater discharge enhances estuarine stratification and hence,

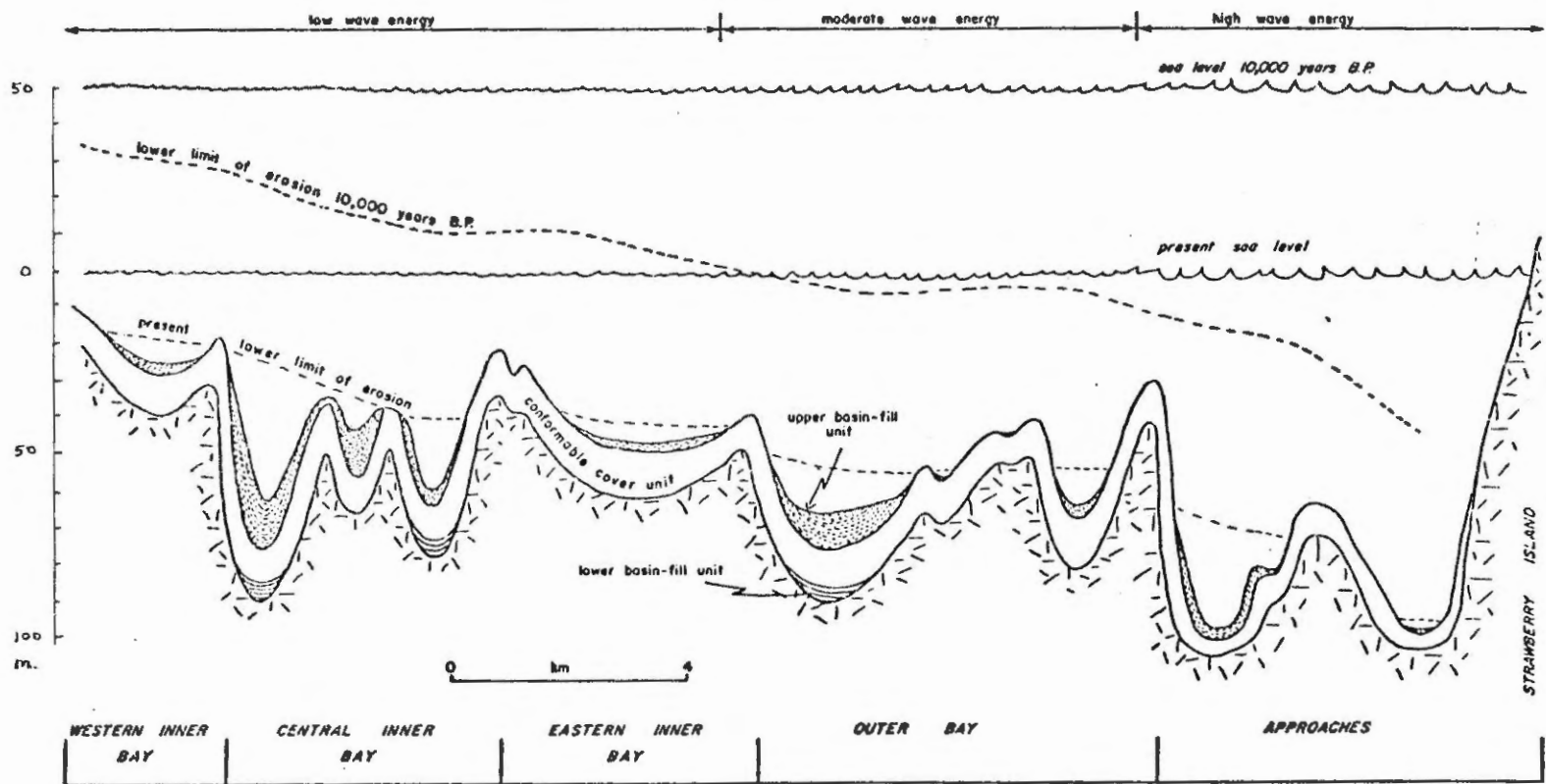


Figure 11.1: Longitudinal profile of Makkovik Bay showing the distribution of the contemporary and basinal muds and the relict conformable cover unit. The dashed lines indicate the contemporary lower limit of erosion (or no net deposition) and that for 10,000 years ago, demonstrating the influence of a 50 m rise in sea level or sedimentation

circulation, and increases sea water exchange across the sill for a partially mixed estuary. The latter concept can be shown by studying the mechanics of salt balance circulation (e.g. McLellan, 1975; Pederson, 1977). The continuity of water mass through any cross section of an estuary can be expressed in simple terms by:

$$O = I + R$$

where O is the volume rate of outflow, I the volume rate of inflow and R, the runoff. Assigning salinities to the outflow ( $S_o$ ) and inflow ( $S_i$ ), a crude salt balance equation can be written:

$$S_o O = S_i I$$

Combining these two equations yields:

$$O = \left( \frac{S_i}{S_i - S_o} \right) R \quad \text{or} \quad I = \left( \frac{S_o}{S_i - S_o} \right) R$$

Thus, the basal rate of inflow can be augmented by increased runoff. Ecologically, this means that a relatively marine environment can be maintained at the base of a stratified estuary during increased freshwater discharge (Fig. 11.2).

As the fresh water input increases past some critical level, the fjord becomes a highly stratified, two-layer type estuary (Pickard, 1961; Pederson, 1977) with a freshwater upper layer, a marine base and greatly reduced salt balance mixing along the interface. Therefore, in both types of estuaries, a relatively marine base is maintained.

The effects of the two major controlling factors, sea level and runoff, are often similar and cannot always be related to one specific mechanism. In addition, other less significant factors exist (e.g. wind circulation, tidal currents, suspended sediment concentration, differential flocculation, etc.).

### 11.2 Facies Model of Deposition

Although the primary factors controlling deposition have not been evaluated directly, their relative influence can be modelled from the lithologic and acoustic data. This is shown in Figure 11.2 with respect to the composite facies sequence interpreted from the piston cores. It is recognized that the two piston cores are from different estuarine environments and caution must be exercised in translating the data from one environment to the other. The following is a facies model of deposition based primarily on the Outer Bay environment.

The clay mineralogy of the conformable cover unit suggests that it had a terrestrial source, probably from the south, transported by a relatively high fluvial discharge northwards along glacially enlarged valleys. The morphology and distribution of this unit suggests a maximum relative sea level and a substantially thick veneer of freshwater to transport the suspended sediment. The low total foraminiferal population, dominated by marine to brackish forms, suggests a relatively high sedimentation rate and relatively good exchange of marine water over the sill, presumably augmented by a high relative sea level. Hence, it is suggested that the estuary was a highly stratified, two-layer, type estuary with a high relative sea level.



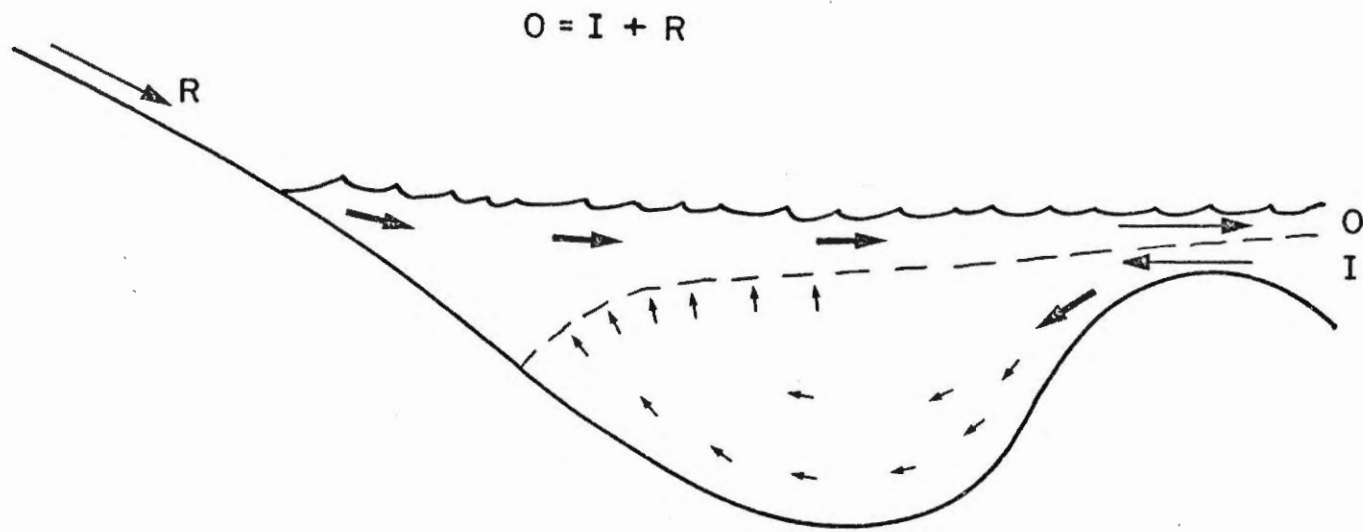


Figure 11.2: Simple model for estuarine circulation of a partially mixed estuary. Moderate and small size arrows denote circulation; long arrows represent terms in the continuity equation: runoff (R), outflow (O) and inflow (I) (from McLellan, 1975)

The freshwater upper layer transported a high load of terrestrially derived, suspended sediment across the fjord, and a brackish to saline basal stratum supported meagre, brackish-marine fauna. Presumably, flocculation would occur along the interface, resulting in relatively rapid, conformable deposition through the lower stratum. Possibly, the quiet conditions of the well stratified estuary may have been augmented by increased ice cover, but there is no direct evidence to support this hypothesis.

Sound interpretation of the genesis of the lower basin-fill unit is inhibited by the paucity of acoustic records and the complete absence of samples. The prominent acoustic strata suggest a high sedimentation rate whereas the basin-fill morphology indicates a high energy environment. Therefore, it is proposed that this unit was deposited during an increasing sea level during a transitional period to the conformable cover unit. The crudely extrapolated age of the earliest sediments is approximately 19,000 to 26,000 years B.P., depending on the assumed rate of sedimentation. Presumably, preservation of earlier strata was prevented either by glacial scouring or by very high energy conditions.

The lowest sampled facies of the upper basin-fill unit, facies D, is very similar to the unconformable unit. However, the upper portion of this unit, subfacies D1, has significant amounts of bioturbation and macrofossils and an increased total population of foraminifera, suggesting a decreased rate of sedimentation. Presumably this condition would be brought about primarily by a decrease in the amount of sediment-laden runoff. This, plus the change in the acoustic morphology of the unit, suggest that the estuarine condition changed to a partially mixed type estuary. A

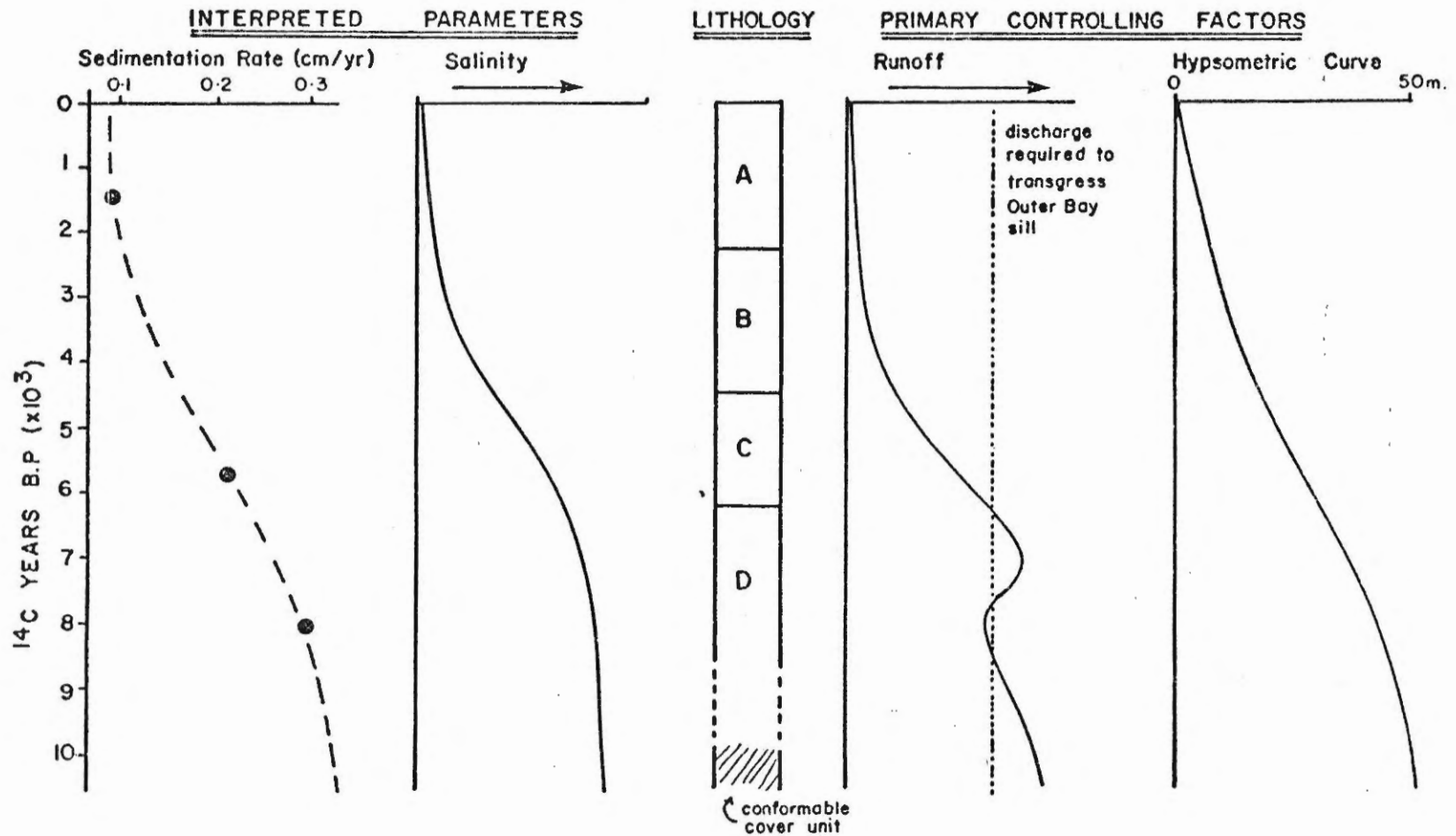


Figure 11.3: Model of primary controlling factors of postglacial development based on the interpreted parameters: sedimentation rate and salinity

moderately strong runoff would maintain stratification and sea water exchange across the sill, sustaining a calcareous-dominated benthonic foraminiferal assemblage. The predominantly agglutinated foraminiferal assemblage in subfacies D2 is problematic. It may be related to different sedimentation rates, decreased salinity or poor sample representation (only 1 sample, containing 7 individuals per gram).

Facies C contains generally the same proportions of clay minerals and exhibits the same distributional trends as D, and therefore the primary source is thought to be terrestrial. However, the decreased illite/feldspar ratio and a slight increase in the proportion of montmorillonite suggest a second, minor source, presumably marginal marine sediments exposed to erosion by a decreasing sea level. The increased bioturbation and fossil abundances, plus the interpreted chronologies, suggest that the sedimentation rate has decreased to approximately 0.2 cm/year. The changes in foraminiferal assemblages are most conspicuous in facies C, from estuarine-marine at the base to estuarine at the top. This reduction in salinity is thought to be related primarily to a decreased relative sea level, effectively restricting exchange of marine water over the sill. This is consistent with the acoustic-basin-fill morphology of the unit. A waning runoff may also have reduced the salinity of the basal strata by starving the estuarine circulation, thereby decreasing the basal inflow of marine water. Facies C also contains the first significant traces of an increase in the energy of environment; these include wispy laminations and a slight increase in grain size.

Facies B indicates the most prominent change into the second generation clays, with higher montmorillonite contents and decreased illite/feldspar ratio. This suggests that the marginally eroded marine sediments are now the dominant source. Other indicators of a decreased sea level include significant increases in grain size, proportion of agglutinated foraminifera (notably, E. advena) and the frequency of wispy laminae. The dwindling rate of sedimentation as evidenced by the proportions of montmorillonite and bioturbation and the absolute chronologies, suggests a decrease in the change of the relative sea level.

Facies A represents the contemporary environment, characterized by a gradually falling sea level, increased wave activity at the sea floor, decreased rate of sedimentation and estuarine-type salinities. These conditions are indicated in total by the sediment textures, structures and composition, by the microfossils and the distribution of the facies unit.

In summary, there are two modes of deposition: one reflected by the conformable cover unit and one by the contemporary sediments. These are shown schematically in Figure 11.4. The conformable cover unit represents runoff-dominated deposition in a two-layer-type estuary wherein terrestrial suspended material is distributed throughout the bay in the upper freshwater layer. Rapid deposition occurs by flocculation when the suspended sediment contacts the basal marine stratum of the fjord. The relative sea level must have been high in order to prevent erosion along the topographic highs.

The contemporary wave-dominated deposition occurs during decreased relative sea level and runoff. The fjord is a partially-mixed-type

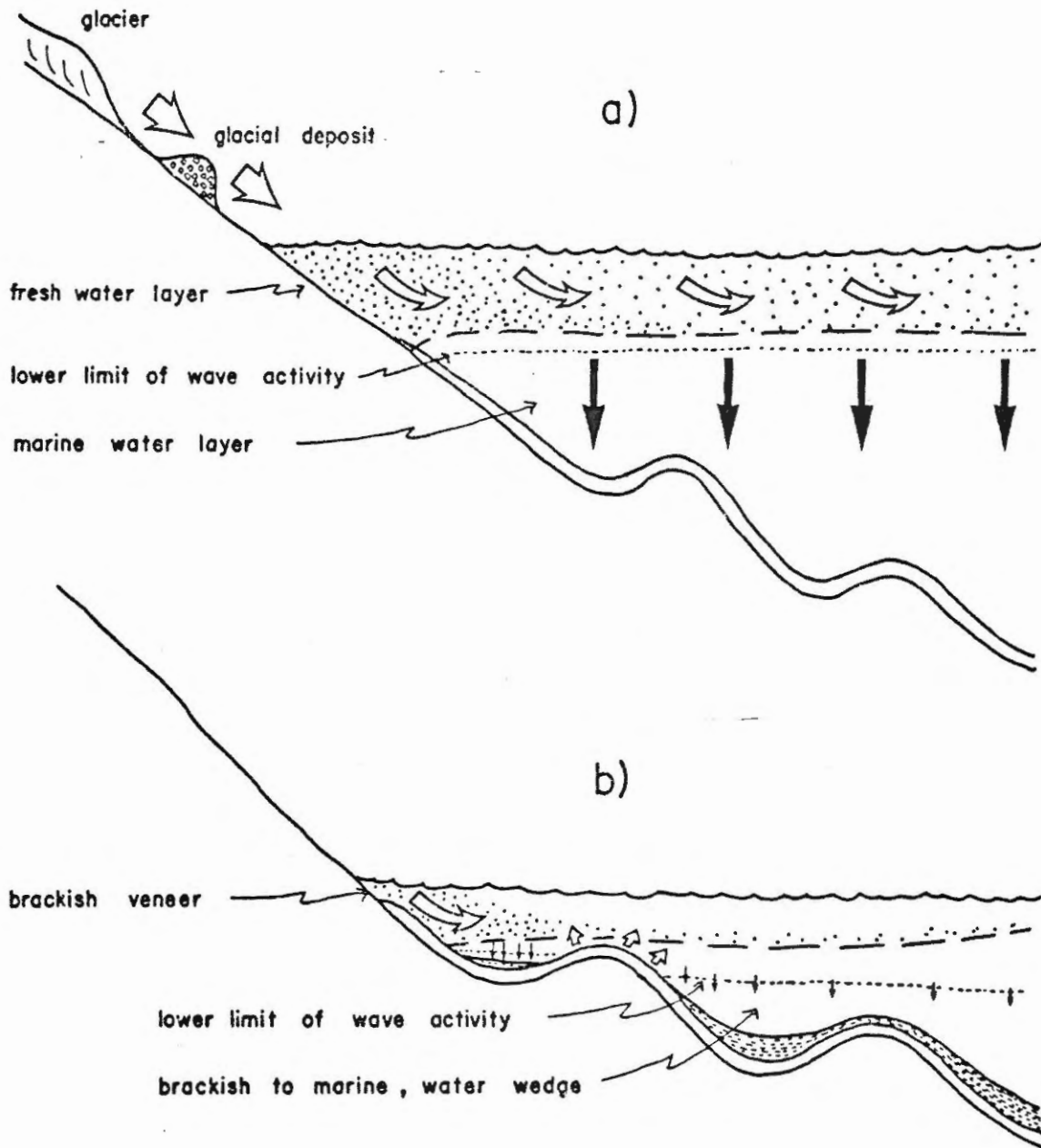


Figure 11.4: Schematic illustration contrasting (a) deep water, runoff-dominated deposition in a highly stratified 2-layer type estuary and (b) shallow water, wave-dominated deposition in a partially mixed estuary. Solid arrows denote deposition.

estuary. Wave energy erodes marginal and shoal marine deposits, distributing them throughout the basins according to the specific wave energy and the height of the water column, effecting onlapping basin-fill morphology. The contribution from eroding bluffs of raised deltas is thought to have only local significance.

### 11.3 Stratigraphic Facies Model of Deposition

Having constructed a vertical facies model, it is now possible to use it as feedback, applying it to the stratigraphic correlation of the piston cores and surficial samples, to set up an environmental summary of basinal deposition in the Makkovik Bay area. This is shown schematically in a stratigraphic facies model of deposition (Fig. 11.5).

Deep water runoff-dominated deposition prevailed throughout the last major transgression until approximately 9,000 years B.P. At this time decreased relative sea level and reduced sediment-laden runoff attenuated the exchange of water across the sill, such that wave-dominated deposition prevailed in the Approaches while runoff-dominated deposition continued in the more protected Outer Bay. At approximately 7,000 years B.P. a resurgent, sediment-laden runoff briefly transgressed the shallowing sill, recording a short interval of runoff-dominated deposition in the Approaches, indicated by facies D and E. Shallow water, wave-dominated deposition of the marginally-derived, basinal mud has recurred since approximately 5,000 years B.P. in the Approaches, and started at approximately 4,000 years B.P. in the Outer Bay.

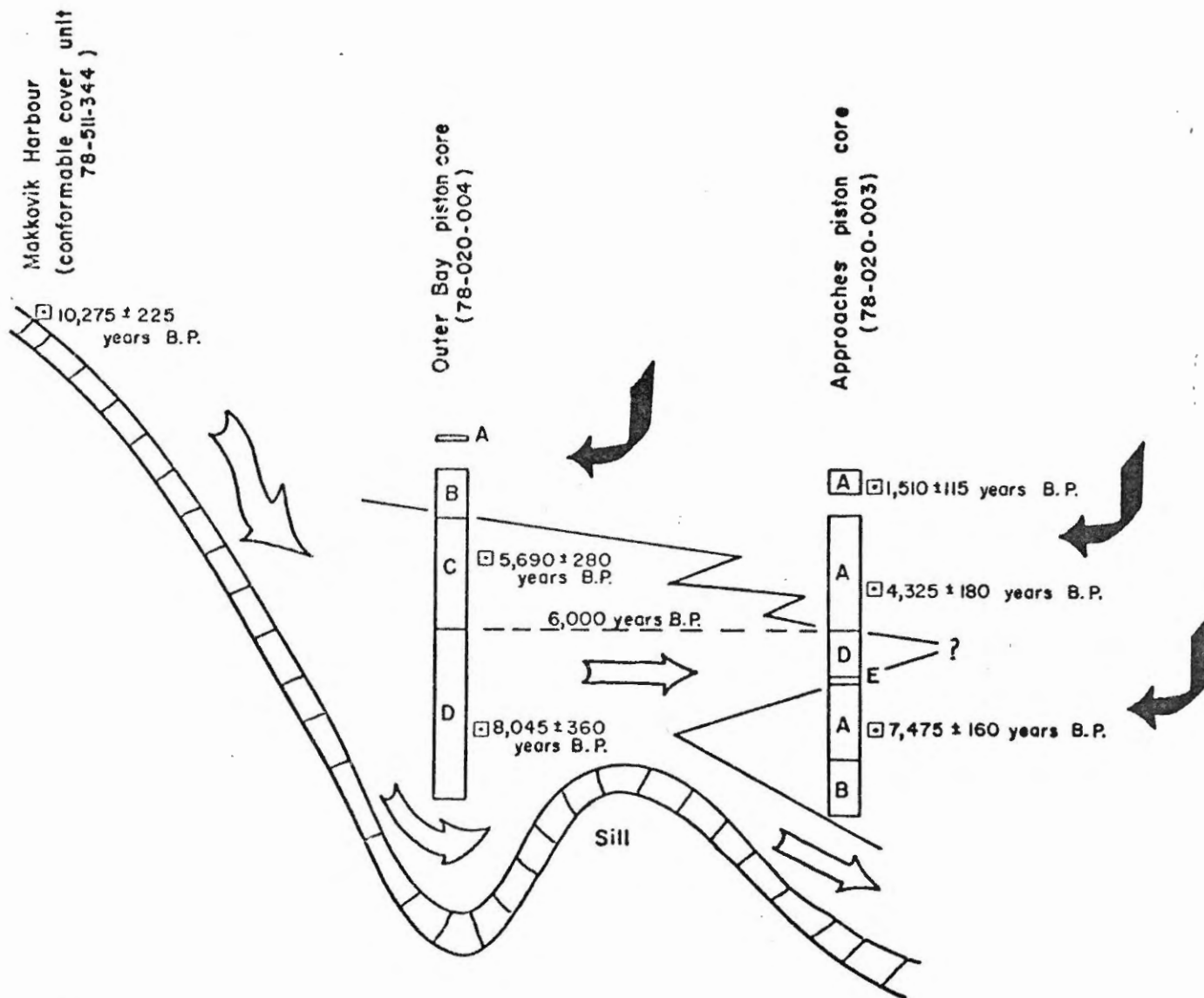


Figure 11.5: Stratigraphic model of deposition. Correlation line discriminates wave-dominated deposition (facies A and B) from transitional runoff-to wave dominated deposition (facies C and D). Open arrows represent input of glacial detritus during periods of high runoff. Shaded arrows represent sedimentation of marginally eroding marine sediments.

Solid



This model suggests that the recurrence of the runoff-dominated deposition experienced at approximately 7,000 years B.P. may have been related to a significant increase in sediment-laden runoff. Presumably, this condition was brought about by increased precipitation or more rapid ablation of an ice sheet, suggesting an amelioration in climate. Furthermore, the basin-wide erosional events observed in the acoustic profiles (e.g. basins F, J and K in Plates 4.6, 4.10 and 4.11) have crudely interpolated ages of 6,000 years B.P. It is speculated here that the increased runoff and the erosional events may be related either (1) concomitantly, such that runoff-enhanced estuarine circulation during a relatively low sea level may have winnowed the basinal muds, or (2) derivationally, such that both respond to a warmer climate. In the latter case, a shorter winter ice cover would expose the sediments to the deeper wave activity associated with the early spring and late fall storms.

A summary of the major factors and the depositional events since 19,000 years B.P. is shown in Table 11.1.

#### 11.4 Application to Recent Concepts of Postglacial Development

Based on the correlation of regional palynology of upland lake cores with Scandinavian stratigraphies, Wenner (1947) believed that deglaciation of southeastern Labrador occurred about 8,000 to 10,000 years ago. With the advent of  $^{14}\text{C}$  dating, Prest (1969) estimated deglaciation at about 14,000 to 16,000 years B.P., using two remote, raised marine deposits. However, consistently young ages (Blake, 1956; Hodgson et al., 1972) combined with indirect morphological evidence (Fillon, 1975, 1976) revived the

TABLE 11-1 Summary of major factors and depositional events  
since 19,000 years B.P.

PERIOD YEARS B.P.	RELATIVE SEA LEVEL	RELATIVE RUNOFF	OUTER BAY FACIES	APPROACHES FACIES	ACOUSTIC UNIT
Present to 3,000	very low	very low	- wave dominated deposition (A) - partially mixed estuary - possible cooling period	- wave dominated deposition (A) - open bay	Upper Basin Fill Unit
3,000 to 4,500	low	low	- wave dominated deposition (B) - partially mixed estuary	- wave dominated deposition (A) - open bay	
4,500 to 6,000	low to moderate	low to moderate	- runoff and wave deposition (C) - partially mixed estuary	- wave dominated deposition (A) - open bay	
ca 6,500	moderate	high	- runoff dominated deposition (D) - partially mixed estuary (highly stratified)	- runoff dominated deposition (D) - partially mixed estuary	
7,000 to 9,000	moderate to high	moderate to high	- runoff dominated deposition (D) - partially mixed estuary (highly stratified)	- wave dominated deposition (A) + - partially mixed estuary to ? open bay (B)	
10,000 to 15,000	high	high	- runoff dominated deposition - highly stratified, 2-layer estuary	- runoff dominated deposition - highly stratified, 2-layer estuary	Conformable Cover Unit
15,000 to 19,000	? moderate	?	- high energy deposition	?	Lower Basin Fill Unit
Prior to 19,000	? low	?	- no deposition - ? scouring	- no deposition - ? scouring	-

later date for deglaciation.

Foraminiferal and palynological evidence from two marine sediment cores from southeastern Labrador Shelf indicate open water shelf conditions and continuous regional tundra vegetation back at least to 23,000  $^{14}\text{C}$  years B.P. (Vilks and Mudie, 1978; Mudie, 1980). This supports at least a deglaciated shelf plus mainland nunataks and coastal refuges by 23,000 years B.P.

In the mainland lake cores, the palynological tundra episode occurs down to at least the top of the highly inorganic sediments, dated at 10,300 years B.P. (Short and Nichols, 1977). The 10,300 year B.P. conformable cover unit of this study, interpreted to have been deposited during the late Holocene maximum transgression, refutes a late deglaciation of Makkovik Bay. Furthermore, crude extrapolation of the Outer Bay piston core sequences suggest an age of approximately 19,000 years B.P. for the oldest preserved sediments in Makkovik Bay (subject to interpreted rates of sedimentation).

Sea floor morphology (Fillon, 1976), sedimentology and micropaleontology suggest that the Central Labrador Shelf has been sinking isostatically since approximately 15,000 years B.P. (Vilks, in press), whereas the data from Makkovik Bay indicate a relative sea level lowering during the last 10,000 years B.P. Uplift rates along coastal Labrador (Andrews, 1970) and eustatic sea level fluctuations (Walcott, 1972) have been minimal during the past 6,000 years B.P. The sum of these observations can be explained by an isostatic readjustment model (Peltier et al., 1978; Quinlan, personal communication). This model is depicted in Figure 11.6. Prior to

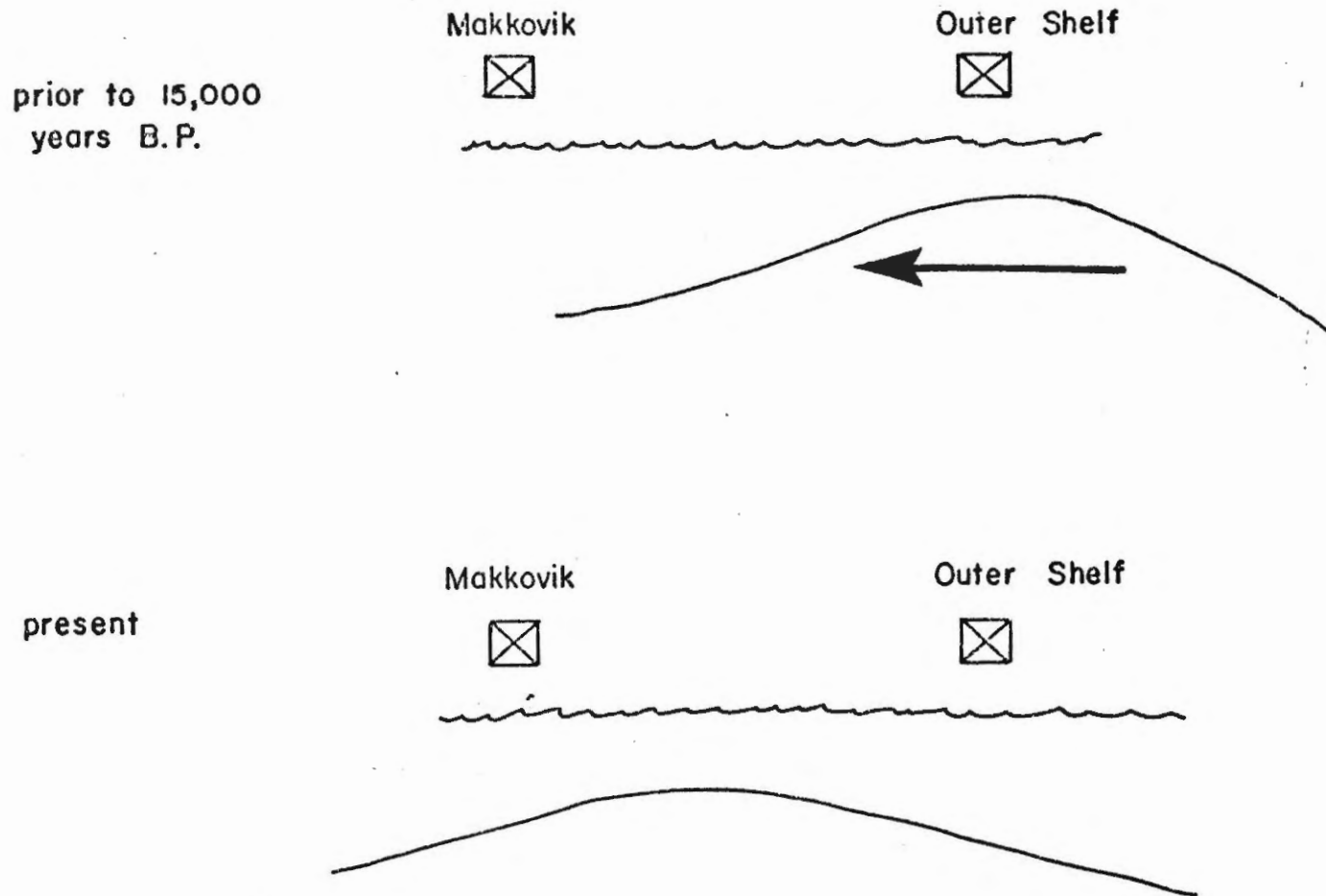


Figure 11.6: Hypothesis for landward migration of glacio-isostatic readjustment (Peltier et al., 1978)

15,000 years B.P. a peripheral bulge existed on the shelf, resulting in lesser water depths in the shelf and greater deposits due to glacio-isostatic depression along the coast. As this depression migrated landwards with the retreating ice, Makkovik was elevated at least 50 metres along the inner bulge slope from 10,000 to 6,000 years B.P. Shelf subsidence occurred along the seaward edge of the peripheral bulge.

Palynomorphs from the Cartwright Saddle record a Holocene hypsithermal phase from approximately 9,500 to 3,000 years B.P., and a major climatic hiatus between 7,000 to 6,000 years B.P. (Mudie, 1980). This hiatus coincides with a warmer and wetter period evidenced by coastal lake pollens (Jordan, 1975; Short and Nichols, 1977). These are consistent with the proposed disappearance of the Labrador-Quebec ice sheet (Short and Nichols, 1977) and the increased runoff at approximately 6,500 years B.P., as presented by this depositional model.

Foraminiferal evidence from Cartwright Saddle (Vilks, inpress), records three recent periods of faunal diversity with 15 to 30% Elphidium clavatum prior to 15,000 years B.P., in gradually decreasing populations. The latter two correlate chronologically with the conformable cover unit, and facies C and D respectively. The Makkovik Bay units are characterized by low but diverse populations dominated by calcareous types, and in place, by E. clavatum. Thus, it appears that similar bottom oceanographic conditions existed during these periods extending from the coastal bays to the open shelf environments.

An overall cooling or neoglacial phase commencing at approximately 3,000 years B.P. (Namias, 1970; Andrews, 1972; Bradley et al., 1972;

Jordan, 1975; Short et al., 1977; Mudie, 1980) coincides with significant decreases in foraminiferal populations within Makkovik Bay. The decrease in total population and the proportion of calcareous foraminifera plus the relative increase of the cold water species R. arctica observed in the upper 3 metres of the Approaches core (since 4,000 years B.P.) is consistent with such a cooling climatic trend.

## CHAPTER XII

### CONCLUSIONS AND SUGGESTIONS FOR FURTHER RESEARCH

#### 12.1 Oceanography

The contemporary oceanographic environment of Makkovik Bay can be considered to be a partially mixed estuary during the summer months with brackish, cold basal strata replenished gradually by sea water exchange across the sill. The low concentrations and the distribution of the suspended particulate matter, and the moderately high sedimentation rates suggest that basinal sedimentation occurs primarily by rapid deposition of wave-resuspended bottom sediments.

#### 12.2 Stratigraphy

Three major acoustic units are recognized using an original technique capable of synthesizing 3.5 kHz analogue records. The lower basin-fill unit is a well stratified, 16 m thick (maximum) unit probably of coarse clastics deposited in the deep basins between approximately 19,000 and 15,000 years B.P. based on extrapolated rates of sedimentation.

The conformable cover unit is a well stratified, 15 m thick unit deposited in a blanket-like form between approximately 15,000 and 10,000 years B.P. The well stratified acoustic nature is probably attributable to the alternation of acoustically transparent gray, clayey silt and acoustically reflective coarser clastic horizons.

The upper basin-fill unit is an acoustically transparent body up to 20 metres thick found filling the basins and exhibiting a flank-onlapping

habit. The degree of onlap is inversely related to the wave energy which decreases upbay. The sediment in general is an olive grayish clayey silt. Four major facies can be recognized that show upward decreasing salinity and sedimentation rate. Facies C and D represent the waning depositional conditions of the conformable cover unit, whereas facies B is transitional to the contemporary facies A. Deposition of facies A has been substantially time-transgressive from the Approaches to the Outer Bay.

The conformable cover unit and facies D are correlatable both chronologically and faunally with respective shelf sediments, suggesting that the controlling processes are widespread. The change from calcareous dominated assemblages of the conformable cover unit and facies C and D, to agglutinated dominated assemblages of facies A and B, indicate a decreasing salinity. The most recent foraminiferal assemblage suggests a deterioration in marine climate since 4,000 years B.P.

### 12.3 Model of Postglacial Development

There are two major factors that control the depositional environment: relative sea level and runoff. Fluctuations in the relative sea level control estuarine circulation, the depth of wave activity and the depth of the sediment-contributing water column. Changes in runoff influence estuarine circulation and the flux and distribution of terrestrially derived sediments. Two main modes of deposition can be resolved from these variables: run-off dominated and wave-dominated.

The sediments of the lower basin-fill unit were probably deposited in a high energy environment, presumably wave- and current dominated,



preventing deposition in all but the deeper basins. This presumably occurred prior to the last major transgression.

It is proposed that the conformable cover unit was deposited (1) when the fjord was responding as a highly stratified, two-layer type estuary as a consequence of increased runoff, and (2) when the relative sea level was approximately 50 m higher than at present, during the last major transgression. Fluvial runoff transported high concentrations of suspended glacial detritus northwards along the glacially enlarged Makkovik Brook Valley. The suspended sediment was dispersed across Makkovik Bay within the upper fresher water layer of the highly stratified fjord, concentrating illite proximally and feldspar distally. Sedimentation would occur rapidly through the halocline and the lower marine water. A calcareous dominated foraminiferal population was able to thrive in the lower marine water of the highly stratified fjord. Contribution of sediment from eroding raised deltaic deposits had some local significance by the end of this depositional period as the relative sea level began to recede.

In contrast, the upper basin-fill unit is characterized by wave-dominated deposition in a partially mixed estuary during a period of falling relative sea level and decreasing runoff. Marginally exposed conformable cover sediments are resuspended by wave activity and redistributed into the basins producing second generation marine clays. Illite is further concentrated along the nearshore zone, whereas chlorite and montmorillonite may be concentrated at the bay head and the bay mouths respectively by estuarine circulation. The lower relative sea level and reduced runoff

have decreased the sea water exchange across the sill. The reduced salinity of the fjord supports a meagre, agglutinated-dominated foraminiferal population.

#### 12.4 Suggestions for Further Research

The need for further research in all fields is evident from the lack of sufficient background required for a multidisciplinary study. The Makkovik Bay site offers a unique opportunity for the study of many academic pursuits because, as a fjord, it is a semi-enclosed environment, operating generally in 2-dimensional space. It is a complex fjord in that it has several sills and allows different levels of examination and interaction. Perhaps foremost is the aspect of an isostatically rising coastline producing differential erosion throughout the fjord. This allows areal examination of both contemporary and relict sedimentary environments.

During the course of this study it became evident that many specific avenues of further research and investigation were needed, viz.

- (1) detailed oceanographic measurements are required to determine the effects of wind, waves, tide and runoff on the estuarine stratification and mixing processes
- (2) the mineralogical compositions and concentration of detailed suspended particulate matter are required to establish the source and nature of the redistributive processes within the bay

- (3) the success of the sediment traps suggests that such an environment is suitable for this type of measurement; a detailed program may make it possible to ascertain longer term sedimentological and biological components
- (4) the distributions of foraminifera within both contemporary and relict surficial sediments need to be documented
- (5) several more piston cores related to the acoustic stratigraphy should be obtained in order to (a) acquire vertical sections of the conformable cover unit and (b) to refine downbay facies variations
- (6) further investigation of both marine and land deposits is needed to determine the nature of the differential sedimentation observed here by the clay-size mineralogy
- (7) clay mineralogy of discrete grain size fractions of bottom and suspended sediments may help determine contemporary estuarine circulation patterns and segregational processes
- (8) investigation of the heavy mineral suite may verify the southern source and determine if any other source component is present
- (9) examination of the geochemistry of piston core with regard to iron monosulphide may allow complete description of the sulphate cycle and its possible use here as a paleosalinity indicator

- (10) further investigation is required on the nature of deposition of the bedded couplets of mud and laminated silt observed in facies D and at the base of the conformable cover unit.

REFERENCES

- Amos, C.L., 1978. The postglacial evolution of the Minas Basin, Nova Scotia: a sedimentological interpretation. *J. Sed. Pet.* 48, 965-981.
- Andrews, J.T., 1969. Shoreline relation diagram: physical basis and use for predicting age of relative sea levels. *Arctic and Alpine Res.* 1, 67-78.
- Andrews, J.T., 1970. Present and postglacial rates of uplift for glaciated northern and eastern North America derived from postglacial uplift curves. *Can. J. Earth Sci.* 1, 703-715.
- Andrews, J.T., 1972. Recent and fossil growths of marine bivalves, Canadian Arctic, and Late Quaternary Arctic marine environments. *Paleogeogr. Paleoclim., Palaeoecol.* 11, 157-176.
- Bandy, O.L. and Arnal, R.E., 1960. Concepts of foraminiferal paleoecology. *Am. Ass. Petrol. Geologists Bull.* 44, no. 12, 1921-1932.
- Barnes, N.E., 1976. The areal geology and Holocene history of the eastern half of Mahone Bay, Nova Scotia. Unpublished M.Sc. Thesis, Dalhousie University, Halifax, Nova Scotia, 125 pp.
- Barnes, N.E. and Piper, D.J.W., 1978. Late Quaternary geological history of Mahone Bay, Nova Scotia. *Can. J. Earth Sci.* 15, 586-593.
- Barrie, C.O., 1973. Preliminary data report on the marine geology of Makkovik Bay, Labrador. pp. 3-29 in Piper, D.J.W. (ed.), 1973. *Geology of coastal bays in Labrador and Nova Scotia*. Progress Report to the Dept. of Energy, Mines and Resources, November 1978.
- Barrie, C.O., 1979. Acoustic reflection stratigraphy of Makkovik Bay, Labrador. pp. 106-132 in *Proceedings on Symposium on Research in the Labrador Coastal and Offshore Region, May 8-10, 1979*, Memorial University of Newfoundland, 317 pp.
- Bartlett, G.A., 1965. Preliminary investigation of benthonic foraminiferal ecology in Tracadie Bay, Prince Edward Island. *Bedford Institute of Oceanography, Report* 65-3.
- Bartlett, G.A., 1966. Distribution and abundance of foraminifera and thecamoebins in Miramichi River and Bay. *Bedford Institute of Oceanography, Report* 66-2, 104 pp. (Unpublished manuscript)
- Beavan, A.P., 1958. The Labrador uranium area. *Proc. Geol. Assoc. Can.* 10, 137-145.
- Bergen, F.W. and O'Neil, P., 1979. Distribution of Holocene foraminifera in the Gulf of Alaska. *J. Paleo.* 53, 1267-1292.

- Berner, R.A., 1970. Sedimentary pyrite formation. *Am. J. Sci.* 268, 1-23.
- Berner, R.A., 1974. Iron sulphides in Pleistocene deep Black Sea sediments and their paleo-oceanographic significance. In Degens, E.I. and Ross, D.A., *The Black Sea-Geology, Chemistry and Biology*. *Am. Assoc. Pet. Geol. Mem.* 20, 524-534.
- Berner, R.A., Baldwin, T. and Holdren, G.R., 1979. Authigenic iron sulfides as paleosalinity indicators. *J. Sed. Pet.* 49, 1345-1350.
- Biggs, R.B., 1970. Sources and distribution of suspended sediment in northern Chesapeake Bay. *Mar. Geol.* 9, 187-201.
- Bird, J.B., 1964. *The physiography of Arctic Canada*. Baltimore, Maryland, John Hopkins Press, 220 pp.
- Biscaye, P., 1965. Distinction between kaolinite and chlorite in Recent sediments by x-ray diffraction. *Am. Mineral.* 49, 1281-1289.
- Biscaye, P., 1965. Mineralogy and sedimentation of recent deep sea clay in the Atlantic Ocean and adjacent seas and oceans. *Geol. Soc. Am. Bull.* 76, 803-832.
- Bjorlykke, E. and Elverhøi, A., 1975. Reworking of Mesozoic clayey material in the northwestern part of the Barents Sea. *Mar. Geol.* 18, M29-M34.
- Blake, Jr. W., 1956. Landforms and topography of the Lake Melville area, Labrador, Newfoundland. *Geogr. Bull.* 9, 75-100.
- Bornhold, B.D., 1977. Echo sounding and subbottom profiling in Douglas channel and Kitimat Arm, British Columbia. Report of Activities, Part B, *Geol. Surv. Can. Pap.* 77-1B, 265-268.
- Bradley, R.S. and Miller, G.H., 1972. Recent climatic change and increased glacierization in the eastern Canadian Arctic. *Nature* 237, 385-387.
- Cockbain, A.E., 1963. Distribution of foraminifera in Juan de Fuca and Georgia Straits, British Columbia, Canada. *Contr. from the Cushman Foundation for Foraminiferal Research* 14, 37-57.
- Cooper, G.E., 1951. The petrology of some syenites and granites in Labrador. Unpublished M.Sc. Thesis, McGill Univ., Montreal, Quebec.
- Cooper, S.C., 1964. Benthonic foraminifera of the Chukchi Sea. Contributions from the Cushman Foundation for Foraminiferal Research 15, 79-104.
- Cranston, R.E. and Buckley, D.E., 1972. Geochemical data from a 25 hour station, LaHave River, Nova Scotia. Project 71-23A, *Inorganic Chemistry Data Series B1-D-72-12*.
- Cronin, T.M., 1977. Champlain sea foraminifera and ostracoda: systematic and paleoecological synthesis. *Geogr. phys. Quat.* 31, 107-122.
- Cushman, J.A., 1948. Arctic foraminifera. *Cush. Lab. Forum. Res., Spec. Publ.* 23, 1-79.
- Dale, C.T., 1979. A study of high resolution seismology and sedimentology of the offshore Late Quaternary sediment northeast of Newfoundland. Unpublished M.Sc. Thesis, Dalhousie Univ., 181 pp.

- Dale, C.T. and Haworth, R.T., 1979. High resolution reflection seismology studies on the Late Quaternary sediments of the northeast Newfoundland continental shelf. *In* Current Research, Part B, Geol. Surv. Can., Pap. 79-1B, 357-364.
- Daly, R.A., 1902. The geology of northeast coast of Labrador. Bull. Mus. Comp. Zool., Harvard, 38, Geol. Ser. 5, no. 5.
- Damuth, J.E. and Hayes, D.E., 1977. Echo character of the East Brazilian Continental Margin and its relationship to sedimentary processes. Mar. Geol. 24, 73-95.
- Darby, D., 1975. Kaolinite and other clay minerals in Arctic Ocean sediments. J. Sed. Pet. 45, 272-279.
- Dobrin, M.D., 1976. Introduction to geophysical prospecting. 3rd ed. New York, McGraw-Hill Book Company, 630 pp.
- Douglas, G.V., 1953. Notes on localities visited on the Labrador Coast in 1946 and 1947. Geol. Surv. Can. Pap., 53-1.
- Dugan, P.R., Pfister, R.M. and Frea, J.I., 1971. Implications of microbial polymer synthesis in water treatment and lake eutrophication. 5th Int. Water Poll. Res. Conf., July-Aug. 1970. Pergamon Press Ltd.
- Dyer, K.R., 1972. Sedimentation in estuaries. *In* The estuarine environment. Barnes, R.S.K. and Green, J. (eds.). Applied Science Pub. Ltd., London, 133 pp.
- Ellison, Jr., S.P., 1951. Microfossils as environment indicators in marine shales. J. Sed. Pet. 21, 214-225.
- Feuillet, J.P. and Fleischer, P., 1980. Estuarine circulation: controlling factor of clay mineral distribution in James River estuary, Virginia. J. Sed. Pet. 50, 267-279.
- Feyling-Hanssen, R.W., Jorgensen, J.A., Knudsen, K.L. and Anderson, A.L., 1971. Late Quaternary foraminifera from Vendsyssel, Denmark and Sandres, Norway. Bull. Geol. Soc. Denmark, 21, 317 pp.
- Fillon, R.H., 1974. Late Pleistocene benthic foraminifera of the southern Champlain Sea: paleotemperature and paleosalinity indicators. Marit. Sed. 10, 14-18.
- Fillon, R.H., 1975. Palaeoglaciology: deglaciation of the Labrador Continental Shelf. Nature 253, 429-431.
- Fillon, R.H., 1976. Hamilton Bank, Labrador Shelf: postglacial sediment dynamics and paleo-oceanography. Mar. Geol. 20, 7-25.
- Gandhi, S.S., Grasty, R.L. and Grieve, R.A.F., 1969. The geology and geochronology of the Makkovik Bay area, Labrador. Can. J. Earth Sci. 6, 1019-1035.
- Gibbs, R.J., 1977. Clay mineral segregation in the marine environment. J. Sed. Pet. 47, 237-243.

- Grant, A.C., 1975. Seismic reconnaissance of Lake Melville, Labrador. *Can. J. Earth Sci.* 12, 2103-2110.
- Gregory, M.R., 1970. Distribution of benthonic foraminifera in Halifax Harbour, Nova Scotia. Ph.D. Thesis, Dalhousie Univ., Halifax.
- Greiner, G.O.G., 1970. Environmental factors causing distributions of recent foraminifera. Ph.D. Thesis, unpublished, Case Western Reserve Univ., 195 pp.
- Grieve, D. and Fletcher, K., 1977. Interactions between zinc and suspended sediments in the Fraser River Estuary, British Columbia. *Estuarine and Coastal Mar. Sci.* 5, 415-419.
- Hargrave, B.T., Phillips, G.A. and Taguchi, S., 1976. Sedimentation measurements in Bedford Basin, 1973-1974. Technical Report No. 608, Fisheries and Marine Science, Environment Canada.
- Hodgsen, D.A. and Fulton, R.J., 1972. Site description, age and significance of a shell sample from the mouth of the Michael River, 30 km. south of Cape Harrison, Labrador. *Can. Geol. Surv. Pap.* 72-1B, 102-105.
- Hooper, K., 1968. Benthonic foraminiferal depth-assemblages of the continental shelf off eastern Canada, *Marit. Sed.* 4, 96-99.
- Hooper, K., 1975. Foraminiferal ecology and associated sediments of the lower St. Lawrence estuary. *J. Foram. Res.* 5, 218-238.
- Howells, K. and McKay, A.G., 1977. Seismic profiling in Miramichi Bay, New Brunswick. *Can. J. Earth Sci.* 14, 2909-2927.
- Hume, H.R., 1972. The distribution of Recent foraminifera in southeast Baffin Bay. M.Sc. Thesis, Dalhousie University, Halifax, 137 pp.
- Ives, J.D., 1958. Mountain-top detritus and the extent of the last glaciation in northeastern Labrador-Ungava. *Can. Geogr.* 12, 25-31.
- Ives, J.D., 1978. The maximum extent of the Laurentide ice sheet along the east coast of North America during the last glaciation. *Arctic* 31, 24-53.
- Johnson, J.P. (Jr.), 1969. Deglaciation of the central Nain-Okak Bay section of Labrador. *Arctic* 22, 373-394.
- Jordan, R., 1975. Pollen diagrams from Hamilton Inlet, Central Labrador, and their environmental implications for the Northern Maritime Archaic. *Arct. Anthropol.* 12, 92-116.
- King, A.F., 1963. Geology of Cape Makkovik Peninsula, Aillik, Labrador. Unpublished M.Sc. Thesis, Memorial Univ. Newfoundland, St. John's, Newfoundland.
- King, L.H., 1967. Use of a conventional echo-sounder and textural analysis in delineating sedimentary facies: Scotian Shelf. *Can. J. Earth Sci.* 4, 691-708.
- Knudsen, M., 1901. Hydrographic tables. Copenhagen, G.E.C. Gad, 1901.
- Kögler, F.C. and Larsen, B., 1979. The West Bornholm basin in the Baltic Sea: geologic structure and Quaternary sediments. *Boreas* 8, 1-22.



- Komar, P.D. and Miller, M.C., 1974. Sediment threshold under oscillatory waves. pp. 756-775. In Proceedings of the Fourth Coastal Engineering Conference, June 24-28, 1974, vol. 11, Am. Soc. Civil Engineers, New York.
- Kranck, E.H., 1939. Bedrock geology of seaboard region of Newfoundland, Labrador. Geol. Surv. Newfoundland, Bull. No. 19.
- Kranck, E.H., 1953. Bedrock geology of the seaboard of Labrador between Domino Run and Hopedale, Newfoundland. Geol. Surv. Can. Bull., 26.
- Kranck, K., 1975. Sediment deposition from flocculated suspensions. Sed. 22, 111-123.
- Lagoe, M.B., 1979. Recent benthonic foraminiferal biofacies in the Arctic Ocean. Micropaleo. 25, 214-224.
- Loeblich, Jr., A.R. and Tappan, H., 1953. Studies of Arctic foraminifera. Smithson. Misc. Coll. 121, no. 7, 150 pp.
- Leslie, R.J., 1965. Ecology and paleoecology of Hudson Bay foraminifera. Bedford Institute of Oceanography, Report 65-6, 192 pp.
- Lisitzin, A.P., 1972. Sedimentation in the world ocean. Soc. Econ. Paleont. Mineral., Spec. Pub. 17, 218 pp.
- Løken, O.H., 1962. The Late-glacial and postglacial emergence and deglaciation of northernmost Labrador. Geogr. Bull. 17, 23-56.
- Lyell, C., 1854. Principles of geology. New York. D. Appleton and Co., 834 pp.
- McCave, I.N., 1971. Wave effectiveness at the seabed and its relationship to bed-forms and deposition of mud. J. Sed. Pet. 41, 89-96.
- McLellan, H.J., 1975. Elements of physical oceanography. Pergamon Press, Toronto, 151 pp.
- Meade, R.H., 1972(a). Transport and deposition of sediments in estuaries. Geol. Soc. Am. Mem. 133, 91-120.
- Meade, R.H., 1972(b). Sources and sinks of suspended matter on continental shelves. In Shelf sediment transport: processes and patterns. Swift, D.J.P., Duane, D.B. and Pilkey, O.H. (eds.), Dowden. Hutchinson and Ross Inc., Pennsylvania, 1972, pp. 249-262.
- McIntyre, A., Kipp, M.G., Bé, W.H., Crowley, T., Kellog, J.V., Gardner, W., Prell, W. and Ruddiman, W.F., 1976. Glacial North Atlantic 18,000 years age: a CLIMAP reconstruction. Geol. Soc. Am. Mem. 145, 43-76.
- McQuillin, R. and Ardue, D.A., 1977. Exploring the geology of shelf seas. London, Graham and Trotman Ltd., 234 pp.
- Millot, G., 1970. Geology of clays. Springer-Verlag, New York, 1970, 429 pp.
- Moore, T.H., 1951. Igneous dyke rocks of the Aillik-Makkovik area, Labrador. Unpublished M.Sc. Thesis, McGill Univ., Montreal, Quebec.

- Mudie, P., 1980. Palynology of later Quaternary marine sediments, eastern Canada. Unpublished Ph.D. Thesis, Dalhousie Univ., Halifax, Nova Scotia, 450 pp.
- Naidu, A.S., Burrell, D.C. and Wood, D.W., 1971. Clay mineral composition and geological significance of some Beaufort Sea sediments. *J. Sed. Pet.* 41, 691-694.
- Namias, J., 1970. Climatic anomaly over the United States during the 1960's. *Science* 170, 741-743.
- Neihof, R. and Loeb, G., 1973. Dissolved organic matter in seawater and the electric charge of immersed surfaces. *J. Mar. Res.* 32, 5-12.
- Nelson, B.W., 1958. Clay mineralogy of the bottom sediments, Rappahannock River, Virginia. In *Clays and clay minerals. Proc. Nat. Conf. on Clays and Clay Minerals.* Swineford, A. (ed.), pp. 135-147.
- Neu, H., 1979. Canadian coastal wave climate [abstract]. p. 219. In *Proceedings on the Symposium on Research in the Labrador Coastal and Offshore Region, May 8-10, 1979.* Memorial University of Newfoundland. 317 pp.
- Nichols, 1972. Sediments of the James River estuary, Virginia. *Geol. Soc. Am. Mem.* 133, 169-212.
- Nutt, D.C., 1952. Blue Dolphin Labrador Expedition, winter project 1952. Operational report, 15 June.
- Nutt, D.C., 1953. Certain aspects of oceanography in the coastal waters of Labrador. *J. Fish. Res. Bd. Canada* 10, 177-186.
- Nutt, D.C., 1963. Fjords and marine basins of Labrador Polar Notes. Occ. pub. of Stefansson collection 5, 9-24.
- Nutt, D.C. and Coachman, L.K., 1956. The oceanography of Hebron Fjord, Labrador. *J. Fish. Res. Bd. Canada* 13, 709-758.
- Osterman, L.E. and Kellogg, 1979. Recent benthonic foraminiferal distributions from the Ross Sea, Antarctica: relation to ecologic and oceanographic conditions. *J. Foram. Res.* 9, 250-269.
- Packard, A.S., 1891. *The Labrador coast.* New York.
- Parker, F.L., 1952. Foraminiferal distribution in the Long Island Sound-Buzzards Bay area. *Harvard Coll. Mus. Comp. Zool., Bull.* 106, 427-473.
- Pederson, F.B., 1977. A brief review of present theories of fjord dynamics. In *Hydrodynamics of estuaries and fjords.* Proc. 9th Int. Liege Colloq. on Ocean Hydrodynamics. Nihoul, J.C.J. (ed.), pp. 407-422.
- Peltier, W.R., Farrell, W.E. and Clark, J.A., 1978. Glacial isostasy and relative sea level - a global finite element model. *Tectonophysics* 50, 81-110.
- Pevear, D.R., 1972. Source of recent rearshore marine clays, southeastern United States. *Geol. Soc. Am. Mem.* 153, 317-335.

- Pfister, R.M., Dugan, P.R. and Frea, J.I., 1969. Microparticulates: isolation from water and identification of associated chlorinated pesticides. *Science* 166, 878-879.
- Phleger, F.B., 1952. Foraminifera distribution in some recent samples from the Canadian and Greenland arctic. *Contributions from the Cushman Foundation for Foraminiferal Research* 3, 80-89.
- Phleger, F.B., 1960. Ecology and distribution of Recent foraminifera. John Hopkins Press, Baltimore, 297 pp.
- Pickard, G.L., 1961. Oceanographic features of inlets in the British Columbia mainland coast. *J. Fish. Res. Bd. Canada* 18, 907-999.
- Pierce, J.W. and Myers, B.L., 1974. Deposition of clay-sized particles [abstract]. *Geol. Soc. Am. Abst. with Prog.*, 1974, pp. 388.
- Pinet, P.R. and Morgan, W.P., 1979. Implications of clay-provenance studies in two Georgia estuaries. *J. Sed. Pet.* 49, 575-580.
- Piper, D.J.W., 1977(a). Manual of sedimentological techniques. Dept. of Geology and Oceanography, Dalhousie Univ., Halifax, Nova Scotia, 106 pp.
- Piper, D.J.W., 1977. Report on samples EC-76-1 to 26 and 101 to 126, Hamilton Bank and Northeast Newfoundland Shelf. B.P. Exploration Canada Ltd.
- Piper, D.J.W. and Iuliucci, R.J., 1978. Reconnaissance of the marine geology of Makkovik Bay, Labrador. *Current Res. Part A., Geol. Surv. Can. Pap.* 78-1A, 333-336.
- Piper, D.J.W. and Keen, M.J., 1976. Geological studies in St. Margaret's Bay, Nova Scotia. *Geol. Surv. Can. Pap.* 76-18, 18 pp.
- Piper, D.J.W. and Slatt, R., 1977. Late Quaternary clay-mineral distribution on the eastern continental margin of Canada. *Geol. Soc. Am. Bull.* 88, 267-272.
- Postma, H., 1967. Sediment transport and sedimentation in the estuarine environment. *In Estuaries*, Lauff, G.H. (ed.). Conf. on estuaries, Jekyll Island, 1964. Pub. No. 83, Am. Assoc. Adv. Sci., Wash., D.C., 1967, 757 pp., pp. 158-179.
- Prest, V.K., 1969. Speculative isochrones on the retreat of Wisconsin and Recent ice in North America. *Can. Geol. Surv. Map.* 125A.
- Pritchard, D.W., 1955. Estuarine circulation patterns. *Proc. Amer. Soc. Civil Eng.*, 81, no. 717.
- Rashid, M.A. and Vilks, G., 1977. Environmental controls of methane production in Holocene basins in eastern Canada. *Org. Chem.* 1, 53-59.
- Riley, G.C., 1951. The bedrock geology of Makkovik and its relation to the Aillik and Kaipokok Series. Unpublished M.Sc. Thesis, McGill Univ., Montreal, Quebec.

- Rosen, P.S., 1979(a). Coastal environments of the Makkovik region, Labrador. In McCann, S.B. (ed.), Coastlines of Canada. Geol. Surv. Canada.
- Rosen, P.S., 1979(b). Boulder barricades in central Labrador. *J. Sed. Pet.* 49, 113-1124.
- Rosen, P.S., 1979(c). Sediment transport by intertidal ice. pp. 133-147. In Proceedings on Symposium on Research in the Labrador Coastal and Offshore Region, May 8-10, 1979, Memorial University of Newfoundland, 317 pp.
- Scott, D.B., 1973. Recent foraminifera from Samish and Padilla Bays, Washington. Unpublished M.Sc. Thesis, Western Washington State College, 63 pp.
- Scott, D.B., 1977. Distribution and population dynamics of marsh-estuarine foraminifera with applications to relocating Holocene sea-levels. Unpublished Ph.D. thesis, Dalhousie University, Halifax. 252 pp.
- Scott, D.B. and Medioli, F.S., 1978. Studies of relative sea level changes in the Maritimes. Progress Report to the Dept. of Energy, Mines and Resources on Research Agreement # EMR 2239-4-31/78, 79 pp.
- Scott, D.B. and Medioli, F.S., 1979. Marine emergence and submergence in the Maritimes. Progress Report to the Dept. of Energy, Mines and Resources on Research Agreement # EMR 45-4-79, 69 pp.
- Scott, D.B. and Medioli, F.S., 1980. Living versus total foraminiferal populations: their relative usefulness in paleoecology. *J. Paleo.* 54, 814-831.
- Scott, D.B., Medioli, F.S. and Schafer, C.T., 1977. Temporal changes in foraminiferal distributions in Miramichi River estuary, New Brunswick. *Can. J. Earth Sci.* 14, 1566-1587.
- Scott, D.B., Schafer, C.T. and Medioli, F.S., 1980. Eastern Canadian estuarine foraminifera: a framework for comparison. *J. Foram. Res.* In press.
- Sholkovitz, E.R., 1979. Chemical and physical processes controlling the chemical composition of suspended material in the River Tay Estuary. *Estuarine and Coastal Mar. Sci.* 8, 523-545.
- Short, S.K., 1978. Palynology: a Holocene environmental perspective for archaeology in Labrador-Ungava, *Arctic Anthro.* 15, 9-35.
- Short, S.K. and Nichols, H., 1977. Holocene pollen diagrams from subarctic Labrador-Ungava: vegetational history and climatic change. *Arctic and Alpine Res.* 9, 265-290.
- Slatt, R.M., 1974. Formation of palimpsest sediments, Conception Bay, southeastern Newfoundland. *Geol. Soc. Am. Bull.* 85, 821-826.
- Slatt, R.M., 1975. Dispersal and geochemistry of surface sediments in Halls Bay, north central Newfoundland: Application to mineral exploration. *Can. J. Earth Sci.* 12, 1346-1361.

- Slatt, R.M. and Press, D.E., 1976. Computer program for presentation of grain-size data by the graphic method. *Sed.* 23, 121-131.
- Slessor, D.K., 1970. Benthonic foraminiferal ecology in Covehead Bay, Prince Edward Island - a preliminary study. *Marit. Sed.* 6, 48-64.
- Spencer, D.W. and Sachs, P.L., 1970. Some aspects of the distribution, chemistry and mineralogy of suspended matter in the Gulf of Maine. *Mar. Geol.* 9 117-135.
- Stanley, D.J., 1968. Reworking of glacial sediments in the Northwest Arm, a fjord-like inlet on the southeast coast of Nova Scotia. *J. Sed. Pet.* 38, 1224-1241.
- Stow, D.A.V., 1977. Late Quaternary stratigraphy and sedimentation on the Nova Scotian Outer Continental margin. Unpublished Ph.D. Thesis, Dalhousie University, Halifax, Nova Scotia, 360 pp.
- Stow, D.A.V. and Bowen, A.J., 1978. Origin of lamination in deep sea, fine-grained sediments. *Nature* 274, 324-328.
- Sundby, B., 1974. Distribution and transport of suspended particulate matter in the Gulf of St. Lawrence. *Can. J. Earth Sci.* 11, 1517-1533.
- Tanner, V., 1939. Om de blockrika strandgördlarna (Boulder barricades) vid sabarktiska oceankustar, förekomst og upkomst: *Terra* 51, 157-165.
- Todd, R. and Low, D., 1961. Nearshore foraminifera of Martha's Vineyard Island, Massachusetts. *Cush. Found. Foram. Res., Contr.* 12, 5-21.
- Van Olphen, H., 1966. An introduction to clay colloid chemistry. Interscience Publishers, New York, 318 pp.
- Van Overeem, A.J.A., 1978. Shallow penetration, high resolution sub-bottom profiling, *Mar. Geotech.* 3, 61-84.
- Van Weering, T.C.E., 1975. Late Quaternary history of the Skagerrak; an interpretation of acoustical profiles. *Geol. en Mijn.* 54, 130-145.
- Van Weering, T.C.E., Jansen, J.H.F. and Eisma, D., 1973. Acoustic reflection profiles of the Norwegian channel between Oslo and Bergen. *Neth. J. Sea. Res.* 6, 24-263.
- Vilks, G., 1967. Quantitative analysis of foraminifera in Bras d'Or Lakes. Bedford Inst. Oceanography Report 67-1, 1-84.
- Vilks, G., 1968. Foraminiferal study of the Magdolen Shallows, Gulf of St. Lawrence. *Marit. Sed.* 4, 14-21.
- Vilks, G., 1969. Recent foraminifera in the Canadian Arctic. *Micropaleo.* 15, 35-60.
- Vilks, G., 1976. Foraminifera of an ice-scoured nearshore zone in the Canadian Arctic. *In Marit. Sed. Spec. Pub.* 1, 267-277.
- Vilks, G. Postglacial basin sedimentation on Labrador Shelf. *Geol. Surv. Can.* (In press)

- Vilks, G. and Mudie, P., 1978. Early deglaciation of the Labrador Shelf. *Science* 202, 1181-1183.
- Vilks, G., Wagoner, F.J.E. and Pelletier, B.R., 1979. The Holocene marine environment of the Beaufort Sea. *Geol. Surv. Can. Bull.* 303, 31 pp.
- Walcott, R.I., 1972. Past sea levels, estuary and deformation of the earth. *Quat. Res.* 2, 1-14.
- Ward, W.H., 1959. Ice action on shores. *J. Glaciology* 3, p. 437.
- Weber, V.V. and Maximov, S.P., 1976. Early diagenetic generation of hydrocarbon gases and their variations dependent on initial organic composition. *Bull. Am. Assoc. Petrol. Geol.* 60, 287-293.
- Weiss, L., 1954. Foraminifera and origin of the Gardiners Clay (Pleistocene), Eastern Long Island, New York. *U.S. Geol. Surv. Pap.* 254-G, 139-163.
- Wenner, C.G., 1947. Pollen diagrams from Labrador. *Geogr. Ann. Årg.* XXIX, Häft. 3, 137-373.
- Whitehouse, U.G., Jeffrey, L.M. and Debbrecht, J.D., 1960. Differential settling tendencies of clay minerals in saline waters. *In Clays and clay minerals. Proc. Nat. Conf. on Clay and Clay Minerals*, Swineford, A. (ed.), pp. 1-79.
- Widess, M.B., 1973. How thin is a thin bed? *Geophy.* 38, 1176-1180.
- Winters, G., Fitzgerald, R., and Buckley, D., 1978. Analyses of water column and bottom sediment samples from the Miramichi Estuary, New Brunswick. *Bedford Institute of Oceanography. Data Series/* B1-D-78-8.

APPENDIX 1

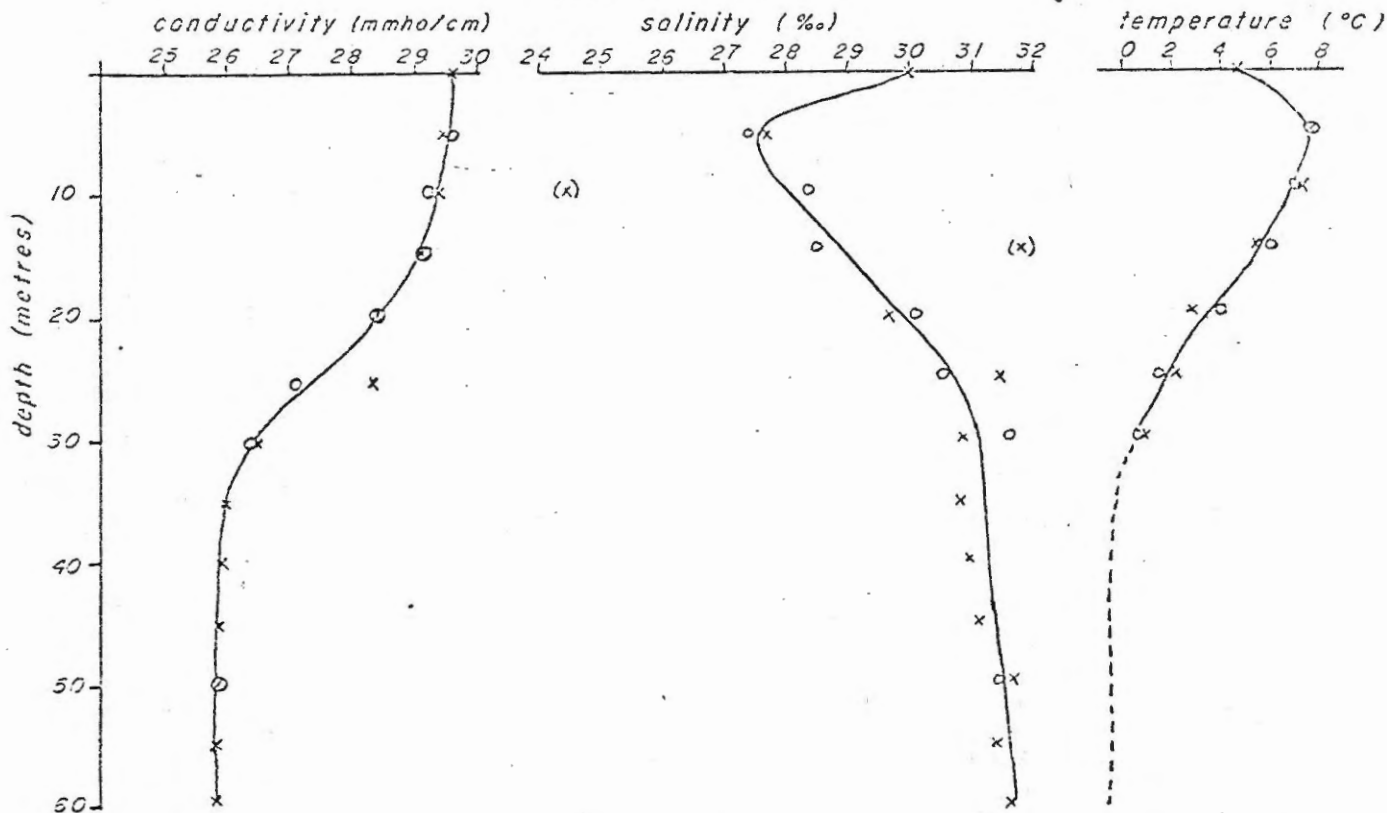
Oceanographic Data

RS-5 PLOT, MATKOVIK BAY

station 1

going down x  
going up o

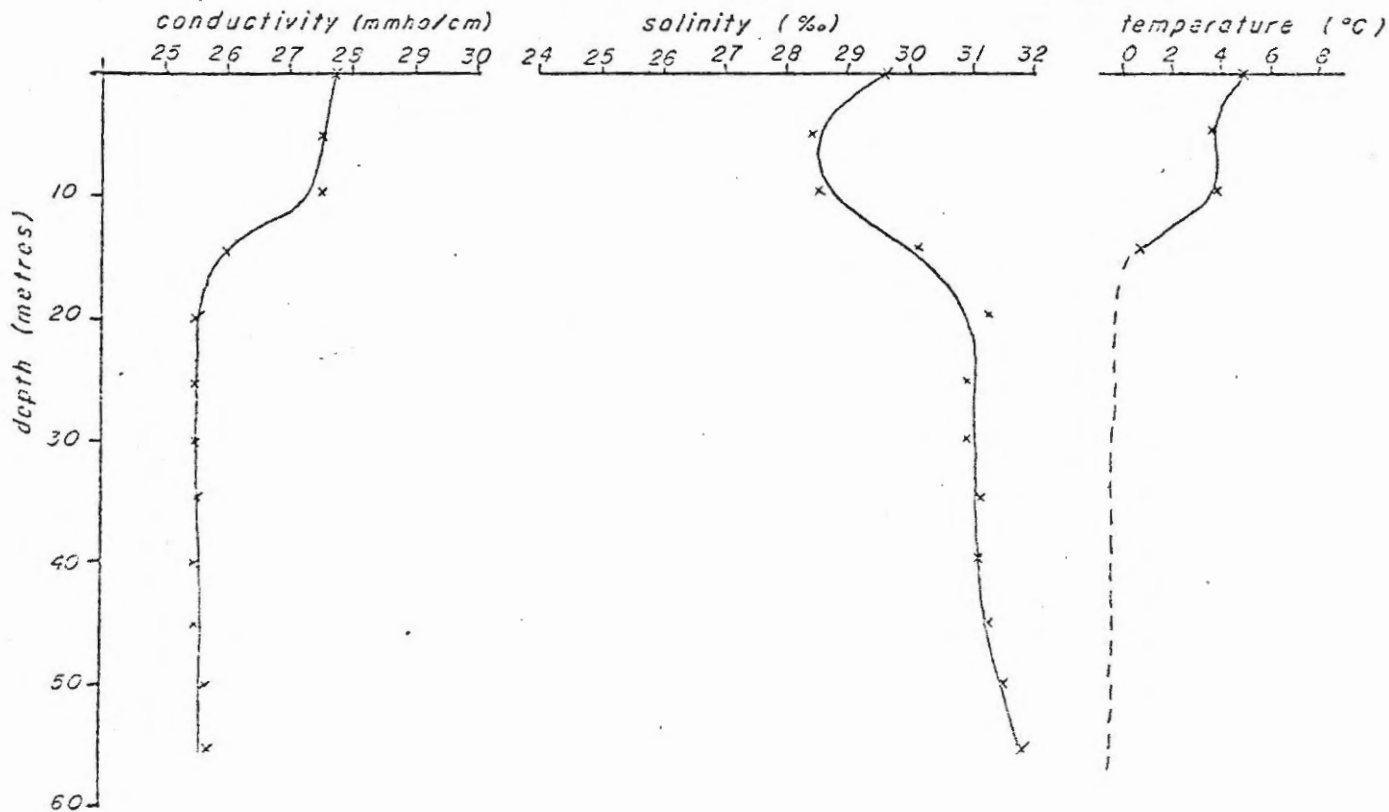
1045 AUGUST 8, 1978  
high tide



station 2

going down x  
going up o

1410 AUGUST 8, 1978  
mid ebb tide



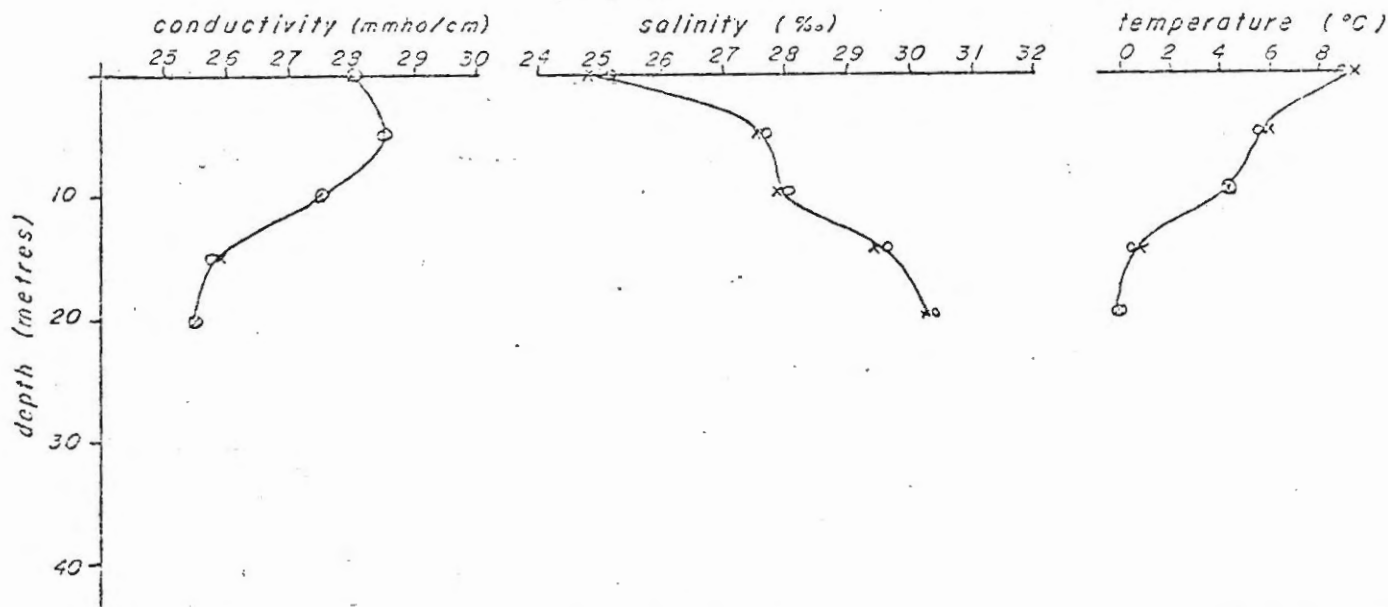


RS-5 PLOT, MAKKOVIK BAY

station 12

going down x  
going up o

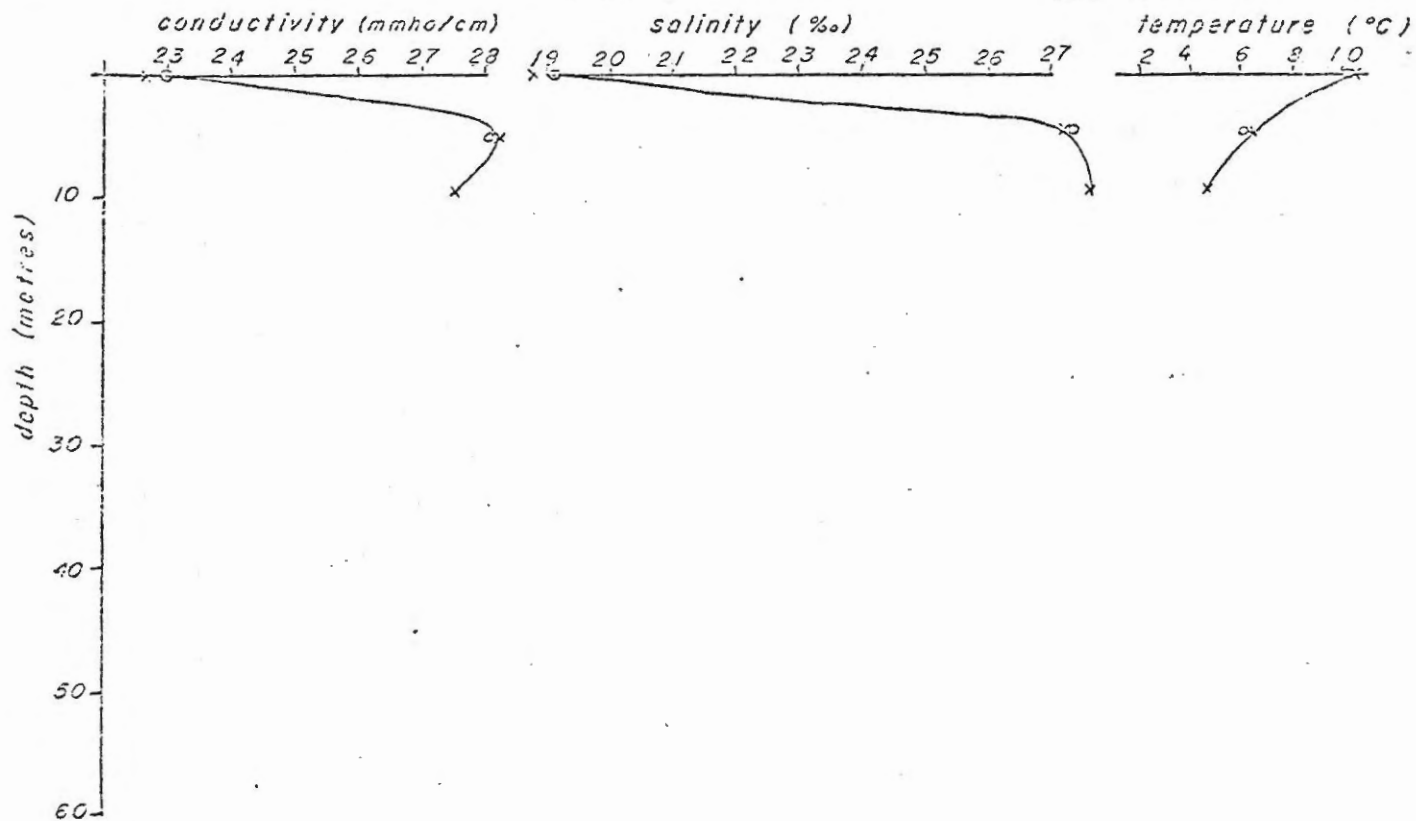
1440 AUGUST 10, 1978  
late ebb tide



station 13

going down x  
going up o

1510 AUGUST 10, 1978  
late ebb tide

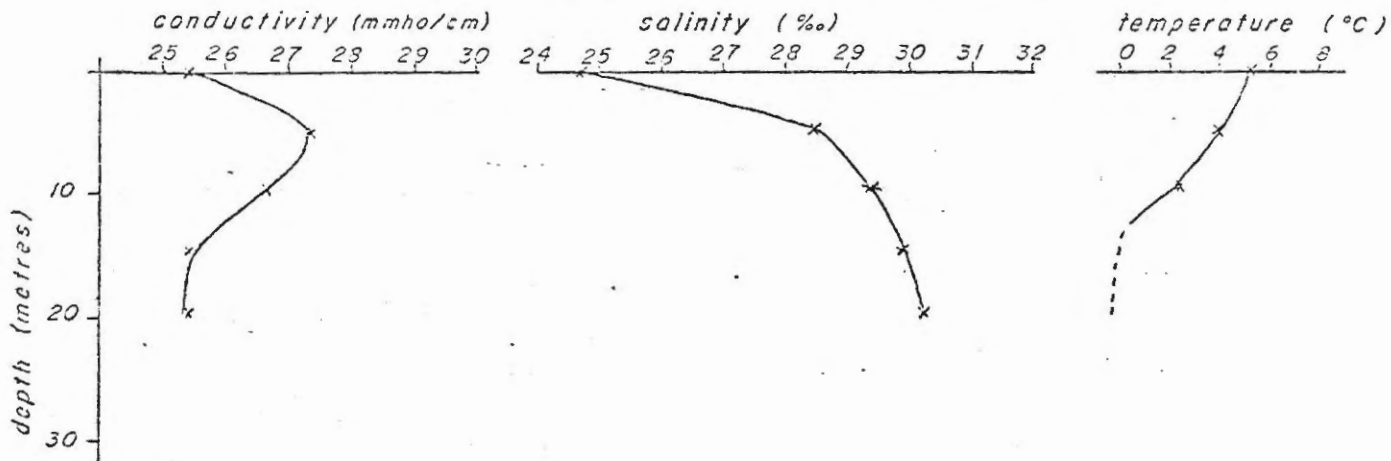


RS-5 PLOT, MAKKOVIK BAY

station 3

going down x  
going up o

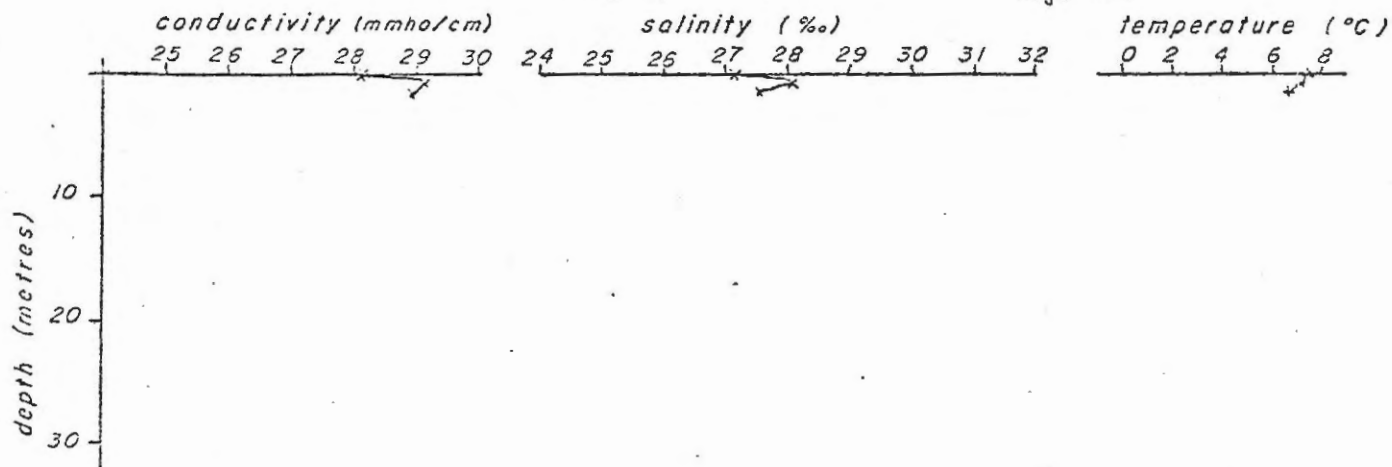
1515 AUGUST 8, 1978  
(late ebb tide)



station 4

going down x  
going up o

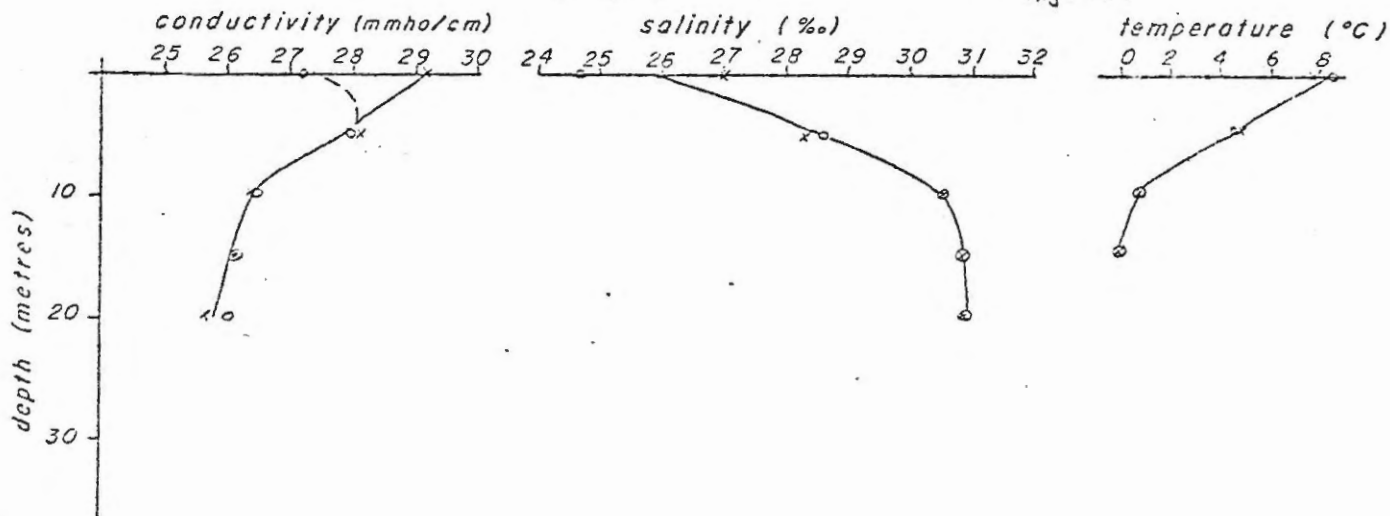
1020 AUGUST 10, 1978  
high tide



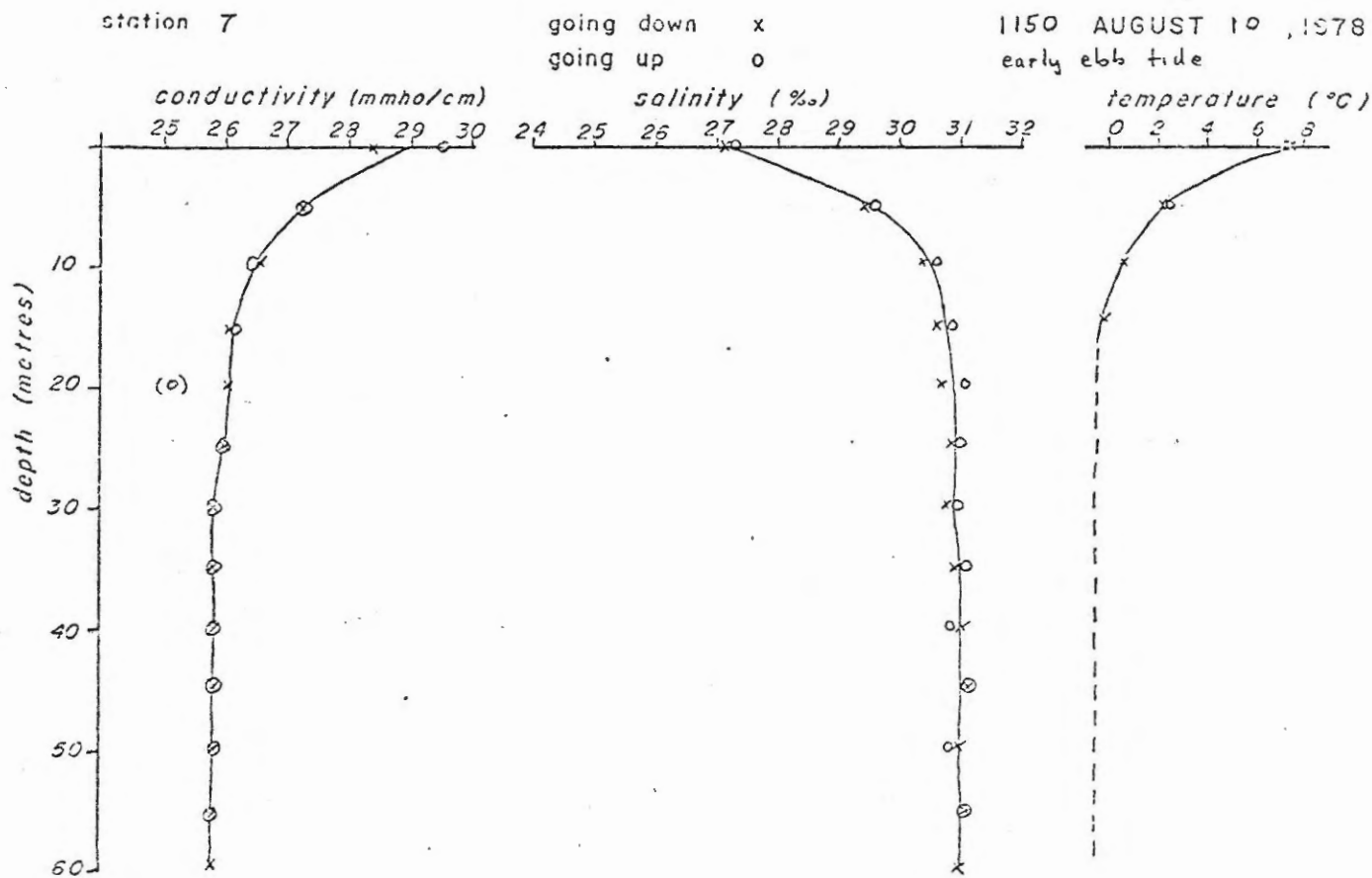
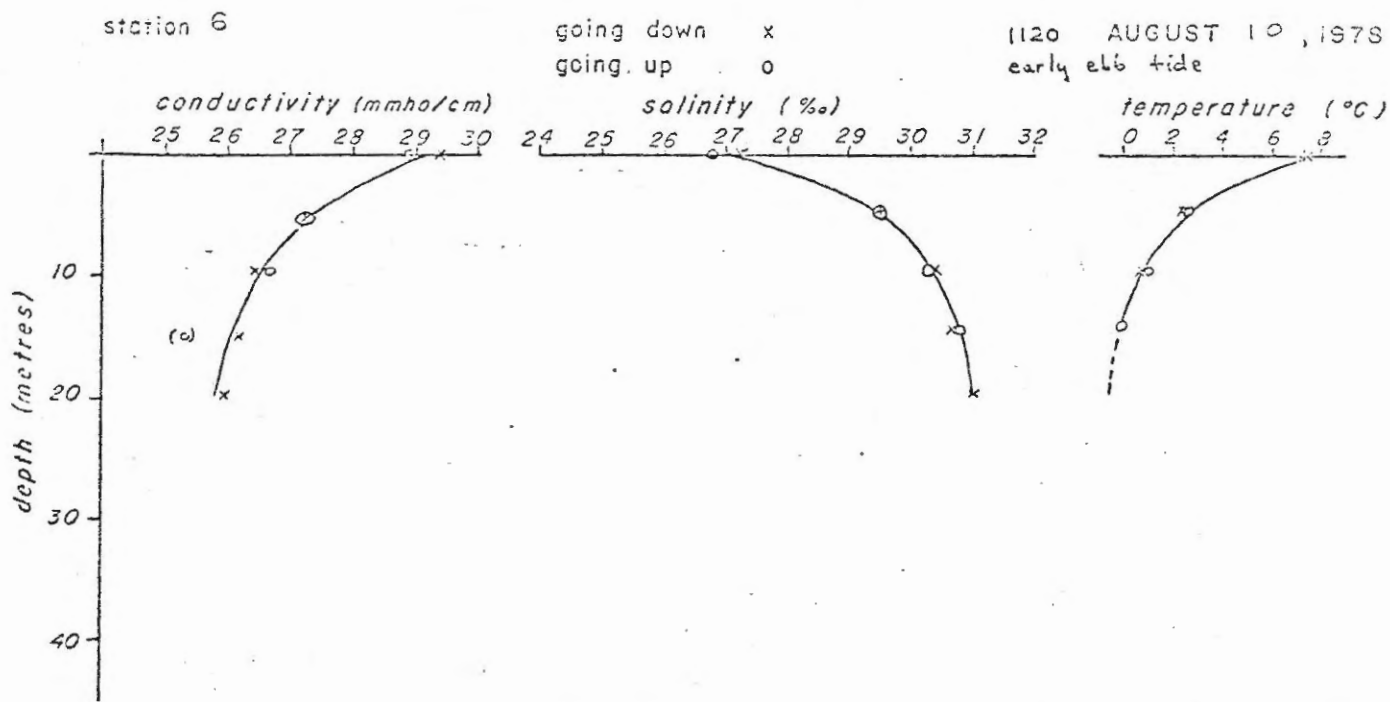
station 5

going down x  
going up o

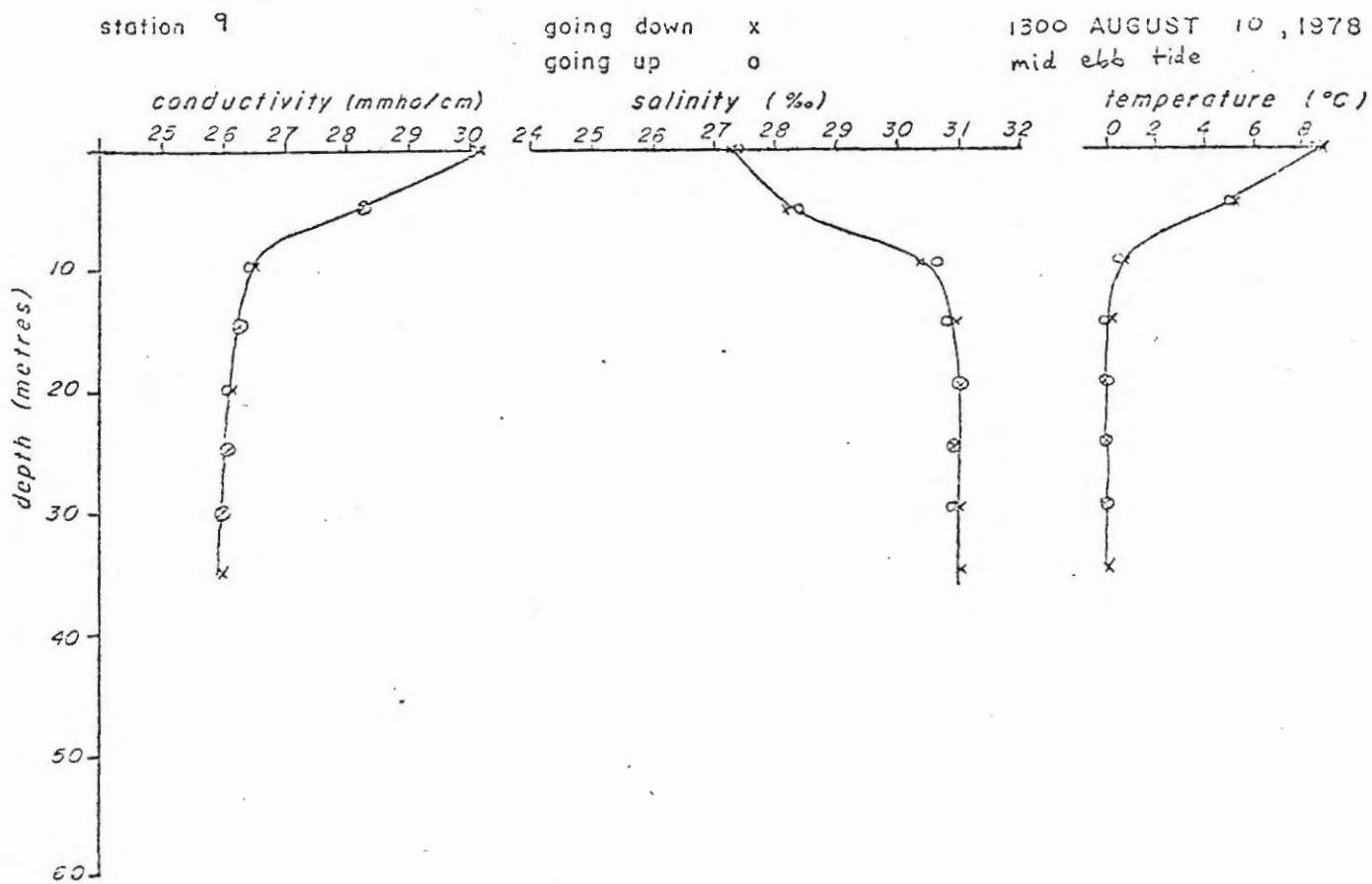
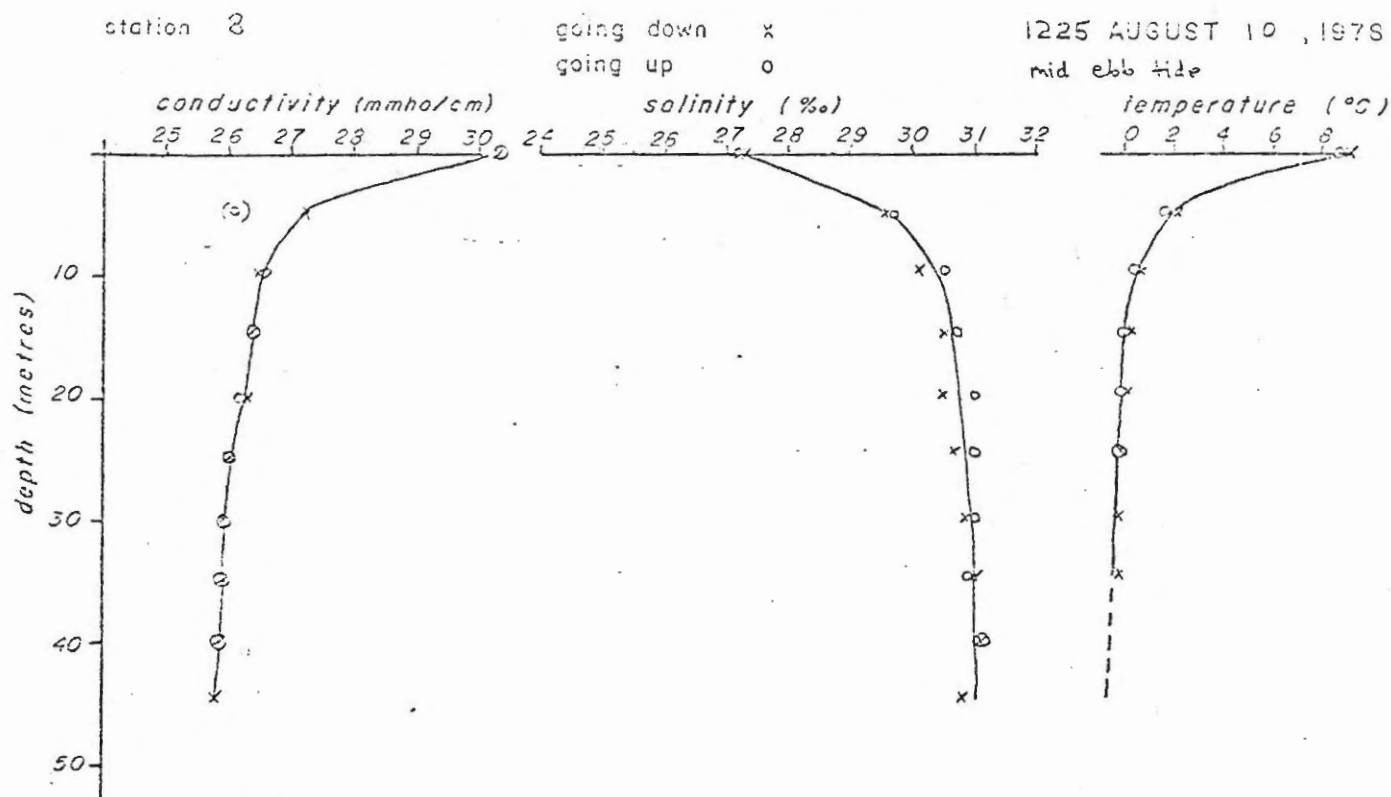
1055 AUGUST 10, 1978  
high tide



RS-5 PLOT, MAKKOVIK BAY



RS-5 PLOT, MAKKOVIK BAY

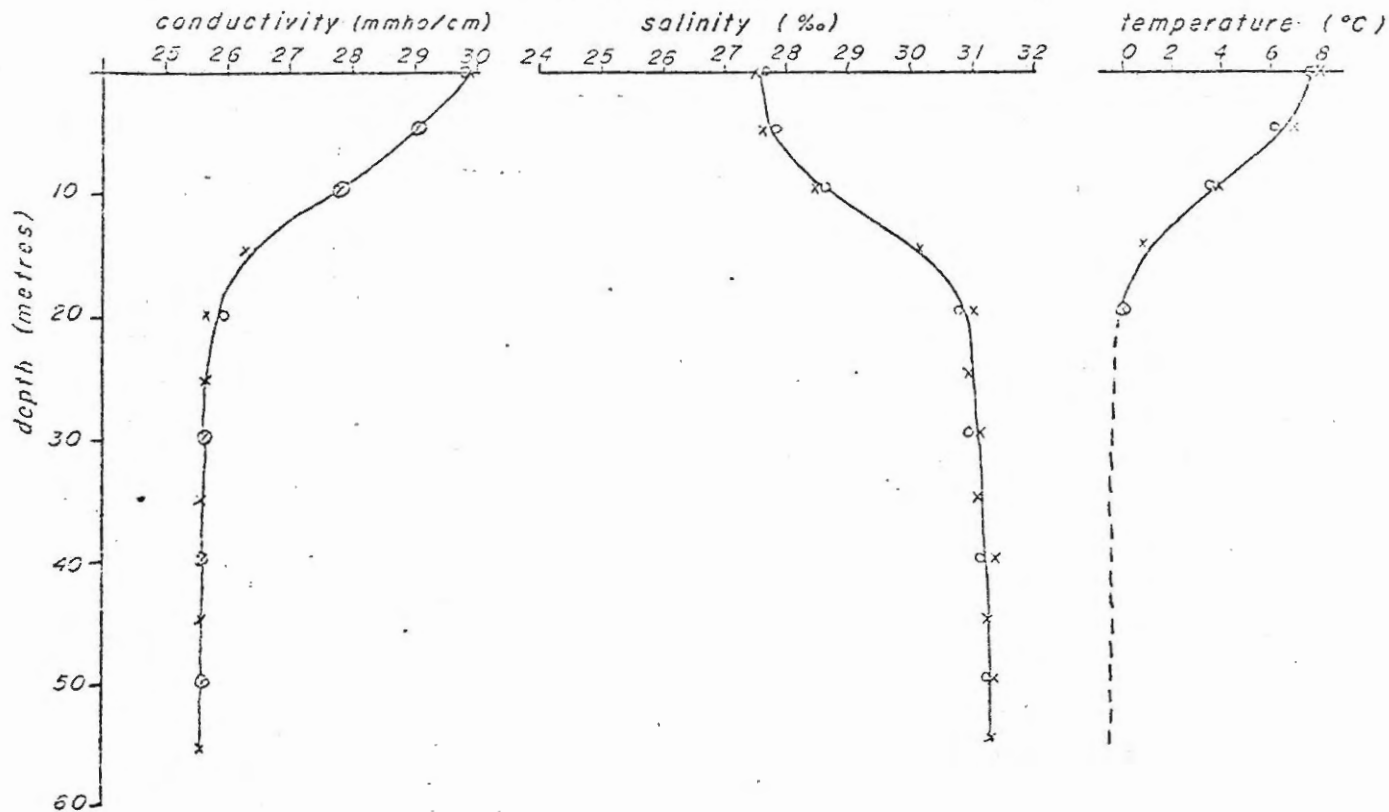


RS-5 PLOT, MAKKOVIK BAY

station 10

going down x  
going up o

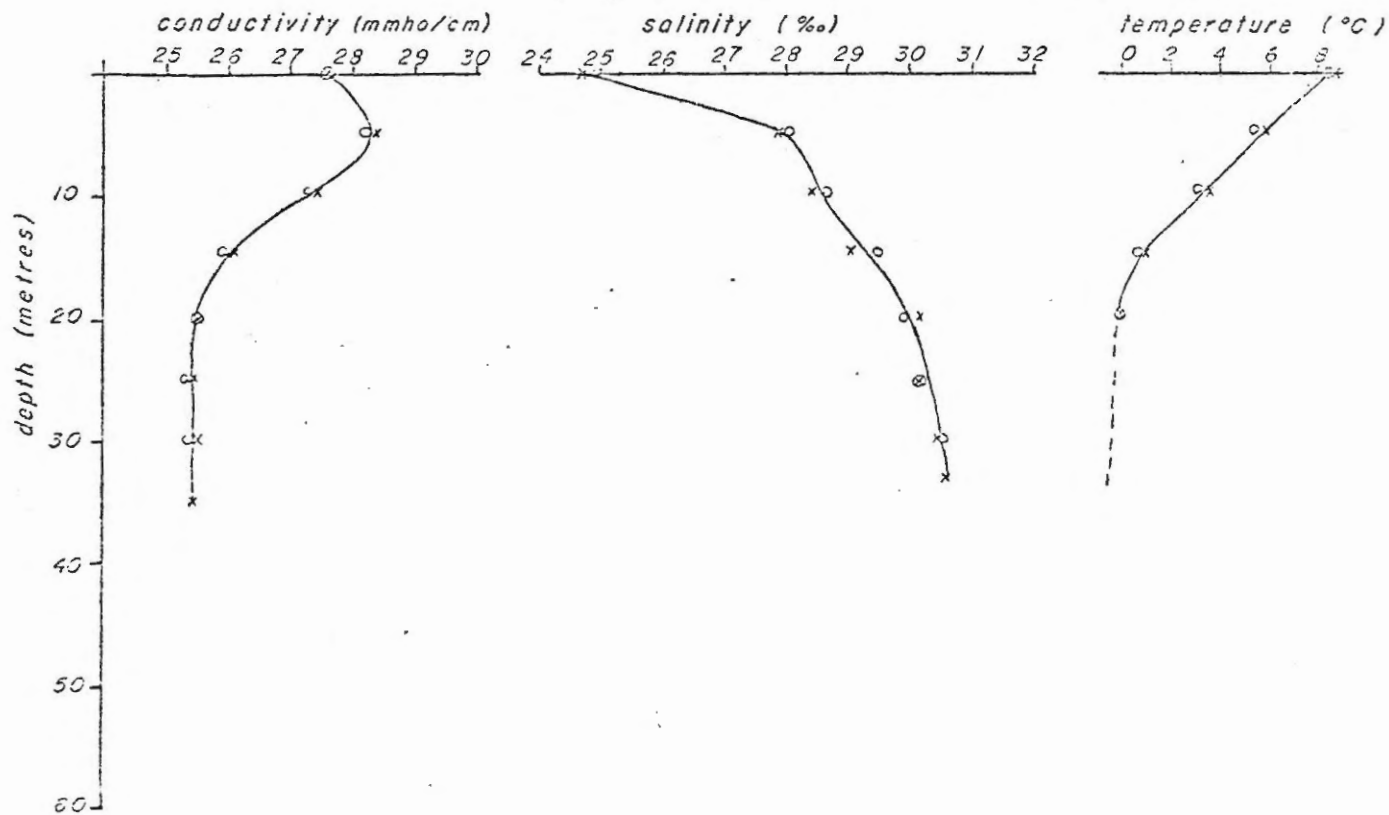
1330 AUGUST 10, 1978  
mid ebb tide



station 11

going down x  
going up o

1415 AUGUST 10, 1978  
late ebb tide



APPENDIX 2

Sediment Trap Data

Outer Bay (Station RS-1)

<u>depth (m)</u>	<u>total weight (g)</u>	<u>mean (g)</u>	<u>standard deviation</u>	<u>sedimentation rate (cm/yr)</u>
60	2.4982			
60	1.0362			
60	1.4066	1.6470	0.8589	
standard deviation too high, omit first datum				
60	1.0362			
60	1.4066	1.2214	0.1852	0.172 ± 15%
40	1.0161			
40	0.9522			
40	0.9756	0.9813	0.0265	0.137 ± 3%

Western Inner Bay (Station RS-3)

18	0.3877			
18	0.3728			
18	0.3666	0.3757	0.0082	0.053 ± 2%
12	0.3560			
12	0.3268	0.3414	0.0146	0.048 ± 4%
12	0.4050 - omit, contaminated			

cross-sectional area of trap - 89.92 cm<sup>2</sup>

duration - 17 days

APPENDIX 3

Piston Core Labelling



The shipboard mislabelling of the piston core section is indicated by the following aspects:

- (1) sediment compaction during storage was significant only at the tops of the "bottom" sections
- (2) the upper sections were firm in contrast to the watery sediment in the "bottom" section
- (3) the  $^{14}\text{C}$  dates were inversed

Less definitive criteria include:

- (1) the upcore trends in the relative proportions of both diatoms and foraminifera
- (2) the upcore trend in clay size mineralogy
- (3) the upcore colour trend from grayish to olive
- (4) the occurrence of sharp textural boundaries between core sections

The conversion from the shipboard labelling to the corrected core interval is depicted in Figure A3.1.

Piston core 78-020-003

Corrected core interval (cm)

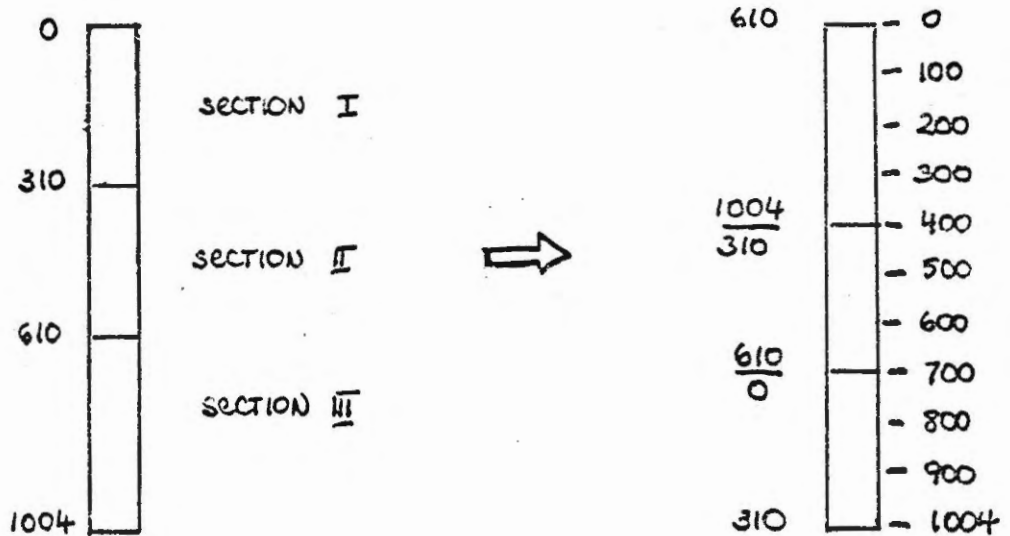
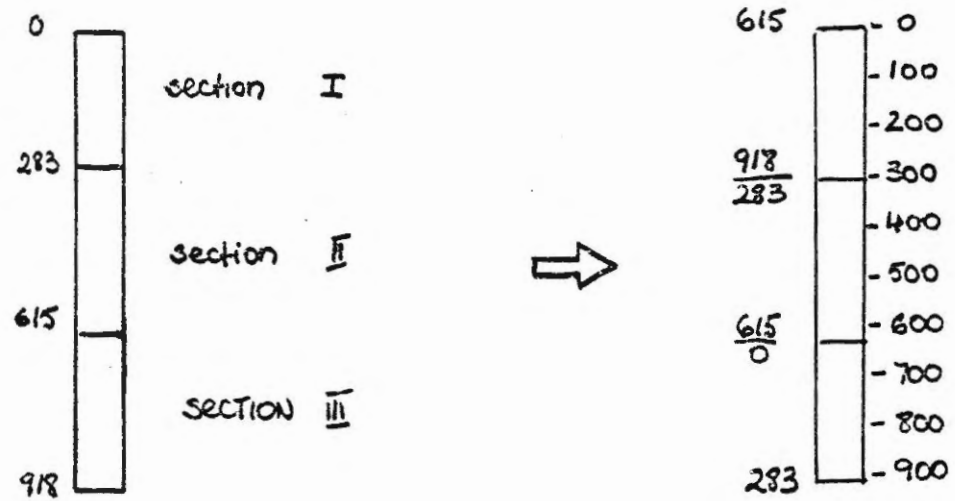


Figure A3.1: Figure showing the conversion of shipboard piston core labels to the corrected core interval

TABLE A4.1 Sediment statistics. Data calculated using HP 9820A calculator; program after Slatt and Press (1976).  
 P = piston core; T = trigger core; S = short core; G = grab sample; L = land sample; ME = median phi diameter; SK = skewness; SD = standard deviation; KE = kurtosis; KGI = normalized kurtosis; \* = flocculated sample.

Sample	Depth (m)	% Gravel	% Sand	% Silt	% Clay	ME	SK	SD	KE	KGI
77-511-										
31G	28	11.65	31.54	32.90	23.91	5.02	.18	4.47	1.04	.51
12G	38	.98	13.07	44.28	41.67	7.65	.17	3.55	.79	.44
34G	51	4.12	23.09	34.45	38.34	6.97	.06	4.20	.88	.47
35G	41	81.48	5.53	9.73	3.27	-1.46	.94	3.06	14.06	.93
36G	34	6.27	13.74	36.71	43.28	7.48	-.82	4.26	.98	.50
37G	28	2.16	16.87	38.16	42.81	7.52	.03	3.91	.86	.46
40G	4	.97	92.62	3.32	3.10	2.64	.09	.98	1.05	.62
41G	41	.15	78.68	13.59	7.58	3.43	.51	1.71	2.85	.74
42G	37	1.60	64.06	22.83	11.51	4.10	.58	2.23	2.32	.70
43G	49	.11	33.57	39.07	27.25	6.19	.53	3.40	.87	.47
44G	55	4.91	21.73	36.93	36.42	6.87	.13	4.20	.96	.48
46G	69	-	6.03	44.86	49.11	8.34	.16	3.20	.77	.43
47G	83	.48	5.39	45.24	48.89	8.29	.15	3.24	.73	.42
48G	56	.18	4.62	42.74	52.47	8.52	.10	3.19	.75	.43
49G	84	.04	9.35	59.50	31.11	7.30	.33	3.09	.94	.48
59G	10	-	50.76	31.63	17.61	5.07	.62	3.98	1.17	.54
52G	44	-	87.28	7.95	4.78	3.04	.27	1.40	2.65	.73
53G	51	.01	88.36	7.73	3.89	3.22	.44	.94	2.21	.69
54G	61	2.52	88.49	5.88	3.11	3.27	.08	.71	1.39	.58
55G	57	-	89.76	7.95	2.29	3.32	.29	.79	1.83	.65
57G	61	28.01	30.42	18.95	22.62	3.64	.40	4.88	.67	.40
58G	100	-	51.20	42.70	6.11	4.65	.50	2.16	.74	.43
60G	77	-	80.08	11.52	8.41	3.52	.69	1.72	3.08	.76
63G	62	-	57.11	34.60	8.09	4.51	.64	2.01	1.41	.56
67G	19	.19	97.03	.64	2.14	2.36	.21	.70	1.18	.54
69G	32	12.94	62.11	16.16	8.79	2.58	.21	3.21	1.53	.60
71G	42	7.39	52.33	28.76	11.51	4.19	.29	2.94	2.71	.73
75S	32	2.17	62.93	25.15	9.75	3.85	.33	3.50	2.22	.69
84G	14	.48	48.56	41.65	9.32	4.17	.28	3.20	2.44	.71
86G	21	.07	29.56	58.16	12.21	5.12	.56	2.19	1.93	.66
87G	23	.09	22.90	55.44	21.54	6.06	.62	2.89	1.18	.54
88S	25	.97	21.99	55.97	21.07	6.04	.58	2.88	1.15	.53
117G	74	-	8.29	47.42	44.30	7.98	.21	3.27	.75	.43
118G	64	-	9.86	47.61	42.54	7.75	.26	3.31	.73	.42
125*G	5	8.59	47.90	41.58	1.93	3.83	-.01	2.65	1.08	.52
126G	8	7.79	15.43	65.90	10.88	5.23	.04	2.94	2.22	.69
129S	9	5.57	37.25	28.66	28.52	6.32	-.03	4.28	.99	.50
130S	13	8.10	30.71	44.92	16.27	4.83	.05	3.66	1.29	.56
133S	18	1.69	15.53	53.63	29.14	7.04	.29	3.39	1.07	.52
135G	30	2.75	16.26	47.91	33.08	7.11	.11	3.72	1.01	.50
136G	29	3.82	13.80	50.49	31.89	7.06	.09	3.88	1.17	.54
137G	14	35.47	8.28	31.18	25.06	4.61	.01	5.02	.64	.39
138G	7	2.00	33.07	50.22	14.71	5.05	.15	3.13	1.40	.58
139G	18	.68	27.24	58.95	13.12	5.14	.22	2.70	1.98	.66
140G	22	8.09	14.15	49.47	28.30	6.50	.13	4.03	1.28	.56
141G	25	6.32	16.74	43.36	33.57	6.86	.01	4.22	1.09	.52
142G	16	58.76	10.82	10.23	20.20	2.27	.95	4.77	.90	.47
143G	28	13.48	25.84	30.81	29.87	5.49	-.15	5.04	.70	.41
144G	43	-	4.93	40.29	54.77	8.82	.09	3.07	.81	.45
145G	26	-	12.76	58.69	28.55	7.11	.30	3.11	1.03	.51
168G	61	5.67	58.82	21.31	14.19	4.15	.45	3.34	1.89	.63
177G	35	.03	64.54	25.59	9.81	4.14	.59	2.03	1.83	.63
178G	25	.19	57.73	35.14	4.94	4.11	.42	1.81	1.76	.64
179G	16	1.44	81.00	13.00	4.33	3.34	.06	1.14	1.69	.63
180G	41	.10	40.34	47.81	11.75	4.97	.45	2.36	1.47	.60

TABLE A4.1 Sediment statistics. (Continued)

Sample 77-511-	Depth (m)	% Gravel	% Sand	% Silt	% Clay	MS	SK	SD	KS	KGI
181G	42	-	61.09	30.78	8.12	4.31	.67	1.68	2.05	.67
185G	34	.12	82.57	13.17	4.14	3.16	.22	1.37	1.95	.66
188G	73	.04	5.62	49.79	44.55	8.04	.22	3.21	.74	.43
217G	76	-	9.88	50.40	39.72	7.67	.29	3.24	.75	.43
218G	79	-	9.79	59.04	31.17	7.02	.52	1.09	.86	.46
223G	29	28.90	28.80	32.30	10.01	2.86	.29	4.06	.65	.40
224G	34	29.71	38.05	18.56	13.69	2.55	.51	4.20	.78	.44
225G	20	22.61	66.06	5.68	5.65	.52	.36	2.38	1.72	.63
226G	39	65.29	22.85	6.66	5.20	.09	.90	2.50	1.64	.62
227G	45	15.68	42.05	21.01	21.26	3.98	.25	4.71	.95	.49
228G	63	-	13.22	47.01	39.77	7.73	.16	3.39	.86	.46
233G	22	-	21.37	54.41	24.23	6.42	.44	3.10	1.11	.53
234G	53	-	3.78	43.50	52.73	8.73	.15	3.02	.81	.45
235G	17	-	5.87	40.19	53.94	8.91	.14	2.99	.86	.46
236G	58	14.90	20.21	49.21	15.68	4.36	-.05	3.95	1.79	.64
237G	39	-	6.42	45.56	48.02	8.30	.16	3.23	.83	.45
238G	51	9.37	18.81	34.55	37.27	6.40	-.08	4.75	.94	.49
239G	21	-	12.64	47.40	29.97	7.15	.36	3.07	.92	.48
240G	24	.42	19.78	40.80	39.00	7.37	.10	3.78	.86	.46
291L	-	-	1.59	52.72	45.69	8.42	.29	2.90	.81	.45
292L	-	.95	4.18	46.47	48.39	8.35	.19	3.14	.78	.44
293L	-	.99	7.72	46.75	44.54	7.94	.16	3.42	.80	.45
297-08	74	1.10	6.05	50.05	42.80	7.82	.26	3.27	.73	.42
297-258	74	.55	7.56	48.52	43.37	7.83	.23	3.33	.71	.42
316L	-	3.21	39.11	47.29	10.40	4.96	.15	2.87	1.72	.63
344L	-	.12	2.12	36.61	61.15	9.15	.00	2.99	.80	.45
359G	17	1.65	94.36	3.82	.17	3.38	-.62	.67	.91	.48
360-08	45	87.13	11.41	1.98	.39	-1.21	.45	.83	7.40	.86
361-08	44	82.98	15.75	.74	.53	-.93	.78	1.87	6.67	.87
362-08	36	18.82	79.42	1.12	.65	1.07	-.23	1.75	.84	.46
363-08	42	-	82.32	10.03	7.63	3.54	.18	1.85	2.97	.74
364-08	43	80.17	17.95	.59	.49	-.87	.79	1.02	5.91	.86
365-08	44	-	68.65	21.79	9.56	3.97	.29	2.43	2.05	.67
366-08	43	-	75.34	15.87	8.79	3.89	.28	2.41	3.04	.75
367-08	36	-	73.78	18.69	7.53	3.68	.16	2.33	2.36	.70
368-08	35	15.17	68.75	17.98	6.09	2.49	.07	2.97	1.80	.64
369-08	32	4.18	83.48	10.30	2.04	3.05	-.49	1.57	1.67	.63
372-08	45	.24	11.88	48.18	39.71	7.69	.17	3.45	.86	.46
373-08	46	10.39	15.87	40.26	33.47	6.38	-.05	4.57	1.00	.50
374-08	47	37.39	11.43	28.05	23.13	4.25	.11	4.93	.65	.39
375-08	45	2.67	20.45	42.19	34.69	7.03	.04	3.96	.95	.49
376-08	45	3.31	10.60	45.41	40.68	7.73	.09	3.64	.95	.49
377-08	42	-	10.44	59.23	30.33	7.37	.29	3.11	1.05	.51
378-08	36	.15	8.74	47.79	43.32	7.97	.18	3.32	.82	.45
379-08	35	.27	9.27	47.41	43.05	7.96	.17	3.34	.84	.46
380-08	30	.19	7.36	50.07	42.38	7.98	.19	3.27	.84	.46
381-08	31	-	6.46	48.62	44.92	7.99	.24	3.25	.75	.43
382-08	31	1.67	6.07	53.53	38.73	7.73	.25	3.26	.89	.46
383-08	14	39.15	37.63	15.24	7.98	1.99	.25	3.45	.94	.48
394-08	54	-	9.92	46.36	43.72	7.99	.14	3.41	.87	.47
426-08	44	4.84	2.39	44.18	48.59	8.33	-.01	3.86	1.14	.53
434-108	16	2.14	28.84	41.42	27.60	6.12	.31	3.86	1.02	.51
434-138	16	20.62	30.87	25.65	22.86	4.16	.18	4.86	.78	.43
434-158	16	35.34	30.83	16.65	17.19	2.69	.60	4.50	.81	.45
434-185	16	4.33	17.63	39.03	39.00	6.84	-.06	4.49	.99	.50
457-08	98	1.30	43.95	33.05	16.70	4.95	.51	3.07	1.37	.58
459-08	74	-	14.57	50.76	34.67	7.07	.47	3.29	.77	.44

TABLE M.1 Sediment statistics. (Continued)

Sample 77-511-	Depth (m)	% Gravel	% Sand	% Silt	% Clay	ME	SE	SD	MC	MC1
462-208	71	.15	10.04	46.53	43.28	7.83	.21	3.36	.75	.43
464-08	100	-	18.69	47.50	33.80	6.99	.41	3.37	.79	.44
468-08	103	-	15.49	50.77	33.75	7.17	.36	3.29	.80	.45
471-108	68	.11	1.60	51.87	46.42	8.24	.26	3.08	.74	.43
474-278	72	.76	12.45	46.40	40.40	7.55	.25	3.48	.81	.45
478-308	86	2.65	8.78	44.41	44.16	7.82	.12	3.65	.87	.47
488-08	45	.21	3.27	46.45	50.07	8.50	.20	3.06	.78	.44
492-08	25	-	8.31	50.93	40.76	7.83	.22	3.32	.86	.46
493-08	20	-	15.11	45.67	39.22	7.61	.11	3.61	.92	.48
497-08	43	.87	8.10	42.04	48.98	8.34	.10	3.36	.87	.47
502-08	84	.44	13.84	40.44	25.29	6.04	.55	3.34	.92	.48
509-208	37	-	2.08	47.87	50.05	8.42	.18	3.11	.74	.43
521-08	73	-	5.99	66.13	27.88	7.38	.30	2.83	1.15	.53
524-108	47	.16	.76	43.00	56.08	8.98	.13	2.89	.76	.43
525-208	40	-	3.34	53.91	42.75	7.92	.31	3.14	.74	.42
530-208	-	-	8.70	51.81	39.49	7.57	.34	3.26	.74	.43
531-208	-	-	29.11	50.66	20.23	5.84	.70	2.79	1.36	.58
531-258	-	-	2.92	48.84	48.24	8.11	.19	3.26	.65	.39
533-08	26	11.86	23.13	38.37	26.64	6.13	.15	4.11	1.21	.55

TABLE A4.1 Sediment statistics. (Continued)

Sample 79-20-003	% Gravel	% Sand	% Silt	% Clay	ME	SE	SD	MS	MSI
107	-	10.27	50.33	39.40	7.57	.31	3.30	.75	.43
307	-	9.03	51.53	39.45	7.55	.34	3.27	.74	.43
507	-	10.03	51.07	38.91	7.54	.31	3.30	.75	.45
707	-	14.71	51.71	33.58	7.11	.41	3.28	.80	.45
1097	-	15.82	47.17	37.01	7.21	.40	3.37	.74	.43
15	-	9.81	48.18	42.02	7.69	.27	3.33	.73	.42
35	-	9.08	44.40	46.52	8.00	.17	3.36	.72	.42
55	-	9.70	45.03	45.27	7.93	.19	3.36	.73	.42
75	-	11.43	42.87	45.70	7.86	.19	3.41	.70	.41
85	-	10.64	43.68	45.67	7.86	.20	3.40	.70	.41
115	-	11.44	45.54	43.03	7.69	.26	3.38	.71	.41
135	-	11.36	46.56	42.08	7.70	.24	3.37	.72	.42
165	-	19.95	52.07	27.98	6.50	.59	3.19	.91	.48
185	-	13.28	48.79	37.93	7.31	.39	3.34	.74	.43
205	-	12.29	50.33	37.38	7.28	.42	3.31	.75	.43
235	-	10.22	45.94	43.85	7.77	.24	3.38	.71	.42
255	-	8.57	45.34	45.99	7.90	.22	3.36	.69	.41
285	-	7.09	42.90	50.01	8.23	.10	3.34	.70	.41
305	-	7.82	41.20	50.98	8.28	.07	3.36	.69	.41
310	-	3.48	49.10	47.42	8.13	.21	3.21	.69	.41
330	-	4.89	46.43	48.69	8.24	.15	3.23	.71	.42
350	-	5.99	49.18	44.83	7.93	.25	3.26	.70	.41
360	16.84	24.57	34.53	24.06	4.56	.05	4.90	.88	.47
380	2.22	5.12	43.21	49.45	8.22	.11	3.25	.74	.42
400	-	5.13	48.23	46.65	8.06	.21	3.24	.70	.41
420	-	5.09	45.50	49.42	8.27	.17	3.22	.68	.41
440	-	4.36	47.62	28.02	8.26	.20	3.17	.73	.42
450	4.46	33.83	36.28	25.42	5.49	.17	4.30	1.04	.51
470	4.29	19.38	41.25	35.07	6.73	.08	4.26	1.01	.50
490	1.76	16.65	41.10	40.49	7.34	.12	3.90	.88	.47
510	13.62	21.87	34.62	29.88	5.21	.04	4.96	.86	.46
530	23.38	17.19	31.90	27.40	4.76	.04	5.09	.67	.40
550	-	8.31	47.55	44.14	7.83	.25	3.32	.71	.41
570	-	8.17	48.00	43.83	7.91	.28	3.25	.76	.43
590	-	11.46	45.56	42.98	7.67	.27	3.39	.71	.42
610	-	9.99	46.40	43.61	7.75	.25	3.37	.72	.42
630	-	9.61	47.86	42.53	7.67	.30	3.30	.71	.42
635	-	10.63	48.89	40.48	7.52	.35	3.35	.73	.42
685	-	9.55	46.31	44.13	7.82	.33	3.35	.70	.42
705	-	9.08	50.32	40.60	7.84	.30	3.29	.73	.42
725	-	6.33	48.27	45.40	7.92	.34	3.29	.69	.41
745	-	7.33	53.82	38.85	7.62	.31	3.23	.74	.43
765	-	8.97	53.29	37.79	7.38	.41	3.25	.74	.42
785	-	8.53	51.23	40.23	7.55	.36	3.28	.72	.42
805	-	8.06	56.49	35.45	7.55	.29	3.16	.80	.45
825	-	8.88	50.93	40.18	7.56	.35	3.28	.73	.42
845	-	9.17	52.12	42.72	7.86	.28	3.20	.71	.42
865	-	6.25	46.24	47.51	8.11	.18	3.28	.71	.42
885	-	4.71	49.15	46.14	8.10	.21	3.21	.71	.42
905	-	6.76	47.41	45.83	8.07	.20	3.26	.73	.42

TABLE A4.1 Sediment statistics. (Continued)

Sample 78-020-004	% Gravel	% Sand	% Silt	% Clay	MS	SK	SD	KS	KGI
07	-	27.21	48.95	23.84	6.15	.63	3.04	1.06	.51
127	-	31.41	46.38	22.21	6.00	.61	3.00	1.01	.50
207	-	21.80	49.53	28.67	6.60	.57	3.18	.86	.46
307	-	28.22	53.31	18.47	5.77	.55	2.72	1.57	.61
30	-	14.54	52.16	33.31	6.99	.51	3.22	.77	.44
70	-	11.17	53.58	35.25	7.31	.39	3.22	.76	.43
110	-	9.24	53.38	37.38	7.36	.43	3.23	.74	.42
150	-	4.62	49.10	46.29	8.02	.24	3.23	.69	.41
190	-	3.28	48.45	48.27	8.20	.20	3.20	.71	.41
230	-	3.07	49.01	47.92	8.23	.20	3.18	.72	.42
270	-	2.84	49.49	47.67	8.21	.21	3.17	.72	.42
290	-	3.03	48.65	48.31	8.31	.18	3.26	.66	.40
350	-	5.62	62.72	31.66	7.10	.54	3.03	.83	.45
384	-	4.74	54.47	40.79	7.67	.37	3.18	.71	.41
392	-	4.91	50.71	44.38	7.92	.29	3.20	.71	.42
404	-	5.40	47.47	47.13	8.15	.20	3.23	.76	.43
360	.25	12.21	45.11	42.43	7.72	.22	3.40	.74	.42
484	-	6.31	44.75	48.94	8.35	.17	3.19	.77	.43
524	.13	3.62	49.55	44.70	8.01	.24	3.21	.74	.42
564	-	3.86	50.39	45.75	8.15	.25	3.14	.74	.43
604	-	6.21	52.78	41.00	7.72	.33	3.21	.73	.42
644	-	2.17	43.71	54.12	8.73	.11	3.06	.74	.43
684	-	1.19	43.23	55.58	8.91	.12	2.95	.76	.43
694	-	.68	37.95	61.37	9.25	.05	2.84	.74	.43
734	-	.74	44.02	55.21	8.88	.14	2.93	.74	.43
774	-	.97	54.30	44.73	8.11	.27	3.10	.74	.42
834	.63	.75	46.17	52.45	8.71	.19	2.95	.74	.43
854	-	.87	47.16	51.97	8.67	.19	2.97	.75	.43
894	-	.40	51.04	48.56	8.42	.23	3.03	.75	.43
934	-	.46	49.09	50.45	8.52	.20	3.03	.74	.43
974	-	.77	46.56	52.67	8.62	.14	3.07	.73	.42

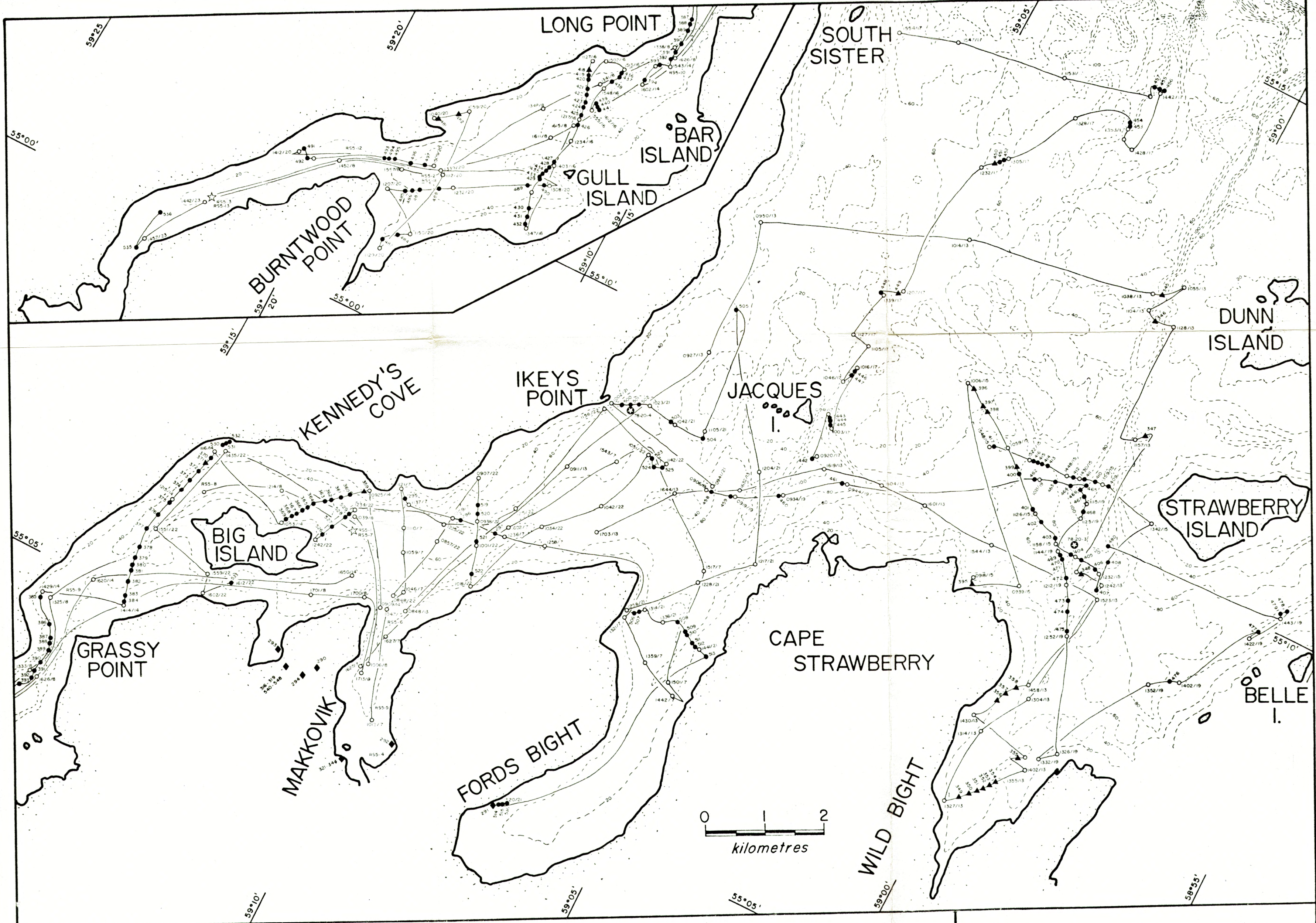
TABLE A5.1 Clay and clay-size mineralogy of the < 2 $\mu$  fraction from short cores and land samples

Sample 78-511-	Clay minerals				Clay-size minerals						
	Mont.	Illite	Kaol.	Chl.	Mont.	Illite	Kaol.	Chl.	Qtz.	Amph.	Felds.
290	1.0	66.8	7.1	25.1	0.3	9.2	0.9	3.1	1.1	5.2	64.7
291	2.0	69.7	3.9	24.3	1.1	37.5	2.1	13.1	4.5	3.0	38.7
292	1.8	70.9	3.8	23.6	0.9	38.1	2.0	12.6	4.6	6.1	35.7
293	1.4	77.1	4.0	17.4	0.8	41.2	2.1	9.3	7.0	4.6	35.0
294	0.4	62.9	4.5	32.2	0.2	25.0	1.8	12.8	7.1	5.2	47.9
297-0	2.4	56.2	10.0	31.4	0.9	20.8	3.7	11.6	8.2	4.5	50.4
297-25	4.6	66.2	7.2	22.0	2.3	33.3	3.6	11.0	7.1	6.0	36.7
316	4.8	46.2	13.0	36.1	0.5	4.6	1.3	3.6	8.2	5.0	76.9
344	1.3	78.6	3.7	16.4	0.7	43.4	2.1	9.1	3.2	2.4	39.2
381-0	1.0	55.3	10.4	33.3	0.3	19.2	3.6	11.5	5.3	4.6	55.5
394-0	7.2	55.9	6.7	30.2	3.1	24.4	2.9	13.2	9.3	5.0	42.0
426-0	3.2	56.1	9.0	31.6	1.2	21.0	3.4	11.9	7.3	4.8	50.4
434-10	7.1	53.3	11.4	28.1	3.2	24.0	5.2	12.7	7.7	5.4	41.9
434-13	3.2	42.1	20.0	34.7	0.8	10.1	4.8	8.3	10.8	3.8	61.4
434-15	2.0	61.1	10.9	26.0	0.7	22.1	4.0	9.4	6.8	2.5	54.5
434-18	2.1	37.4	14.0	46.4	0.8	14.7	5.5	18.3	4.8	1.7	54.1
459-0	2.7	64.9	8.6	23.9	1.0	24.3	3.2	8.9	6.4	6.1	50.1
462-20	3.7	48.6	7.2	40.5	1.3	17.7	2.6	14.8	7.7	5.0	50.8
464-0	4.8	54.4	9.2	31.6	1.3	15.1	2.6	8.8	7.6	5.2	59.5
468-0	2.8	69.7	4.5	23.0	0.9	21.2	1.4	7.0	9.1	3.5	57.0
471-10	0.6	61.0	5.1	33.4	0.3	26.7	2.2	14.6	3.8	5.8	46.7
474-27	1.2	48.7	11.2	38.9	0.4	16.6	3.8	13.2	8.2	3.5	54.4
478-30	3.3	37.2	14.0	45.6	1.0	10.8	4.1	13.3	9.3	3.4	58.3
488-0	5.4	56.5	9.5	28.6	2.1	21.3	3.6	10.8	11.9	4.6	45.9
489-0	2.6	56.6	6.9	33.9	1.1	24.5	3.0	14.6	14.1	5.0	47.8
492-0	5.9	51.3	5.5	37.3	2.9	25.1	2.7	18.3	4.1	4.3	42.7
497-0	4.4	50.3	14.3	31.0	1.6	18.4	5.2	11.3	4.9	5.8	52.8
502-0	3.7	49.7	8.7	37.9	0.6	8.5	1.5	6.5	12.2	5.3	65.4
509-20	2.2	56.9	5.8	35.0	0.8	20.6	2.1	12.7	6.1	4.0	53.7
524-10	3.9	64.3	8.1	23.8	1.7	27.7	3.5	10.2	9.1	6.7	41.1
525-20	2.3	54.7	6.7	36.3	0.8	19.9	2.4	13.2	7.4	3.3	53.0
530-20	0.7	62.8	10.2	26.4	0.3	29.4	4.8	12.4	5.8	6.8	40.5
531-20	5.1	51.3	6.8	36.8	2.4	23.5	3.1	16.9	7.1	2.5	44.6
531-25	2.0	54.2	9.2	34.6	1.0	25.6	4.4	16.3	5.9	4.3	42.6



TABLE A5.2 Clay and clay-size mineralogy of the < 2 $\mu$  fraction from piston cores 78-020-003 and 78-020-009

Core Interval (cm)	Clay minerals				Clay-size minerals						
	Mont.	Illite	Kaol.	Chl.	Mont.	Illite	Kaol.	Chl.	Qtz.	Amph.	Felds.
<u>Piston core 78-020-003</u>											
trigger- 10	5.1	57.3	5.5	32.1	1.3	14.7	1.4	8.2	7.3	3.5	63.6
trigger- 70	3.9	58.4	18.9	18.9	1.0	14.7	4.8	4.8	16.4	4.1	54.4
trigger- 105	8.3	55.7	7.7	28.4	2.2	14.7	2.0	7.5	14.6	5.5	53.5
15	9.0	66.0	7.0	18.0	1.9	14.2	1.5	3.9	14.8	3.2	60.4
105	4.9	66.7	6.4	22.1	1.5	20.9	2.0	6.9	6.3	4.4	58.0
185	5.9	63.6	6.4	24.2	1.8	19.4	1.9	7.4	8.9	6.2	54.4
285	6.3	60.0	7.6	26.1	2.1	19.9	2.5	8.7	9.8	10.5	46.5
330	6.7	64.9	6.2	22.2	2.8	27.3	2.6	9.3	11.6	5.0	41.4
360	2.0	62.8	10.1	25.1	0.8	25.7	4.1	10.3	9.2	5.3	44.5
420	5.8	61.3	8.6	24.4	2.1	22.0	3.1	8.7	10.1	4.1	50.0
450	2.2	54.7	5.6	37.4	1.1	26.0	2.7	17.8	5.9	5.4	41.0
490	5.1	56.3	2.9	35.7	2.4	26.5	1.4	16.9	3.2	5.9	43.8
510	0.7	64.1	9.5	25.7	0.3	29.1	4.3	11.7	1.8	4.7	48.1
530	1.0	64.0	11.7	23.3	0.4	28.3	5.2	10.3	7.3	6.0	42.4
550	5.9	56.3	6.0	31.8	1.9	18.4	2.0	10.4	6.3	4.8	56.3
570	2.8	58.1	11.9	27.2	0.7	15.5	3.2	7.2	9.7	5.6	58.1
590	9.0	52.1	8.2	31.0	3.0	17.1	3.3	9.6	13.1	6.2	49.0
610	7.8	52.9	9.2	30.0	3.2	21.7	3.8	12.3	9.0	5.0	45.1
630	5.3	61.2	8.4	25.2	1.4	16.5	2.3	6.8	10.3	6.7	56.0
635	3.6	57.6	7.2	31.6	1.9	30.2	3.8	16.6	6.5	4.2	36.9
725	3.7	61.5	5.8	28.9	1.6	26.3	2.5	12.4	9.1	8.0	40.1
825	6.7	63.9	8.4	25.2	1.1	27.1	3.6	10.7	4.8	4.2	49.6
<u>Piston core 78-020-004</u>											
trigger- 20	3.5	53.4	9.8	33.3	1.7	25.4	4.7	15.8	8.6	4.5	39.3
30	4.1	62.2	8.6	21.1	2.2	35.4	4.6	11.3	5.4	2.7	38.4
150	2.4	66.4	5.2	26.1	1.2	34.2	2.7	13.4	6.1	3.8	38.5
350	1.8	62.1	4.5	31.7	0.9	31.1	2.2	15.9	7.6	3.8	38.4
564	1.3	66.6	4.1	28.1	0.7	35.3	2.2	14.9	8.2	3.5	35.4
684	2.0	70.0	4.1	23.9	1.1	38.9	2.3	13.3	5.8	7.1	31.4
894	1.1	66.9	2.8	29.2	0.6	36.5	1.5	15.9	9.2	4.0	32.3



**LEGEND**

- PISTON CORE
- SHORT CORE
- ▲ GRAB SAMPLE
- ◆ LAND SAMPLE
- ☆ SEDIMENT TRAP
- R55-x OCEANOGRAPHIC STATION
- SEXTANT FIX
- - - BATHYMETRY (METRES)

**TRACK CHART  
MAKKOVIK BAY**